

Forest dynamics at regional scales: predictive models constrained with inventory data

Emily Rebecca Lines

Downing College

University of Cambridge

Dissertation submitted to the University of Cambridge for the Degree of

Doctor of Philosophy

This dissertation is my own work and contains nothing which is the outcome of work done in collaboration with others, except as specified in the text.

For Denis and Margaret Oates, who inspire me.

Acknowledgements

I would like to thank my two supervisors, David Coomes and Drew Purves, for their unending and invaluable help and support during my PhD, and without whom this research would not exist. David, you taught me pretty much everything I know about trees (which you may or may not see as a compliment), and without your advice I would still be floundering in the world of kerplunk modelling. Drew, you taught me that enjoying maths and computing, and producing valuable, applicable ecological research are not mutually exclusive, and that the environment needs mathematicians! My sincere thanks also go to my collaborators in Spain: Miguel Zavala, whose insights and perspectives have enriched my knowledge of Mediterranean ecology, and Paloma Ruiz-Benito, whose patience and good humour enabled me to understand and use the Spanish forest inventory. Thank you to Microsoft Research for funding and supporting this project.

The many members and visitors of the Forest Ecology Group who have passed through during my time here have all helped me out and broadened my understanding of ecology, so thank you to you all: David Wright, Raffaele Laforteza, Olivier Flores, Robbie Holdaway, Andrew Tanentzap, Laura Spence, Mindy Syfert, Irantzu Primicia, Andres Plaza-Aguilar, Pieter De Frenne, Rebecca Spriggs, Tommaso Jucker and Beatrice Wedeux. Special thanks to Will Simonson and Paco Rodriguez-Sanchez for helping me out with my Spanish ecology, and to Beccy Wilebore and Jessica Royles (though not strictly a group member), frankly for putting up with me. If I've forgotten anyone, I'm sorry, and thank you too.

Thanks to my family: my Mum, Dad and sister Kate, for your understanding and support. Hannah Slater, sharing this experience with you has made it so much easier! Finally, the list of things I have to thank Christopher Bosworth for is endless, so thank you for them all.

Summary

Forest ecosystems store more carbon than the atmosphere and harbour the majority of the world's biodiversity, yet their response to changing climate is uncertain. Forest simulation models make landscape-level predictions of forest dynamics by scaling from key tree-level processes, but models typically have no climate dependency. In this thesis I demonstrate how large-scale national inventories combined with improvements in computational methods mean that models that incorporate the climate dependency of demographic processes may be parameterised at regional scales.

In **Chapter One** I outline historical approaches to modelling forest dynamics and present a discussion of competing methods of parameterisation and model selection. In **Chapter Two** I present a model of individual tree mortality in the eastern United States which incorporates species, climatic and competitive effects parameterised using Markov Chain Monte Carlo methods. The remainder of the thesis concentrates on modelling Spanish forest dynamics, so in **Chapter Three** I present a brief introduction to Spanish forest ecology. In **Chapter Four** I examine how aboveground allometry - the scaling of tree height and crown shape - varies with climate and competition in Spain for 26 species. Hierarchical modelling suggests that scaling theories based on wood properties do not explain differences between species, but climatic factors, and in particular hydraulic limitations, do. In **Chapter Five** I parameterise a model of recruitment in Spanish forests using Approximate Bayesian Computation, a novel computational method which allows parameterisation of individual-based models without individual-based data, and demonstrate that it produces ecologically reasonable results. **Chapter Six** presents a forest dynamics model parameterised for the major native species in Spain and tests whether it is able to reproduce observed species-climate distributions. Finally, in **Chapter Seven** I discuss the main findings of the thesis and avenues for extending this research.

To facilitate publication of the thesis, Chapters Two and Four-Six are written as manuscripts for peer-reviewed journals. Since multiple authors contributed data and supervisory support, I use the pronoun "we" rather than "I", and the contributions of each author is described at the end of each of these chapters. At the time of submission, Chapter Two has been published and Chapter Four is in press:

Lines, E.R., Coomes, D.A., Purves, D.W., 2010. Influences of forest structure, climate and species composition on tree mortality across the Eastern US. *PLoS ONE* 5, e13212.

Lines, E.R., Zavala, M.Á., Purves, D.W., Coomes, D.A., *in press*. Predictable changes in aboveground allometry of trees along gradients of temperature, aridity and competition. *Global Ecology and Biogeography*.

Contents

List of tables.....	vi
List of figures.....	vii
1 Introduction	1
1.1 Motivation for modelling forest dynamics.....	2
1.1.1 Forests in models of global vegetation.....	2
1.1.2 Models of the effects of human-induced and natural disturbance	3
1.2 Approaches to modelling forest dynamics.....	4
1.2.1 Patch, gap and individual-based spatially explicit models.....	4
1.2.2 The Perfect Plasticity Approximation: reducing model complexity	6
1.2.3 Physiology-based gap models.....	7
1.2.4 Metabolic scaling theory: scaling from individual metabolism and biomechanics to whole-forest dynamics.....	7
1.3 Specifying models of forest processes	9
1.3.1 Growth	9
1.3.2 Allometry	10
1.3.3 Mortality	10
1.3.4 Recruitment.....	11
1.4 Parameterisation and model selection.....	12
1.4.1 Frequentist approaches to parameterisation	12
1.4.2 Philosophical problems of frequentist hypothesis testing.....	13
1.4.3 Frequentist likelihood-based approaches to parameterisation	14
1.4.4 Bayesian inference	14
1.4.5 Parameterisation without sufficient data.....	17
1.4.6 Models selection: methods for testing ecological hypotheses	18
1.4.7 Bayesian methods for forest dynamics modelling	20

2	Influences of forest structure, climate and species composition on tree mortality across the Eastern US	23
2.1	Introduction.....	23
2.2	Materials and methods	25
2.2.1	Forest Inventory data	25
2.2.2	Environmental data	26
2.2.3	Model description	27
2.2.4	Parameter estimation.....	28
2.2.5	Model selection.....	29
2.2.6	Parameter significance	31
2.2.7	Interpretation of the results	31
2.3	Results.....	33
2.3.1	Model selection.....	33
2.3.2	Species-mortality relationships.....	34
2.3.3	Size-mortality relationship.....	34
2.3.4	Environment-mortality relationships	36
2.3.5	Geographical variation in mortality	37
2.4	Discussion.....	38
2.4.1	Size and stand structure.....	38
2.4.2	Within vs across species variation in mortality along climatic gradients	40
2.4.3	Species-mortality responses to changing climate	42
2.4.4	Limitations	42
2.4.5	Conclusion	43
3	A brief introduction to Spanish forests.....	45
3.1	Introduction.....	45
3.2	Climate, topography and tree species distributions.....	47
3.3	Adaptation to drought	49
3.4	Adaptation to forests fires.....	50
3.5	Land use change, threatened species and climate change.....	51

3.6	The Spanish Forest Inventory	52
4	Predictable changes in aboveground allometry of trees along gradients of temperature, aridity and competition	53
4.1	Introduction.....	54
4.2	Materials and Methods.....	56
4.2.1	Inventory data and climate variables.....	56
4.2.2	Species-level wood traits and critical buckling heights	57
4.2.3	Statistical models	57
4.2.4	Interpreting the results	59
4.3	Results.....	59
4.3.1	Height and crown allometries varied among species and along environmental gradients	59
4.3.2	(H1) Tree heights were greater and crown diameters narrower in competitive neighbourhoods	61
4.3.3	(H2) The elastic similarity model provided an upper limit on height at a given DBH and trees in dense forests will grow to their critical height.....	61
4.3.4	(H3) Tree height and crown diameter for a given DBH was lower in areas of longer drought	62
4.3.5	(H4) Within-species height increased with temperature, but there was no trend in crown diameter	64
4.4	Discussion.....	65
4.4.1	Allometric scaling varies substantially with species.....	65
4.4.2	Asymmetric competition for light was a strong determinant of DBH-H allometry.....	67
4.4.3	Species were shorter in drought areas but individuals did not respond consistently	67
4.4.4	Within-species height increased with temperature, but across species the trend was the opposite.....	67
4.4.5	Within-species variation in allometry along climatic gradients is smaller than across-species differences.....	68
4.4.6	Sources of unexplained variation.....	69
4.4.7	Conclusions.....	69

5	Inferences from aggregated count data using Approximate Bayesian Computation: deriving juvenile recruitment rates from inventory data.....	71
5.1	Introduction.....	72
5.2	ABC Algorithms	74
5.3	Materials and Methods.....	76
5.3.1	Data.....	76
5.3.2	Prior information for growth and mortality rates.....	78
5.3.3	Simulation model	78
5.3.4	Assessing the algorithm on test data: method.....	79
5.3.5	Performance of the algorithm on test data and choice of metric.....	80
5.3.6	Implementation of the ABC-SMC algorithm on the inventory data.....	80
5.4	Results from inventory data	82
5.4.1	Convergence of the ABC-SMC algorithm.....	82
5.4.2	Average recruitment rates and the effect of canopy cover	82
5.4.3	Relationships between recruitment, growth and mortality.....	86
5.5	Discussion.....	87
5.5.1	Parameterisation and predicted recruitment rates	87
5.5.2	Other factors affecting Mediterranean juvenile recruitment	87
5.5.3	Implementation of ABC.....	88
5.5.4	Applications of ABC in Ecology	89
6	Regional successional dynamics simulated from tree-level processes.....	91
6.1	Introduction.....	91
6.2	Simulation model	93
6.2.1	Canopy area of taller trees, CAI_h , as a measure of competition.....	93
6.2.2	Demographic rates and allometric equations	94
6.2.3	Predictions of successional dominance.....	95
6.2.4	Simulation steps	96
6.2.5	Observed species dominance	97
6.3	Results.....	98

6.3.1	Models of growth and mortality.....	98
6.3.2	Observed and predicted pine dominance	99
6.3.3	Observed and predicted angiosperm dominance.....	104
6.4	Discussion.....	106
6.4.1	Growth and mortality rates varied with size, climate and competition.....	106
6.4.2	Early successional dominance was determined by both growth and mortality.....	107
6.4.3	Mismatches in pine dominance are likely due to lack of fire dynamics	107
6.4.4	Late successional dominance dynamics.....	108
6.4.5	Conclusions: climate-driven simulation models at a regional scale.....	108
7	Discussion	113
7.1	Tree size and competition as primary determinants of individual-level rates.....	113
7.2	Climate dependency of tree-level processes and inventory data.....	115
7.3	Limitations of the use of forest inventory data for simulation models	116
7.4	Concluding remarks	118
	Appendix A: Eastern US mortality	121
	Appendix B: Aboveground allometry	131
	Appendix C: ABC recruitment model	141
	Appendix D: Simulation model.....	157
	References.....	171

List of tables

Table 2.1	Species' predicted annual mortality rates.	34
Table 4.1	Wood, modulus of elasticity and number of samples used for allometric models for each species.	62
Table 5.1	Number of plots, shade tolerance and recruitment, growth and mortality rates in a fixed environment for each species.	81
Table 6.1	The 14 species modelled, their maximum observed DBH and the upper limit of drought length the species was simulated in.	97
Table A.1	Comparison of 36 models tested using AIC and BIC.	121
Table A.2	Fitted parameter values for each of the 21 common species.	122
Table B.1	Parameter values for species-level covariates of height-DBH relationships fitted using the hierarchical Gibbs sampler.	135
Table B.2	Parameter values for species' height-DBH scaling relationships.	136
Table B.3	Across-species correlations between predicted heights and crown widths and species' mean environment.	137
Table B.4	Priors and initial values for height-DBH and crown diameter-DBH model parameters used in MCMC model fitting.	137
Table C.1	Amount of data for each species used to parameterise the crown diameter model.	144
Table C.2	Comparison of crown diameter models tested with AIC scores for each model.	145
Table C.3	List of species in the dataset, number of plot each is found in and the crown diameter allometric equations used to calculate crown area for each species.	146
Table C.4	Comparison of stem growth rate models tested with AIC scores for each model.	149
Table C.5	Comparison of mortality rate models tested with AIC scores for each model.	149
Table C.6	Best-fit growth rate model parameter values and credible intervals.	150
Table C.7	Best-fit mortality rate model parameter values and credible intervals.	151
Table D.1	Details of the data used for each model for the 14 species included in the analysis.	161
Table D.2	Growth model comparison with functional forms and AIC values.	162
Table D.3	Mortality model comparison with functional forms and AIC values.	163
Table D.4	Parameter values for the best-fit growth model for each species.	164
Table D.5	Parameter values for the best-fit mortality model for each species.	165
Table D.6	Parameter values for the height-diameter allometric model for each species.	166

List of figures

Figure 1.1	The horizontal structure of a JABOWA-style patch model, a gap model, and a SORTIE-style individual-based model.	6
Figure 2.1	Observed and predicted mortality against stem size and environmental gradients.	36
Figure 2.2	Predicted changes in species' mortality rates with increases in temperature and precipitation.	39
Figure 2.3	Regional variation in mortality due to variation in each component of the model.	41
Figure 3.1	Maps of average annual temperature (°C) and annual precipitation rate (mm) in Spain in the period 1940-1996.	45
Figure 3.2	Distribution of the approximately 90,000 forest plots in the Second Spanish Forest Inventory (IFN2) representing the distribution of Spanish forests.	46
Figure 3.3	Forest species dominance across Spain.	48
Figure 4.1	Fitted parameters for each species' height-DBH scaling relationship.	60
Figure 4.2	Height-DBH data and fitted models for two common species (<i>Pinus halepensis</i> and <i>Quercus robur</i>).	63
Figure 4.3	Predicted changes in height along gradients of climate and competition.	64
Figure 4.4	Predicted changes in crown diameter along gradients of climate and competition.	66
Figure 5.1	Observed large juvenile count densities for each species.	77
Figure 5.2	Predicted growth and mortality rates used as priors for simulation model.	83
Figure 5.3	Estimated and true parameter values using simulated test data.	83
Figure 5.4	Fitted values and credible intervals for recruitment, growth and mortality parameters.	84
Figure 5.5	Predicted recruitment rates for each species against total plot canopy area.	85
Figure 5.6	Boxplots of differences between conifer and angiosperm recruitment rates and their responses to changes in plot canopy area.	86
Figure 6.1	Observed 95% climatic distribution of species in the inventory.	98
Figure 6.2	Predicted growth and mortality rates for each species along stem size and competitive gradients.	99
Figure 6.3	Observed climatic range of dominance of the six pine species.	101

Figure 6.4	Model predictions for climatic range of dominance of the six pine species.	102
Figure 6.5	Predicted dominance, growth, mortality and crown diameter for pine species along a temperature gradient.	103
Figure 6.6	Observed climatic range of dominance of the eight angiosperm species.	105
Figure 6.7	Model predictions for changes in climatic range of dominance of the eight angiosperm species simulated over 500 years.	109
Figure A.1	Observed and predicted mortality rates against maximum wind speed.	126
Figure A.2	Observed and predicted mortality rates against soil type.	126
Figure A.3	Observed and predicted mortality rates against plot basal area.	127
Figure A.4	Observed versus predicted plot-averaged mortality rates.	127
Figure A.5	Patterns of mortality due to regional variation in stand structure and environmental conditions alone.	128
Figure A.6	Regional patterns of differences between observed and predicted mortality rates.	129
Figure B.1	Height-diameter data, fitted allometric relationship and critical buckling height.	138
Figure B.2	Predicted changes in height along gradients of climate and competition with species names.	139
Figure B.3	Predicted changes in crown diameter along gradients of climate and competition with species names.	140
Figure C.1	Observed and predicted crown diameters for each species.	152
Figure C.2	Observed and predicted diameters for each species at the second time step.	154
Figure C.3	Observed and predicted mortality rates for each species.	155
Figure D.1	Predicted and observed tree growth rates for each species along size, competition and climatic gradients.	161
Figure D.2	Predicted and observed tree mortality rates for each species along size, competition and climatic gradients.	162
Figure D.3	Predicted and observed tree height for each species along size, competition and climatic gradients.	163
Figure D.4	Climatic distribution of predicted tallest pine species after 30 years of simulation.	164

1 Introduction

Simulation models form a vital part of ecological research, allowing for the exploration of systems at larger geographic scales and over longer time frames than is possible through field measurements or experimentation alone. This thesis aims to develop methods for parameterising a forest simulation model from inventory data collected on a regional scale. No previous forest simulations have explicitly modelled multiple processes for multiple species as a function of environment, but without these factors long-term predictions of forest dynamics in the face of climate change and disturbance cannot be made.

Many forest simulation models have been developed from data collected in small, intensively studied areas of forest comprising of a handful of species. This is predominantly for two reasons: firstly, many forest models have large numbers of parameters, for which many measurements must be taken (e.g. the detailed light environment measurements in SORTIE, Pacala et al. 1996)- data which are not available for large numbers of species and sites (Lichstein et al., 2010). Secondly, computational limitations have prevented detailed models being simulated at regional or global scales (Moorcroft et al., 2001; Purves and Pacala, 2008).

Long-term forest inventory data, which are becoming increasingly available in many parts of the world, provide valuable information that may be used to parameterise forest models for many species and across wide environmental gradients (Didion et al., 2009). Moreover, careful examination of the detail required to reproduce observed forest dynamics (e.g. Deutschman et al. 1999), and new simplified forest models, e.g. PPA (Purves et al., 2008), mean that simulation models may now be developed on regional scales and rigorously parameterised for large numbers of species, and can incorporate climatic and environmental dependency in their demographic functions. Combined with increased computational power and more sophisticated algorithms, these advances mean that more detailed models than ever before can be parameterised, and simulations run in greater detail and over wider areas.

In this chapter I explain the motivations for modelling forest processes at large scales in terms of the importance of better understanding the effects of climate change and human and natural disturbance on biodiversity, species composition, succession, productivity and carbon storage. I also describe some approaches and methods used to construct and parameterise models, and in particular I discuss the appropriateness and effectiveness of different statistical approaches in terms of ecological models.

1.1 Motivation for modelling forest dynamics

Simulation models are particularly important for making predictions in forest ecology research, since processes of interest often happen at substantially longer time scales than the average research project (or even career) and predictions are often made over decades or centuries. As I discuss in this section, questions about the effect of management practices, long term disturbance events and climate change on forest structure and productivity, biodiversity, carbon storage, species composition and succession must therefore be interrogated by carefully building models that capture the observed behaviour of a forest system, and by running simulation experiments.

1.1.1 *Forests in models of global vegetation*

Forests store more carbon than is held in the atmosphere (Millenium Ecosystems Assessment, 2005), but ecologically realistic models of their dynamics are not currently included in global vegetation models (Purves and Pacala, 2008). The response of forests to changing climate and atmospheric CO₂ levels, as well as their role in mitigating the effects of human-induced greenhouse gases through feedbacks to the atmosphere, is a large source of uncertainty in current vegetation models and therefore the global climate models (GCMs) coupled to them (Purves and Pacala, 2008; Sitch et al., 2008; Lapola et al., 2009; Fisher et al., 2010; Galbraith et al., 2010). Globally, forests are currently thought to act as a significant sink for carbon dioxide (Pan et al., 2011), but it is not known for how long they will continue to act in this way (Lewis, 2006; Hyvönen et al., 2007). Empirical studies in many parts of the world have shown forests accumulating carbon (per unit area). In temperate regions this is attributed to regeneration following land abandonment (Caspersen et al., 2000) and the fertilizing effects of nitrogen deposition from human activities (Thomas et al., 2010), whilst in old-growth tropical forests it may be a result of increased productivity under increased atmospheric CO₂ levels (Lewis, 2006; Phillips et al., 2008). However, some studies of coupled vegetation-atmosphere models predict large scale dieback of forests due to climate change, such as increased drought in Amazonia (e.g. Cox et al. 2004). Moreover, some forest-climate feedbacks have been shown to amplify the impact of human-induced greenhouse gas emissions on global temperatures: in boreal regions increased forest productivity and cover in coniferous forests is thought to accelerate global warming as the associated reduction in winter surface albedo (compared with snow on unforested land) causes temperature to increase (Bonan, 2008).

Dynamic global vegetation models (DGVMs) include many simplifying assumptions about forest dynamics which strongly influence the predictions they make (Sitch et al., 2008; Fisher et al., 2010). Species are grouped together and assigned parameter values according to plant functional types (PFTs) (Prentice et al., 2007). For trees, these groupings may be extremely simplistic (e.g. broadleaf and needleleaf in TRIFFID, Cox 2001) or may differentiate both between tree types (e.g. deciduous or

evergreen, broadleaf or needleleaf) and climatic region (tropical, temperate, boreal) (e.g. ORCHIDEE, Krinner et al., 2005). However, within DGVMs there is little consensus on which PFT classification is sufficient and the approach has been criticised for a number of reasons, such as ignoring important species' differences that drive vegetation composition (Quillet et al., 2010). Species within PFTs are modelled as having the same *effect* on ecosystem functioning and showing the same *response* to environmental factors such as climate stressors (McMahon et al., 2011), but in many instances this is unlikely to be true (Lavorel et al., 2007).

A mismatch in the level of detail modelled for different forest processes in many DGVMs makes them unsatisfactory for making long-term predictions. Forest growth, represented as carbon assimilation, is described in great detail using photosynthesis, stomatal conductance and respiration models which, in the most detailed DGVMs, are applied in half-hour steps. Other processes are not represented in anything like such detail: seeding establishment is modelled uniformly in each grid cell for climatically appropriate PFTs, and tree mortality is described as a function of carbon balance and simple disturbance events (Sitch et al., 2008), despite the fact that these processes are key components of the terrestrial carbon cycle and have been shown to be sensitive to climate change (e.g. Camarero and Gutiérrez, 2007; van Mantgem and Stephenson, 2007). Moreover, DGVMs assume no limit on rates of migration of species or PFTs in response to climate (Prentice et al., 2007), yet timescales of species migration are likely to be highly variable within PFTs (Neilson et al., 2005) and for many lowland areas species migration is unlikely to be fast enough to keep up with changing climate (Loarie et al., 2009).

1.1.2 *Models of the effects of human-induced and natural disturbance*

Simulation models are vital tools for addressing questions on the impact that management and disturbance have on forests. Stand models have long been used in the forestry sector to calculate growth rates and yields (Changhui, 2000a), and are usually parameterised with site-specific data to make predictions for commercial timber production over large areas (Liu and Ashton, 1995). Changes in forest management practices in many parts of the world, from monospecific even-age plantations to multi-age multi-species stands, have increased the role of detailed ecologically-structured forest models that simulate the effects of management strategies on a wider set of forest goods and management objectives (Wolfslehner and Seidl, 2010). For example, simulation models have been used to assess the effects of forest management strategies on ecosystem structure and function (Changhui, 2000b), biodiversity and carbon stocks (Hynynen et al., 2005; Taylor et al., 2008; Swanson, 2009), nutrient reserves (Blanco et al., 2005) and forest structure (Newton et al., 2011), and to assess the need for different management practices under climate change scenarios (Linder, 2000; Garcia-Gonzalo et al., 2008). Simulations may also be used to predict the long-term impact of human activity on forest structure, for example the impact of land use on species diversity in a tropical forest

(Teixeira et al., 2009; Uriarte et al., 2009), or the regrowth of temperate forests after land abandonment (Evans and Kelley, 2008).

Simulation models are particularly valuable when predicting the effects of natural disturbance events at landscape scales, such as hurricanes, storms, forest fires and diseases, because such events are typically highly infrequent but have extreme impacts. Models of the relationship between wind and fire events and vegetation have revealed impacts on species composition and stand biomass (Hickler et al., 2004), size structure (Liedloff and Cook, 2007; Uriarte et al., 2009) and net primary productivity (Keane et al., 1996). Simulations also allow predictions to be made about the effects of changes in disturbance occurrence rates, for example the effect of large-scale disturbance on forest carbon flux (Coomes et al., 2012), the effect of climate change-induced changes to fire frequency on carbon storage (Thornley and Cannell, 2004), pest and disease outbreaks (Bergot et al., 2004; Kurz et al., 2008), and interactions between different disturbances and management practices (He and Mladenoff, 1999; Mitchell et al., 2009; James et al., 2010).

1.2 Approaches to modelling forest dynamics

The many different structures of forest simulation models reflect both their diverse purposes and the data available with which to parameterise them. Models may have as their smallest component an individual tree or a small patch of forest, and may be spatially explicit (recording the exact location of each tree in relation to all others) or implicit (assuming a uniform horizontal structure within each component of the model). Models which omit the individual variation of each tree have been found to have significant limitations in terms of predictive ability (Grimm and Railsback, 2005). Spatial structure is fundamental to understanding community structure (Crawley, 1997), so whole stand models require many simplifying and unrealistic assumptions that are unnecessary in individual-based models and can only approximate a few aspects of forest dynamics (Huston et al., 1988; Vanclay, 1995). In this section I summarise the different types of forest dynamics models according to their structure, smallest unit of interest, assumptions and applications.

1.2.1 Patch, gap and individual-based spatially explicit models

Patch models simulate forest dynamics as a mosaic or composite of small patches of forest, with a patch (the smallest spatially referenced unit) usually corresponding to the size of either one or a small number of mature individual trees (Shugart and Smith, 1996; Bugmann, 2001). The aim of patch models is often to simulate and therefore better understand changes in species composition and succession in relation to environmental conditions (Grimm and Railsback, 2005).

Patch models may be subdivided into two categories (Gratzer et al., 2004): those which model the transitions of vegetation types between patches (cellular automata/state-transition models) but omit within-patch dynamics, and those which model the dynamics of individual trees within a simulated patch (e.g. JABOWA, Botkin et al., 1972, FORET, Shugart & West 1977). Cellular automata/state-transition models are structured on regular lattices or arrays and the state of each cell is followed over time, with the transition of a given cell between states determined by a transition rule and some local interaction with a defined neighbourhood of other cells (Karafyllidis and Thanailakis, 1997; Balzter et al., 1998). Such state transition models have been used to describe succession (Kessell and Potter, 1980) and dispersal dynamics (Green, 1989), the impact of disturbances such as fire (Karafyllidis and Thanailakis, 1997), and land-use change (Soares-Filho et al., 2002).

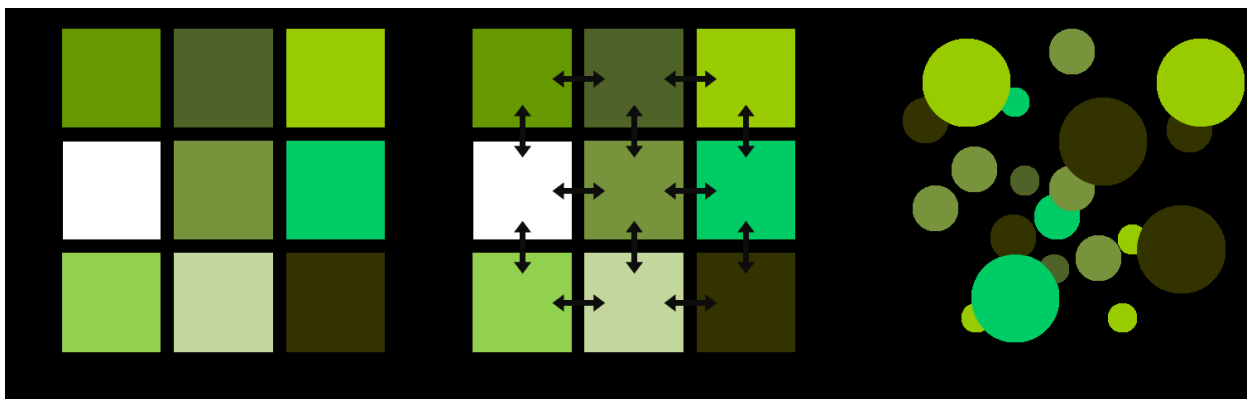
Patch (gap) models based on individual trees follow birth, growth and death processes as functions of abiotic and biotic environmental variables such as available light, crowding, temperature and evapotranspiration, but only consider vertical spatial structure and assume horizontal homogeneity within a patch. Patch size is set to correspond with the size of a very large tree (100m² in JABOWA), and leaves are located at the top of each tree in a thin layer. This means that the light environment of each patch is controlled by the largest tree and ‘gaps’ are opened up in a patch when the large trees die, leading to successional dynamics governed by interspecific competition for light. Growth (usually calculated annually) is strongly determined by the light available, and mortality is often negatively dependent on growth. Patches within a forest are modelled as having different successional statuses, but early forms of gap models assumed, for computational reasons, no interaction between patches, and therefore ignored important processes such as dispersal and shading between patches (Bugmann et al., 1996, Fig 1.1a).

Later gap models relaxed the assumption of no interactions between patches and model the forest landscape as a mosaic of interconnected patches (e.g. ZELIG, Urban, 1990, Fig. 1.1b), meaning that trees in a given cell may be shaded by those in neighbouring cells as well as within their own (Urban et al., 1991). Patch interactions also allow the inclusion of long-range dispersal, thereby improving the representation of understory dynamics, and allow studies of the impact of large herbivores which move between patches (e.g. FORGRA, Jorritsma et al., 1999). The realism of gap models has also been improved by removing the assumption of ‘flat top’ leaf arrangement, which resulted in strong asymmetry of competition for light and the largest trees having a very large advantage over all smaller ones (Leemans, 1991), and instead modelling vertical canopy structure through individual tree crown depths, which allows shading within crowns (e.g. FORSKA, Leemans and Prentice, 1989).

Individual-based spatially explicit models also simulate the recruitment, growth, allometry and mortality of individuals in a plot, but record the specific location of each tree (Fig. 1.1c). These models typically involve detailed calculation of the effect of competition on the light available to each stem using three-dimensional calculations of crown geometry (e.g. SORTIE, Pacala et al. 1993), and

therefore require detailed field measurements for parameterisation. Since they model each stem individually, these models allow gaps of any size to be created (rather than fixing patch size), and are therefore better able to reproduce successional dynamics (Pacala and Deutschman, 1995). However, such a high level of detail may not be required to accurately reproduce forest dynamics in all cases (Busing and Maily, 2004; Strigul et al., 2008), and modelling small patches on the scale of a few trees instead of individual stems may be sufficient for predicting forest dynamics (Deutschman et al., 1999).

Figure 1.1 The horizontal structure of a) a simple JABOWA-style patch/gap model with non-interacting patches of forest, b) a patch/gap model with interactions between patches, for example through shading or seed dispersal, and c) a SORTIE-style individual-based spatially-explicit model.



1.2.2 The Perfect Plasticity Approximation: reducing model complexity

The high number of parameters and correspondingly detailed field data needed to parameterise spatially explicit individual-based models such as SORTIE reduces their practicality for simulating forest dynamics at large scales or in novel locations. The Perfect Plasticity Approximation (PPA) model (Purves et al., 2007, 2008) is a cohort-based canopy competition model that models individual tree processes but treats all stems within a cohort as the same. By considering height-structured competition for light as the most important process governing forest dynamics, and assuming that the canopy of a forest is space filling and plastic in its response to gaps, the need for the light environment of individual trees to be calculated is removed. This assumption not only dramatically reduces the computational effort required to run simulations (compared to spatially-explicit models such as SORTIE), but also reduces the number of parameters required, making the model able to be parameterised from standard inventory data collected over thousands of sites. For example, two parameters for each species are required for modelling each of growth and mortality rates – one describing the rates of understory trees and one for those in the canopy. A more recent adaptation of the PPA framework has relaxed the ‘in or out’ of canopy assumption by predicting growth and mortality as a function of individual tree size and the projected area of crowns taller than the tree

(Bohman and Pacala, 2011; Caspersen et al., 2011; Coomes et al., 2012). This gives a more continuous definition of asymmetric competition for light than simple canopy/understory status classification, and has been used to gain insight into how individual growth and mortality rates determine stand productivity. However, this framework requires the continuous competition-dependency of demographic processes to be specified.

1.2.3 *Physiology-based gap models*

Physiology-based gap models seek to link ecosystem structure with physiological processes at the tree level such as photosynthesis, respiration and water and nutrient use, which are modelled on timescales of a day or even less (e.g. HYBRID, Friend et al., 1993). These models respond to changes in atmospheric CO₂ and climate, and therefore contain the detail necessary to predict the response of both individual tree processes such as growth, seed production and phenology, and whole-forest characteristics such as succession and carbon storage (e.g. van der Meer et al., 2002). Physiology-based models have also been used to examine the effects of fires on ecosystem characteristics such as net primary productivity and nutrient cycling (Keane et al., 1996), and to predict productivity in managed stands (e.g. PROMOD, Sands et al., 2000). Because of the level of detail included, physiology-based models typically require very large numbers of parameters whose values are poorly known and often constrained only for special cases (Mohren and Burkhardt, 1994; Mäkelä et al., 2000), and despite the inclusion of physiological processes which respond to the environment, models formulated for one region may not perform well in other climates (e.g. seasonal drought in the Mediterranean, Morales et al., 2005).

1.2.4 *Metabolic scaling theory: scaling from individual metabolism and biomechanics to whole-forest dynamics*

Metabolic scaling theory (West et al., 1997, 1999, 2009; Enquist et al., 1999, 2009; Enquist and Niklas, 2002) makes a variety of predictions about individual tree and whole-forest properties based on assumptions about individual metabolic rates. The theory assumes that resources are used efficiently and are distributed through the tree (or organism in general) through an optimal, self-similar, hierarchical, volume-filling vascular branching network, through which hydraulic resistance is minimised. These assumptions lead to the fundamental scaling relationship that leaf mass, and hence whole-plant photosynthetic (metabolic) rate, scales as a 3/4 power of body mass. This, along with the specified relationship between mass (M) and stem diameter (D), $M \propto D^{8/3}$, leads to a set of predictions about individual tree allometry and function. Metabolic scaling theory predicts that tree height (H) scales with D as $H \propto D^{2/3}$, that diameter growth rate, (dD/dt) scales with D as $dD/dt \propto D^{1/3}$, and that individual mortality is solely derived from competitive thinning and scales with $D^{-2/3}$ (Enquist et al., 2009). The theory predicts that the exponents in these power-law relationships are invariant

with body size and that differences between species may be accounted for with differences in the coefficients of the power function (Enquist et al., 1999). The appeal of such a model as a framework for individual-based models is therefore strong, because only the coefficient need be determined for each of these three processes and each species, thereby reducing the amount of data required to parameterise the models.

The theory is scaled up to whole-forest dynamics by assuming no recruitment limitation, that resource use and supply are equal, birth and death rates are equal and that stems' allometry and demographic rates are as defined above, allowing predictions such as stand size distribution, canopy structure and resource use (West et al., 2009). The effects of disturbance on succession and temporal dynamics are also predicted, but there are discrepancies between model predictions and data. In particular mismatches are caused by the simplifying assumptions that there is no recruitment limitation and that mortality is solely size dependent and caused by competitive thinning (Enquist et al., 2009).

Metabolic scaling theory has proved contentious for several reasons. The theory has been found to be effective in explaining body size from metabolism across very large scale differences in body size, but within a ten-fold difference in size, the theory explains only 20 per cent of variation in body size, and even less in more similar-sized organisms (Tilman et al., 2004). Whilst the theory may therefore be useful in examining entire ecosystems, for example in terms of resource use, it has much more limited applicability within communities with similar-sized members, such as forests. The theory ignores the effect on growth of asymmetric competition between plants of different sizes and the effects of gap-creating disturbances within a forest (Coomes et al., 2003), for example increases in crown area in trees next to a gap to take advantage of extra light available. The use of invariant fixed scaling laws for describing forest structure and dynamics has therefore been questioned by many using comparison with data (e.g. Muller-Landau et al. 2006a, 2006b, Russo et al. 2007, N avar 2009). The very fact that the predictions of the metabolic theory are independent of species, competition (in particular asymmetric competition for light), forest location and tree age conflicts specifically with studies which have found relationships between these and allometry (Canham et al., 1994; Niklas, 1995; Mencuccini, 2002; Chen and Li, 2003), growth (Li et al., 2005; Reich et al., 2006; Coomes and Allen, 2009) and mortality (Muller-Landau, Condit, Chave, et al., 2006). In this way the wisdom of ignoring the variability in experimental data and forcing species to share certain invariant traits has been questioned (Agutter and Wheatley, 2004).

1.3 Specifying models of forest processes

Forest simulation models such as SORTIE and PPA typically contain a set of submodels that describe individual growth and mortality, aboveground allometry and recruitment or regeneration, and a representation of the effects of competition on these processes. Functional forms for these processes and methods to parameterise them from data vary, and choice depends on considerations such as the forest type of interest and the purpose of the model. The choice of functional form for a model is highly dependent on the purpose of the model or the hypotheses to be tested. For example, if species diversity and succession are of interest then species-specific parameters to describe species' interactions are required, but in tropical forest communities this is likely to be impossible due to the very large number of species, so species may be grouped by functional type (e.g. Vanclay, 1989).

The earliest forest dynamics models used simple functional forms with no climatic dependency of processes, and may be appropriate for simple models, for example of plantation productivity, whereas large-scale long-term models which address questions of climate change require submodels to be responsive to climatic changes. The choice of predictors and functional forms is therefore critical to a model being sufficient for purpose and will impact the model's transferability to other ecosystems and climatic conditions. Climatic, competitive, resource and disturbance dependencies will be highly dependent on the forest system of interest, so data exploration should always be an important part of model building. Although competition for light is often considered the most important limitation in closed-canopy forests, other factors such as drought, nutrient limitations and belowground competition (e.g. root competition for nutrients, Platt et al., 2004) may be more important in other ecosystems, which must be taken into consideration when re-parameterising any model for a region for which it was not built. In this section I discuss some approaches to determining appropriate models for four major forest processes: growth, canopy development, mortality and recruitment.

1.3.1 Growth

Models of tree growth abound in ecological and forestry literature, and are frequently parameterised using diameter increment data collected over two or more time steps from permanent plots. Differences in species' growth rates are important for succession (Huston and Smith, 1987), and may be related to species' traits such as wood density (Poorter et al., 2010) and xylem hydraulic traits (Russo et al., 2010). Models frequently include the effect of competition for light, a key limitation to tree growth (e.g. Canham et al., 1994, 2004; Pacala et al., 1996; King et al., 2005; Wyckoff and Clark, 2005). Competition for, or limitations of, other resources such as water (Karin, 1996) and soil nutrients (Coomes and Grubb, 1998), has also been found to be a key driver of growth in many regions. The climate dependency of growth, with effects of temperature and altitude (Coomes and

Allen, 2007a), evapotranspiration (Wickramasinghe, 1988) and drought (Martínez-Vilalta et al., 2011), has also been well documented. These effects are often included as scalars to an hypothesised ‘maximum’ growth rate, although a more mechanistic, physiology-based approach has been taken for the effects of some factors on photosynthesis and respiration (e.g. temperature, Bonan and Sirois, 1992).

1.3.2 *Allometry*

Models of aboveground allometry define relationships between stem diameter and tree height, crown width and crown depth. The shape a tree takes within its environment determines the amount of light its leaves are able to intercept, which is an important driver of individual tree growth, mortality and fecundity, and therefore of whole forest structure (Kohyama, 1991; Pacala et al., 1996; Purves et al., 2007). Whole canopy structure determines understory light conditions, knowledge of which allows prediction of which species' saplings will grow and survive to the reach the canopy and form the next generation of adult trees (Horn, 1971). Accurate prediction of tree and crown shape through allometric relationships from diameter is therefore vital for accurate simulation models, which have been shown to be sensitive to allometric scaling (e.g. ALLOCATE, Tilman 1988; SORTIE, Pacala et al. 1996; PPA, Purves et al. 2008).

Aboveground allometry has been found to be affected by competition, because trees grow taller to capture more light and restrict their crown width in densely pack stands (Henry and Aarssen, 1999; Bragg, 2001; Muth and Bazzaz, 2003; Weiner, 2004) , and by temperature, because long and severe frosts can cause embolism and branch loss (Lemoine et al., 1999; Wang et al., 2006). Most field-parameterised allometric relationships have been defined for small samples in single locations, and surprisingly little is known about how scaling relationships vary within and among species along environmental gradients at regional scales (Wang et al., 2006; Méndez-Alonzo et al., 2008), although my work in Chapter Four has shown that such variation can be very pronounced.

1.3.3 *Mortality*

Models of individual tree mortality are less developed than those for growth and allometry. Approaches to simulating stem loss commonly stress the role of suppression of smaller stems beneath the forest canopy by linking a higher probability of mortality with lower growth (e.g. FORMIX, Bossel and Krieger 1991; SORTIE, Pacala et al. 1993) and the effects of large-scale natural disturbances such as fire and windthrow (e.g. FORSKA, Prentice et al. 1993). One reason why mortality models are not as common as those for growth and allometry is that mortality is a rare, discrete event that requires long-term, large-scale monitoring in order to pick up both quantifiable continuous patterns in mortality along environmental gradients and the effects of rare large-scale disturbance events (e.g. hurricanes and earthquakes).

Mortality has been found to vary along gradients of precipitation and temperature (Voelker et al., 2008; van Mantgem et al., 2009), and my work in Chapter Two shows that both average rates and variation along gradients may be highly species-specific. U-shaped, size-dependent mortality appears to be a common and quantifiable feature of forests (Buchman et al., 1983; Monserud and Sterba, 1999; Umeki, 2002; Coomes and Allen, 2007b; Chao et al., 2008) and one that I have found from examining mortality in the eastern United States (Chapter Two). This pattern is likely to be a result of high mortality in small suppressed trees, low mortality in canopy trees, and an increase in mortality in larger and older trees due to senescence and/or increased exposure to disturbances, although the relative importance of these processes may depend on stand age (Coomes and Allen, 2007b). Small trees do not, however, always suffer from the presence of adults; in Mediterranean conditions where water is limited and desiccation risk from direct sunlight is high, and in areas with high wind speed, the survival of small trees may be higher in the presence of adults (Taylor and MacLean, 2007; Gómez-Aparicio et al., 2008).

1.3.4 Recruitment

Since juvenile recruitment and dynamics are crucial determinants of forest community dynamics (Shibata and Nakashizuka, 1995; Kobe, 1996), accurate representation of dispersal and recruitment limitation is vital to produce realistic simulations of succession and spatial dynamics (Ribbens et al., 1994). Models of recruitment vary in their treatment of seedling dispersal and recruitment, with the simplest ones assuming that seed is always available for regeneration (Clark et al., 1998) and many combining dispersal and establishment together in one process (Busing and Mailly, 2004). On the other hand, spatially-explicit individual-based forest simulation models typically model recruitment using a seed dispersal kernel, where seedlings establish in a location with probability related to the distance to conspecific adults, and the number of seedlings established per adult varies with species, adult size and shading from adult trees (e.g. Busing, 1991; SORTIE, Pacala et al. 1996; TROLL, Chave, 1999). The spatially implicit PPA simulates recruitment as a function of adult canopy tree density (Purves et al., 2008) with species-specific functions. Long-distance dispersal mechanisms are generally ignored in models of forest dynamics, but are likely to be important for determining shifts in species' distributions with rapid climate change (Hampe, 2011). Permanent-plot datasets such as national inventories rarely contain detailed information on recruitment rates, but approximate juvenile densities are sometimes recorded and in Chapter Five I parameterise a model of recruitment rates using such data.

The presence and density of conspecific adults is a well-recognised determinant of seedling recruitment, but many other factors may affect seedling dynamics. For example, small scale spatial heterogeneity and microsite quality are important for seedling establishment (Nathan and Muller-Landau, 2000), although such effects are difficult to measure and quantify. Canopy gaps and competition from understory shrubs (Beckage et al., 2000), soil moisture and drought (Lloret et al.,

2004; Urbietta et al., 2008; Mendoza et al., 2009), facilitation through protection from water stress and direct sunlight by 'nurse' plants (Lookingbill and Zavala, 2000; Smit et al., 2008; Plieninger et al., 2010), and fire frequency (Lloret et al., 2003) have all been found to affect seedling recruitment, yet there are few models describing continuous changes in recruitment rates along climatic or competitive gradients.

1.4 Parameterisation and model selection

In this section I discuss the different statistical methods commonly used to select and parameterise ecological models from data. I discuss classical frequentist methods (e.g. null-hypothesis least-squares regression) and frequentist likelihood methods (e.g. simulated annealing), and compare them with Bayesian inference to demonstrate why Bayesian methods may often be a better approach for forest models. Frequentist and Bayesian methods differ fundamentally in their treatment of models and data. Frequentist methods assume parameter values (the underlying model) to be fixed and consider all datasets which those parameters could generate, whereas Bayesian methods assume the data to be fixed and consider all parameter values that could have led to them.

I also compare frequentist and Bayesian methods of model selection, and present the reasons why I consider Bayesian methods to be the more natural approach for comparing ecological hypotheses posed using competing models, as they can calculate the probability of each hypothesis being true when given the available data.

1.4.1 *Frequentist approaches to parameterisation*

The most commonly used method for parameterising ecological models of continuous processes is undoubtedly frequentist least-squares linear regression, typically using an ordinary least squares (OLS) optimisation. Its appeal lies in the simplicity with which OLS predicts a response Y from a single variable X and states whether a relationship is significant. However, underlying this approach are assumptions that are inappropriate for many ecological situations. For example, fitting a linear model between only two variables assumes a fixed linear relationship that, as the predictor variable increases, the dependent variable will also increase proportionally. Extrapolation of such relationships beyond the range of the data is likely to give unrealistic predictions in many ecological problems, since few processes are controlled only by one variable and multiple limitations act in different conditions (Bloom et al., 1985) - for example, water availability may dominate variation in growth rates in deserts and light fluxes in rainforest understories. Such considerations may not be important in many small-scale studies but ought to be taken into account when translating a model from one location to another. These issues may be resolved by employing multivariate and generalised (for

example polynomial or logistic) regression techniques. Regression in its classical frequentist form also makes strict assumptions about the normality of the data and the error. The assumption that the error distribution is homogeneous regardless of the value of X may well not be valid for many situations (e.g. increased variance in height with stem diameter, Chapter Four). In addition, if systematic variation in the error structure is present, methods which account for this should be used, such as weighted least squares or an appropriate transformation. Another assumption of standard regression is that there is no error in the independent variable X , which is unrealistic in many ecological applications where measurement error is likely in both variables. Reduced major axis line fitting (RMA – also known as standardised major axis line fitting, SMA) has become commonly used in ecology because, unlike OLS, it assumes error in X as well as Y (which is often true of biological measurements), although it fails to address the distinction between measurement/sampling error and equation error ("natural variation" or "intrinsic scatter", Warton et al., 2006). A key difference between OLS and RMA is that RMA is a symmetric method (it produces the same line of best fit regardless of which variable is the predictor and which the response) whereas OLS regression is asymmetric. The choice of one or the other may therefore depend on not only the measurement error but on consideration of whether the aim is finding the relationship between two variables or predicting one from the other (Warton et al., 2006).

1.4.2 Philosophical problems of frequentist hypothesis testing

There are some drawbacks of classical regression that cannot be addressed using related frequentist methods. For example, when parameterising a model using frequentist methods, parameter values are assumed to be fixed, with no underlying variation, which may be unrealistic for ecological processes. This is a consequence of the frequentist philosophy of statistics, which assumes that parameters are fixed and that data is drawn randomly from some underlying population distribution. Therefore, when a p-value is calculated for a linear regression (typically for the null hypothesis of the slope equalling zero), it represents the probability of obtaining, on repeating the experiment, the observed data or data more extreme given that the model is true (the model being the null hypothesis of no relationship). Similarly, a 95% confidence interval in frequentist analysis does not represent the range over which there is a 95% probability that the parameter value lies; rather it is the range over which, if the *same* experiment was repeated a very large number of times, the regression parameter estimate would fall within 95% of the time (Gelman et al., 2004). By testing against null-hypotheses of 'no effect', frequentist statistics assume no knowledge or relevant information about a system such as previous experiments or observations. This is an inefficient use of data, since it means that tests are carried out to disprove null-hypotheses that may have been falsified before.

1.4.3 Frequentist likelihood-based approaches to parameterisation

Well-recognised drawbacks and limitations of classical null-hypothesis frequentist approaches have led to increased interest and uptake of frequentist likelihood-based approaches to model parameterisation. These methods provide increased flexibility for parameterisation, and more useful and intuitive methods for model comparison (see below), because instead of testing a null and alternative hypothesis and reporting a significance, likelihood methods compare different models and select the best (defined by comparing the support given to each model by the data).

Suppose we wish to parameterise a model M which depends on parameters θ to describe the relationship between variables X and Y . Likelihood-based methods differ in their approach to hypotheses from classical frequentist-based ones (such as OLS) because they select parameter values by maximising the probability of the model given the data, $P(M(\theta, X)|Y)$, and by calculating and maximising the *likelihood* (L) of the data given the model (although in practice to ease computation, methods often minimise the log-likelihood, which is equivalent):

$$L(Y|M(\theta, X)) \propto P(M(\theta, X)|Y) \quad (\text{Eqn 1.1})$$

Thus, likelihood-based methods rely on the specification of the likelihood of a model and apply an iterative optimisation strategy (such as simulated annealing) to search for the set of parameters θ that maximise the likelihood (called the maximum likelihood estimators, MLEs). As the number of iterations of the optimisation increases, the MLEs converge to the true parameter values, and the sampling distribution of the MLEs is asymptotically normal for all parameters (Gatti, 2005), so confidence intervals can easily be calculated if parameter distributions are specified. However, these are frequentist confidence intervals so suffer from the misconceptions discussed earlier (see above), and likelihood methods still treat parameters as being fixed in the underlying model. Likelihood-based methods also allow for evaluation of covariance between parameters through examination of the Hessian matrix (the inverse of which approximates the variance-covariance matrix), which can be used to derive the multidimensional curvature of the log-likelihood parameter surface. Likelihood methods are substantially more computationally demanding than classical regression methods, and can be time inefficient if the likelihood space has multiple local maxima.

1.4.4 Bayesian inference

Bayesian methods are fundamentally different from frequentist methods, both classical and likelihood-based (as described above), and both philosophically and practically, in ways that make them attractive to ecologists trying to solve real-world problems (e.g. Dennis 1996; Hilborn & Mangel 1997; Ellison 2004; Hobbs & Hilborn 2006; Kruschke 2010a,b). Bayes' rule is the only statistical method for quantifying the probability of competing hypotheses being true given available data (Hobbs and Hilborn, 2006). During optimisation, frequentist methods iterate across parameter values to find the MLEs, whereas Bayesian methods integrate the likelihood of all possible values of each parameter, given all others.

Although Bayesian methods have led to some controversy, it is not Bayes' theorem itself that is in doubt, even for the most ardent frequentist, but merely how it is interpreted and applied in parameter estimation methods. Bayes' theorem states that, for a given model M which depends on parameters θ and data X to describe data Y , then:

$$P(M(\theta, X)|Y) = \frac{P(Y|M(\theta, X))P(M(\theta, X))}{P(Y)} \quad (\text{Eqn 1.2a})$$

assuming fixed data Y , this leads to the *unnormalised posterior density*:

$$P(M(\theta, X)|Y) \propto P(Y|M(\theta, X))P(M(\theta, X)) \quad (\text{Eqn 1.2b})$$

which is more frequently written simply as:

$$P(\theta|Y) \propto P(Y|\theta)P(\theta) \quad (\text{Eqn 1.2c})$$

In Bayesian terminology, the term $P(\theta|Y)$ is called the *joint posterior probability distribution*, and gives the distribution of parameter values that best fit the data, which is the distribution of interest but which in many cases cannot be directly sampled from. The term $P(Y|M(\theta, X))$ or simply $P(Y|\theta)$, when regarded for fixed Y and variable θ , is the *likelihood* function, and $P(\theta)$ is the *prior* of model M dependent on parameters θ (often denoted $\pi(M(\theta))$ or simply $\pi(\theta)$).

For multiple parameter models, Bayesian methods seek the *marginal* posterior distribution for each parameter conditioned on all others. Thus, for a model with two parameters, equation 1.2c takes a slightly different form (Gelman et al., 2004):

$$P(\theta_1, \theta_2|Y) \propto P(Y|\theta_1, \theta_2)P(\theta_1, \theta_2) \quad (\text{Eqn 1.3a})$$

Finding the conditional posterior distribution given the data for a single parameter, say θ_1 , requires integrating over all other parameters:

$$P(\theta_1|Y) = \int P(\theta_1, \theta_2|Y)d\theta_2 \Rightarrow P(\theta_1|Y) = \int P(\theta_1|\theta_2, Y)P(\theta_2|Y)d\theta_2 \quad (\text{Eqn 1.3b})$$

It is rare to be able to directly sample from the right hand side of equation 1.3b (e.g. using the Gibbs sampler, see below) because this requires the prior distributions of all parameters to be conjugate – that is, of the same family – so numerical integration techniques are often required (e.g. MCMC sampler, see below).

Monte Carlo simulation algorithms such as the Gibbs sampler and the Metropolis-Hastings algorithm are extremely useful tools for parameterisation. These methods work by taking a random walk through parameter space to estimate the conditional posterior distribution $P(\theta|Y)$. In a multiparameter model, parameters are not sampled from the full conditional distribution, but rather individual parameters are chosen and sampled from the conditional distribution given all other parameters, $P(\theta_1|\theta_2, \dots, \theta_N, Y)$, so-called *alternative conditional sampling*. Sampling then continues for many iterations until the Markov chain has converged to the joint posterior of all parameters. When the prior distributions of the parameters are *conjugate* (that is, the conditional distribution $P(\theta_1|\theta_2, \dots, \theta_N, Y)$ is known and can be directly sampled from) this is done directly using the Gibbs sampler. If $P(\theta_1|\theta_2, \dots, \theta_N, Y)$ is not known then a rejection method such as the Metropolis or Metropolis-Hastings algorithm may be used.

The Metropolis algorithm works as follows. At each step in a random-walk, a parameter is selected and a new value θ^* drawn from some pre-defined distribution. The likelihood of the new parameter set is calculated and compared with the likelihood of the previous parameter set θ (the likelihood ratio). Then the new parameter set is accepted with probability equal to the ratio of the posterior distributions (the posterior odds):

$$\text{Accept } \theta \text{ with Probability} = \min\left(1, \frac{P(\theta^*|Y)}{P(\theta|Y)}\right) = \min\left(1, \frac{P(\theta^*)P(Y|\theta^*)/P(Y)}{P(\theta)P(Y|\theta)/P(Y)}\right) = \min\left(1, \frac{P(Y|\theta^*)}{P(Y|\theta)} \frac{P(\theta^*)}{P(\theta)}\right)$$

(Eqn 1.4)

That is, the posterior odds are equal to the prior odds multiplied by the likelihood ratio (Gelman et al., 2004) and in practice the right hand side of equation 1.4 is calculated during optimisation.

Such Bayesian methods not only sample parameter values that are better according to the likelihood than the previous sample (as frequentist likelihood methods do), but they also accept some parameter sets with lower likelihood if the likelihood is close, thereby sampling (asymptotically) directly from the posterior distribution of parameter values. By sampling directly from the posterior, Bayesian methods provide intervals of belief for parameter values that differ from the frequentist confidence interval: a Bayesian 95% credible interval is exactly the interval within which it is believed (given the data) that there is 95% probability that the true value of the parameter lies. Some Markov chain methods require individual parameter distributions to be specified (e.g. Gibbs sampling, a method which allows the posterior distribution to be sampled from directly), but others do not, which can be an advantage when there is no particular reason to choose a certain distribution.

When fitting multiple parameter models using environmental predictors, Bayesian methods provide a substantial advantage for ecologists, because such variables are often partially correlated (e.g. denser forests are often found in wetter places). This means that the parameters associated with their effects are also likely to be partially correlated (Kruschke, 2010a), whereas frequentist-fitted confidence intervals can be misleading because such methods are unable to account for high levels of correlation among estimated parameters (Straume and Johnson, 2010). Bayesian methods provide an easy solution to such a problem because, instead of providing an estimate of the mean and variance of each parameter separately from all others, they provide parameter estimates in sets, each dependent on the other (estimating one parameter requires integrating across all others). These joint parameter estimates, drawn from the joint distribution of the model parameters, may therefore be used to make model predictions in a way that robustly accounts for correlation within a dataset (and can be used in a straightforward way for future research). In Chapters Two and Four, I demonstrate how MCMC methods allow the parameterisation of models with partially correlated variables (such as drought length and annual precipitation) on forest processes, and how the posterior distribution samples produced by the MCMC runs easily allow for the effect of one variable to be examined whilst controlling for variation in all others. Although frequentist approaches such as generalised linear modelling do allow the variance and covariance of parameters to be estimated, the approach is less

intuitive and flexible, and requires specification of parameter distributions, which are not easily well chosen.

The use of priors, representing prior belief in a parameter set or model, is often cited as an argument against Bayesian methods, since priors imply prior belief, which is subjective, and therefore Bayesian methods cannot be objective statistical tests. There are two main arguments as to why this is not a good reason to reject Bayesian methods. Firstly, with all but very small amounts of data, the strength of the prior can easily be set to be weak (or ‘uninformative’) so that information from the data far outweighs the prior's influence on the final estimated parameter values (Kruschke, 2010a), and the influence of prior strength on parameter estimation may easily be examined (e.g. Dietze, et al. 2008). Secondly, prior beliefs may be highly logical in nature, for example the height of a particular species of tree should be positive and less than 50m. Intelligent use of priors can get the most out of scarce data when there is good knowledge of a system from previous experiments. For example, in forest dynamics, good data on processes for rare species may be extremely difficult to collect, but through hierarchical modelling, strength can be ‘borrowed’ from other species to constrain processes in order to take sensible parameter values via constraint through priors (see below for further discussion). In addition, there is nothing inherently Bayesian about using prior information, and within a frequentist likelihood framework knowledge may be accumulated from one experiment to another (Hobbs and Hilborn, 2006).

1.4.5 Parameterisation without sufficient data

There are many times when parameterisation of particular ecological models may be difficult due to insufficient data to constrain the desired model. Parameterising species-specific models can pose difficulties when species are rare and there is not enough data to constrain models for each individually. Hierarchical Bayesian modelling (HBM) provides a solution to this problem by fitting both individual species' models and a 'universal' model relationship for all species together, essentially reducing the number of free parameters by constraining the models of less common species to be more similar to the population average (Gelfand et al., 1990; Gelman and Hill, 2007). Parameters for the ‘species-average’ model may simply be fitted as averages of all species or they may be fitted as functions of species’ traits, therefore allowing for systematic variation in the average model, where species with similar traits have more similar parameters. For example, Dietze et al., (2008) use HBM to construct both species-specific and an across-species allometric relationship based on species traits of shade tolerance and wood properties. This approach not only constrains the value of rare species’ parameters to be informed by those of more common ones with similar trait values, but also allows for future estimation of parameters for unobserved species based on these traits alone, and without having to collect field measurements. The advantages of the hierarchical approach have been recognised in many areas of ecology and HBM techniques have been used, for example, to model species’ distributions accounting for spatial random effects (Hooten et al., 2003), to estimate tropical tree

species' growth rates (Feeley et al., 2007) and to evaluate scaling models (Price et al., 2009; Coomes et al., 2011).

Maximum likelihood, MCMC and HBM methods all require the calculation of a likelihood – that is, the probability of the data given the model – but there are times when such a calculation is impossible or impractical, for example when the process we wish to model is either unobservable or too difficult or expensive to observe directly. Approximate Bayesian Computation (ABC) methods present a mathematically rigorous solution to such problems, because they may be used to fit models to data when the likelihood cannot be formulated or is computationally prohibitive to analyse (Tavaré et al., 1997; Pritchard et al., 1999; Tanaka et al., 2006; Sisson et al., 2007, 2009). ABC methods may be used to estimate parameters for models of fine-scale complex processes for which only coarse-scale aggregated data are available. Instead of comparing candidate parameter sets using likelihoods, ABC methods use simulation models to create simulated datasets, then summarise the simulated data and compare it with the real summarised data. These techniques typically take a truly Bayesian yet likelihood-free approach to parameterising models by incorporating both summary data and prior knowledge of unobserved processes to estimate parameter values. Over the last decade these likelihood-free ABC methods have increasingly been applied to data in areas such as epidemiology, for example to estimate disease transmission dynamics when only data on clusters of cases with identical genotypes are available (Tanaka et al., 2006), and population genetics (Foll et al., 2008), but have barely reached ecology (but see Jabot and Chave, 2009). In Chapter Five, I demonstrate the power of these methods to estimate annual recruitment rates using count data of small trees and carefully constructed priors to describe juvenile growth and mortality.

1.4.6 Models selection: methods for testing ecological hypotheses

All models are wrong, and models to describe simulate ecological and environmental processes make explicit assumptions that are known to be wrong, yet they are necessary to reduce the overwhelming level of complexity in the natural world. Questions in ecology often arise from a desire to find the best model to describe a process, and pose two or more competing models formulated to represent competing ecological hypotheses to be compared (Hobbs and Hilborn, 2006). Complex models with more parameters inevitably leads to better fits to training data, but overfitting can cause problems with covariance between parameters, and leads to overcomplicated model structures that are too difficult to analyse. Sensible model comparison and selection is therefore vital to ensure that patterns in processes are described in a way that is sufficient to capture the variation of interest, whilst taking care not to create models whose complexity makes them too difficult to understand.

Model selection in classical frequentist statistics is, in its most basic form, null hypothesis testing. Simple 'no effect' versus 'some effect' p-value significance tests do not provide much information about the best model structure when presented with a set of competing models. ANOVA and F-tests can be used to compare nested models, and to perform stepwise regression to construct the

best model by analysing the amount that residual variation changes with the inclusion (or exclusion) of explanatory variables. Maximising fit using adjusted R^2 or Mallows's C_p are both methods of selecting the best model fitted using OLS regression, which penalise models with higher numbers of parameters and can be used to compare non-nested models.

The likelihood ratio test (LRT) compares the likelihood of two competing nested models and selects the more complex one only when its likelihood is significantly greater according to a χ^2 statistic. It is the most commonly used null-hypothesis approach (Johnson and Omland, 2004) and, since it compares nested models, may be used with a stepwise selection approach to construct the best model. Stepwise algorithms are particularly important when there are a large number of models in the candidate set, because comparing all models may be impractical. However, the selected best model using such an approach may depend on the order in which the models were tested, and if not all possible models have been tested may therefore not be the best overall model.

LRTs are unsatisfactory for all but the simplest situations for a number of reasons. They can only be used for nested models and rely on the choice of significance level to accept or reject a model (Posada and Buckley, 2004), when in reality we are often interested in comparing competing non-nested models and wish to know not just which is the best model to represent the data, but also *how much better* it is. Some stepwise methods of LRTs are so sensitive that they may even result in different models being selected as the best depending on their initial configuration (Pol, 2004). Information criteria bypass these problems and provide much more flexible approaches to model comparison. The Akaike information criterion (AIC; Akaike, 1974) is the most common and is derived from the Kullback-Leibler information distance (K-L; Kullback and Leibler, 1951), which defines the distance between two models or the information lost when a poorer model is used to approximate a better one (Burnham and Anderson, 2002). K-L cannot be used directly because it relies on knowledge of the 'true' model, but AIC is an asymptotically unbiased estimator of the *expected* relative distance (the K-L distance). AIC is defined using the maximum likelihood ($L(Y|M_i(\hat{\theta}, X))$), where $\hat{\theta}$ are the maximum likelihood estimators) for model M_i with m_i parameters give as:

$$\text{AIC} = -2 \log(L(Y|M_i(\hat{\theta}, X))) + 2m_i \quad (\text{Eqn 1.5})$$

The term $-2\log(L(Y|M(\theta, X)))$ is sometimes called the *deviance*. AIC values for a set of models M_1, \dots, M_N are calculated and compared, and the model with the minimum AIC is chosen. It is important to know the relative support for each model tested in the data. Absolute AIC values have no meaning on their own, and it is the difference between the AIC for the best model and each of the others that is used to determine the relative support for each,

$$\Delta_i = \text{AIC}_i - \text{AIC}_{\text{MIN}} \quad (\text{Eqn 1.6})$$

Models with $\Delta_i < 2$ are judged to be as well supported as the best model, and those with $\Delta_i > 10$ have no support (Burnham and Anderson, 2004). AIC is difficult to apply for multilevel or hierarchical models, because the number of parameters is not well defined for these situations. Instead, the

deviance information criterion (DIC; Spiegelhalter et al., 2002) is used to perform model comparison for hierarchical models, and is calculated from posterior samples from an MCMC chain:

$$\text{DIC} = -2 \log(L(Y|M(\bar{\theta}, X))) + 2p_D \quad (\text{Eqn 1.7})$$

where $\bar{\theta}$ is the mean parameter value, the term $-2 \log(L(Y|M(\bar{\theta}, X)))$ represents the mean deviance and p_D is the effective number of parameters (calculated by comparing the mean of the deviances from the posterior chain and the mean deviance). DIC was constructed to be a generalised version of AIC, and in a non-hierarchical model DIC and AIC should be approximately the same (Wagenmakers and Farrell, 2004).

The Schwarz or Bayesian information criterion (BIC; Schwarz, 1978) is formulated in a similar way to AIC in that it also uses the likelihood and the number of parameters to compare different models, but BIC also considers the number of data points used and penalises models with more parameters more strongly (so it overfits less in comparison). For a model M_I with m_I parameters fitted to n data points, BIC is defined using the maximum likelihood $L(Y|M_I(\hat{\theta}, X))$ as:

$$\text{BIC} = -2 \log(L(Y|M_I(\hat{\theta}, X))) + m_I \log(n) \quad (\text{Eqn 1.8})$$

AIC and BIC can often be used in the same situation, but since both may be considered Bayesian and both may be derived from non-Bayesian approaches, selecting one over the other does not depend on being a Bayesian practitioner or not (Burnham and Anderson, 2004). There are conditions under which AIC will outperform BIC and visa versa, which can be demonstrated using simulated data with known model structure and parameter values (e.g. Acquah, 2010). BIC is likely to choose a simpler model than AIC, and unlike AIC is both consistent as sample size increases and accounts for parameter uncertainty (Wagenmakers and Farrell, 2004). However, the derivation of BIC assumes that the 'true' model is amongst the model set being tested (Burnham and Anderson, 2004), which may be unrealistic for ecological applications.

Both AIC and BIC can be used to produce weights for a set of models. Akaike weights are calculated for each model from the difference in its AIC value relative to the whole set, and can be interpreted as the probability of each model conditioned on the set, thereby giving insight into the relative confidence in the best model (Wagenmakers and Farrell, 2004). BIC weights are also calculated using the difference in BIC value for each model relative to the whole set, and can incorporate prior belief in each model (although commonly priors are set as equal for all models). They represent the posterior model probability; that is, the probability that each model is correct given the data, and therefore also show the level of confidence in the best model relative to the others.

1.4.7 Bayesian methods for forest dynamics modelling

Bayesian approaches provide a straightforward way of comparing competing hypotheses for the four processes typically included in forest dynamics models (growth, allometry, mortality and recruitment) described in section 1.3. For many forest types, the extent to which these processes are dependent on

stem size, climate and competitive environment, and the amount of variability between different species, is not well studied. Moreover, incomplete or insufficient inventory data and high species diversity means that defining such dependencies is not necessarily straightforward. In this thesis I present applications of Bayesian methods for model selection and parameterisation for these processes, using forest inventory data from two regions: the Eastern US and Spain. I fully parameterise models for all four processes for the major tree species in Spain, and demonstrate how these models may be incorporated into a model of whole-stand dynamics.

2 Influences of forest structure, climate and species composition on tree mortality across the Eastern US

Abstract

Few studies have quantified regional variation in tree mortality, or explored whether species compositional changes or within-species variation are responsible for regional patterns, despite the fact that mortality has direct effects on the dynamics of woody biomass, species composition, stand structure, wood production and forest response to climate change. Using Bayesian analysis of over 430,000 tree records from a large eastern US forest database we characterised tree mortality as a function of climate, soils, species and size (stem diameter). We found (1) mortality is U-shaped vs. stem diameter for all 21 species examined; (2) mortality is hump-shaped vs. plot basal area for most species; (3) geographical variation in mortality is substantial, and correlated with several environmental factors; and (4) individual species vary substantially from the combined average in the nature and magnitude of their mortality responses to environmental variation. Regional variation in mortality is therefore the product of variation in species composition combined with highly varied mortality-environment correlations within species. The results imply that variation in mortality is a crucial part of variation in the forest carbon cycle.

2.1 Introduction

An understanding of tree mortality is central to any predictive understanding of forest dynamics. The long-term dynamics of woody biomass are regulated by the difference between gains through individual growth and losses through mortality. This makes tree mortality a crucial determinant of the forest carbon cycle, the future of which is a major source of uncertainty in Earth System Model predictions of future climate (Sitch et al., 2008). Moreover, differences in mortality rates among species appear to be major determinants of ecological succession (Kobe et al., 1995; Purves et al., 2008), the geographical ranges of species (Loehle, 1998; Purves, 2009), stand structure (e.g. stem size distributions: Coomes et al. 2003; Muller-Landau et al. 2006), and responses of forests to climate change and disease (van Mantgem and Stephenson, 2007; Kurz et al., 2008). However, we currently

have little quantitative information about the nature, magnitude or causes of geographical variation in tree mortality.

The simplest approach to making predictions about mortality in a changing world would be to correlate stand-level mortality obtained from permanent plot data with climatic variables, and use these relationships to predict changes under future climate scenarios. The problem with this approach is that it neglects the effects of species, individual size and competition, factors that individually have been shown to strongly affect mortality at the scale of the individual tree, with potentially serious consequences for landscape-level predictions. In order to predict the impacts of changing climate on forest-level mortality, it is therefore important to isolate the effects of these factors because they are likely to show complex, semi-independent changes in the future. For example, in much of the temperate zone, many forest stands are successional and regenerating, undergoing directional change in species composition independent of any changes in the environment (Rhemtulla et al., 2009; McMahan et al., 2010). Additionally, species are unlikely to disperse rapidly enough to track their optimal climatic conditions under rapid anthropogenic climate change, leading to combinations of species composition and environment that do not occur currently (He et al., 1999; Morin and Thuiller, 2009). Tree-level mortality patterns can also be confounded by external actions: harvesting can create various novel combinations of basal area, size distributions and species composition (e.g. de Graaf et al., 1999; Villeda et al., 2006), and pests and pathogens are often highly species-specific (e.g. sudden oak death: Rizzo and Garbelotto, 2003; Lovett et al., 2006). To estimate the individual effects of each factor, it is necessary to study factors simultaneously in order to tease apart their individual effects, otherwise the apparent effect of one is likely to be confounded by the others (e.g. apparent differences in species' average mortality rates might reflect differences in the average environments occupied by those species: Caspersen and Kobe, 2001).

Here we use the Eastern USA Forest Inventory and Analysis (FIA) dataset to parameterise, for each of 21 common US tree species, a logistic regression model that assigns an annual probability of mortality to an individual tree given its size, species identity, competitive environment (plot basal area) and physical environment. We estimate the nature and relative magnitude of the different factors affecting tree mortality and parameterise a model that could be useful in predicting potential responses of US forest carbon stocks to climate change (e.g. Joyce, 1995). Here we report: (1) how each factor affects the mortality rate of individual trees; (2) whether, and how, species differ in their underlying mortality rates and responses to size, competition and the environment; and (3) differences in the environmental dependency of forest stand-level vs. species-level mortality, which determine the level of model complexity required to accurately predict forest mortality in a changing environment.

2.2 Materials and methods

2.2.1 Forest Inventory data

We used the pre-1999 USA Department of Agriculture Forest Inventory and Analysis (USDA FIA) dataset containing tree-level data for 182 species from a network of plots distributed across the Eastern USA (Smith, 2002). The data comes from forest inventory plots which were surveyed in the 1980s and again in the 1990s, although the interval between surveys differs between states between 1 and 21 years (93% of survey intervals were between 6 and 15 years). Surveys were taken using a two-phase sampling procedure known as double sampling for stratification. In the first phase random points were chosen on aerial photographs and classified by land cover and forest type, and in the second a random subsample of each class were selected and established as field plots. Five or more points were chosen within each plot, around which several sub-plots were established and sampled using variable radius sampling, whereby the effective subplot size differs according to tree size (for more details see Purves et al., 2004). Species, size (diameter breast height, DBH) and status (alive, dead from harvesting, dead from natural causes) were recorded for each tree sampled, along with plot basal area ($\text{m}^2 \text{ha}^{-1}$). The FIA survey was designed specifically to allow accurate estimates of average forest characteristics such as species composition and average tree size through scaling from the tree, through the stand, to the regional level (Smith, 2002; Purves et al., 2004).

Before analysis began, the dataset was filtered to include only those dead trees that we could be certain were not removed by human activity, and to remove various kinds of errors in the data (e.g. false mortality events corresponding to subplots that were measured in the first, but not the second, survey). The model was parameterised for 21 of the most common species, using 438,401 individual tree records in total, accounting for around 60% of all trees in the reduced dataset. Due to the high number of possible predictors being considered, only species with over 10,000 individuals in the data set were used for parameterising the model. Of these, two species (*Ulmus americana* and *Abies balsamea*) were known to have suffered severely from disease and pests during the survey period. Other species are likely also to suffer a variety of impacts from diseases which are part of the mortality patterns studied here. However, the disease impacts on *Ulmus americana* and *Abies balsamea* are known to be so severe, episodic, and localised, that in our opinion it was better to exclude both species from the analysis. Since these factors were not included as predictors of mortality in our model we did not include these species in the model fitting. We also did not consider the effects of other disturbances, both natural (e.g. fire and hurricanes) and human, on the observed mortality in the dataset. Such disturbances are likely to have had a marked effect on current species composition (Russell et al., 1993; Fuller et al., 1998; Bürgi et al., 2000) and demographic rates (Foster, 1988), but are likely to be complex and interacting and, combined with a lack of a detailed

land-use history, the quantification of such disturbances and evaluation of their effects may be unachievable in many areas (Motzkin et al., 1999).

2.2.2 *Environmental data*

Since little is known about the geographical variation in tree mortality we had little information to judge which climatic factors might correlate with mortality. However, there have been many studies linking growth with a wide variety of climatic variables; for example, solar radiation, (Rolland, 1993; Vaganov et al., 2009), precipitation and drought (Pacala et al., 1994; Hanson et al., 2001; Miao et al., 2009), temperature (Matala et al., 2005), severe frost (Liu and Muller, 1993) and wind speed (Kronfuss and Havranek, 1999). Since many studies link individual rates of mortality within a species as a function of growth (e.g. Kobe et al., 1995; Wyckoff and Clark, 2002; Muller-Landau, Condit, Chave, et al., 2006; Wunder et al., 2006) there is good reason to believe that mortality also varies with many different climatic variables. Our approach was therefore to assess which of these variables were most closely correlated with observed mortality patterns, rather than to attempt to generate hypotheses, in order to determine which were most important within our data.

We assigned environmental factors to each tree using two sources of environmental data, both available on a 0.5° x 0.5° degree. The first source was the CRU05 climatology product (Climatic Research Unit, University of East Anglia: New et al., 1999) which provides monthly averages for many climate variables including temperature, precipitation, radiation, frost frequency, vapour pressure, cloud cover and wind speed (monthly average refers to the average over the period 1961 – 1990). We took the mean of each climate variable rather than climate observed over the survey period associated with each tree (which differs from tree to tree). From the CRU05 data we calculated the additional metrics of minimum temperature, degree days and average warm season (as opposed to annual) precipitation. The second source of environmental data was the Vegetation/Ecosystem Modelling and Analysis Project (VEMAP) (Kittel et al., 1995), a multi-institutional project to develop a database of climate, soils and vegetation on a 0.5° latitude/longitude grid across the United States for use with ecosystem physiology models. From this source, we took only the data on US soil, which included over 20 different metrics including soil depth, and measures of soil texture. In addition the FIA provided data on soil texture for each inventory plot, divided into five classifications from xeric (normally low or deficient in available moisture), through mesic (normally moderate but adequate available moisture) to hydric (normally abundant or overabundant moisture all year) (FIA-DB, 2008). The classification of each FIA site into one of these five soil classes is intended to be independent of the climate (e.g. rainfall) at that site.

To avoid convergence problems during parameter estimation, we applied principal component analysis (PCA) to the 14 different environment variables (both from the VEMAP and CRU05 data) to remove highly correlated variables. Among highly correlated variables, the variable with the highest weighting in the principal components was retained and the rest discarded. This left four CRU05-

derived climatic variables (radiation, yearly precipitation, mean annual temperature and maximum wind speed) to be included as possible mortality predictors, plus one FIA soil texture classification associated with each tree. We normalised each factor (i.e. subtracted the mean value and divided by the standard deviation) to allow for a simple comparison between the magnitudes of effects of each of the factors. We also checked that plot basal area was not highly correlated with the remaining climate variables.

2.2.3 Model description

Tree mortality is a difficult property to estimate because unlike growth, it has only 2 possible outcomes from each re-measured tree (survived or died), and typical tree mortality rates are low (on the order of 0.1 to 2% year⁻¹), such that large sample sizes and / or long re-measurement periods are required. Moreover this dataset contained varying re-measurement intervals, meaning that a simple 'proportion dead' would not have been informative (Purves et al., 2008). We therefore chose to parameterise a model describing the annual probability of death for each individual tree i , $P(\text{mortality}, i)$. Since $P(\text{mortality}, i)$ must lie between 0 and 1, we used a logistic transformation

$$P(\text{mortality}, i) = 1 / (1 + \exp(-k_i)) \quad (\text{Eqn 2.1})$$

where k_i (which can vary from $\pm \infty$) is a function of the predictor variables.

We included different combinations of the predictor variables: DBH (continuous); soil type (discrete, ranging from 1-5); plot basal area (i.e. FIA inventory plot) (continuous); and environmental variables (all continuous) as follows:

$$k_i = \alpha + f_1 + f_2 + \dots \quad (\text{Eqn 2.2})$$

where α is a constant parameter, and f_1 is a function of the first predictor variable (e.g. DBH), f_2 is a function of the second (e.g. precipitation), and so on. Initial analysis indicated that the relationship between DBH and mortality was U-shaped, corresponding to high mortality in small trees, low mortality for medium sized trees (typically 25-40 cm) and increasing mortality in larger trees. To describe this relationship we tried several different model equations and found the best fit to the data using the following functional form

$$f_{\text{size}, i} = \beta_1(\text{dbh}) \exp(\beta_2 \text{dbh}) \quad (\text{Eqn 2.3})$$

where β_1 and β_2 are parameters. In keeping with the qualitative pattern visible in the initial assessment of the size-dependency of mortality, equation 2.3 allows the initial decrease in mortality vs. size for small trees to be steeper than the increase in mortality for size for larger trees whilst giving high flexibility to the shape of the response. For each environmental variable V (i.e. climate and soil measures) we considered two alternative functional forms:

$$f_{V, i} = \beta_V V_i \quad (\text{linear}) \quad (\text{Eqn 2.4})$$

$$f_{V, i} = \beta_V V_i + \gamma_V V_i^2 \quad (\text{non-linear}) \quad (\text{Eqn 2.5})$$

where V_i is the value of environmental variable V associated with tree i , and β and γ are parameters. We used the same functional forms to include the effects of plot basal area B ($\text{m}^2 \text{ha}^{-1}$):

$$f_{B,i} = \beta_V B_i \quad (\text{linear}) \quad (\text{Eqn 2.6})$$

$$f_{B,i} = \beta_B B_i + \gamma_B B_i^2 \quad (\text{non-linear}) \quad (\text{Eqn 2.7})$$

where B_i is the plot basal area B associated with tree i , and β and γ are parameters. Although we chose to use a quadratic functional form, we did not constrain the shape further so that, within a species' range, it could predict shallow or steep monotonic curves, as well as U-shaped (or hump-shaped) responses. Since we had no strong evidence for a particular across-species response for any of the environmental variables we felt that a quadratic functional form would be sufficiently complex to capture essential patterns without being too complex. Together, equations 2.1-2.7 allow for a very large possible number of models, with a wide variety of numbers of parameters, depending on which predictor variables are included, and depending on whether each variable is included using a linear or non-linear (quadratic) functional form. We allowed each parameter in any given model to be either species-specific (e.g. in equation 2.4 this would give us 21 separate β_V parameter values, one for each species, each of which is unaffected by data from other species) or global, that is, shared among species (e.g. in equation 2.4 there would be a single β_V value for all trees regardless of their species). To avoid having to fit all possible models, we used a selection procedure that compared models with major differences in their predictor variables (see *Model selection*, below).

2.2.4 Parameter estimation

We used Bayesian methods based on Metropolis-Hastings Markov Chain Monte Carlo sampling (Gelman et al., 2004) to estimate values and confidence intervals for each of the parameters in each model. These methods were chosen because they allow for simple, efficient estimation of parameters, including confidence intervals. However, we did not use informative priors, so the outcome of the analysis can be expected to be similar to the outcome of a Maximum Likelihood analysis using the same data and models. The first step of the analysis was to define, for a given candidate model M , the log-likelihood of the inventory data (referred to here as X), given a particular set of parameters (referred to here as $\underline{\theta}$) values for model M :

$$l(X | M, \underline{\theta}) = \sum_i \ln \begin{cases} [1 - P(\text{mortality}, i)]^{S_i} & \text{if tree } i \text{ survived} \\ 1 - [1 - P(\text{mortality}, i)]^{S_i} & \text{if tree } i \text{ died} \end{cases} \quad (\text{Eqn 2.8})$$

equation 2.8 represents a sum, over all trees i , of the logarithm of the probability of the observation for i (survived or died), given the model structure M and parameter set $\underline{\theta}$, where S_i is the survey interval (years) for tree i .

We used non-informative uniform priors on all parameters so the MCMC algorithm (see below) needed to refer to the log-likelihood only. However, for numerical reasons we imposed upper and lower limits on the allowable values of all parameters, i.e., a prior probability of 0 on parameter values outside of the allowable range. We set the allowable range much wider than the plausible values, and also checked the posterior distributions to make sure the tails of the posterior distributions were a long way from the edge of the allowable range.

The next step was to estimate values for the parameter set $\underline{\theta}$ in model M , given the definition of the log-likelihood (equation 2.8). We did this using an adaptive Metropolis MCMC algorithm (Gelman et al., 1999, 2004), which returns random samples from the posterior distribution of $\underline{\theta}$. At each iteration, a particular parameter p_k is chosen and altered by adding a random value from a normal distribution $N(0, v_k)$ where v_k is specified for each parameter. The likelihood of the data given the new parameter is calculated and the parameter change is 'accepted' based on the ratio of the new likelihood and the previous likelihood:

$$P(\text{acceptance of new parameter set } \tilde{\theta}) = \min \left[1, \frac{l(x|M, \tilde{\theta})}{l(x|M, \theta)} \right]$$

The variance v_k for each parameter was tuned during a 'burn-in' period to achieve an optimal parameter acceptance rate of 25% (Gelman et al., 2004) so the samples returned from the MCMC can be said to have efficiently sampled the posterior of each parameter.

We implemented the MCMC algorithm by initializing each parameter value at a random point close to the middle of the allowable range, allowing a suitable burn-in period (between 25,000 and 1,000,000 iterations) for the algorithm to reach quasi-equilibrium, then recording every 100th sample of $\underline{\theta}$ (to avoid auto-correlation) from a post burn-in period of between 50,000 and 250,000 iterations (the number required depended on the speed of model convergence and the number of parameters). This provided us with a set of between 500 and 2,500 samples of $\underline{\theta}$ for each model M that we parameterised. From these samples, we calculated the mean, and 95% confidence interval, of each parameter p within $\underline{\theta}$. For the best-fit model we re-ran the model four times with differing starting parameter values and found the results were unchanged.

2.2.5 Model selection

As metrics to compare alternative models, we calculated, for each model M that we parameterised, the Akaike Information Criterion (AIC; Akaike, 1974) and the Bayesian Information Criterion (BIC; Schwarz, 1978). Both criteria reward models for providing a better fit to the data, but penalise models according to the number of free parameters that they contain, thus allowing for model selection from sets of models that differ in model complexity. However, the AIC penalises complexity less strongly than the BIC, so it is useful to compare the two criteria. Simple likelihood-ratio based comparisons would not have been appropriate since the models were, in general, non-nested (Hilborn and Mangel,

1997). Both criteria require an estimate of the maximum likelihood, for which we used the maximum value of the log-likelihood encountered by the MCMC algorithm in the post burn-in period.

Given the high number of possible mortality predictors, the options of functional forms presented by equations 2.2-2.7 and the choice of species-specific or global for any parameter, there was a very large set of possible models M . We wished to select an appropriate best model from this set, but without having to examine every possible combination of possible predictors. To do this we used the procedure outlined in the next three paragraphs.

First, we established which of the possible predictor variables was the best single predictor of mortality by parameterising all possible mortality models featuring one predictor variable (referred to here as 1-d models). This set of models was still relatively large (28 different models), since the predictor variable in question could be included using a linear or non-linear function, and with species-specific or global parameters (see equations 2.4-2.6). We also tested some of the closely correlated alternative climate predictors in this way, but none gave a better fit than the set we had already chosen. Comparing the AIC and BIC values associated with each model allowed us to determine whether, considered in isolation, each predictor variable was best described using species-specific vs. global parameters, and a linear vs. non-linear functional form (see equations 2.4-2.6). This analysis suggested that all predictor variables were best described using non-linear, species-specific functional forms. Therefore we decided to retain, within the larger set of all possible models, only those models that included non-linear functional forms. Further, comparing the maximum likelihood of the different 1-d models allowed us to rank the predictor variables in descending order of importance (meaning importance considered in isolation). The rank was: size >> radiation > yearly precipitation > mean annual temperature > plot basal area > maximum wind speed > soil type. Since size (DBH) was by far the best single predictor of mortality, we decided at this point to discard, from the large set of all possible models, any models not including DBH as a predictor variable.

Second, we sought, within the remaining set of models, the best set of environmental variables to include in the model. Since radiation was the best single environmental predictor, we tested each additional environmental predictor to find the best two-predictor combination, using species-specific responses, giving a model of the form:

$$k = \alpha + \beta_1(\text{DBH})\exp(\beta_2(\text{DBH})) + \beta_3(\text{radiation}) + \beta_4(\text{radiation})^2 + \beta_5(\text{environment}) + \beta_6(\text{environment})^2$$

We found that adding in yearly precipitation gave the best fit. We repeated this procedure to find the best three and four parameter models, and finally checked that including all five predictors (radiation, yearly precipitation, mean annual temperature, maximum wind speed and soil type) gave a better fit than the other models, using AIC and BIC.

These steps gave us for types of predictor variable: the constant α (equation 2.2), DBH (equation 2.3), the set of five non-linear environmental effects (equation 2.5) and the non-linear competition effect (plot basal area: equation 2.7). To determine the final model form we generated a

set of models which allowed us to test whether each type of predictor should be species-specific or shared, and whether the extra model complexity added by including environmental and competition effects in the simple size model was justified by the improvement in fit. We tested models using every combination of species-specific or shared effects for each type of predictor, as well as every combination with or without environment and competition effects (36 models in total). The full list of different models tested are shown in Table A.1 (in Appendix A page 121), along with AIC and BIC scores. The score of the best model was a very large improvement on the next best, although it is worth noting that models without environmental effects performed significantly worse than those without plot basal area as a predictor.

2.2.6 Parameter significance

The majority (74%) of parameters' 95% posterior distributions did not include 0, indicating significant effects. None of the posterior distributions for the constant or size parameters (α_j , β_{1j} and β_{2j} in equation 2.4) included 0, while the least significant deviations from zero were seen for soil type and maximum wind speed parameters, and for the species *Liquidambar styraciflua*, *Thuja occidentalis* and *Nyssa sylvatica*. In principle many additional parameterisations could be used to eliminate some effects for some species (i.e. remove terms associated with species-parameters with posteriors including zero), but we considered that this extra computational effort could not be justified in terms of increased scientific understanding.

2.2.7 Interpretation of the results

In order to compare the different mortality rates predicted for each species we calculated a single 'baseline' mortality of each species as the predicted mortality of a tree of standard size growing in a standard environment (we used both the mean environment, taken over the study region, for all variables together with a 'mesic' soil texture; and the species' own median environment). We chose to use 20 cm as the standard stem diameter because it is approximately the size of a canopy tree in this region (Purves et al., 2008).

In order to visualise geographical patterns in observed mortality rates, we calculated a mortality rate for each plot ("plot-averaged mortality") by fitting a single-parameter logistic model to the data, and used the coordinates of each to create a regional mortality map. We visualised geographical patterns in predicted mortality rates by creating simulated datasets which were identical to the original dataset except that whether each tree died or not was determined using the model's posterior parameter values. We then used the simulated data to calculate a model-predicted mortality rate for each plot. For each tree i we calculated its annual mortality rate based on the model equation generated from the randomly chosen parameter set. From this we determined the probability it died, P_i , over the whole survey period, and then assigned it as dead with probability P_i and alive with probability $1 - P_i$ within the simulated dataset. We generated 100 simulated datasets in this way, using

different parameter sets randomly drawn from the joint posterior of the parameters, and combined their results using likelihood profile methods to predict a single model-predicted mortality rate for each plot. Using multiple randomly chosen samples from the joint posterior instead of simply the mean value of each parameter accounts for any co-variance in the parameters and the effect this would have on the predictions. By comparing the predicted and observed maps we were able to examine how well our predictions fitted the observed mortality and in which regions there were mismatches.

We also wanted to create maps showing how mortality varies regionally in response to variation in species identity, stand structure (stem size and plot basal area) and environmental conditions, whilst controlling for variation in the other factors. We devised an approach to do this, based on creating simulated datasets in various different ways which selectively removed variation in the predictors which were not of interest. For example, to analyse the mortality patterns arising from variation in stand structure, we generated new 100 simulated datasets in which the tree alive/dead column was predicted from our model by using size and plot basal area, but assuming all trees were *Acer rubrum* (the most common and wide-ranging species in the dataset) and every tree experienced the same environmental conditions (the region's average). Similarly, to analyse mortality patterns arising from species composition, we retained species information but assumed all trees had the same size (20 cm DBH), basal area (the average density) and environmental conditions (the region's average) when creating the dead/alive column of the simulated datasets. Finally, to analyse mortality patterns arising from variation in environmental conditions we retained environmental information but assumed all trees were *A. rubrum*, and had the same size (20 cm DBH) and were in plots of average density.

Our maps are an imperfect way to partition spatial variation but this method does allow us to partition variation in mortality due to each factor by selectively controlling for variation in the others. Had we chosen a different size of tree or a different set of environmental conditions, we would expect to have seen similar spatial variation in mortality rates but a different overall level of mortality. Since different species responded in different ways to changes in environment and stand structure, we also calculated variation in mortality due to these factors but using *Pinus taeda* (the most common gymnosperm species) instead of *A. rubrum*. However, this species has a much smaller range than *A. rubrum* so we only considered variation in mortality in the region in which the species is found.

We were also interested in seeing how mortality varied along the range of each predictor, both for all species together ("forest-averaged mortality") and for each individual species ("species-averaged mortality"). We generated estimates of how observed mortality varied along the range of each predictor by binning the raw data according to the predictor of interest into equal sized bins (i.e. each containing the same number of stems) and found the best single annual mortality rate for the whole bin in the same way as before, using a single parameter logistic model. We did this both for the raw data (for just the 21 species for which we parameterised the model) and for all the data (including

the rare species). In order to compare this to the model predictions for all species together (the forest-averaged mortality) we created 100 sets of simulated data as before (i.e. data of the same form as the original dataset but with alive/dead status based on our model predictions), ordered and binned these according to the variable of interest and calculated a single mortality rate for each bin, and a 95% confidence interval on this rate. Thus the forest-averaged mortality accounted for simultaneous changes in species composition and size structure across whichever gradient was being considered, and could be compared to the observed data.

Finally, for each species we were interested in how mortality varied with changes in the variable of interest alone, but since the predictors (size, environment and stand basal area) all covaried along each gradient we calculated the median conditions in which each of the species was found. For each model predictor we created 100 simulated datasets using parameter values randomly chosen from the joint parameter posterior distributions. In these datasets, each tree was given the median condition of its species (apart from the predictor of interest) and was assigned as dead or alive based on its predicted annual mortality rate. For example, in order to examine the sole effect of temperature change on mortality we re-assigned each tree the median size, precipitation, radiation, maximum wind speed, soil type and stand basal area in which its species was found in the original dataset, and kept only the temperature information for each individual tree and then created the 100 simulated datasets as before by selecting 100 parameter sets at random from the joint posterior. This gave us a spread of mortality vs. temperature functions for each species, where the spread represents parameter uncertainty (variation in parameters causing variation in probability of mortality) and sampling (random variation in whether lived or died given the probability of mortality). This allowed us to consider only the effect of temperature on that species mortality, whilst modelling the species in a reasonable environment.

2.3 Results

2.3.1 Model selection

Using AIC and BIC, we found that the 7 best performing models all included species-specific environment effects, even when other predictors were not species-specific, or when plot basal area was not included. Plot basal area was only found to be a worthwhile predictor if its effects were species specific but did not benefit the model if the effect was shared among species. Models with non species-specific constant or size effects performed well, but the model with all predictors included as species-specific performed substantially better than all the others, according to both AIC and BIC. Therefore in our final model the function k (equation 2.1) took the form:

$$\begin{aligned}
k_j = & \alpha_j + \beta_{1j}(\text{DBH})\exp(\beta_{2j}(\text{DBH})) + \beta_{3j}(\text{radiation}) + \beta_{4j}(\text{radiation})^2 + \beta_{5j}(\text{precipitation}) \\
& + \beta_{6j}(\text{precipitation})^2 + \beta_{7j}(\text{mean annual temp}) + \beta_{8j}(\text{mean annual temp})^2 \\
& + \beta_{9j}(\text{max wind speed}) + \beta_{10j}(\text{max wind speed})^2 + \beta_{11j}(\text{soil type}) + \beta_{12j}(\text{soil type})^2 \\
& + \beta_{13j}(\text{plot basal area}) + \beta_{14j}(\text{plot basal area})^2
\end{aligned} \tag{Eqn 2.9}$$

where j is the species and the α_j and β_j s were the parameters estimated (so a different function k_j was estimated for each species). The MLEs, Bayesian means and confidence intervals for the parameters for each species of the best fit model (equation 2.9) are given in Table A.2 (Appendix A page 122). The predicted trends in mortality were close to the observed patterns across all predictor variables included in the model (Fig. 2.1, A.1-A.3 in Appendix A pages 126-127) suggesting that the structure of the model was appropriate for capturing mortality patterns within these data.

2.3.2 Species-mortality relationships

Species showed very different baseline mortality rates, even when other effects were factored out (Table 2.1), and as a consequence plot-level mortality was found to be highly sensitive to species composition. To illustrate this point we compared species mortality rates calculated at the median environment of each individual species. These mortality rates differed widely: the highest, for *Populus tremuloides*, was 80 times larger for than for the lowest, *Quercus prinus* (Table 2.1). In addition to the differences in baseline mortality, species showed contrasting responses to environmental variation. For example, the model predicts substantial species differences in the direction and magnitude of responses to hypothetical increases in temperature and precipitation (Fig. 2.2).

2.3.3 Size-mortality relationship

The relationship between size (DBH) and mortality was U-shaped for all species (Fig. 2.1a: $p \ll 0.001$ for all species). The highest mortality rates were found for the smallest trees and the lowest rates for trees of 18-37 cm DBH. The rate at which mortality decreased with size in saplings and increased with size in larger trees varied considerably among species, from relatively flat (e.g. *Thuja occidentalis*) to dramatic (e.g. *Acer saccharum*). However, species with higher minimum mortality consistently showed both higher sapling mortality and higher mortality at larger stem sizes (Spearman's Rank Correlation $p < 0.05$ for both trends). Predicted forest-averaged mortality was U-shaped mortality vs. size (i.e. when all data were grouped together, the model applied to each individual and the total average mortality calculated). However, the upturn in forest-averaged mortality in large trees was less pronounced as larger size classes became increasingly dominated by species with low mortality rates.

Table 2.1 Predicted baseline annual mortality rate (deaths tree⁻¹ year⁻¹) calculated for each species in the mean environment of the dataset for 20 cm DBH trees, and at each species' median environmental conditions (that is the conditions at which the highest number of individuals within the dataset were found), using the best fit model. 95% confidence interval for the mortality rates are also given.

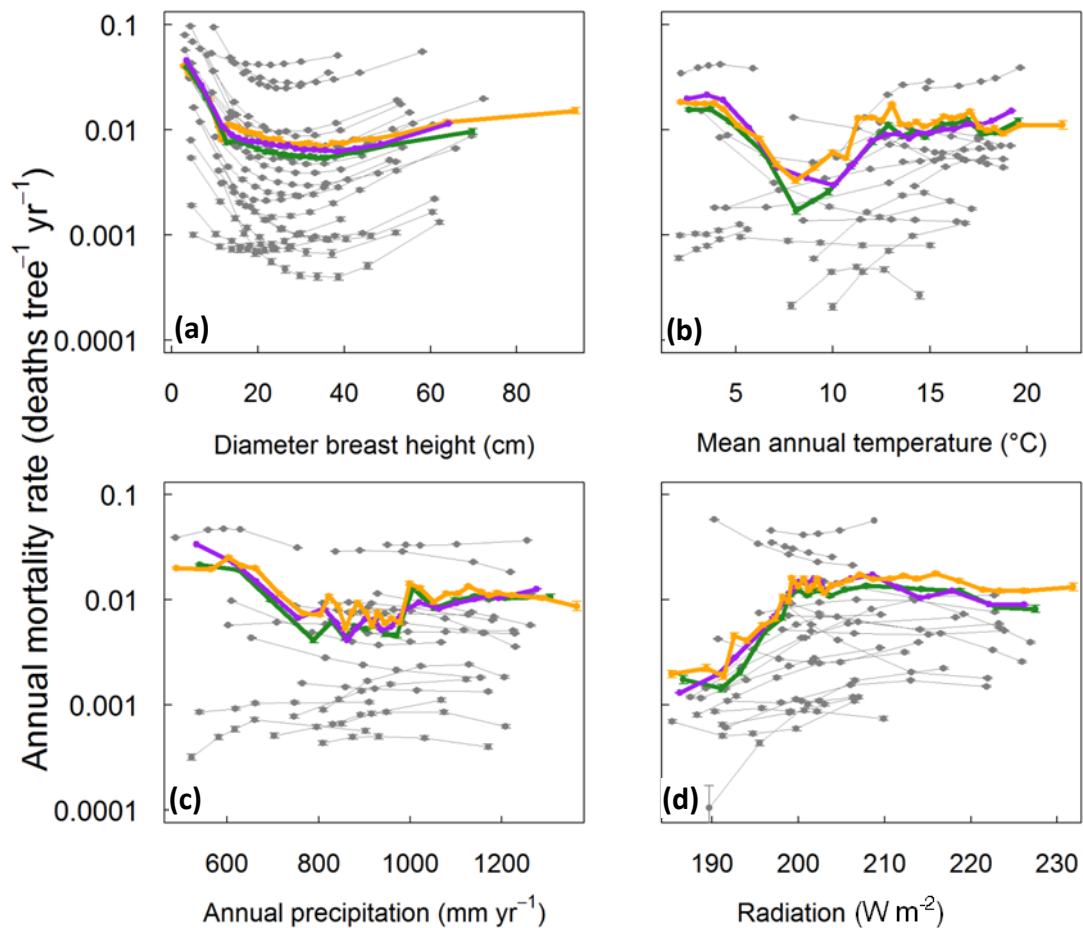
Species	Mortality in forest mean environment		Mortality in each species' median environment	
	Annual mortality rate	95% CI	Annual mortality rate	95% CI
<i>Acer rubrum</i>	0.0035	(0.0034, 0.0038)	0.0022	(0.0020,0.0023)
<i>Acer saccharum</i>	0.0108	(0.0104, 0.0112)	0.0052	(0.0049,0.0054)
<i>Betula papyrifera</i>	0.0012	(0.0010, 0.0014)	0.0009	(0.0008,0.0011)
<i>Carya spp</i>	0.0011	(0.0009, 0.0012)	0.0026	(0.0023,0.0028)
<i>Fagus grandifolia</i>	0.0020	(0.0018, 0.0022)	0.0017	(0.0014,0.0019)
<i>Fraxinus americana</i>	0.0016	(0.0014, 0.0018)	0.0008	(0.0007,0.0010)
<i>Liquidambar styraciflua</i>	0.0040	(0.0037, 0.0042)	0.0048	(0.0045,0.0052)
<i>Liriodendron tulipifera</i>	0.0005	(0.0004, 0.0006)	0.0009	(0.0008,0.0010)
<i>Nyssa sylvatica</i>	0.0180	(0.0170, 0.0187)	0.0323	(0.0311,0.0336)
<i>N. sylvatica (biflora)</i>	0.0044	(0.0040, 0.0049)	0.0098	(0.0090,0.0104)
<i>Populus tremuloides</i>	0.0017	(0.0015, 0.0018)	0.0407	(0.0399,0.0414)
<i>Quercus alba</i>	0.0016	(0.0015, 0.0017)	0.0013	(0.0012,0.0014)
<i>Quercus nigra</i>	0.0094	(0.0088, 0.0102)	0.0068	(0.0063,0.0074)
<i>Quercus prinus</i>	0.0004	(0.0003, 0.0005)	0.0005	(0.0004,0.0006)
<i>Quercus rubrum</i>	0.0062	(0.0059, 0.0064)	0.0035	(0.0033,0.0038)
<i>Quercus stellata</i>	0.0392	(0.0384, 0.0399)	0.0083	(0.0078,0.0088)
<i>Quercus velutina</i>	0.0114	(0.0110, 0.0119)	0.0072	(0.0068,0.0075)
<i>Pinus echinata</i>	0.0157	(0.0151, 0.0163)	0.0054	(0.0051,0.0057)
<i>Pinus taeda</i>	0.0020	(0.0018, 0.0022)	0.0054	(0.0052,0.0057)
<i>Pinus virginiana</i>	0.0047	(0.0042, 0.0052)	0.0282	(0.0271,0.0299)
<i>Thuja occidentalis</i>	0.0114	(0.0110, 0.0119)	0.0011	(0.0010,0.0013)

2.3.4 *Environment-mortality relationships*

Of the several environmental factors included in the model, temperature and precipitation are particularly important in this region because they are likely to change substantially, and perhaps rapidly, under anthropogenic climate change (IPCC, 2007). Forest-averaged mortality was U-shaped against annual mean temperature. The minimum mortality, which occurred at a temperature of around 8-10 °C, was 6-9 times lower than the rate at low or high temperatures (mean annual temperature <5 or >15 °C) (Fig. 2.1b). This observed pattern was robust to whether all species, or only the 21 common species, were considered (Fig. 2.1b, green and orange lines respectively), and was reproduced by our model (Fig. 2.1b, compare green and purple lines). This occurred despite the fact that the observed forest-averaged mortality pattern across the temperature gradient was not always reflected in the species-averaged responses of the particular species present at those temperatures. In the range 10-15 °C, both the forest-averaged mortality and the species-averaged mortality for the majority of the species increased with temperature (Fig. 2.1b, grey lines). However, forest-averaged mortality decreased with increasing temperature below 10 °C and increasing mortality with increasing temperature above 15 °C. In contrast, species-averaged mortality for the majority of species found in these temperature ranges showed the opposite trend. Analogous mismatches in the response of particular species vs. the forest average were also found for precipitation (Fig. 2.1c) and radiation (Fig. 2.1d).

Forest-averaged mortality rates decreased with increasing precipitation up to a threshold of around 800 mm yr⁻¹ and showed no clear trend thereafter (Fig. 2.1c), but individual species showed both increasing and decreasing mortality in the driest part of the range. At higher precipitation levels the forest-averaged mortality pattern was less clear, with some species showing increasing species-averaged mortality with higher precipitation (producing an overall U-shaped response to precipitation), and some a flat response. The opposite effect was found in the relationship between mortality and radiation, with a strong trend for increasing forest-averaged mortality up to a threshold point of about 200 W m⁻² (Fig. 2.1d), after which the response was much flatter. For most species we found that species-averaged mortality vs. basal area was hump-shaped ($p < 0.05$ for 16 of 21 species), with 50% of species showing maximum mortality in stands of 10-37 m² ha⁻¹ (Fig. A.3 in Appendix A page 127). The inclusion of less common species raised the observed forest-averaged mortality rate, but otherwise left the patterns unchanged (Fig. 2.1 and Fig. A.1-A.3 in Appendix A page 126-127).

Figure 2.1 Observed and predicted forest-averaged and species-averaged annual mortality rates (deaths $\text{tree}^{-1} \text{yr}^{-1}$, log scale) plotted against (a) DBH (cm), (b) mean annual temperature ($^{\circ}\text{C}$), (c) total annual precipitation (mm/year), and (d) solar radiation (W m^{-2}). Each panel shows the observed trends in mortality calculated using data from all species (orange) and from the 21 common species (green), and the predicted curves for 21 common species individually (grey) and together (purple). Individual species mortality rates are shown vs. changes in the predictor variable of interest alone, i.e. with all other predictor variables held at the median for that species. Error bars on the predictions (grey and purple) are 95% confidence intervals calculated from an error propagation procedure that accounted for parameter uncertainty. Error bars on the observations for the whole forest including rare species (orange) and 21 species combined (green) are 95% confidence intervals for mortality rates in the data (see Table A.2 in Appendix A page 122 for parameter values).



2.3.5 Geographical variation in mortality

The model reproduces most of the geographical patterns in plot-averaged mortality observed in the FIA dataset (compare Fig. 2.3d and Fig. 2.3e) with a high correlation seen between observed and predicted mortality in plots with more than 10 stems (Fig. A.4 in Appendix A page 127: $r^2 = 0.89$). Since the model reproduced geographical variation well, we were able to decompose the variation into

the separate effects of stand structure (stem-size distributions and plot basal area), environment and species (Fig. 2.3a-c). According to this decomposition, variation in species composition and environmental conditions were much more important than variation in stand structure in determining geographical patterns in plot-averaged variation in mortality. High observed plot-averaged mortality in the southeast is reproduced by considering only the environmental conditions of the region, but not when only stand structure or species composition are considered (Fig. 2.3c). In particular, several species common in the southeast (e.g. *Nyssa sylvatica*, *A. rubrum* and *Quercus nigra*) showed strongly increasing species-averaged mortality with the higher average temperatures, but this effect doesn't appear when only species composition is considered since temperatures in the region are much higher than these species' median environments. High plot-averaged mortality in the west is driven primarily by species composition (Fig. 2.3b); whilst variation in stand structure has relatively little impact on plot-averaged across the region (Fig. 2.3a). We checked whether our conclusions were dependent on our choice of species (i.e. *A. rubrum*) by creating the equivalent maps using the most common gymnosperm species, *P. taeda* (Fig. A.5 in Appendix A page 128). We again found that variation in environmental conditions resulted in higher variation in mortality than variation in stand structure.

However, not all variation predicted by the model was explained by a simple sum of the three components, indicating strong interactions between them. For example, both stand structure and species composition (Fig. 2.3a-b) predict higher plot-averaged mortality in the northeast than is predicted by the model or is observed (Fig. 2.3d-e), indicating an interaction with environmental conditions (Fig. 2.3c), which predict lower plot-averaged mortality in the area. The largest differences between model predictions and observations of plot-averaged mortality were all in plots with less than 100 stems. Differences were mostly due to underestimated plot-averaged mortality by the model, particularly in the furthest northwest and southeast of the region where many plots were dominated by species too rare across the whole region to be included in our analysis (see Fig. A.6 in Appendix A page 129).

2.4 Discussion

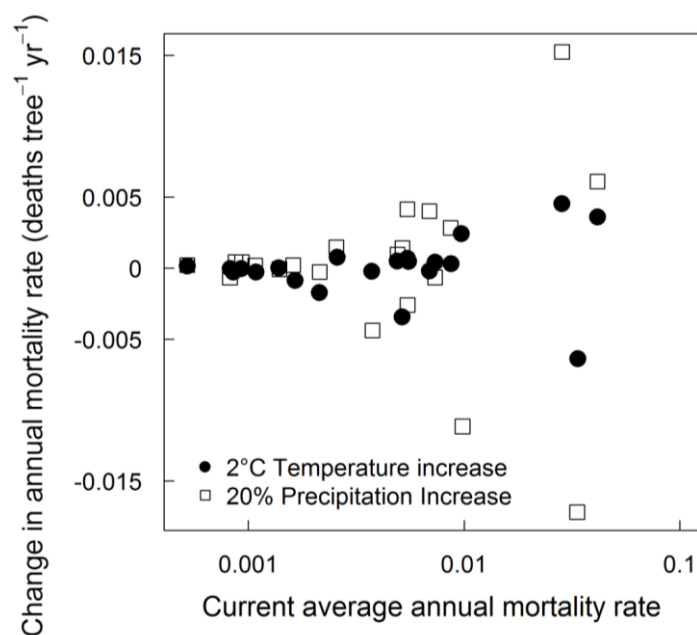
2.4.1 Size and stand structure

We found that size (DBH) was the single variable with the greatest effect on mortality rate at the level of the individual tree, with trees of intermediate size exhibiting mortality rates much lower than smaller, or larger, trees. This U-shaped relationship between size and mortality appears to be a common feature of forests, whether from sub-boreal (Umeki, 2002), temperate (Buchman et al., 1983; Monserud and Sterba, 1999; Coomes and Allen, 2007b) or tropical (Chao et al., 2008) regions. It

seems likely that this feature results from two opposing effects: (i) mortality is often high when trees are small because they are competitively inhibited by taller neighbours, but with higher light levels show an increase in growth rate and reduction in mortality (Kobe et al., 1995); and (ii) a general increase in mortality in larger individuals due to senescence and/or increased exposure to strong wind and other disturbance agents (Busing and Pauley, 1994; Yang et al., 2003; Coomes and Allen, 2007b). This explanation is supported by the fact that species exhibit their minimum mortality rates at around the size they enter the canopy (around 20 cm DBH, corresponding to a height of around 20 m for a typical Eastern US deciduous tree; Purves et al., 2008): once in the canopy, individuals are less affected by competition for light with neighbours. U-shaped mortality has potentially major implications for understanding forest structure and the forest carbon cycle, because larger trees contain a disproportionate fraction of above-ground woody biomass, such that any increase in their mortality has a large effect on carbon storage (Coomes et al., 2003).

However, despite size being the most important single predictor of mortality at the tree scale, variation in stand size structure had almost no effect on geographical variation in plot-averaged mortality (Fig. 2.3a). This may be simply because stand structure does not vary systematically across the region, otherwise geographical variation in size distributions would result in geographical variation in plot-averaged mortality. However, the precise way in which the dynamics of size distributions might interact with climate change and/or changes in tree harvesting to induce future changes in plot-averaged mortality remains largely unexplored.

Figure 2.2 Predicted changes in species' average annual mortality rate (calculated at each species' median size and environment) when subjected to a hypothetical 2°C temperature increase (●) and a 20% increase in annual precipitation (□), shown plotted against the current average mortality rate without this change.

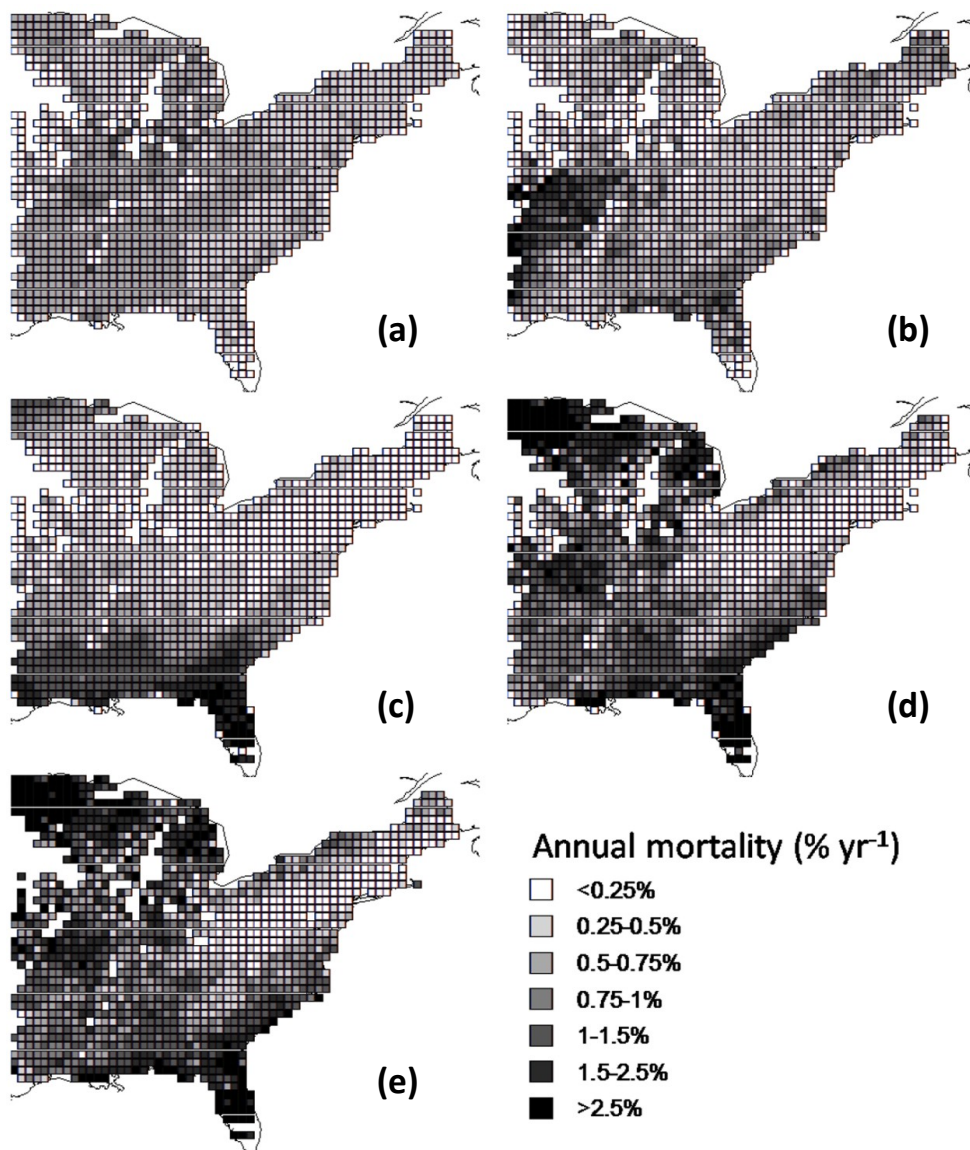


2.4.2 *Within vs across species variation in mortality along climatic gradients*

The mismatches we found between species-averaged and forest-averaged mortality-environment correlations imply that, under climate change, forest-averaged mortality will change in ways that cannot be anticipated by examining the current relationship between observed mortality and climate. Given that mortality is highly dependent on species identity, size and environmental factors, it is important to include all these factors in predictive models of climate-change effects. For example, consider the response of carbon stocks in the coldest regions of the Eastern US to a scenario of increased temperature. Forest-averaged mortality is currently greatest in the coldest locations, suggesting that warming should decrease mortality rates, and increase carbon stocks (Fig. 2.1b). In contrast, species that currently dominate cold regions had higher species-averaged mortality rates in warmer areas, implying that the warming might increase mortality in cooler regions dominated by these species. Although warming-induced mortality increases have been observed in other temperate forests (van Mantgem and Stephenson, 2007; van Mantgem et al., 2009), even this extrapolation must be viewed with caution, because it ignores any simultaneous changes in species composition.

At the forest-averaged level, wind speed did not effect mortality yet several species-averaged mortality rates showed a strong correlation with it (Fig. A.1 in Appendix A page 126). The effect may be confounded with other variables, for example trees may experience higher mortality with higher wind speed in low density areas where there is little protection from neighbouring trees (Taylor and MacLean, 2007). At the forest-averaged level, we found that mortality increased with radiation (Fig. 2.1d). A similar pattern of increasing mortality in higher light conditions has been found for oak seedlings in the Mediterranean (Gómez-Aparicio et al., 2008) and linked to higher desiccation risk. Although several species followed this pattern, many others showed the opposite trend of decreasing mortality with increasing radiation, in agreement with many other studies linking light to survival (e.g. Chen and Klinka, 1998; Kobe, 1999; Gratzler et al., 2004).

Figure 2.3 Maps of estimated annual forest-level mortality across the Eastern United States illustrating the contributions of each of the components of the model (a-c), the full model results (d), and the observed mortality for the 21 common species (e). (a) Variation in forest structure alone (stem size and plot basal area), illustrated by removing environmental effects and modelling just the most common species (*A. rubrum*). (b) The effect of variation in forest species composition alone, illustrated by removing environmental variation, and stand structure variation (i.e. modelling a 20 cm DBH tree). (c) The effect of variation in environment alone, illustrated by modelling *A. rubrum* without stand structure variation (i.e. modelling a 20 cm DBH tree) across the region. Full model results (d) are strongly affected by species-environment interaction, and closely match the observed geographical pattern of average mortality (e).



2.4.3 *Species-mortality responses to changing climate*

Our results suggest that species show contrasting responses to changing environmental conditions, and these mortality responses were strongly non-linear which suggests that individuals within a species may respond at different rates to a change in conditions, depending on where they sit within the species range. Changes in mortality have been correlated with changing temperature and precipitation levels in the USA in other studies (Voelker et al., 2008; van Mantgem et al., 2009), and since many parts of the Eastern USA are predicted to experience increases in temperature and precipitation under climate change (IPCC, 2007), we examined changes in mortality under scenarios of blanket increases in temperature and precipitation only (Fig. 2.2). We found that the largest changes were seen in the species with the highest mortality rates, implying that under these climate change scenarios the largest changes in carbon dynamics might be seen in highly-disturbed landscapes where fast-growing species dominate. Such changes in mortality could have repercussions for forest structure and species composition, but any consequences would need to be understood in the context of compounding effects of species-specific changes in growth and recruitment rates (Ibáñez et al., 2007; McMahon et al., 2010), and frequency of disturbance events, such as pest and pathogen outbreaks, which may change with climate change (Dale et al., 2001). However, since observed wood anatomy and demographic rates within a species may have adapted to local climatic conditions (Esteban et al., 2010), the future response of mortality to rapid climate change may follow different patterns to the correlations between current climate and mortality documented here.

2.4.4 *Limitations*

Although this work presents strong evidence for marked variation in mortality with a variety of different factors, we recognise several shortcomings in terms of a lack of inclusion of external disturbance factors, forest management and history, which are all likely to affect mortality. It is also important to note a significant limitation of the study, namely that the data used cover a single survey period only (1980s-1990s), so particular quantitative results are dependent on conditions in this period and must be treated with caution. This raises the possibility that some of the patterns reported here reflect particular episodic events that may not be representative of mortality patterns averaged over the longer term. However, our four main conclusions (that mortality is U-shaped against DBH, hump-shaped against plot basal area, and species exhibit both different underlying mortality rates and different responses to changes in environmental conditions) are robust unless: (a) over longer periods temporal variation completely or nearly removes all effects of species, size or environment on mortality, (b) the apparent effects of the different predictor variables on mortality uncovered here were caused *entirely* by temporally varying factors not considered by this study, for example pests and pathogens (Lovett et al., 2006), forest management practices or extreme weather events (Batista and Platt, 2003). Fortunately, national forest inventories are beginning to provide re-surveyed data

covering more than one time interval (e.g. FIA-DB, 2008). In principle, this kind of data can be used to estimate the magnitude of inter-decadal variation in tree mortality directly. These limitations are important and call for caution in interpreting the results given here, and/or in utilising our models of mortality (Table A.2 in Appendix A page 122). More importantly, these limitations, together with the marked correlations between climate and mortality documented here, call for further research into tree mortality and its potential contribution to the response of the terrestrial carbon cycle to climate change.

2.4.5 *Conclusion*

We found large and statistically significant differences in mortality among species not only in baseline mortality rates (Table 2.1), but also in their responses to environmental variation (Fig. 2.1, A.1-A.3 in Appendix A pages 126-127), along with marked effects of individual size and plot basal area. Importantly, both species composition and stand structure are likely to continue to undergo directional changes over decadal timescales, independent of any effects of climate change. Therefore, projections of future forest carbon dynamics will be in error unless they incorporate the effects of projected changes in species composition and stand structure. The good news is that recent decades have seen the appearance of a variety of simulation models that can make accurate predictions of forest dynamics, whether within the context of forest community ecology (e.g. Purves et al., 2008) or silviculture (e.g. Mitchell, 1969), as well as Dynamic Global Vegetation Models which in principle can predict forest responses to changing CO₂ concentrations (e.g. Bonan et al., 2003). These models, together with the large forest inventory databases that are rapidly becoming available for many of the world's forests, suggest that believable predictions of future forest dynamics and the forest carbon balance which incorporate ecological processes are within reach.

Author contributions

Designed the study, analysed the data and performed statistical analysis: Emily Lines with support from Drew Purves and David Coomes. Wrote the paper: Emily Lines with supervisory support from David Coomes and Drew Purves.

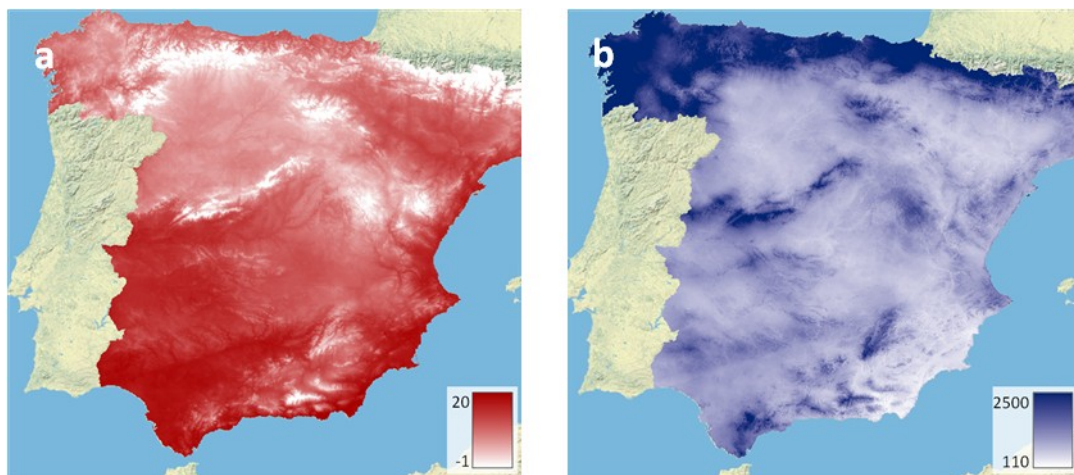
3 A brief introduction to Spanish forests

The second part of this thesis concentrates on modelling forest processes in Spain. In this chapter I therefore provide a brief description of Spanish forest ecology to introduce the context for the following chapters.

3.1 Introduction

Mainland Spain, spanning from 36°N to 44°N and 9°W to 3°E, has an extremely varied landscape containing a wide range of soil and climatic conditions which produce many different vegetation types. It has been identified as part of the Mediterranean basin biodiversity hotspot (Myers et al., 2000), making it an important place in terms of conservation to investigate the response of individual tree and whole-forest dynamics to changing environmental conditions. Although the predictions of climate models for future temperature and precipitation levels are conflicting for many regions of the world, most of them agree that Spain will become hotter and drier under future climate change (IPCC, 2007), allowing a more straightforward investigation into the effect of climate change on Spanish forests than in many other cases.

Figure 3.1 Maps of a) average annual temperature (°C) and b) annual precipitation rate (mm) in the period 1940-1996 (MMA).



Forests, as defined by the UN, cover around over 18 million ha or 36 per cent of mainland Spain, making it the most heavily forested country in Southern Europe (Fig. 3.2), with around 14 per cent of forest in formally protected areas (FRA, 2000). Vegetation types in Spain are controlled to a large extent by the strong climatic gradient across the country, from wet Atlantic conditions in the

north to arid Mediterranean conditions in the south, along which temperature and precipitation regimes vary substantially (Fig. 3.1). Although much of the country is characterised by seasonally dry Mediterranean conditions, northern and mountainous parts of central Spain have much higher levels of rainfall, and are accordingly the most densely forested regions. In the south, precipitation varies greatly with season, with Atlantic fronts bringing higher precipitation in winter (Millán et al., 2005) and the lowest levels in summer. Precipitation can also be highly variable between years, with the south and east coasts experiencing periodic autumn deluges (>200 mm in 24 hours, Grove and Rackham, 2001).

Forests, both natural and managed, are found at altitudes from sea-level to over 2000 m and three-quarters of Spanish forests are found in hilly and mountainous areas, on slopes greater than 20 per cent. Woody-plant dominated landscapes in Spain include shrub land (matorral), savannah (dehesa) and as well as more familiar forest forms (Grove and Rackham, 2001). Many Mediterranean tree species, notably *Quercus coccifera* and *Q. ilex*, can take a shrub form, creating matorral ecosystems in areas which are dry, where soils are poor, or where there is intense pressure from grazing animals or frequent fires. Savannah (wood-pasture) systems exist in areas with low rainfall (400-700 mm/year; Grove and Rackham, 2001) and are often dominated by the evergreen oaks *Q. ilex* and *Q. suber* (holm and cork oak) at densities of 20-40 mature trees per ha (Joffre et al., 1988), although some *Pinus* species can also form dehesas. Dehesas have a long history of management for acorn production, livestock grazing, wood and charcoal production, and cork harvesting. Oaks have commonly been pruned and pollarded to maximise crown spread and therefore acorn production (Plieninger et al., 2004).

Figure 3.2 Distribution of the approximately 90,000 forest plots in the Second Spanish Forest Inventory (IFN2) representing the distribution of Spanish forests.



3.2 Climate, topography and tree species distributions

The very high diversity of Spanish forest types make it both an attractive and a challenging system to study. The Iberian peninsula's forests are dominated by a wide variety of species (Fig. 3.3), primarily determined by the high variation in climate and topography, as well as a long history of human activity. Spain contains both temperate forests in the northern and central parts, and Mediterranean-type forests in the south. In the early Holocene *Pinus* forests dominated in many parts of Spain, but a wetter and warmer period in the mid Holocene (around 7000-5000 BP) led to increased dominance of angiosperm species such as *Quercus*, *Fraxinus* and *Betula* (Carrión et al., 2001; Rubiales et al., 2008; Pérez-Obiol et al., 2011). Since the mid Holocene, increasing aridification and more frequent fires (possibly causing changes in soil quality) combined with increase human activity, has led to an increased dominance by evergreen *Quercus* species over *Pinus* and deciduous species in the south of Spain (Carrión et al., 2000, 2001; Valbuena-Carabaña et al., 2010; Pérez-Obiol et al., 2011).

The Mediterranean Basin is a biodiversity hotspot containing 25,000 species of plant (50 per cent of which are endemic), including 100 tree species; compared to just 6,000 plant and 30 tree species in the whole of northern and central Europe (Scarascia-Mugnozza et al., 2000). Successional dynamics and species composition in Mediterranean communities are qualitatively different to those in temperate zones because the distributions of species in the Mediterranean are more affected by water limitation than light availability (Zavala et al., 2000).

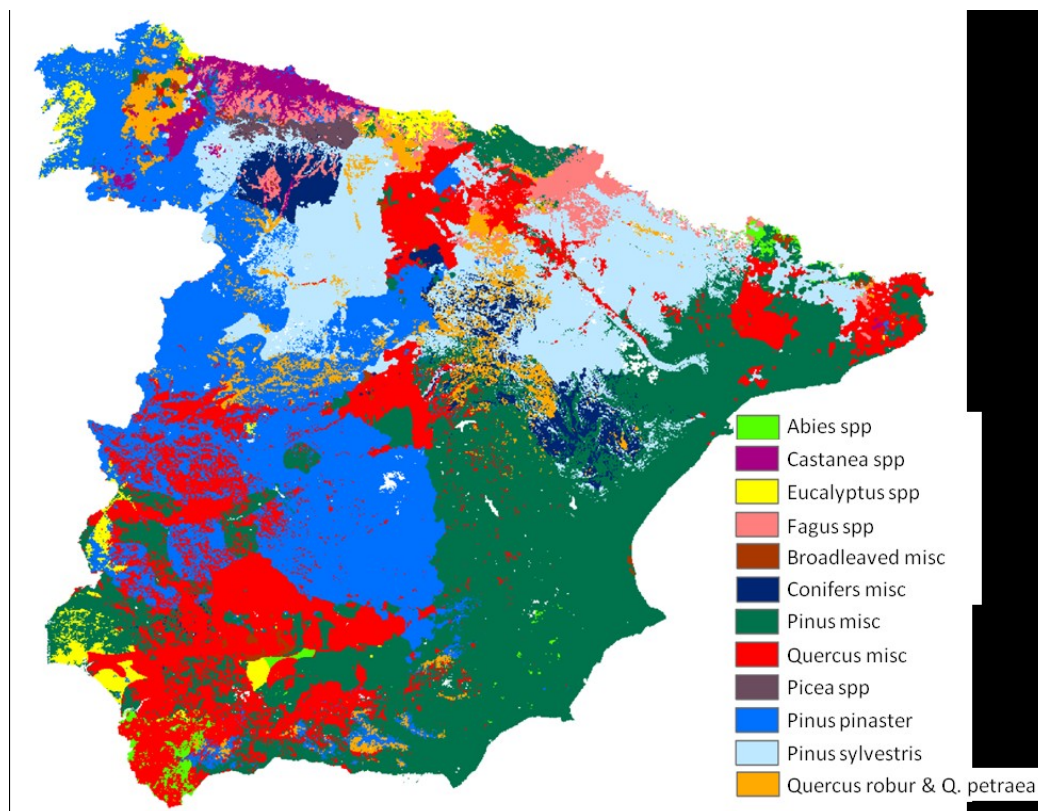
The northern part of Spain lacks a distinct dry summer season, and temperate forests dominate. Conifer-dominated forests form a large part of all Spanish forests, accounting for about 40 per cent of forested land, with about 25 per cent of forests dominated by *Pinus* species (Barbéro et al., 1998). Temperate conifer forests are found in the northern and central mountainous regions in areas with Atlantic climates that have regular long frosts and cool summers with no drought, and on slopes above 1500m (García Viñas et al., 2006). They contain species such as the mountain pines *Pinus sylvestris*, *P. uncinata* and *P. nigra*, along with some fir (*Abies alba*). Temperate broadleaf forests are also found in the north in areas without drought, but are generally on lower slopes. *Fagus sylvatica*, a species that doesn't tolerate drought, dominates many montane forests in the north of Spain, representing the southern range edge of its distribution (Jump et al., 2006). Deciduous oak species such as *Quercus petraea* and *Q. robur* are commonly found on lower slopes in northern and central parts (Benito Garzón et al., 2008).

The southern part of Spain is characterised by a Mediterranean climate with mild autumns and winters, during which most of the rainfall occurs, and hot dry summers, along with a highly varied topography and nutrient-deficient soils (Zavala et al., 2000). Deciduous species are found in the south of Spain, but are restricted to riparian areas and moisture-retaining soils. Oak species such as *Q. pyrenaica* and *Q. faginea* are strongly limited by water availability (Benito Garzón et al., 2008),

whilst even in arid areas species such as *Ulmus minor* and *Populus nigra* are able to survive alongside rivers and in areas with a high water table (Tabacchi et al., 1996; Grove and Rackham, 2001).

Two evergreen oak species, *Q. ilex* and *Q. suber*, dominate in areas too dry for deciduous oaks, but are outcompeted by pine species in the very driest parts of southern Spain as well as in very frequently disturbed areas (Rodà, 1999; Zavala et al., 2000). For example, *Q. ilex* forms a dense forest in regions with 500-600mm rainfall/year but is sparse in areas with 400-450 mm/year, whereas *Pinus halepensis* plantations may survive in areas with as low as 300 mm/year precipitation (Rodà, 1999).

Figure 3.3 Forest species dominance across Spain (adapted from Brus et al., 2011).



The Mediterranean pines, *Pinus pinea*, *P. halepensis* (Aleppo pine) and *P. pinaster*, are more drought resistant than the mountain pines and Mediterranean oak species. The relative abundance of oaks and pines is strongly related to water availability and topography (Zavala et al., 2000). Mixed stands are found in areas with droughts lasting between 4 and 8 months per year, but pines also form monospecific stands in drier regions. Along gradients of altitude and slope aspect, higher densities of light-demanding pines are found on warmer south-facing or lower slopes, with higher densities of oak found on cooler north-facing or higher slopes. Although in many parts of Spain pine-dominated stands are the early successional stage ending with broadleaf dominance, for example *P. halepensis* to *Q. ilex* and *P. pinaster* to *Q. suber*, in the very driest regions broadleaves are unable to establish and pine communities represent a stable or climax vegetation (Barbéro et al., 1998).

3.3 Adaptation to drought

The Mediterranean region has an environment characterised by soils that are commonly nutrient-poor (Thompson, 2005) and a long drought in the summer that limits growth in the warmest period of the year. Trees living in the region are adapted to tolerate drought and low nutrient levels through strategies such as physiological acclimation (e.g. altering photosynthesis rates), having longer-lived and thicker sclerophyllous leaves, smaller leaf area index and higher root-to-leaf area ratio (Bréda et al., 2006).

A high proportion of rainfall in the Mediterranean occurs in winter, meaning winter deciduous species with a more limited photosynthetically-active period may be at a disadvantage (Thompson, 2005). Evergreen woody-vegetation, often with small, thick, sclerophyllous leaves, is therefore often dominant in areas with the longest droughts (Joffre et al., 1999). Sclerophyllous angiosperms (e.g. *Q. ilex* and *Q. suber*) and conifer species have been found to have higher levels of stomatal control than deciduous species and may therefore be better able to avoid water loss during drought than deciduous species (Duhme and Hinckley, 1992; Mediavilla and Escudero, 2003), although there is evidence this is not the case in all environments where deciduous and sclerophyllous species coexist (e.g. Damesin and Rambal, 1995).

Both angiosperm and gymnosperm species adopt deep and wide rooting systems to maximise water availability and access to deep reservoirs during drought (Joffre et al., 1999; David et al., 2004; Moreno et al., 2005), which, along with stomatal response, reduces the risk of cavitation and leaf damage by avoiding low water potentials. Deep rooted trees may benefit their surrounding vegetation because they can reduce the water stress experienced during drought by increasing upper soil layer moisture through hydraulic lift (Filella and Peñuelas, 2004).

Sclerophylls tend to have low levels of nutrients in their leaves (Turner, 1994), which is an advantage in low-nutrient conditions due to higher nutrient use efficiency (Aerts, 1995), but may be less responsive than deciduous species to increases in nutrient levels, for example after fires (Valladares et al., 2000). Sclerophyllous angiosperms have lower photosynthetic capacity than deciduous species leading to lower growth rates, and are therefore outcompeted by deciduous species in areas with shorter droughts or higher nutrient levels (Thompson, 2005). Sclerophylls did not evolve under current Mediterranean conditions (Herrera, 1992) and the mechanism for the dominance of sclerophylls over deciduous species or vice-versa is not always a straightforward product of drought length or intensity (Blumler, 1991).

3.4 Adaptation to forests fires

Forest fires are frequent occurrences in many parts of Spain, with an average of more than 14,000 ha per year in the period 1980-2000 (Civil Protection and Environmental Accidents Unit, 2001). Forest fires play a substantial role in influencing vegetation composition and dynamics and have done so for at least the last 5000 years (Carrión et al., 2001).

Many Mediterranean tree species have developed specific adaptations to aid survival and regeneration following fire, both to avoid damage (by growing thicker bark) and to regenerate quickly post-fire (through resprouting and reseeded), and post-fire dynamics are strongly dependent on the ability of species to regenerate (Gracia et al., 2002). When burnt, both *Q. ilex* and *Q. suber* are able to resprout from stem and basal buds (Pausas, 1997; Broncano et al., 2005), while *Q. suber* is also protected from milder fires by its thick bark (Pausas, 1997). Many shrublands are dominated by these resprouters along with others such as *Q. coccifera* and *Arbutus unedo* (Pausas et al., 2008). Individuals of resprouting species recover faster in the short term than reseeders because they maintain live biomass underground, but light-demanding conifer reseeders tend to dominate in frequently disturbed stands and after intense fires (Zavala et al., 2000). *P. halepensis* and *P. pinaster* have adapted to the effects of intense crown fires by reproducing at a young age and by having serotinous cones that allow rapid seed dispersal and regeneration after a fire (Tapias et al., 2004; Calvo et al., 2008). Levels of serotiny is, however, highly variable between species and populations, and may also be related to the length and severity of drought in the area (Tapias et al., 2001). *P. halepensis* has thin bark and is easy killed by fire, whereas *P. pinaster* has a thicker and more protective bark. *P. pinea* is not serotinous but reduces fire damage through a thicker, more insulating and more resistant bark. It also escapes more intense crown fires because it is naturally found in areas of poor sandy soil, which typically do not support dense flammable understories (Grove and Rackham, 2001; Rigolot, 2004; Tapias et al., 2004). Other species such as the mountain species *P. nigra* and *P. sylvestris* are not serotinous and are unable to either survive intense crown fires or regenerate after them, although *P. nigra* has a thick bark and is able to survive low-severity understory fires (Pausas et al., 2008).

Although there were forest fires in Spain in pre-human times (Grove and Rackham, 2001), humans have managed the forests with fire for so long that it is difficult to establish what effect a natural fire regime would have had on species distributions. For example, *P. halepensis* burns very fiercely but reproduces so profusely (Pausas et al., 2004) that more frequent burning due to human activity may have increased its range over less tolerant species (Agee, 1998). It has also been suggested that the dominance of *Q. ilex* over deciduous oaks in the subhumid south of Spain could be attributed to human-induced fires lit to create clearings from around 4000 BC (Reille and Pons, 1992).

3.5 Land use change, threatened species and climate change

All Mediterranean forests have a long history of human activity and management and Spain is no exception. Fire regimes, herbivory, and a long history of human land use and disturbance have influenced current species' distributions (Zavala and Marcos, 1993; Zavala et al., 2000). Anthropogenic effects have influenced vegetation composition and structure since at least 10,000 yr BP and driven major changes since the late Holocene (3,000 yr BP), particularly through forest clearing at low altitudes (Ramil-Rego et al., 1998). The combination of human activity and climatic changes, for example warming after the last ice age, has changed forest species composition, for example causing the reduction in *Pinus sylvestris* seen in north-western Spain in the Holocene (Rubiales et al., 2008).

In the latter half of the 20th century a large amount of agricultural land in Spain was abandoned resulting in increases in forest cover (e.g. Barbero et al., 1990; Poyatos et al., 2003), which may have interacted with fire regimes to cause changes to forest structure and dynamics (Viedma et al., 2006; Chauchard et al., 2007). In the last few decades, the abandonment of agricultural land combined with new EU policies have led to the re-forestation of substantial areas of land (3.2 million ha in the period 1940-1980 and 450,000 ha in 1994-1999; Campos et al., 2005). Planted forests account for around 2.7 million ha, around 40 per cent of which is introduced species such as *Pinus radiata* and *Eucalyptus spp.*

Many forest types in Spain are considered threatened. For example, *Abies pinsapo* (Spanish fir) is found in only three areas in the high mountains of southern Spain, and has had its range greatly reduced by fire and human activity (Esteban et al., 2010). The oaks of the dehesas of south-west Spain provide important ecosystem services such as preventing soil erosion, enriching soil nutrients, and providing habitats and food for many animals; but a decrease in their use for pastoral agriculture combined with a lack of natural regeneration in many areas has led to aging and degraded stands, threatening ecosystem functionality (Joffre et al., 1999; Plieninger et al., 2003, 2004).

The impact of climate change on Spanish forests is not clear, as some studies have predicted positive and others negative impacts. For example, climate change is expected to have a detrimental effect on the distributions of many Iberian species, and under future warming, mountain conifers are predicted to be limited to the few high altitude areas into which they are able to disperse (Benito Garzón et al., 2008). Individual tree growth has been shown to have been affected by increased water stress in recent decades (Andreu et al., 2007), however some species may also benefit from a longer growing season (Sabaté et al., 2002).

3.6 The Spanish Forest Inventory

The data used in this thesis have come from the second and third Spanish Forest Inventories (Inventario Forestal Nacional IFN2 and IFN3; MMA, 1996, 2007), national databases which have already been used to investigate patterns in forest dynamics (e.g. Montoya et al., 2008) but have not yet been applied to construct and parameterise an individual-based model for Spanish forest dynamics. These database contains details of the species, size, height, volume, growth, damage and survival of over a million trees of over 40 species, monitored at 10-year intervals from 90,000 plots distributed over a 1 km² grid across all the currently forested areas of Spain (Fig. 3.1). The plots each contained four concentric circular subplots of radius 5, 10, 15 and 20m, within which all trees larger than the minimum subplot tree diameter were measured (7.5, 12.5, 22.5 and 42.5 cm respectively). The surveys include details of tree height, crown size and depth for several randomly chosen trees within each plot, and plot-level data on altitude, slope, land use, major tree species, forest type and cover, and management has also been recorded. Further details of the inventory are given in Chapters Four, Five and Six.

4 Predictable changes in aboveground allometry of trees along gradients of temperature, aridity and competition

Abstract

Trees are often observed to get shorter and narrower-crowned in dry regions and at high elevations. We explore how this pattern is driven by two opposing factors: competition for light makes it advantageous to extend branches to their biomechanical limit, whereas in cold or arid conditions it is advantageous to have shorter branches, thereby reducing the length of the hydraulic transport system and embolism risk.

Using data from the Spanish forest inventory of 700,000 trees of 26 species, we quantify how environmental conditions influence the scaling of height (H) and crown diameter (CD) with stem diameter (DBH). We compare our predictions with those of Metabolic Scaling Theory (MST), which suggests allometry is invariant of environment. We fit DBH-H and DBH-CD functions using Bayesian methods, allowing comparison of within and across-species trends in allometry along gradients of temperature, precipitation, drought and competition for light (i.e. the basal area of taller trees).

Competitive environment had a strong influence on aboveground allometry, but all trees were far shorter than predicted by biomechanical models, suggesting that factors other than biomechanics are important. Species that dominate in arid and cold habitats were much shorter (for a given diameter) than those from benign conditions; but within species heights did not vary strongly across climatic gradients.

Our results do not support the MST prediction that DBH-H and DBH-CD allometries are invariant, or that biomechanical constraints determine height allometry. Rather, we highlight the role of hydraulic limitations in this region. The fact that intraspecific adjustment in DBH-CD-H allometry along environmental gradients was far weaker than across-species changes may indicate genetic constraints on allometry which might contribute to niche differentiation among species.

4.1 Introduction

Aboveground allometry - the scaling of tree height and crown width with stem diameter - has a strong influence on plant performance, but the way in which it changes along environmental gradients is poorly understood. The biomechanical limitation hypothesis suggests there is strong selective pressure for trees to extend to their critical buckling height in order to project their leaves above those of neighbours and maximize competitiveness in the battle for light (McMahon, 1973; Chave et al., 2005; Mäkelä and Valentine, 2006; Dietze et al., 2008; Kaitaniemi and Lintunen, 2008). In contrast, the hydraulic limitation hypothesis suggests that resistance to sap flow within the plant vascular system limits height growth, particularly in arid regions, and that plants compensate by adjusting their morphology, allocation patterns, and wood anatomy (Ryan and Yoder, 1997). In this paper we investigate how aboveground allometry varies along environmental gradients. It is well known that vegetation becomes shorter and more open in dry regions and that cavitation risk is reduced at the sacrifice of increased hydraulic resistance per unit pipe length (Pockman and Sperry, 2000; Martínez-Vilalta et al., 2002). Similar patterns are observed up altitude gradients (Coomes and Allen, 2007a). In this study we investigate whether aboveground allometry also changes systematically, or whether trees growing in arid and cold environments are simply miniaturised versions of those growing in benign environments.

Whilst allometric studies are numerous, most have been undertaken using a small sample of trees at single locations, and applying the functions to different sites, species or scales is challenging (Chave et al., 2005). Surprisingly little is known about how scaling relationships vary within and among species along environmental gradients at regional scales (Wang et al., 2006; Méndez-Alonzo et al., 2008). The need for more accurate and generalisable allometric relationships which incorporate climatic variation has been highlighted by the sensitivity to allometric scaling of individual based simulation models such as ALLOCATE (Tilman, 1988), SORTIE (Pacala et al., 1996) and PPA (Purves et al., 2008), as well as dynamic global vegetation models (Scheiter and Higgins, 2009). Moreover, ecotypic variation in tree allometry is expected due to local adaptation and plastic responses (e.g. due to crowding) (Weiner, 2004). The lack of studies quantifying inter- and intra-specific allometric variation across the landscape may reflect the paucity of allometry datasets spanning wide environmental gradients and the under-use of computational methods to effectively separate co-varying correlates.

We investigate how aboveground allometry of Iberian tree species varies with wood traits, climate and competitive environment using data extracted from 48,000 forest plots in the Spanish Forest Inventory. The large amount of data contained in the inventory, combined with the high variation in climatic and competitive environments in Spain enable us to make strong inferences about both inter- and intra-specific variation in allometry along gradients, as well as comparing the two. The

height (H) vs. stem diameter at breast height (DBH) dataset comprises over 700,000 stems of 26 native species, and the crown diameter (CD) vs. DBH dataset comprises 225,000 stems of 14 species.

Our first hypothesis is that asymmetric competition for light has strong influences on aboveground allometry, particularly in wetter regions of Spain where forests are denser and aboveground competition more intense. It is well established that trees adjust aboveground allometry in response to their local competitive environment: trees growing in dense young stands tend to invest more into height growth than into diameter growth or crown expansion (Henry and Aarssen, 1999). Individuals in dense stands restrict their crown development in response to competition for light from neighbours (Bragg, 2001), whereas open-grown trees develop much wider crowns (Muth and Bazzaz, 2003). Yet we know of no studies that have compared the responses of multiple species to competitive effects in the context of environmental gradients.

Our second hypothesis is that tree heights never exceed the theoretical height above which they are unable to avoid buckling under small horizontal displacement of the top of the trunk, but that trees growing in neighbourhoods with many taller competitors may attain heights close to the theoretical limit. The critical buckling height of a tree height is given by the Euler–Greenhill formula:

$$H_{crit} = C \left(\frac{E}{G\rho} \right)^{\frac{1}{3}} D^{\frac{2}{3}} \quad (\text{Eqn 4.1})$$

where H_{crit} (m) is a function of trunk diameter (D : m), the green wood density (ρ : kg/m³) and modulus of elasticity (E : N/m²), with G being the gravitational force (9.8 N/kg), and C a constant of proportionality (0.792) (Greenhill, 1881; Niklas, 1994). Maximizing height growth is essential for plants growing under strong competition for light. In lowland Malaysian forests, King et al. (2009) found that some Dipterocarp trees grew very close to their H_{crit} in sheltered understory conditions. However, growing close to the critical value is risky, and several studies have found that trees have heights 2–5 times lower than the theoretical maximum (e.g. McMahon, 1973; van Gelder et al., 2006).

Our third hypothesis is that water shortage reduces tree height and crown diameter relative to DBH, and that hydraulic constraints are more important than biomechanical ones in xeric conditions. Water shortage has a direct effect on aboveground allometry, because plants reduce height and branch growth in order to reduce cavitation within xylem tissues (Bréda et al., 2006). Water supply may indirectly affect allometry by changing competitive interactions within forests: there is evidence that asymmetric competition for light is more intense in mesic forests because they have greater leaf area indices and capture more light than xeric forests (Coomes and Grubb, 2000), so we predict a shift towards height growth in mesic forests, where the battle for light is most intense (Henry and Aarssen, 1999).

Our final hypothesis is that the height and crown diameter attained by a tree will decrease in colder areas. Long or severe frosts may cause embolism and branch loss (Lemoine et al., 1999) and have been found to limit forest height (Wang et al., 2006). There may also be an altitude–temperature

effect on allometry, since growth and biomass have been found to decline in higher, cooler areas (e.g. Coomes and Allen, 2007) and DBH-H and DBH-CD allometry may be affected by stronger winds (Bruchert and Gardiner, 2006).

By testing these hypotheses we intend to demonstrate the influences of competition, aridity and temperature in regulating aboveground allometry, with potentially important implications for carbon storage and forest dynamics.

4.2 Materials and Methods

4.2.1 Inventory data and climate variables

Data on height (H) and DBH were taken from the second Spanish Forest Inventory (IFN2) (MMA, 1996) for over 700,000 stems of 26 native tree species (see Appendix B page 131), sampled from over 48,000 plots arranged systematically on a 1 km grid across Spain. For each tree a variety of attributes including position within the plot, species, two measurements of DBH (perpendicular to each other) and H (to the nearest 0.5 m) were taken. For a subset of the database (around 150,000 stems of 14 species of silvicultural interest), two measurements of crown diameter were recorded for around four trees per plot. Spanish forests have a long history of human management, so for five species that are commonly coppiced/pollarded (see Appendix B page 131) we used a smaller database of trees that showed no signs of cutting at the time the inventory was taken. For both DBH and crown diameter we used the average of the two measurements taken in the inventory in the model.

The IFN2 plots were sampled using a sampling technique whereby trees of different sizes were measured in concentric plots of varying plot radius. All trees of DBH > 7.5 cm were measured in a plot of radius 5 m, all of DBH > 12.5 cm in a plot of radius 10 m, all of DBH > 22.5 cm in a plot of radius 15 m and all of DBH > 42.5 cm in a plot of radius 25 m. Estimates of plot basal area are therefore calculated using only basal area of trees over 7.5 cm DBH.

Estimates of precipitation, temperature (annual and seasonal for both) and drought length were taken from data layers extracted from Gonzalo Jiménez (2008). These were created by interpolating data from Spanish weather stations (from the State Meteorological Agency AEMET) recorded between 1951 and 1999. Drought length (months) was calculated using the Gaussen-Bagnouls method (ombrothermic curves; Bagnouls and Gaussen, 1957). Plot altitude and slope were measured during the inventory. We removed highly correlated predictor variables from the climate data before models were fitted (excluding those with $|r| > 0.7$), leaving three climate variables to consider in the analysis (mean annual temperature, mean annual precipitation and drought length).

We calculated three different possible predictors of the effect of competition from neighbouring trees on allometry (plot basal area (m^2/ha), basal area of larger trees (those larger in

diameter than the target tree) (m^2/ha) and tree density (stems/ha)) and compared models fitted with each of them to find the best by comparing model fit using Akaike and Bayesian Information Criteria (AIC and BIC; Akaike, 1974; Schwarz, 1978).

4.2.2 *Species-level wood traits and critical buckling heights*

We compared observed heights with H_{crit} values predicted by the elastic similarity model. These comparisons were made for the 14 species with more than 1000 samples in the dataset, and for which we found green wood density and modulus of elasticity (Young's modulus) data in the literature (see Appendix B page 131). We calculated the theoretical maximum attainable height curve using equation 4.1. We characterised species' shade tolerance using Ellenberg scores (Ellenberg, 1988).

4.2.3 *Statistical models*

Hierarchical Gibbs Sampler

To test whether wood density, elastic modulus or shade tolerance affect allometric relationships we constructed a hierarchical normal Gibbs sampler to fit species-trait constrained parameters to traditional power-law allometric equations, $y_{ij} = \alpha x_{ij}^\beta$ to describe the relationship between DBH of a given tree i of species j (x_{ij}) and H and CD (y_{ij}), following the methods used by Dietze et al., (2008) (see Appendix B page 131 for details). We fitted this for a subset of 14 species for which we used data for both wood density and modulus of elasticity. We recognised that DBH-H relationships are non-linear on log-log axes when a very wide range of plant sizes is used (e.g. Niklas and Spatz, 2004) but since all our trees were >7.5 cm DBH and Enquist et al., (2007) found power laws to be adequate for trees greater than about 5 cm DBH, we determined that a power law was appropriate.

MCMC Metropolis algorithm

We used a Markov Chain Monte Carlo (MCMC) Metropolis algorithm to fit models of DBH-H and DBH-CD allometric relationships and examine how they varied with the climate and competition. Justification for the choice of these methods is discussed in Appendix B page 131. Since we had information on the environmental conditions of each sampling plot we were able to quantify both inter- and intra-specific variation along gradients. We constructed an adaptive MCMC Metropolis algorithm (Lee, 1997; Gelman et al., 1999), which searches parameter space efficiently, to find best fit values and credible intervals for model parameters.

The MCMC algorithm searches parameter space and returns not only a best-fit value for each parameter given the data but also estimates its distribution. For a set of starting parameter values θ for each model M tested, the algorithm calculates the predicted H (or CD) h_{ij} for each tree i with recorded H (or CD) y_{ij} and then calculates the log-likelihood of the data (X) given the model and parameters:

$$l(X | M, \theta) = \sum_i \ln \left\{ \left(\frac{1}{\sigma \sqrt{2\pi}} \right) \exp \left(-\frac{(h_{ij} - y_{ij})^2}{2\sigma^2} \right) \right\} \quad (\text{Eqn 4.2})$$

At each iteration the algorithm selects a parameter to alter and recalculates the likelihood (equation 4.2). If the new parameter improves the likelihood then it is accepted by the algorithm. If not, it is accepted with probability of the ratio of the new and old likelihoods. The algorithm has two periods: burn-in and sampling. During the burn-in period (between 500,000 and 5,000,000 iterations of the algorithm for our models) the algorithm alters its parameter search range ("jumping distance") to achieve an optimal acceptance ratio of 25% (Gelman et al., 1999). After the burn-in period, the jumping distance is fixed (independently for each parameter). During sampling, parameter values are recorded every 100 iterations and the resulting parameter samples are taken as samples from the distribution of each parameter.

We fit traditional power-law allometric equations of the form $y_{ij} = \alpha x_{ij}^\beta$ to describe the relationship between DBH (x_{ij}) and H(y_{ij}), and a linear relationship between DBH and CD. We chose to use a power-law rather than asymptotic relationship as we wanted to compare our results with the predictions of the elastic similarity model (a power function). The models were fitted separately for each species and took the forms:

$$y_{ij} \sim N(b_2 x_{ij}^{b_3}, \sigma_1^2) \quad (\text{Eqn 4.3a})$$

$$y_{ij} \sim N(b_2 + b_3 x_{ij}, \sigma_2^2) \quad (\text{Eqn 4.3b})$$

where (in equation 4.3a) y_{ij} is the H of each tree i of species j of DBH x_{ij} , and (in equation 4.3b) y_{ij} is the CD of each tree i of species j of DBH x_{ij} . The standard deviation of residual errors around the fitted power function is well known to increase with increasing DBH, so we modelled it as:

$$\sigma = b_0 + b_1 x_{ij} \quad (\text{Eqn 4.3c})$$

We fitted different models and compared them using information criteria. We generated models in which parameter values were either the same for all species or species-specific. We compared models in which b_2 and b_3 of equations 2a and 2b were constants (i.e. not varying with environment) with models in which they were linear functions of the environmental predictor variables:

$$b_2 = a_0 + \sum a_i e_i ; \quad b_3 = c_0 + \sum c_i e_i \quad (\text{Eqn 4.4})$$

where e_i is a climatic or competition variable.

We normalised all environmental variables to allow easy comparison of their effects and fit the model given in equations 4.3a and 4.3b with parameters b_2 , b_3 as:

$$b_2 = a_0 + a_1(\text{competition index}) + a_2(\text{annual precipitation}) + a_3(\text{drought length}) \\ + a_4(\text{average temperature}) \quad (\text{Eqn 4.5})$$

$$b_3 = c_0 + c_1(\text{competition index}) + c_2(\text{annual precipitation}) + c_3(\text{drought length}) \\ + c_4(\text{average temperature}) \quad (\text{Eqn 4.6})$$

We fitted the full 12 parameter model for all species together, and with species-specific parameters. Details of the specifications of the MCMC model are given in Appendix B and Table B.4 (page 137). We used AIC and BIC to select the best model. All models were fitted using an adaptive Metropolis algorithm written in C (compiled using MS Visual Studio 2008).

4.2.4 Interpreting the results

The results of the MCMC algorithm are presented by predicting the change in H and CD for a fixed DBH (15 cm) across the central range of each species along each predictor (i.e. between \pm one standard deviation of the mean environment in which the species is found). We chose 15 cm as the standard size but we also investigated the across-species correlations using 10 cm and 20 cm DBH, and found that patterns remained consistent across these sizes (Table B.3 Appendix B page 137).

4.3 Results

4.3.1 Height and crown allometries varied among species and along environmental gradients

The scaling exponent of a simple across-species DBH-H model (equation 4.3a with constant b_2 and b_3) was 0.609 (95% credible interval 0.606–0.611) but this model has much less statistical support than a model including different curves for each species ($\Delta\text{AIC} \gg 1000$). Thus, there is strong support for the hypothesis that DBH-H allometry varies among species (Fig. 4.1 and see Fig. B.1 Appendix B page 138). There were clear differences between angiosperms (17 species) and gymnosperms (9 species): when species were fitted separately, the mean scaling coefficient (b_2 in equation 4.4) of the angiosperms was much higher than the mean of the gymnosperms (300 vs. 155 respectively, t-test $T = 4.7$, $P < 0.05$), whilst the mean scaling exponent (b_3 in equation 4.4) was lower (0.40 vs. 0.58 respectively, t-test $T = 4.5$, $P < 0.05$), and all species showed increases in variation in height with size (b_1 in equation 4.3c). This indicates that, in general, gymnosperm species were relatively short at small diameters but caught up with, then overtook, angiosperms at larger diameters (Table B.2 and Fig. B.1 Appendix B pages 136 and 138). However, there was no support for a trade-off between exponents and coefficients because despite a negative association when all species were considered together (Spearman's $P < 0.05$), there was no correlation when angiosperm and gymnosperm species were considered separately.

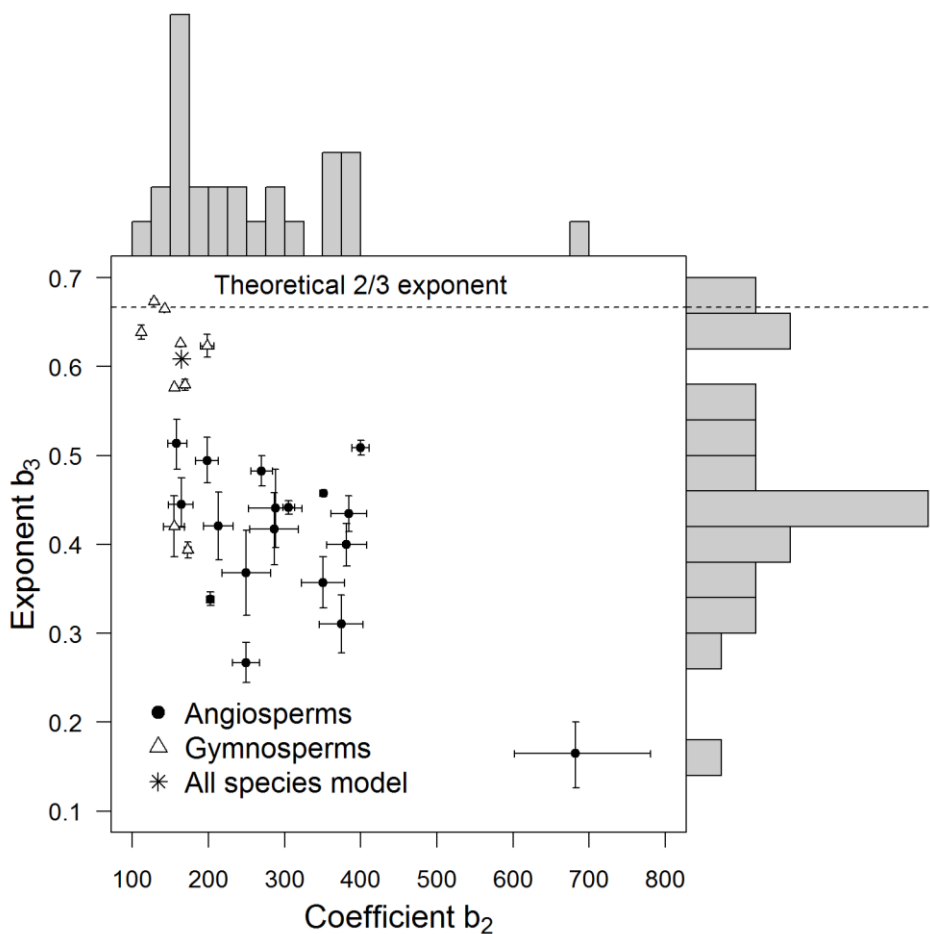
For both H and CD, species-specific models which included environmental predictors (equations 4.5 and 4.6) were more strongly supported (i.e. had much lower AIC and BIC values) than models lacking environmental predictors, except in the case of *Pinus uncinata*. However, along all the gradients we considered, across-species patterns were stronger than within-species variation (Fig.

4.2), and species did not, in general, change height rank along gradients. Climate and site dependency of the coefficient of DBH-H relationships has been found previously (López-Serrano et al., 2005; Wang et al., 2006), but we also found dependency in the exponent, indicating a compounding effect of climate on species' allometry and height growth.

DBH-CD allometry varied strongly among species (Fig. 4.3) with mean CD for individuals of 15 cm DBH ranging between 220–590 cm, and angiosperm crowns were significantly wider than gymnosperms (t-test $T = 3.0$, $P < 0.05$). Neither H nor CD allometry were significantly related to wood density, modulus of elasticity or shade tolerance (hyperparameter 95% credible intervals contained 0, tested using a Hierarchical Gibbs Sampler, Appendix B and Table B.1, page 135).

Figure 4.1

Fitted parameters (coefficient b_2 , exponent b_3) for the simple height-DBH scaling relationship (equation 4.3a) with 95% credible intervals for each of the 26 species, and histograms of the mean parameter values. Angiosperm species (closed circles) had, in general, lower exponents and higher coefficients than gymnosperm species (open triangles). Most species' exponents lay below the theoretical 2/3 exponent (dotted line) predicted by the elastic similarity model.



4.3.2 (H1) *Tree heights were greater and crown diameters narrower in competitive neighbourhoods*

All 26 species were taller (at 15 cm DBH) in stands with more large neighbours. Of the three indicators of competitive intensity – total stand basal area, basal area of larger trees (m²/ha) and tree density (stems/ha) – we found that basal area of larger trees was by far the best predictor of the effect of competition on allometry ($\Delta\text{AIC} \gg 1000$), suggesting that asymmetric competition is a more important determinant of allometry than symmetric competition. Among the angiosperms, light demanding species had a stronger response to changing neighbourhood crowding (Pearson's correlation between change in height (at 15 cm DBH) across the central 67% of each species' range of competitive environments and species' Ellenberg scores: $P < 0.05$), but there was no relationship for gymnosperms. There was correlation between the heights of species (at 15 cm DBH) and their mean competitive environments (Table B.3 Appendix B page 137): species that tended to have more large neighbours were relatively tall for a given diameter (Fig. 4.2 and Fig. B.2 Appendix B page 139).

Most species showed an effect of crowding in their crowns, with 11 of the 14 having narrower crowns in areas with more larger neighbours (Fig 4.3 and Fig. B.3 Appendix B page 140) and this narrowing of crown diameter was greater for gymnosperms than angiosperms (t-test $T = 3.9$, $P < 0.01$). There was no correlation between the standardised crown diameter of species (i.e. predicted value for a 15 cm tree) and the mean competitive environment (mean basal area of larger trees) of that species (Table B.3 Appendix B page 137).

4.3.3 (H2) *The elastic similarity model provided an upper limit on height at a given DBH and trees in dense forests will grow to their critical height*

Critical buckling height H_{crit} depends on the ratio of modulus of elasticity to wood density, E/ρ (equation 4.1). We found E/ρ varied among species (0.011–0.027, Table 4.1) resulting in large variation in predicted H_{crit} curves (Fig. B.1 Appendix B page 138). The upper boundary of height data approached the critical curve at small DBH values (Figs 4.4 and Fig. B.1 Appendix B page 138), and species grew closer to the critical height in warmer areas with shorter droughts and more larger trees, but these effects were not strong for all species (red lines, Fig. 4.4). Very few trees approached their critical buckling height: for small trees (<15 cm DBH) about 3% of stems had heights greater than 66% of their predicted critical height, but this was true of <0.1% of large trees (Fig. B.1 Appendix B page 138). Interestingly, there was no evidence that species with high critical buckling heights were the taller species in the dataset; if the elastic similarity model were important, we would expect to see a close correlation between $\left(\frac{E}{G\rho}\right)^{\frac{1}{3}}$ and predicted height at a given DBH (see equation 4.1), but we found no such correlation at 15 cm DBH (Pearson's correlation, $P > 0.1$) or at other diameters we tried. This result indicates that factors other than biomechanics are important in determining the relative heights of tree species in our dataset.

Table 4.1 Values of wood density (WD: oven dry mass/fresh volume kg/m^3) and modulus of elasticity (MOE: green wood GPa) used in equation 4.1 to find H_{crit} , and the number of samples for 14 native and not commonly coppiced species with over 1000 samples in the dataset (see Appendix B page 131 for sources of data). The species for which we could not find WD and MOE information were *Arbutus unedo* (A), *Corylus avellana* (A), *Ilex aquifolium* (A), *Juniperus communis* (G), *J. thurifera* (G), *Olea europaea* (A), *Pinus nigra* (G), *P. pinea* (G), *P. uncinata* (G), *Quercus faginea* (A), *Q. pyrenaica* (A), *Sorbus spp.* (A).

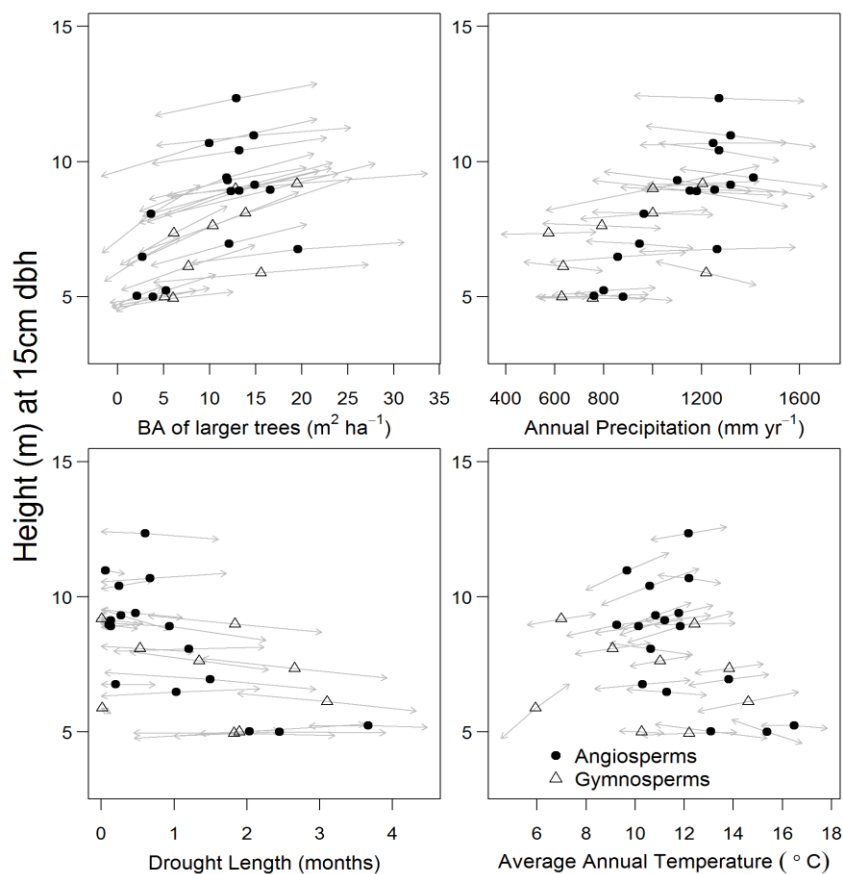
Species	Angiosperm/ Gymnosperm	WD (kg/m^3)	MOE (GPa)	Number of
<i>Acer campestre</i>	A	525.21	6.00	2194
<i>Alnus glutinosa</i>	A	439.11	8.00	3825
<i>Betula</i> spp.	A	510.00	9.25	7238
<i>Castanea sativa</i>	A	463.33	6.00	1162
<i>Fagus sylvatica</i>	A	585.48	8.60	51479
<i>Quercus ilex</i>	A	820.00	14.70	21551
<i>Quercus</i> <i>petraea</i>	A	559.65	9.20	13809
<i>Quercus robur</i>	A	559.65	9.20	26550
<i>Quercus suber</i>	A	770.00	2.00	3450
<i>Salix</i> spp.	A	450.00	5.40	2281
<i>Abies alba</i>	G	353.01	9.50	3961
<i>Pinus</i> <i>halepensis</i>	G	460.00	6.14	88437
<i>Pinus pinaster</i>	G	412.07	8.20	178622
<i>Pinus sylvestris</i>	G	421.89	8.55	145446

4.3.4 (H3) Tree height and crown diameter for a given DBH was lower in areas of longer drought. Most species (17 of 26) were shorter (for given DBH) in areas of longer drought, and gymnosperms and angiosperms did not differ significantly in their responses (t-test $T = 1.2$, $P > 0.1$). However, some species were shorter in areas of higher annual precipitation: 10 of the 13 species with the wettest average environment showed decreasing heights in wetter areas (within the dataset, annual precipitation and drought length were not highly correlated), indicating a possible non-linear height response to changes in precipitation. The species with the largest decreases in height (for given DBH) in wetter areas were generally the less shade-tolerant (Ellenberg scores: Spearman's $P < 0.05$), although the most shade-tolerant species, *Fagus sylvatica*, did not follow the pattern. Species growing in

regions with long drought length and low annual precipitation invested less in height (i.e. had lower heights at 15 cm DBH) than species from wetter regions (Fig. 4.2, Spearman's $P < 0.01$). This correlation was also observed when other diameters were used to calculate standardised heights (Table B.3 Appendix B page 137).

Crown diameter (for given DBH) was responsive to changes in annual precipitation, with 12 of the 14 species having wider crowns in wetter areas, but the effects were small for most species (Fig. 4.3). The predicted mean crown diameter (at 15 cm DBH) of angiosperm species was greatest for species specialising in wetter regions with shorter drought lengths (Spearman's $P < 0.05$: see Table B.3 Appendix B page 137), but no such pattern was observed when conifers were considered or when all species were included in the analysis.

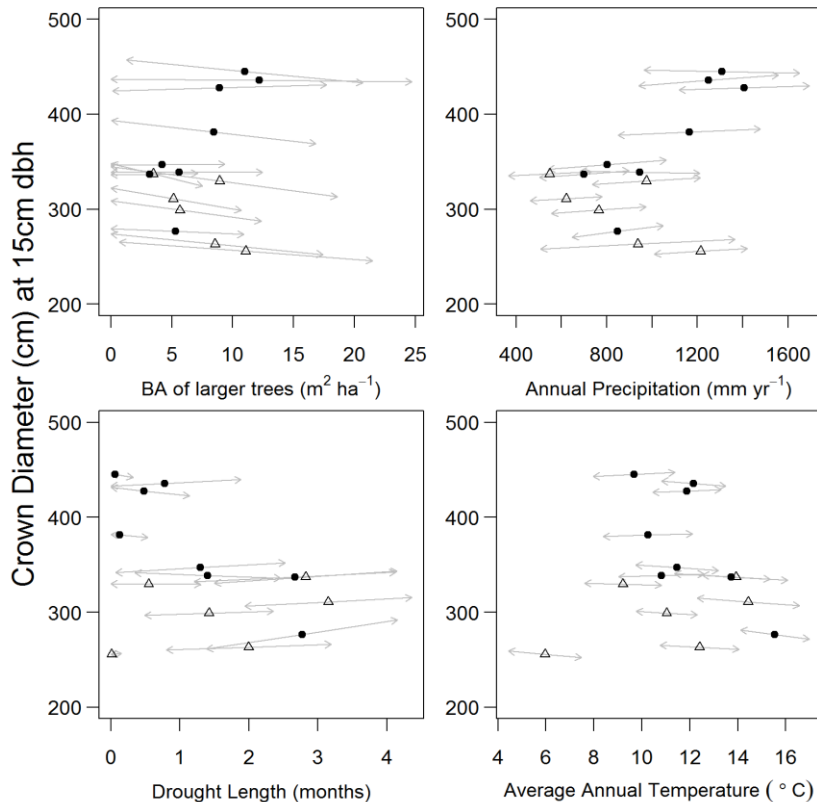
Figure 4.2 Predicted changes in height of 15 cm DBH stems of 26 species in relation to (a) basal area of larger trees, (b) precipitation, (c) drought length and (d) mean annual temperature. The symbols show height at the mean value of the environmental variables for the species – angiosperms (filled circles) and gymnosperms (open triangles) – whilst predicted variation in height is shown for ± 1 standard deviation in the environmental variable around the species' distribution mean (grey arrows). Predictions were produced using posterior estimates of the distribution of the parameters.



4.3.5 (H4) Within-species height increased with temperature, but there was no trend in crown diameter

Most species (19 of 26) were taller (at 15 cm DBH) in warmer locations. Surprisingly, the opposite effect was observed in the across-species patterns: taller species were associated with cooler regions (Spearman's rank correlation between predicted mean height and average annual temperature at the centre of the species' range was negative, $P < 0.05$) irrespective of the diameter (Table B.3 Appendix B page 137), but this may be a temperature-drought interaction since the very warmest areas are also dry. There was no consistent pattern, either within or among species, in responses of crown diameter to temperature.

Figure 4.3 Predicted changes in crown diameter of 15 cm DBH stems of 14 species in relation to (a) basal area of larger trees, (b) precipitation, (c) dry season length and (d) mean annual temperature. The symbols show crown diameter at the mean value of the environmental variables for the species – angiosperms (filled circles) and gymnosperms (open triangles) – whilst predicted variation in crown diameter is shown for ± 1 standard deviation in the environmental variable around the mean (grey arrows). Predictions were produced using posterior estimates of the distribution of the parameters.



4.4 Discussion

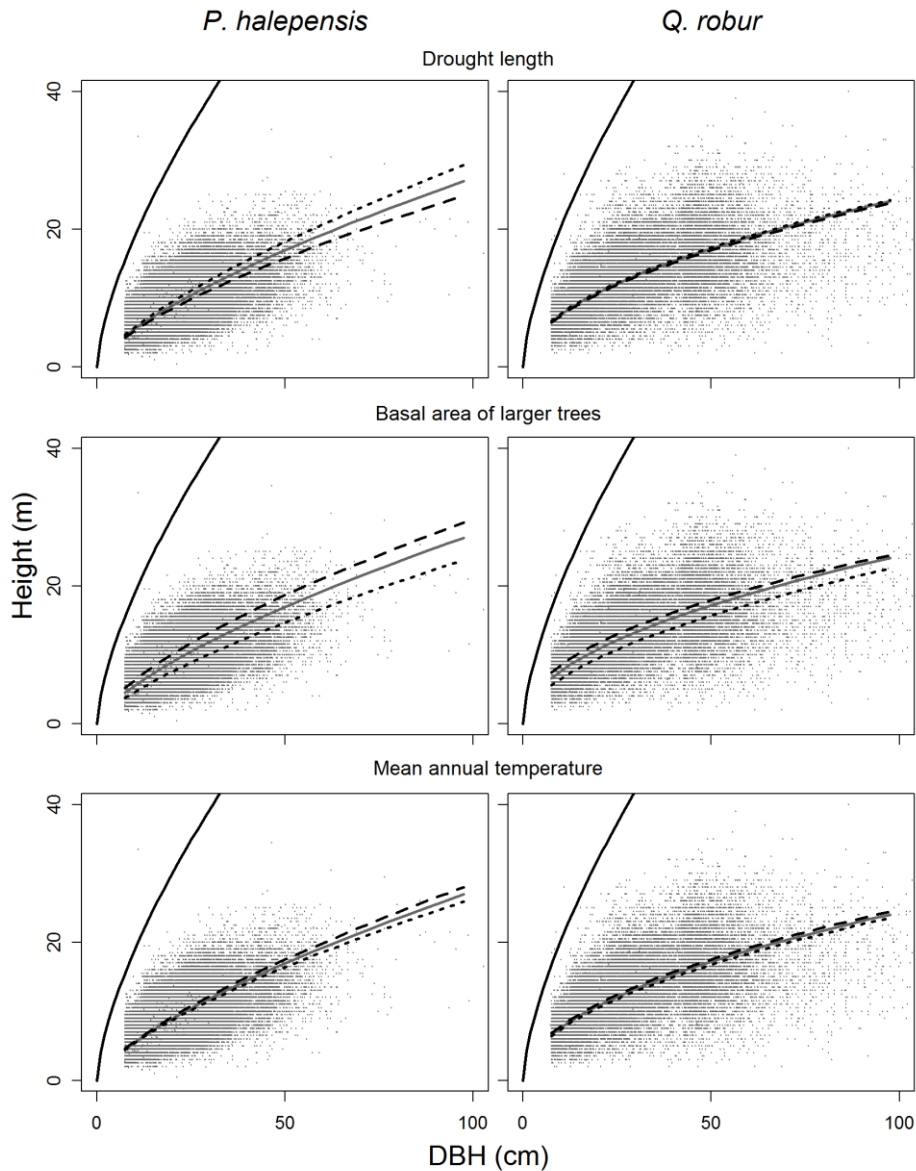
4.4.1 *Allometric scaling varies substantially with species*

Species varied greatly in their DBH-H and DBH-CD allometric relationships, in agreement with other studies reporting variation among species and functional groups (Bragg, 2001; López-Serrano et al., 2005), and we found evidence against both the original MST theory of a fixed $2/3$ exponent (West et al., 1999) and the later extension of MST that exponent values vary between species but cluster around $2/3$ (Price et al., 2007): for these data there was no fixed exponent to the DBH-H scaling relationship either across or within species. However, it is interesting to note that the conifers had, in general, exponents close to $2/3$. Indeed many may have had exponents indistinguishable from $2/3$ if we had used SMA line fitting approaches, as this method is likely to give slightly larger estimates than regression methods. Elastic similarity defines the scaling relationship between the diameter and length of individual stems, and extensions of the theory have applied the same scaling relationship to stem diameter-tree height. Since many conifers have apical dominance, a single tapering stem, the extension of elastic similarity from branch to whole tree scaling may be more reasonable. In contrast, many angiosperms have fractal-like branching, making the extension to tree height scaling less appropriate.

We found no relationship between the empirical DBH-H curve and modulus of elasticity or wood density, suggesting that biomechanics had little influence on the mean height of trees in the Mediterranean (Fig. 4.4 and Fig. B.1 Appendix B pages 134 and 138). However, for many species we were able to find only one value of modulus of elasticity or wood density measured on green wood and we assumed fixed values for these within species. These wood traits are likely to vary within species with age and climatic and other environmental conditions.

Further evidence of the lack of influence of biomechanics on mean height came from our analyses of the critical buckling height model: almost all empirical data were situated far below the upper constraint curves predicted by the model (Fig. B.2 Appendix B page 139). This situation contrasts with that observed in Asian tropical forests trees, where trees grow much closer to their critical height in the wettest areas where competition for light was most intense (King et al., 2009). Strong water deficits and management practices in the Mediterranean result in relatively open canopied trees, resulting in more light getting through to the subcanopy (Coomes and Grubb, 2000); our results suggest there is little impetus to battle for light by growing taller in these conditions.

Figure 4.4 Scatter plots of height-DBH data for two common species (*Pinus halepensis* and *Quercus robur*), showing the theoretical maximum attainable height predicted by the elastic similarity model (black line) and the fitted height-DBH relationship in the species' mean environment (grey). For three of the model variables, the effect of decreasing (dotted line) and increasing (dashed) each variable by 1 standard deviation (within each species' distribution) on the predicted height is shown plotted against diameter.



4.4.2 *Asymmetric competition for light was a strong determinant of DBH-H allometry*

The basal area of larger trees was a better predictor of allometric variation than either total stand basal area or density, and all species had a more elongated form when surrounded by more larger trees (Figs. 4.2 and 4.4). The importance of competition from larger trees shown by our data suggests that allometric relationships and biomass allocation patterns are affected by asymmetric competition, meaning that trees may invest more in height growth and increasing light capture when under more intense competition (Berntson and Wayne, 2000). Competition for light also influenced crown size, with most species having smaller crowns in more competitive environments (Fig. 4.3), in agreement with studies showing that crown area adapts to local competition (Bragg, 2001).

4.4.3 *Species were shorter in drought areas but individuals did not respond consistently*

Species living in areas of longer drought and lower annual rainfall were shorter than those in wetter areas. This pattern of reducing tree height with increasing aridity is well documented for many parts of the world (e.g. Devakumar et al., 1999; Méndez-Alonzo et al., 2008) and may be a result of changing vessel hydraulic structure in drought areas to reduce the risk of embolism (Corcuera et al., 2004). Wood hydraulic properties have been found to be more important for demographic rates than wood density (Russo et al., 2010), and they are not closely correlated (Zanne et al., 2009). A well-established trade-off in the plant hydraulics literature is that morphological traits which confer transport efficiency make the xylem vulnerable to cavitation. Cavitation risk is reduced when conducting pipes have thick cell walls, thick pit membrane and narrow lumens, but all these properties increase resistance to sap flow, leading to a fundamental trade-off between safety and efficiency (Tyree and Zimmermann, 2002). Smaller vessels may be more resistant to cavitation under drought conditions but have high resistivity (resistance per unit cross-sectional area) and are less efficient (Markestijn et al., 2011). More sapwood is therefore needed to transport the same amount of water and so trees in drought areas that reduce their risk of catastrophic failure of water flow by having small vessels may do so at the cost of reduced height growth. However, tree size may affect ability to respond to drought, with larger trees more able to recover from drought (Martín-Benito et al., 2008).

Within-species responses did not always agree with the across-species pattern of increasing height in wetter areas, especially for light-demanding species in areas with high annual rainfall, where an interacting impact of increased competition, not modelled in this study, may reduce any benefit of additional water (Fig. 4.2). Periods of soil moisture saturation and flooding may also act as a stressor in arid-climate forests by reducing tree height (Rodríguez-González et al., 2010).

4.4.4 *Within-species height increased with temperature, but across species the trend was the opposite*

The observed within-species increases in height with temperature (Fig. 4.2) are in agreement with studies finding a temperature stimulus specifically to height growth (e.g. Lopatin, 2007). This

stimulus may cause a shift in biomass allocation and change in allometry so that trees are taller for a given diameter in warmer areas, perhaps as a result of more rapid increases in photosynthetic capacity than respiration rates causing a higher rate of carbon assimilation (Way and Oren, 2010). Taller trees in warmer areas may also be caused by changing vessel structure and flow properties. It has been suggested that since warmer water is less viscous, this leads to higher flow rates within vessels causing a higher mass concentration of dry matter, but evidence of this has only been observed in gymnosperm species (Roderick and Berry, 2001). Another explanation of the pattern is that cooler temperatures are associated with higher altitudes, and tree allometry may be affected by exposure to strong winds (Bruchert and Gardiner, 2006) in the many forests found in the mountainous areas of Spain.

Across-species we found that species were shorter in warmer areas, but this is likely to be a temperature-drought effect since although the model corrected for drought in intra-specific relationships, it does not account for across-species temperature-drought correlations. Areas of Spain with high average temperatures are also those with longer droughts, which affect the average height at which each species occurs. This mismatch between across- and within-species responses to temperature has implications for predictions of the response of tree allometry to climate, since the observed negative correlation between temperature and tree height was caused by the dominant across-species pattern. Taken naively, this correlation would imply that Spanish trees are likely to become shorter in response to the predicted increases in temperatures across Spain (IPCC, 2007), but this could be confounded by simultaneous changes in precipitation patterns. In the short term however, species composition is likely to remain approximately constant, so in response to simple temperature increases, heights are likely to increase in line with the within-species pattern.

4.4.5 *Within-species variation in allometry along climatic gradients is smaller than across-species differences*

Landscape-level trends in observed tree height and crown diameter allometries were found to be primarily a result of changing species composition along environmental gradients rather than within-species changes in response to environment. The importance of aboveground architectural allometry for succession has long been recognised (Tilman, 1988; Pacala et al., 1996; Purves et al., 2008), but little consideration has been given as to whether variation in height-DBH scaling along environmental gradients could influence the outcome of competition among trees. Our results suggest that it is unlikely that aboveground allometry is a primary driver of changes in competitive interactions and community structure at the landscape level, as few species changed height rank along climatic gradients (Fig. 4.1). However, relatively small differences in allometry between species along gradients may be an important component in defining a species' niche, since species showed little ability to adapt their allometry to systematic changes in climatic conditions.

4.4.6 Sources of unexplained variation

Although we found evidence for environmental influence on allometric scaling relationships, substantial intraspecific variation remains unexplained by our model (Fig. 4.4). Our measure of the effect of competition is taken from current conditions in each plot and may not well reflect past conditions since forests in Spain are subject to fire and management. Moreover, competition was averaged over each plot and therefore doesn't take into account local heterogeneity in soil conditions and light availability, which are likely to strongly influence an individual tree's allometry. The Mediterranean climate has high inter-annual variability (Valladares et al., 2002) but we considered only long-term averages of climatic variables, despite the fact that a tree's observed allometry is a product of its entire life-history. Individual events such as extremely severe droughts or pathogen outbreaks, as well as small-scale variation in soil properties may impact observed allometry (King et al., 1999; Bréda et al., 2006) but these factors were not considered here. Breakage of branches is likely to be linked to wind conditions (Bruchert and Gardiner, 2006), so wind exposure may also be a significant predictor of allometry. Forest fires, a common occurrence across Spain, may also affect biomass allocation and observed allometry, but were not accounted for in our model. On a regional scale, changes in allometry may be confounded by phenotypic plasticity and local adaptation creating differences within species, although further work would be required to test this.

4.4.7 Conclusions

Our results indicate that, whilst biomechanical constraints provide an upper limit to allometric scaling, almost all trees in Spain were substantially shorter than their critical heights. Intense competition for light and more favourable hydraulic conditions did, however, push species towards their critical buckling heights. We found strong evidence for variation in allometric scaling along environmental gradients, and our results are inconsistent with the MST proposition of a fixed exponent of $2/3$ to the DBH-H allometric scaling relationship, or that the exponents cluster around $2/3$ (Price et al., 2007). Interspecific variation in allometry along climatic gradients was substantially stronger than systematic variation within species, and for some predictors showed opposite trends. Intra-specific differences in height allometry were apparent along gradients of drought length, showing that water limits the height attainable by trees in Spain, but competition in mesic forests confounded the pattern.

Allometric regression equations are crucial to estimating aboveground biomass and carbon stocks from forest inventories, which often lack height measurements. Carbon stock estimates are highly dependent on the formulation of such equations and the errors and assumptions they incorporate (Chave et al., 2005). In this study we demonstrate that using a large dataset it is possible to quantify for a large number of species both region-scale variation in allometry and individual species' changes in response to climatic gradients. Improvements in the accuracy of allometric equations will lead to better estimates of current biomass and carbon stocks, and climate-dependent allometric equations will improve estimates for the future.

Author contributions

Designed the study: Emily Lines with support from Drew Purves, Miguel Zavala and David Coomes.
Provided the data: Miguel Zavala. Analysed the data and performed statistical analysis: Emily Lines.
Wrote the paper: Emily Lines with supervisory support from David Coomes, Miguel Zavala and Drew Purves.

5 Inferences from aggregated count data using Approximate Bayesian Computation: deriving juvenile recruitment rates from inventory data

Abstract

Approximate Bayesian Computation (ABC) is a powerful likelihood-free approach to model fitting which may be used to parameterise models of unobserved processes by simulating data. In this study we demonstrate a practical application of ABC by fitting models of juvenile recruitment, growth and mortality to sapling count data obtained from the Spanish forest inventory, which is typical of many national inventories in providing a rich source of data for large tree demographic rates, but little information on small trees, despite the importance of the juvenile life-stage for forest succession and dynamics. Using a sequential Monte Carlo (ABC-SMC) approach, we find that ABC methods provide an effective approach to deriving unobserved juvenile recruitment rates from small tree count data provided by the inventory. We utilised priors for growth and mortality rates derived from the more detailed adult inventory data.

Recruitment rates varied among species, with conifers having significantly higher rates than angiosperms in open areas, but that their rates also decreased the most under dense canopies. The change in recruitment rates from open to dense plots was significantly correlated with the species' shade tolerance, as was the effect of increased canopy cover on both growth and mortality rates.

Recruitment rates derived using this approach were in keeping with what is known about the species' life histories, suggesting that ABC may be a valid approach for tackling this type of problem. We suggest that ABC methods may have many applications for ecological modelling, particularly in situations where data collection is expensive, difficult or impossible (for example to derive historical dynamics), as well as to parameterise models whose likelihoods are prohibitively complex to compute.

5.1 Introduction

Complex, computationally-intensive process-based simulation models are vital tools in many areas of ecological research and parameterisation of demographic processes is a major part of building realistic models. Methods such as Markov Chain Monte Carlo (MCMC) and simulated annealing allow the parameterisation of complex functions from data but require the computation of a likelihood function, for which the calculation of the probability of the data given a model is needed. For many situations this may be too computationally intensive to be practical, for example where the probability of a model relies on summing over very large numbers of hidden states (Beaumont, 2010). For other models the data needed to accurately describe processes may be unavailable or impractical to collect, leading to unsatisfactory approximations or forced simplification of model structure.

Approximate Bayesian Computation (ABC) methods are a significant advance for fitting models to data when the likelihood cannot be formulated or is computationally prohibitive to analyse (Sisson et al., 2007). They provide a means of estimating parameters to describe fine-scale complex processes but for which only coarse-scale, aggregated data are available, for example to estimate disease transmission dynamics when only data on clusters of cases with identical genotypes are available (Tanaka et al., 2006). These techniques typically take a truly Bayesian, yet likelihood-free, approach to parameterising models by incorporating both summary data and prior knowledge of unobserved processes to estimate parameter values where traditional methods present no mathematically rigorous approach. Over the last decade, these likelihood-free ABC methods have increasingly been applied to data in areas of biology such as epidemiology (e.g. Tanaka et al., 2006) and population genetics (e.g. Foll et al., 2008), but have barely reached ecology (but see Jabot and Chave, 2009;) and we know of no examples using ABC methods combined with large-scale ecological data to estimate unobserved demographic processes.

Modelling the performance of juvenile trees using data collected in permanently marked inventory plots provides an excellent opportunity to test ABC methods in an ecological context. Juvenile responses to competition form a central component of predictive models of forest succession and dynamics, because the juvenile stage of the life-cycle is a critical filter (Shibata and Nakashizuka, 1995; Kobe, 1996), yet permanent plot datasets rarely contain detailed information on juveniles. For example, the Spanish Forest Inventory (IFN) (MMA, 1996, 2007) is typical of many datasets originally collected for timber stock evaluations in that it systematically sampled millions of mature trees in thousands of locations across the country, but contains no information on the performance of individual trees < 7.5 cm in diameter, with only categorical and count data being recorded. This lack of detailed data for many species is a major stumbling block to the development of a forest dynamics model for Spain.

In this study we infer the underlying dynamics of juvenile recruitment (defined in our model as the annual rate of establishment of stems of 1 cm DBH), growth and survival from large-scale aggregated juvenile data and examine their response to changes in competitive environment.

Accurate representation of dispersal and recruitment limitation is vital to produce realistic simulations of succession and spatial dynamics (Ribbens et al., 1994). Models of recruitment within simulation models often estimate rates at the stand level (Porté and Bartelink, 2002), and vary in their treatment of seedling dispersal and recruitment. The simplest models assume that seed is always available for regeneration (Clark et al., 1998), whilst others treat recruitment as a function of asymmetric competition for light and shade tolerance (Busing, 1991) or simply a function of total stand basal area and basal area of conspecifics (Kolbe et al., 1999). Many do not explicitly model the steps of seed dispersal, germination and establishment together but combine them in one process (Price et al., 2001; Busing and Mailly, 2004). On the other hand, spatially-explicit individual-based forest simulation models typically model recruitment using a seed dispersal kernel, where seedlings establish in a location with probability related to the distance to conspecific adults, and the number of seedlings established per adult varies with species, adult size and shading from adult trees (e.g. Busing, 1991; SORTIE, Pacala et al. 1996; TROLL, Chave, 1999).

The presence and density of conspecific adults and competition for light are well-recognised determinants of seedling recruitment (e.g. Gómez-Aparicio et al., 2006), but many other factors may affect seedling dynamics. For example, small scale spatial heterogeneity and microsite quality are important for seedling establishment (Nathan and Muller-Landau, 2000), although such effects are difficult to measure and quantify. Canopy gaps and competition from understory shrubs (Beckage et al., 2000), soil moisture, drought and precipitation (Lloret et al., 2004; Gómez-Aparicio et al., 2008; Urbieto et al., 2008; Mendoza et al., 2009), facilitation through protection from water stress and direct sunlight by 'nurse' plants (Lookingbill and Zavala, 2000; Gómez-Aparicio et al., 2004, 2008; Smit et al., 2008; Plieninger et al., 2010), and fire frequency (Lloret et al., 2003) have all been found to affect seedling recruitment.

Improved knowledge of recruitment processes is a pressing need given the widespread concern about low regeneration rates in Spanish forests (e.g. Plieninger et al., 2010; Urbieto et al., 2011). However, most studies of recruitment rates in Spanish forests have focussed on a very small number of species in a few locations. The national scope of the Spanish Forest Inventory allows the examination of recruitment rates of many species across the whole region.

Using a simple simulation model, we use ABC methods to infer best-fit parameters for each process for different species by comparing simulated with observed data, and choosing those which best predict the data to within a defined 'tolerance' level. We believe that the approach presented here is applicable to estimating functions for use in individual based simulation models when individual-based data are not available, and that the use of ABC methods will enable the parameterisation of ecological models for which data is difficult or impossible to obtain. Due to the small amount of data

available for several of the species (Table 6.1) we examined only the effects of two commonly used variables, conspecific adult density and competition for light (represented by canopy area of tall trees), on recruitment rates, and fitted recruitment as:

$$\text{Recruitment (\# new stems /ha/year)} = p_0(\text{conspecific adults})\exp(-p_1(\text{competition for light}))$$

However, we believe that the method used here could be used to model more complex processes affecting recruitment for the most common species and/or through the use of prior information from other studies. Our function predicts that recruitment increases with conspecific adult canopy area (which is proportional to basal area) and decreases with total canopy area - which is a measure of competition for light.

5.2 ABC Algorithms

Conceptually, ABC algorithms are as easy to understand as any basic parameter space-searching algorithm. To illustrate the idea of ABC we first describe a simple ABC rejection algorithm (Tavaré et al., 1997; Pritchard et al., 1999; Beaumont et al., 2002). Suppose we wish to fit a given model M which depends on some unknown parameter set p . Without observed data (y_0) we cannot use a traditional likelihood method to estimate the parameter set p . However, with one or more observed summary statistics of data $S(y_0)$ we can still infer values of the parameter set by sampling from a distribution that approximates the posterior. For example, given a simulation model M and summary statistic(s) S , a simple ABC rejection algorithm would be as follows:

BASIC ABC REJECTION ALGORITHM:

1. Sample a candidate model parameter set \hat{p} from the prior $\pi(p)$.
2. Generate a simulated dataset using the model M , $\hat{y} \sim f(y|\hat{p})$.
3. From the simulated data \hat{y} , calculate the summary statistic(s) $S(\hat{y})$.
4. Using a given metric d and tolerance level ε , compare the observed ($S(y_0)$) and predicted ($S(\hat{y})$) summary statistic(s). If $d(S(y_0), S(\hat{y})) \leq \varepsilon$, accept parameter set \hat{p} , if not, reject the parameter set and return to step 1. (Eqn 5.1)

Each accepted simulated dataset generated in this algorithm is an independent sample from the distribution $\pi(p|d(S(y_0), S(\hat{y})) \leq \varepsilon)$, and if ε is small enough, this will approximate the true posterior $\pi(p|y)$. This method is likely to be extremely slow to converge without a good knowledge of the prior; many improvements have been suggested to improve speed of convergence and to ensure efficient searching of parameter space (Marjoram et al., 2003; Del Moral et al., 2006; Sisson et al., 2007; Toni et al., 2009).

In this study we use an ABC Sequential Monte Carlo (SMC) approach first proposed by Sisson et al. (2007) and later amended to correct a bias by Beaumont et al. (2009). Although random walk ABC-MCMC algorithms have been described (e.g. Marjoram et al., 2003), parameter chains risk spending long periods of time in areas of low probability and, since samples may be highly correlated, very long chains are likely to be needed (Toni et al., 2009). The main advantage of SMC methods is that they bypass the risk of collecting a set of highly correlated samples by repeatedly sampling from a series of approximations to the posterior with decreasing tolerance levels, within which samples are not correlated (Sisson et al., 2007). ABC-SMC works as follows: at each iteration t from $t=1$ to $t=T$, N independent particles (parameter sets) are sampled from the distribution $\pi(p|d(S(y_0), S(\hat{y})) \leq \varepsilon_t)$ with a defined decreasing vector of tolerances $\varepsilon_1 > \varepsilon_2 > \dots > \varepsilon_T \geq 0$. Particles are sampled from weighted samples (with weights $\omega_i^{(t)}$) from the previous distribution, ensuring that particles that better approximate $\pi(p|y)$ are re-sampled more often, and those that are a poor fit are discarded. The version of the algorithm we used is taken from Beaumont (2009) (but is very similar to those given by Sisson et al., 2009; Toni et al., 2009). We constructed the algorithm (using C code) as follows:

ABC-SMC ALGORITHM:

1. When $t=1$, for $i=1 \dots N$
 - a. Sample a particle from the prior, $p_i^{(1)} \sim \pi(p)$, and generate $\hat{y} \sim f(y|p_i^{(1)})$ until $d(S(y_0), S(\hat{y})) < \varepsilon_1$,
 - b. Set all weights equal, as $\omega_1^{(1)} = 1/N$,
 - c. Set Σ_1 to be twice the empirical variance of particles $\{p_j^{(1)}\}$.
2. For $t=2 \dots T$
 - a. For $i=1 \dots N$
 - i. Sample particle p^* from the previous distribution $\{p_j^{(t-1)}\}$ with weights $\omega_j^{(t-1)}$,
 - ii. Perturb the particle according to a transition kernel, $p^* \sim N(p^*, \Sigma_{t-1})$, and generate $y^{**} \sim f(y|p^{**})$,
 - iii. If $d(S(y_0), S(y^{**})) < \varepsilon_t$, set $p_i^{(t)} = p^{**}$, otherwise return to **2ai**.

- b. For $i=1 \dots N$

Calculate the weight of each particle according to:

$$\omega_i^{(t)} \propto \frac{\pi(p_i^{(t)})}{\sum_{j=1}^N (\omega_j^{(t-1)} K_t(p_i^{(t)}, p_j^{(t-1)}))}$$

where $K_t(p_i^{(t)}, p_j^{(t-1)})$ is the multinormal density with variance Σ_{t-1} .

- c. Set Σ_t to be twice the empirical variance of particles $\{p_j^{(t)}\}$. (Eqn 5.2)

5.3 Materials and Methods

5.3.1 Data

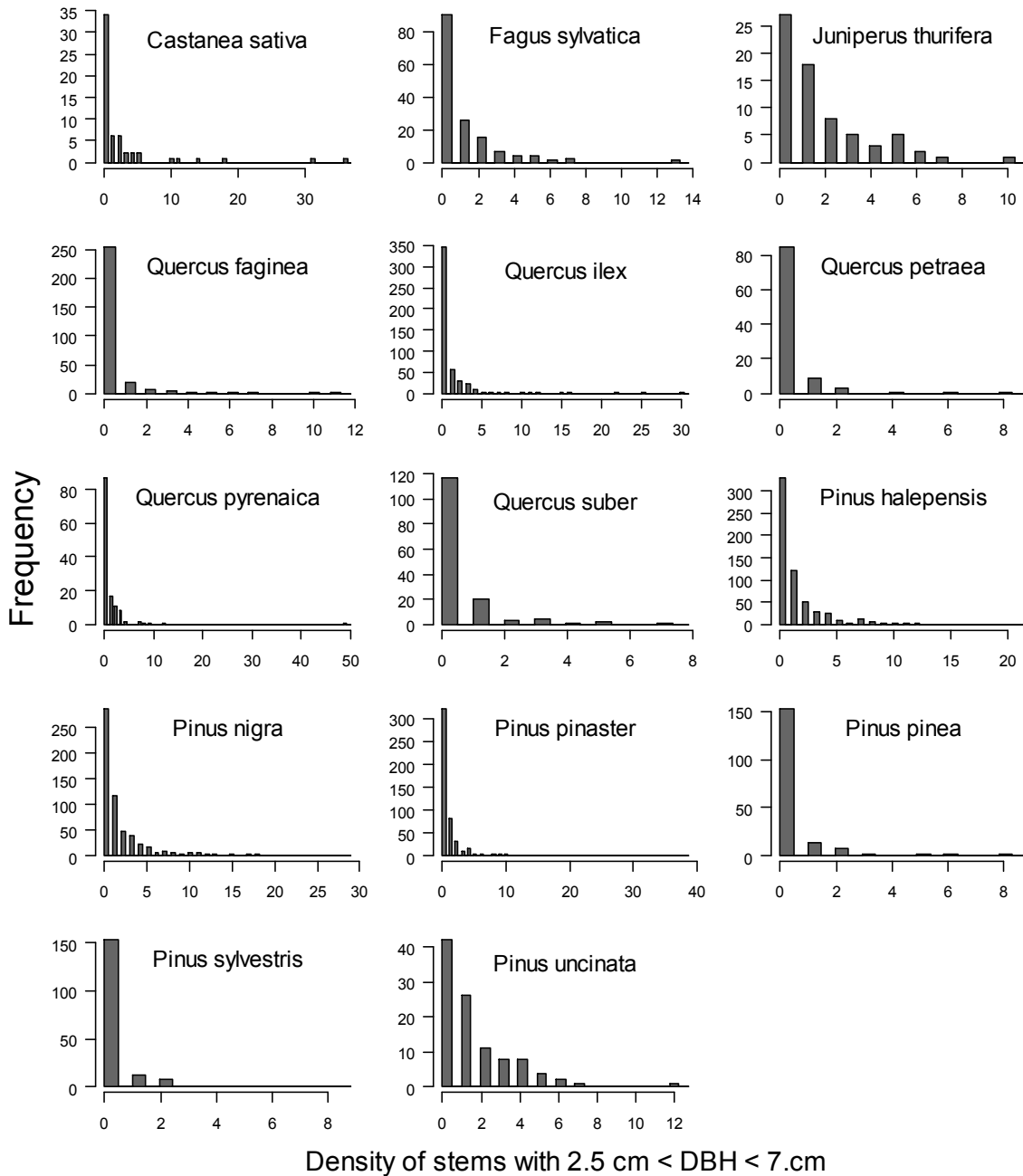
The inventory data used for this study came from the second and third Spanish Forest Inventory (IFN2 and IFN3; MMA, 1996, 2007), sampled from over 70,000 remeasured plots arranged systematically on a 1 km² grid across Spain. The IFN plots were sampled using a variable radius technique, whereby trees of different sizes were measured in concentric plots of varying size. All trees of DBH > 7.5 cm were measured in a plot of radius 5 m, all of DBH > 12.5 cm in a plot of radius 10 m, all of DBH > 22.5 cm in a plot of radius 15 m and all of DBH > 42.5 cm in a plot of radius 25 m. Although no individual sapling data were recorded, densities of large juveniles (heights > 130 cm and DBH in the range 2.5-7.5 cm) were recorded within the central 5 m radius plot in IFN3.

We selected plots for recruitment modelling carefully so as to fit only recruitment which arises during succession, i.e. we removed data that could have arisen from pulses of recruitment following large scale disturbances such as fire, as we did not have information on the occurrence or impact such events. Our criteria were: 1) plots must be thinning (stand density decreasing and mean stem size increasing over the time period of the two surveys)- around 26% of the remeasured plots, 2) juveniles must have been recorded as being of 'natural' origin in the inventory, and 3) plots must have at least one adult (DBH>7.5 cm) of the species of interest in IFN2 plot (largest 25 m radius plot). There was no record of whether the recorded stems were resprouts (a feature of some Spanish tree species; Grove and Rackham, 2001) or saplings, so we were unable to differentiate between these two cases. We selected the 14 species with at least 50 plots matching these criteria to parameterise the model, comprising seven conifers (*Pinus pinea*, *P. halepensis*, *P. pinaster*, *P. sylvestris*, *P. uncinata*, *P. nigra*, *Juniperus thurifera*) and seven angiosperms (*Quercus faginea*, *Q. ilex*, *Q. suber*, *Q. petraea*, *Q. pyrenaica*, *Fagus sylvatica* and *Castanea sativa*). Number of plots selected for each species are shown in Table 5.1. Histograms of the number of large juveniles in each selected plot for each of these species are shown in Fig. 5.1.

We expected recruitment to be proportional to conspecific adult density (potential parent trees) and be negatively affected by aboveground competition for light. We chose to use crown area to represent both these processes, which has been used to represent asymmetric competition within forest dynamics models (e.g. Bohlman and Pacala, 2011; Caspersen et al., 2011; Coomes et al., 2012). We calculated total crown area and total basal area of adults (stems > 7.5 cm DBH) of each plot and each species for both inventories using adult data, and used these as measures of conspecific density and competition (Caspersen et al., 2011; Coomes et al., 2012). For each plot we defined two values, the crown cover of adults of the species of interest (CAI_{sp} , m²/ha) and of all adults on the plot (CAI_{pl}), using species-specific crown width allometric equations derived from data collected on a subset of IFN2 sites (see text and Tables C.1-C.3, Fig. C.1 in Appendix C page 141). We also calculated basal

area of each species (BA_{sp} , m^2/ha) and all species on the plot (BA_{pl}). In order to compare recruitment rates among species we took shade tolerance scores from Niinemets and Valladares (2008), and when species-specific values were not available we took genus averages.

Figure 5.1 Histograms of the recorded number of large juveniles in the central 5 m radius circular subplot of each selected plot for each of the 14 species. Total numbers of plots used for each species are given in Table 5.1.



5.3.2 Prior information for growth and mortality rates

Many combinations of recruitment, growth and mortality rates may combine to give the observed juvenile density patterns, yet not all are reasonable given prior knowledge of demographic processes. We used information from larger trees in the inventories to construct priors for parameters for growth and mortality rates of juveniles. We fit species-specific growth and mortality functions to data from trees between 7.5 and 10 cm DBH that had been remeasured in the inventory (see Tables C.4 and C.5 in Appendix C page 149). For both processes, we tested several alternative models and used Akaike Information Criteria (AIC: Akaike, 1974) to select the best models for the largest number of species (see Appendix C page 141). The best fit models were size-independent models but included the canopy area of taller trees in the plot (CAI_h) as a measure of competition:

$$\begin{aligned} \text{Annual growth rate (cm/year)} &= p_2/(1+ p_3CAI_h) \\ \text{Annual mortality rate (stems/year)} &= \text{logistic}(p_4+ p_5CAI_h) \end{aligned} \quad (\text{Eqn 5.3})$$

where p_2 - p_5 are fitted parameters (see text and Tables C.4-C.7 and Figs. C.2 and C.3 in Appendix C page 141). These functional forms (Fig. 5.2) were used within the simulation model, and their parameter values were estimated during the ABC-SMC algorithm with strong priors defined by the values estimated from the adult data. As the inventory data contained only trees > 7.5 cm DBH, and we simulated juveniles of < 7.5 cm DBH only, when including these rates within the simulation model we took $CAI_h = CAI_{pl}$, the total canopy area of trees in the plot > 7.5 cm DBH (so it took the same value for all simulated juveniles).

5.3.3 Simulation model

In order to estimate juvenile recruitment, growth and mortality rates we constructed a model which simulated the size structure and density of juveniles given a set of parameter values. The model was based on a simple forest stand dynamics model (the PPA, Purves et al. 2008) which predicts the fate of cohorts of individuals of the same species and age rather than individual stems, and therefore does not contain spatial references. We simulated cohorts C_i (introducing a new one at each time step) within a 5 m radius circular plot to make comparison with our data sample, over T years (time steps), and recorded their densities $den_{i,t}$ (#stems / 5m radius plot) at each timestep and diameters $DBH_{i,t}$ (cm), producing a predicted size distribution with corresponding density of juveniles in the 5 m radius plot. The simulation model ran as follows:

SIMULATION MODEL:

For each time step ($t=1\dots T$)

For each plot ($p=1\dots P$)

1. For all existing cohorts ($i=1\dots N$)

a. Kill off a proportion according to the mortality rate:

$$den_{i,t} = (1 - P(\text{mortality}_{i,t-1})) \times den_{i,t-1}$$

b. Increase the size of trees in the cohort according to growth rate:

$$DBH_{i,t} = DBH_{i,t-1} + \text{growth}$$

2. Create a new cohort of DBH = 1 cm and density according to the recruitment rate.

3. $N=N+1$. (Eqn 5.4)

Mortality and growth rates were as in equation 5.3. We fitted recruitment rates as:

$$\text{Recruitment (\#stems 1cm DBH/ha/year)} = p_0 CAI_{sp} \exp(-p_1 CAI_{pl}) \quad (\text{Eqn 5.5})$$

which allowed the recruitment rate within the central 5 m radius plot to vary with the crown area of conspecifics (CAI_{sp}) in the larger 25 m radius plot, and included an effect of shading and competition effect by total plot crown area (CAI_{pl}). Although the prior distribution for p_1 was set to be $U(0,15)$ (i.e. the prior was positive), the ABC-SMC was able to sample negative values for this parameter (for example to represent a facilitation effect of aboveground competition for species found in areas of intense drought). We chose to use crown area rather than the more common basal area (or some function of it, e.g. Ribbens et al., 1994) as it had provided a better fit to the data as a predictor in the growth and mortality functions (see Tables C.4 and C.5 in Appendix C, page 149).

Since both CAI_{sp} and CAI_{pl} changed in each plot between the two inventories for the first part of the simulation model we used values calculated from IFN2, but varied these during the final 10 time steps (corresponding to an average 10-year time interval between inventories) using a simple linear relationship between the measurements calculated from IFN3 data. This meant that for the first period of the simulation model the conspecific canopy and aboveground competition was held constant but in the second part it varied according to the observed canopy area dynamics between the two inventories.

5.3.4 Assessing the algorithm on test data: method

We initially tested the ability of the method to recover parameter values from simulated test data created using the structure of the inventory but replacing juvenile counts with counts simulated with known parameter values. To create the simulated data we took the inventory data for a common species - *Pinus sylvestris* - and our calculated values of CAI_{pl} and CAI_{sp} for each plot in which it was found. We simulated juvenile densities using the simulation model described above. We specified growth, recruitment and mortality models as given in equations 5.3 and 5.5. We ran the model for 200 iterations (each representing a year) to ensure that in all plots there were stems of at least 7.5 cm

DBH. We simulated two different datasets, with and without variability in the parameters. For the dataset without variability we simply simulated data using fixed parameter values (p_0 - p_6 in equations 5.3 and 5.5) as follows:

$$p_0=2; \quad p_1=0.8; \quad p_2=0.45; \quad p_3=1.75; \quad p_4=-5.6; \quad p_5=1.28 \quad (\text{Eqn 5.6})$$

To create variability within the data, during the creation of the simulated data, at each time step and for each cohort we drew values of the parameters from specified normal distributions:

$$p_0 \sim N(2, 0.2^2); \quad p_1 \sim N(0.8, (0.08)^2); \quad p_2 \sim N(0.45, (0.045)^2); \\ p_3 \sim N(1.75, (0.18)^2); \quad p_4 \sim N(-5.6, (0.56)^2); \quad p_5 \sim N(1.28, (0.13)^2)$$

To test whether the ABC algorithm was able to reproduce the parameters, we fitted the ABC-SMC sampler to the simulated data. We set uniform priors ($\pi(\cdot)$) on the recruitment parameters (p_0 - p_1): $\pi(p_0) \sim U(0,5)$; $\pi(p_1) \sim U(0,2)$. We set normal priors on the growth and mortality parameters (p_2 - p_5) which were informative but randomly chosen: we drew a mean value for each parameter from normal distributions with mean values as given in equation 5.6 and standard deviations of 0.05. Standard deviations for the priors were set as 5% of the selected mean. Priors were used as initial sampling distributions for all parameters.

The choice of metric used to compare predicted and observed densities can affect the convergence of the algorithm (Beaumont et al., 2009), and we therefore tested two metrics, d_1 and d_2 , to compare the predicted and observed densities (P_{den} and O_{den}):

$$d_1 = \sum_{\text{plots}} |P_{\text{den}} - O_{\text{den}}|; \quad d_2 = \sqrt{\sum_{\text{plots}} (P_{\text{den}} - O_{\text{den}})^2}; \quad (\text{Eqn 5.7})$$

We ran 10-20 iterations of the ABC-SMC algorithm using 100 particles on the four data-metric combinations. We set tolerance levels as a multiple of the number of plots simulated and decreased levels by 5% at each iteration, and continued to decrease the tolerance level until the algorithm was unable to find parameter values satisfying it.

5.3.5 Performance of the algorithm on test data and choice of metric

For both sets of simulated test data the ABC-SMC algorithm was able to recover the parameters of interest, although as expected parameter values were better recovered for the data without variation, with much tighter ranges in fitted values (Fig. 5.3). However, we did find that parameterisations run using metric d_1 (equation 5.7) were much better able to recover the true parameter value than those using d_2 , (Fig. 5.3), for both sets of simulated test data (with and without variation in parameter values). We therefore chose to use metric d_1 to fit parameters with the real data.

5.3.6 Implementation of the ABC-SMC algorithm on the inventory data

We used the fitted growth and mortality parameters (given in Tables C.6 and C.7 in Appendix C page 150) as prior means for the parameters p_2 - p_5 , (equation 5.3), with standard deviations set as 2% of the prior value, and the prior distribution was used as the initial sampling distribution. Priors for the parameters p_0 and p_1 (equation 5.5) were set as $U(0,15)$ with initial sampling distribution $U(0,5)$. We

simulated cohorts from 1 cm DBH and summed densities of all cohorts with DBH values between 2.5 and 7.5 cm to give the same form as the count data presented in the inventory. We used metric d_I (equation 5.7) to compare predicted and observed densities, as this had performed better in the simulated data example. Starting and final tolerance levels varied between species according to how well the model fitted the data. Tolerances were defined as a multiple of the number of plots for each species, with starting values in the range 0.9-0.1, and reduced by 25% at each simulation step (t in equation 5.2). We used the means of the predicted values of parameters p_0 and p_1 (equation 5.5) to compare recruitment rates among species.

Table 5.1 The fourteen species included in the analysis and the number of plots used, as well as their shade tolerance scores (from Niinemets & Valladares, 2008). The predicted average recruitment rates (number of 1cm DBH stems $ha^{-1} year^{-1}$), the predicted annual growth ($cm year^{-1}$) and predicted annual mortality rate (stems $stem^{-1} year^{-1}$), all calculated in a fixed environment ($0.25 ha ha^{-1}$ conspecific adult crown area (CAI_{sp}) and $0.5 ha ha^{-1}$ total adult crown area of the plot (CAI_{pl})), are also shown (see equation 5.5 for rate equations).

Species	Number of plots	Shade tolerance	Recruitment rate in fixed environment	Annual growth rate in fixed environment	Annual mortality in fixed environment
<i>Castanea sativa</i>	58	3.15	4.740	0.258	0.035
<i>Fagus sylvatica</i>	150	4.56	0.899	0.210	0.005
<i>Juniperus thurifera</i>	70	1.61	1.238	0.075	0.006
<i>Pinus halepensis</i>	600	1.35	3.009	0.177	0.019
<i>Pinus nigra</i>	583	2.1	5.427	0.193	0.013
<i>Pinus pinaster</i>	488	1.35	1.038	0.262	0.042
<i>Pinus pinea</i>	178	1.35	0.240	0.249	0.026
<i>Pinus sylvestris</i>	691	1.67	1.619	0.264	0.010
<i>Pinus uncinata</i>	103	1.2	5.148	0.176	0.009
<i>Quercus faginea</i>	294	2.88	0.093	0.122	0.007
<i>Quercus ilex</i>	489	3.02	0.159	0.131	0.008
<i>Quercus petraea</i>	100	2.73	0.165	0.165	0.004
<i>Quercus pyrenaica</i>	131	2.88	1.142	0.140	0.015
<i>Quercus suber</i>	148	3.02	0.182	0.143	0.012

5.4 Results from inventory data

5.4.1 Convergence of the ABC-SMC algorithm

Convergence of the parameters varied among species, with the 95% credible intervals smallest for recruitment parameters of the species with more data (Fig. 5.4). It is difficult to interpret the effect on recruitment rates from individual parameter values alone, as CAI_{pl} and CAI_{sp} will always at least partially covary (as $CAI_{sp} \leq CAI_{pl}$). All species showed decreases in growth and increases in mortality with increasing CAI_{pl} , with angiosperms showing less response than conifers (Fig. 5.2). Growth and mortality parameters, which were strongly constrained by priors, converged much more strongly with 95% credible interval limits on average just 3% from the prior value (Fig. 5.4), however when we re-ran the model with much larger standard deviations on the growth and mortality rates we found that the convergence of the recruitment rates was substantially reduced (data not shown).

5.4.2 Average recruitment rates and the effect of canopy cover

Both average recruitment rates (Table 5.1) and how competition affected species (Fig. 5.5) varied across species, with most species showing a strong negative response to increased whole-plot density (CAI_{pl}). One species, *C. sativa*, showed almost no reduction in recruitment rates in the most dense plots and had the highest recruitment rates in all but the most open areas (Fig. 5.6). In open, low density plots, angiosperm species had lower average recruitment rates than conifer species (Fig. 5.6a) though the difference was weak (t test $p < 0.1$). The two evergreen Mediterranean oak species (*Q. ilex* and *Q. suber*), along with the semi-deciduous *Q. faginea* had low recruitment rates in all environments. On average the Mediterranean species had lower recruitment rates in the fixed environment of $0.25 \text{ ha ha}^{-1} CAI_{sp}$ and $0.5 \text{ ha ha}^{-1} CAI_{pl}$ (0.85 vs 2.73 , Table 5.1) but the difference was only weakly significant (Spearman's $p < 0.1$) and disappeared in higher density plots.

Among species, we found a significant positive correlation between the mean fitted values of the two recruitment parameters (p_0 and p_1 in equation 5.5) (Spearman's $p < 0.05$), so that species with higher recruitment rates in open areas were also more negatively affected by increased competition from canopy cover overhead. This corresponded to a split in recruitment rates under different plot conditions between angiosperm and conifer species. In low density, monospecific plots ($CAI_{sp} = CAI_{pl} = 0.25 \text{ ha ha}^{-1}$), conifer species had higher recruitment rates than angiosperms (Fig. 5.6b), but this difference disappeared in more dense plots as the conifer species had much stronger negative responses to increases in CAI_{pl} than angiosperm species (Fig. 5.6b). There was a significant negative correlation between shade tolerance and the change in recruitment rate from low to high density stands (Pearson's $p < 0.05$ between shade tolerance and the difference between predicted rates in a plot with $CAI_{sp} = CAI_{pl} = 0.25 \text{ ha ha}^{-1}$ and in a plot with $CAI_{sp} = 0.25 \text{ ha ha}^{-1}$ and $CAI_{pl} = 1 \text{ ha ha}^{-1}$), with the most shade intolerant species suffering the largest drops in recruitment rate with higher canopy cover.

Figure 5.2 Predicted growth and mortality rates used as priors for the simulation mode (equation 5.5, tables C.2 and C.3) for the 14 species across the range of competitive environment (crown area of taller trees CAI_h) in which they are found. Species are split into four groups according to type and geographical distribution: Mediterranean conifer (*Pinus pinea*, *P. halepensis*, *P. nigra*, *P. pinaster*, *Juniperus thurifera*), temperate conifer (*P. sylvestris*, *P. uncinata*), Mediterranean angiosperm (*Quercus faginea*, *Q. ilex*, *Q. suber*) and temperate angiosperm (*Q. petraea*, *Q. pyrenaica*, *Fagus sylvatica*, *Castanea sativa*).

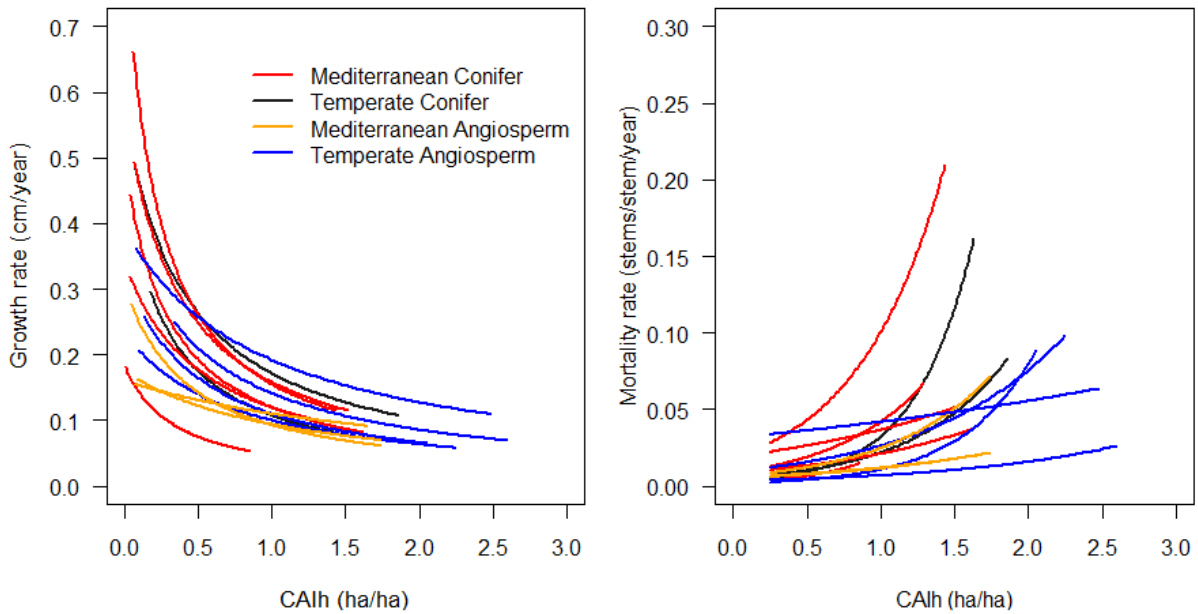


Figure 5.3 Estimated parameter values for simulated test data without and with variation in the data, fitted using two different metrics (equation 5.7). True values of each parameter are shown by the dotted red line. Metric 1 was better able to recover the true parameter values.

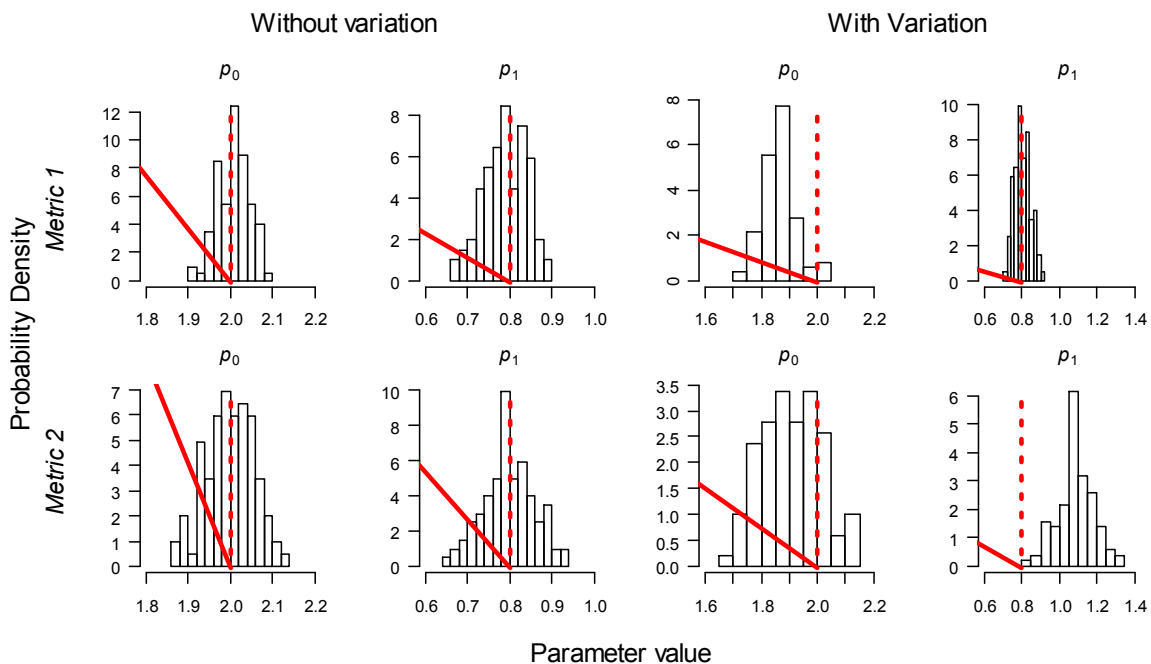


Figure 5.4 Fitted mean values and 95 % credible intervals for each of the six parameters (equation 5.3 and 5.5) estimated in the ABC-SMC algorithm for each of the 14 species (Species abbreviations: *P. sy* = *Pinus sylvestris*, *P. un* = *P. uncinata*, *P. pa* = *P. pinea*, *P. ha* = *P. halepensis*, *P. ni* = *P. nigra*, *P. pr* = *P. pinaster*, *J. th* = *Juniperus thurifera*, *Q. pe* = *Quercus petraea*, *Q. py* = *Q. pyrenaica*, *Q. fa* = *Q. faginea*, *Q. il* = *Q. ilex*, *Q. su* = *Q. suber*, *F. sy* = *Fagus sylvatica*, *C. sa* = *Castanea sativa*).

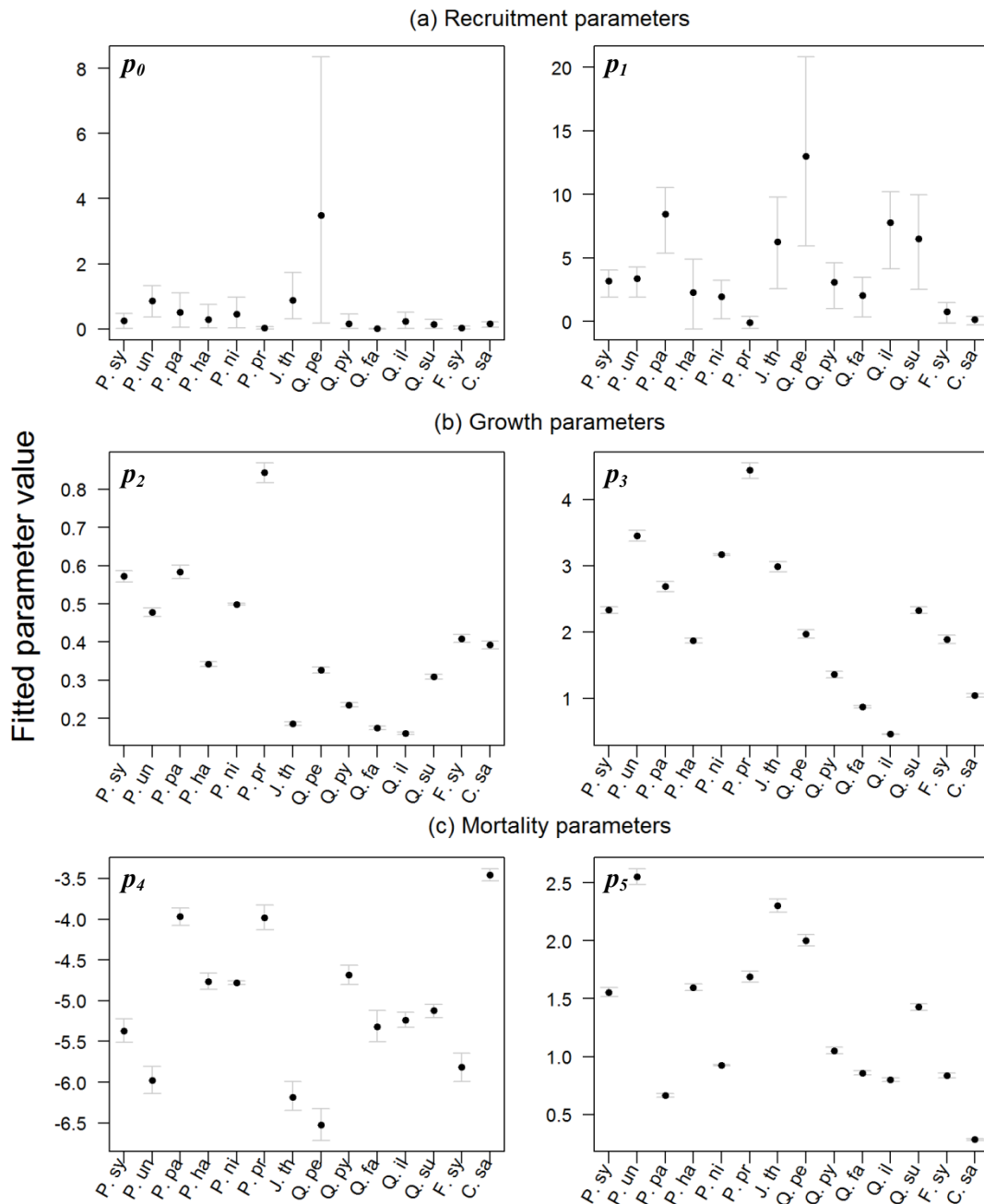
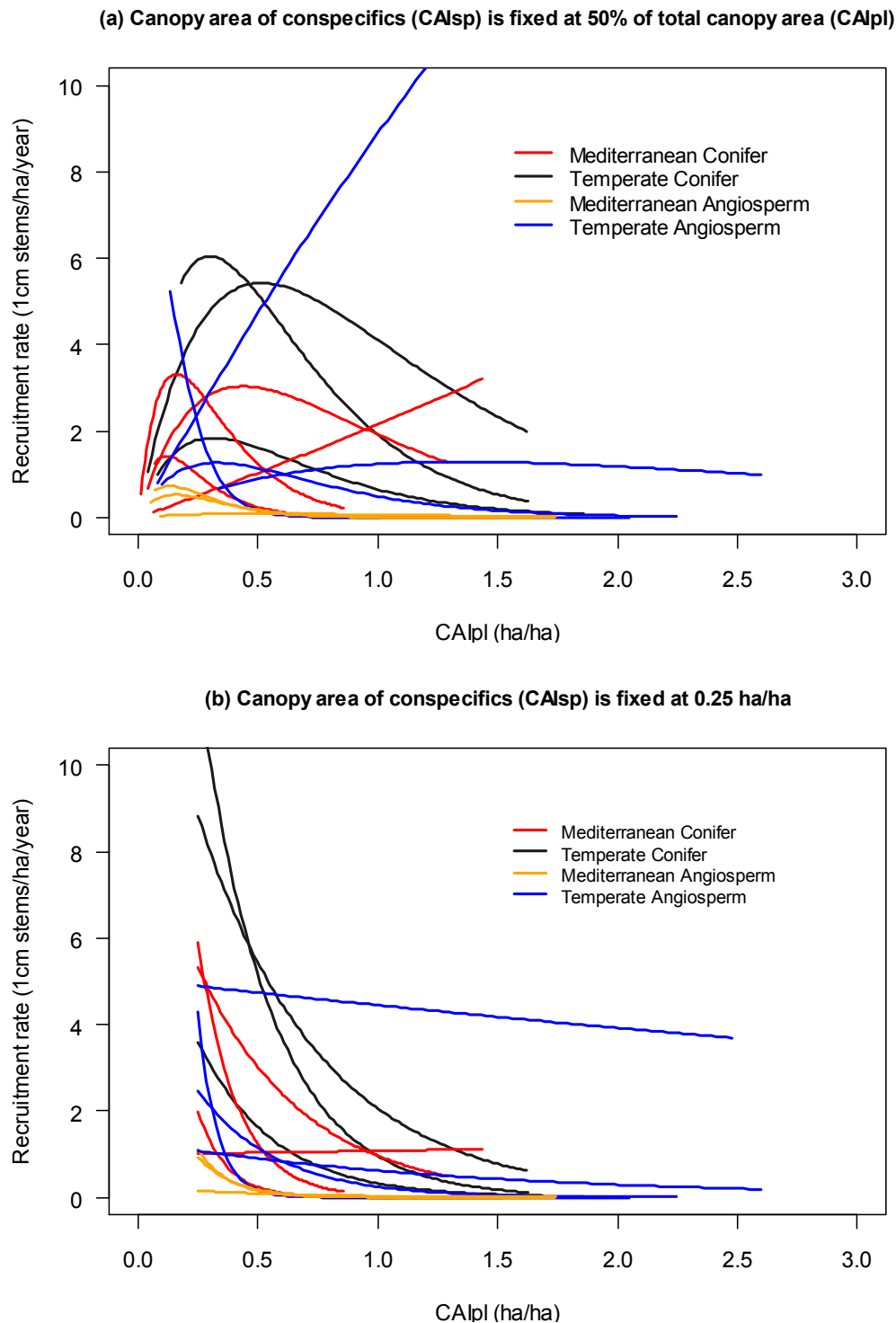


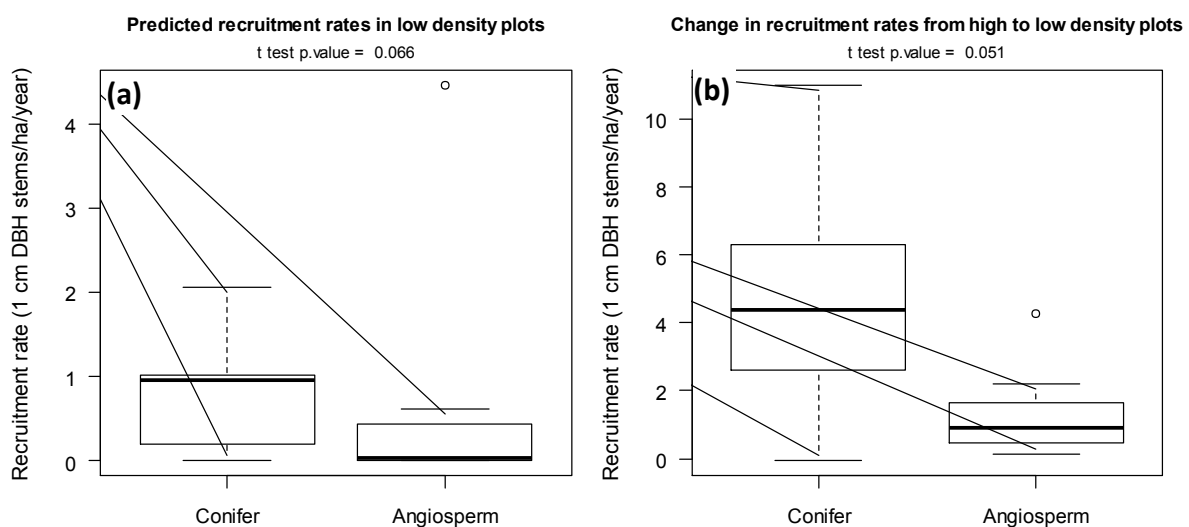
Figure 5.5 Predicted recruitment rates (number of new 1 cm stems $\text{ha}^{-1} \text{year}^{-1}$) for each of the 14 species plotted along the range of plot canopy area (CAI_{pi}) in which they are found, with CAI_{sp} as a) a fixed proportion of CAI_{pi} , and b) fixed at $\text{CAI}_{sp} = 0.25 \text{ ha ha}^{-1}$. Species are split into four groups according to type and geographical distribution: Mediterranean conifer (*Pinus pinea*, *P. halepensis*, *P. nigra*, *P. pinaster*, *Juniperus thurifera*), temperate conifer (*P. sylvestris*, *P. uncinata*), Mediterranean angiosperm (*Q. faginea*, *Q. ilex*, *Q. suber*) and temperate angiosperm (*Q. petraea*, *Q. pyrenaica*, *Fagus sylvatica*, *Castanea sativa*).



5.4.3 Relationships between recruitment, growth and mortality

Average recruitment rates in the fixed environment ($0.25 \text{ ha ha}^{-1} \text{ CAI}_{sp}$ and $0.5 \text{ ha ha}^{-1} \text{ CAI}_{pl}$) did not correlate with growth or mortality rates, though species with higher growth rates had significantly higher mortality rates (Spearman's $p < 0.05$, Table 5.1). We found a significant negative correlation between parameters p_0 and p_4 (equations 5.3, 5.5), suggesting that in open areas the species with the highest recruitment rates also had the lowest mortality rates. Across species and rates the effect of competition was not consistent, with no correlation between either p_3 (the effect of CAI_{pl} on growth) or p_5 (the effect of CAI_{pl} on mortality) and p_1 (the effect of CAI_{pl} on recruitment), nor was there a correlation between the change in growth or mortality rates from low to high density plots with the change in recruitment rates. There was however a positive correlation between p_3 (the effect of CAI_{pl} on growth) and p_5 (the effect of CAI_{pl} on mortality) (equation 5.5), so that species whose growth rates dropped most in more dense plots had the largest increases in mortality rates (Spearman's $p < 0.05$). Among species, the effect of CAI_{pl} on both growth and mortality was significantly related to shade tolerance, with the most shade tolerant species being least affected by increases in canopy cover (Pearson's $p < 0.05$, negative correlation between shade tolerance and both p_3 and p_5).

Figure 5.6 Boxplots showing differences between conifer and angiosperm species in a) predicted recruitment rates in a low density plot ($\text{CAI}_{sp} = \text{CAI}_{pl} = 0.25 \text{ ha ha}^{-1}$), and b) their predicted changes in recruitment rates from low to high density plots (the predicted rate in $\text{CAI}_{sp} = \text{CAI}_{pl} = 1 \text{ ha ha}^{-1}$ plot minus the predicted rate in $\text{CAI}_{sp} = 0.25 \text{ ha ha}^{-1}$ and $\text{CAI}_{pl} = 1 \text{ ha ha}^{-1}$ plot).



5.5 Discussion

5.5.1 *Parameterisation and predicted recruitment rates*

We have demonstrated the ability of the ABC parameterisation framework to infer dynamic rates using summarised data and partial knowledge of a system. By utilising the extensive data of the Spanish forest inventory we were able to calibrate a recruitment model for a much larger number of sites and competitive conditions than could have been examined had we collected more detailed data. Since many forest inventories do not include detailed data for small trees we suggest that this method may prove useful for constructing recruitment models in other parts of the world. We found large variation in recruitment rates among species, and that, in less dense stands at least, conifer species had higher recruitment rates than angiosperms, in agreement with comparisons between Mediterranean pine and oak regeneration levels (Urbieto et al., 2011).

We found that for almost all species (with the exception of *C. sativa*) canopy density strongly negatively affected juvenile recruitment, growth and mortality rates, but that the effect was correlated with the reported shade tolerance of the species, suggesting that all aspects of juvenile dynamics are affected by aboveground competition. However, facilitative effects from neighbouring trees and shrubs are known to aid seedling survival and growth in the Mediterranean, by preventing desiccation by reducing water stress and protecting from high levels of irradiance (Gómez-Aparicio et al., 2006; Quero et al., 2006; Smit et al., 2008; Mendoza et al., 2009), with the strongest facilitation benefits reported for deciduous and *Quercus* species and the weakest for evergreen and *Pinus* species (Gómez-Aparicio et al., 2004, 2006). Therefore we might expect a positive interaction between the effect of drought length and canopy cover on recruitment for some species in the areas with the longest drought. However, the small amount of data we had for many species in this study prevented a full investigation of how large an effect facilitation might have on this process. The high predicted recruitment rates and lack of negative response to increased canopy cover for *C. sativa* may be a result of historical management of the species, which has been a very commonly planted and coppiced species in the Mediterranean (Grove and Rackham, 2001; Giudici and Zingg, 2005). This species also had some of the highest observed sapling densities (Fig. 5.1) so much of the data may be a result of multi-stemmed regeneration from stools rather than seedling establishment.

5.5.2 *Other factors affecting Mediterranean juvenile recruitment*

The low amount of data for several of our species meant that we only included the effects of conspecific adults and competition for light on intraspecific variation in recruitment rates. However, several studies have identified environmental factors affecting variation in seedling establishment and performance in the Mediterranean which may be relevant to our study area. Fine-scale site variables such as soil water content and light availability are important determinants of germination, but

responses are complex; for example both seasonal drought and waterlogging may negatively affect establishment of Mediterranean oaks (Rey Benayas, 1998; Urbietta et al., 2008).

At a larger scale, climate and topographic factors affect regeneration, though responses are different among species. For example, high rainfall has been found to increase regeneration rates of the deciduous *Q. pyrenaica* but decrease rates of the evergreen *Q. ilex* (Plieninger et al., 2010), and temperature has been found to be important for differential regeneration rates between species (Gómez-Aparicio et al., 2009), whilst in southern France grazing pressure has been found to be a primary determinant of regeneration (Chauchard et al., 2007). Climate change and in particular warming is likely to cause an upwards altitudinal shift in species' distributions, and indicators of this have been found in higher recruitment rates on higher slopes in mountainous areas for several species in mountainous areas of Spain (Camarero and Gutiérrez, 2007; Peñuelas et al., 2007).

5.5.3 Implementation of ABC

Whilst the form of the data in this study made the use of ABC methods necessary to derive annual recruitment rates, the method presented here is inefficient for parameter estimation compared to traditional likelihood-based techniques, if available. The multiple elements involved in ABC methods mean that they are not necessarily straightforward to implement, and this must be considered when specifying the algorithms. Since the algorithm relies on the design of an underlying simulation model, the careful construction of this to describe the underlying processes of interest is paramount to the success of the parameter estimation.

Methods of model selection for ABC have been suggested, for example by calculating the posterior probability of a given model over a set of other models (Toni et al., 2009; Leuenberger and Wegmann, 2010) in a method analogous to traditional Bayes' factors. One such method of model comparison approximates Bayes factors using a simple rejection algorithm (similar to equation 5.1) where model indicators are treated as categorical parameters and the ratio of acceptance rates of one model over another gives the Bayes factor (Grelaud et al., 2008). This approach may be made more efficient if it is implemented using an SMC approach (Toni et al., 2009). However, when used to compare a set of models, it can also result in less informative models being given a Bayes factor of 0, since a low tolerance level could exclude them from being selected at all.

Model parameterisation itself may be dependent on the choice of summary statistic, and many studies have suggested methods of selecting the best summary statistics (Joyce and Marjoram, 2008; Wegmann et al., 2009; Jung and Marjoram, 2011). However, it is likely to be difficult or even impossible to know if a selected set of summary statistics is sufficient (Marjoram et al., 2003) and the optimal statistics are likely to be highly dataset specific (Nunes and Balding, 2010). Although it may be intuitive to think that adding more summary statistics would improve model performance, studies have shown this is not always the case as acceptance rates can be dramatically reduced when they are based on both informative and uninformative summary statistics (Blum, 2010; Fearnhead and Prangle,

2010). The use of multiple summary statistics may also make the choice of tolerance levels difficult, as convergence of the model to reproduce multiple statistics well may not be possible with variable data. The credible intervals on posterior parameter estimates arising from ABC simulation models are likely to be inflated due to a loss of information from summarising the data (Csilléry et al., 2010).

By far the most computationally expensive element of the parameterisation algorithm was the simulation model which produced new juvenile count data for each candidate parameter set, making practical application of ABC methods at least partially dependent on its efficiency. One major advantage of ABC-SMC is that, within any iteration of the model, parameter samples are independent and so simulations can be run easily in parallel on multiple CPUs or clusters. Although we constructed our own code in C to implement the algorithm, statistical packages for implementing a range of different ABC algorithms are available, including several R packages (such as *abc*; Csilléry et al., 2012) and the stand alone program *DIY-ABC* (Cornuet et al., 2008).

5.5.4 *Applications of ABC in Ecology*

We have demonstrated the ability of Approximate Bayesian Computation techniques to parameterise individual-based demographic models in a mathematically rigorous way with data that could not have been done using traditional likelihood-based techniques. These methods have been regularly adopted in some areas of biological research, and have potential applications in many areas of ecology, for example to infer unobserved historical processes that have led to an observed state of a system (e.g. Thornton and Andolfatto, 2006). These methods also allow parameter inference for stochastic models for which likelihoods cannot be constructed, for example parameters for the neutral model of biodiversity (Jabot and Chave, 2009).

ABC methods are also likely to have applications in areas of pattern orientated modelling (POM), where emphasis is placed on simulation models reproducing ecological patterns in data. POM focuses on the most essential information in a system (Grimm et al., 2005), and ABC methods provide an analogous way of selecting the best model, as by selecting summary statistics to represent the patterns of interest, rigorous parameterisation and model comparison can be focussed on how well the models reproduce patterns.

One major advantage of the structure of ABC modelling when applied to ecological situations is that they allow us to incorporate partial knowledge of the processes within a complex ecological simulation model, as we have demonstrated in this study. Whilst direct measurements of some processes may be lacking, it is unlikely that nothing is known about the direction or magnitude of *any* process within an ecological system. The inclusion of prior information is likely to dramatically improve the convergence and realism of estimated parameters, and uncertainty in priors can easily be incorporated and explored within the algorithm. ABC methods therefore take a truly Bayesian approach by allowing the use of partial knowledge of systems to infer unmeasured processes, and thus fully parameterise complex models that previously could not be fully specified.

Author contributions

Designed the study, analysed the data and performed statistical analysis: Emily Lines. Provided the data: Miguel Zavala. Wrote the paper: Emily Lines with supervisory support from David Coomes and Miguel Zavala.

6 Regional successional dynamics simulated from tree-level processes

Abstract

Forest simulation models have been used to understand forest dynamics, structure and productivity, and species dominance and succession but typically contain no climatic dependency in their underlying processes, meaning that they have limited use in understanding climate-driven changes in forest dynamics, or in predicting the impact of changing climate on them.

In this study we parameterise a spatially-implicit individual-based forest model, the PPA, for 14 major native tree species in Spain using national inventory data. We parameterise growth, mortality and allometry subroutines of the model as functions of both competition and climate, and run simulations of forest development from open stands over the climatic conditions found in Spain.

The model was able to reproduce observed patterns of *Pinus* dominance across Spain, and decomposing the underlying processes revealed that inter and intraspecific variation in both growth and mortality along climatic gradients determined regional shifts in species dominance. We used the model to predict long-term successional dynamics over 500 years, and found that the inclusion of competition-dependent recruitment within the model produced predictions for the eventual dominance of angiosperm species over *Pinus* species in most parts of Spain.

Despite its simplicity, we found that including climate dependency of growth, mortality and allometry produced realistic predictions of species dominance as emergent properties of the model. We suggest that this approach could be repeated in other parts of the world using national forest inventories to improve understanding of the climatic drivers of species dominance.

6.1 Introduction

Simulation models are vital tools for forest ecology research as they allow questions posed on large geographical scales and over long periods of time to be answered. Forest simulators which incorporate individual rates of tree growth and mortality have been shown to be able to reproduce forest properties such as stand structure (e.g. Lindner et al., 1997), productivity (e.g. Caspersen et al., 2011; Coomes et al., 2012) species composition and successional dynamics (e.g. Pacala et al., 1996), and have been parameterised for boreal (e.g. Zhang et al., 2009), temperate (e.g. Kunstler et al., 2009) and tropical forests (e.g. Bohlman and Pacala, 2011).

Uncertainty in the response of forests to climate change forms a large part of the uncertainty in Earth systems models, and incorporating ecological processes through a better representation of species diversity and competition will fundamentally improve the realism of simulations (Purves and Pacala, 2008). Large-scale long-term forest datasets, combined with increasing computational processing power with which to parameterise and run simulations, mean that the development of forest dynamic models which incorporate the effects of multiple environmental drivers on demographic processes for many species is now possible in many parts of the world.

In order to simulate landscape level forest dynamics it is axiomatic that forest models must include representation of the drivers of variation in forests at a landscape level. The dynamics of succession are known to be sensitive to climatic variation (Kardol et al., 2010), as are individual tree level processes of growth (Coomes and Allen, 2007a; Martínez-Vilalta et al., 2011), mortality (van Mantgem and Stephenson, 2007; Voelker et al., 2008) and recruitment (Mendoza et al., 2009). Forest simulators are usually parameterised from detailed site data, and despite often complex calculations of light availability and local competition, do not typically include climate dependency in model processes, which means that they have very limited use in understanding the role that climate plays on determining successional dynamics and species dominance on a regional scale, or in predicting future forest dynamics under climatic change.

The perfect plasticity model (PPA) is a cohort-based spatially-implicit model which uses individual-tree based allometry, growth and mortality functions to describe whole-forest dynamics and which was originally developed for forests in the lake states of the US (Purves et al., 2007, 2008; Strigul et al., 2008). In order to calculate the level of competition for light within a stand the PPA assumes plasticity in each tree's crown area position, meaning that the crown of a tree of a given height may be placed anywhere within the horizontal plane it occupies in order to maximise light capture. This means that recording the exact location of the crown (and the stem) within the stand is not necessary, making the model spatially-implicit, and dramatically reducing the level of complexity compared to spatially-explicit individual-based forest models such as SORTIE (Pacala et al., 1996).

In this study we test the ability of a PPA-type forest simulation model based on climate-dependent individual-based demographic rates to reproduce observed species distributions at a regional scale. We parameterise the model for 14 major tree species in Spain using inventory data (the Spanish forest inventory; MMA, 1996, 2007) to constrain climate and competition dependent model processes and use simulations to predict early and late successional dominance across Spain. The idea that species dominance and successional dynamics on a regional scale are a product of climate is not a new one, nor is the interest in predicting the response of vegetation to changing climate through simulation modelling (Shugart and West, 1980; Hall et al., 1991; Glenn-Lewin et al., 1992). However, we know of no study which tests whether a forest simulation model can reproduce observed species' dominance at a regional scale as an emergent property from individual-based demographic rates parameterised from inventory data.

We test the ability of the model to reproduce species dominance patterns across the landscape using species dominance observations recorded in the inventory. We simulate successional dynamics by initialising a stand with small trees of many species, and recording how species dominance changes over time under the demographic rules driving the simulations. *Pinus* species are frequently the early-successional dominants in Spain, whilst angiosperms species, primarily *Quercus*, are often observed to be late successional (Lookingbill and Zavala, 2000; Pausas et al., 2004; Capitano and Carcaillet, 2008; Santana et al., 2010). The inventory did not include stand age or successional stage so we used pine/angiosperm dominance as a proxy for this. We use the simulations to predict geographic variation in which *Pinus* species rise to dominance after 30 years of stand development, and to predict which angiosperm species dominate up to 500 years after initialising the model. These predictions are then compared with observed distributions. Forests in Spain have a long history of human management which has driven forest dynamics in some areas (Urbieto et al., 2008), and are frequently disturbed by forest fires (Grove and Rackham, 2001). As in many parts of the temperate world, forest area is increasing due to land abandonment in the second half of the twentieth century (Campos et al., 2005), meaning that much of the forested land in the region is unlikely to be in equilibrium. The simulation models do not explicitly consider the effects of fire or human management. Therefore, by parameterising the model using only competition and climate dependency of individual species' processes we hypothesise that there will be some mismatches between what we predict and the observed patterns of species dominance across the region.

6.2 Simulation model

6.2.1 Canopy area of taller trees, CAI_h , as a measure of competition

The simplest form of the PPA uses a binary definition of competition for light by assigning each stem as either being in the overstory (and receiving full sunlight) or in the understory, with two corresponding sets of growth and mortality rates per species. In this form, the PPA has been shown to be able to reproduce species composition, canopy structure, forest dynamics and succession in the US lake states (Purves et al., 2007, 2008).

Subsequent applications of the PPA model have utilised the crown area of the plot as a continuous measure of competition, using either total crown area and an individual tree's crown position in multiple understory layers (Bohman and Pacala, 2011), or a metric CAI_h : the total crown area of trees taller than a given height h as a proportion of total area (Caspersen et al., 2011; Coomes et al., 2012). Although previous studies have varied the height at which CAI_h is calculated for a given tree, either at the midpoint of the crown (Caspersen et al., 2011) or at both the top of the crown and

several lower points (Coomes et al., 2012), we had no information on crown depth for these data so chose to calculate CAI_h from the top of the tree. The metric CAI_h is defined for a given height h as:

$$CAI_h = \frac{\sum_i^N CA_{h,i}}{A} \quad (\text{Eqn 6.1})$$

where $CA_{h,i}$ is the projected crown area of crown i at height h , N is the total number of trees in the stand and A is the ground area of the stand, for which we used 1 ha (Caspersen et al., 2011). For a tree of height h the metric CAI_h is therefore the projected crown area of all taller trees as a proportion of the total crown area. A tree with a CAI_h value of at least 1 would be completely in the understory, as the crown area of taller trees would fill at least the area of the stand above it, whereas a value less than one would imply that some of its crown has exposure to direct sunlight, proportional to the area of canopy filled above it. Full details of the fitting of CAI_h are given in Appendix C (page 141).

6.2.2 Demographic rates and allometric equations

The simulation model depends on four subroutines for recruitment, growth, allometry (tree height and crown width) and mortality. These processes were parameterised using data from the second and third Spanish forest inventory (IFN2 and IFN3; MMA, 1996, 2007), which surveyed all forested land in mainland Spain on a 1 km² grid approximately 10 years apart. We used Bayesian methods and tested many different model functional forms before selecting the one that best fit the data (see Appendix D page 157 for details). All processes were fitted with species-specific parameters.

For the recruitment model we simply used the functions fitted in Chapter Five, which predicted the total number of new 1 cm diameter breast height (DBH) stems per hectare per year as a function of conspecific adult crown area (CAI_{sp} , calculated as the sum of all crown areas of conspecific stems >7.5 cm DBH), and total plot crown area (CAI_{pl} , calculated as the sum of all crown areas of conspecific stems >7.5 cm DBH), as:

$$\text{Recruitment (\#1 cm DBH stems /ha/year)} = \varphi_0 CAI_{sp} \exp(-\varphi_1 CAI_{pl}) \quad (\text{Eqn 6.2})$$

where φ_0 and φ_1 are estimated parameters. This function describes recruitment as increasing with conspecific crown area, but being negatively affected by aboveground competition for light.

Annual growth rate (stem diameter increase, cm year⁻¹) was fitted as a power function of stem size (DBH) with an exponential decline in growth for large stems, with additional dependencies on drought length (DL), annual precipitation (PA) and average annual temperature (AVT) as well as the competition measure CAI_h , using a size dependent standard deviation:

$$\text{Annual growth rate (cm year}^{-1}\text{)} \sim N\left(\alpha DBH^\beta \exp(-\rho_9 DBH), (\rho_0 + \rho_1 DBH)\right) \quad (\text{Eqn 6.3})$$

where α , β and ρ_0 - ρ_9 are parameters and α is dependent on climate and competition as:

$$\alpha = \rho_2 (1 + \rho_7 DL)(1 + \rho_8 PA)(1 + \rho_6 AVT) / (1 + \rho_2 / \rho_4 \exp(\rho_5 CAI_h)) \quad (\text{Eqn 6.4})$$

This equation describes growth as increasing initially with stem size but a possible decline in growth for large trees (depending on the value of ρ_9), and decreasing with asymmetric competition (CAI_h).

The climate dependency of growth is not pre-determined, since parameters ρ_6 - ρ_8 may take either positive or negative values.

Annual mortality rate (stems stem⁻¹ year⁻¹) was fitted using a logistic function (similar to the method in Chapter Two), with the same predictors as the growth function. The best fit function was:

$$\text{Annual mortality rate (stems stem}^{-1} \text{ year}^{-1}) = 1/(1 + \exp(-k)) \quad (\text{Eqn 6.5})$$

where k is dependent on stem size, competition and climate as:

$$k = \tau_0 + \tau_1 DBH \exp(\tau_2 DBH) + \tau_3 CAI_h + \tau_4 DL + \tau_5 AVT + \tau_6 PA \quad (\text{Eqn 6.6})$$

where τ_0 - τ_6 are estimated parameters. This equation describes mortality as decreasing initially with stem size but the functional form also allows a possible increase in mortality in larger trees (depending on the value of τ_2). The climate and competitive dependency of mortality is not pre-determined, since parameters τ_3 - τ_6 may take either positive or negative values

Growth and mortality functions were strongly size dependent but were developed from trees > 7.5 cm DBH in the inventory, which does not provide individual-level information on smaller trees. To avoid extrapolating these rates to small sizes and producing unreasonable results, for trees smaller than 7.5 cm we used the growth and mortality functions derived for juveniles in Chapter Five.

Allometry, tree height and crown diameter, were also modelled as functions of climate. Tree height was fitted as a power function of stem size (DBH), using a simplified version of the model in Chapter Four, using a size dependent standard deviation:

$$H \sim N\left((\phi_2 + \phi_4 PA + \phi_5 AVT + \phi_6 DL + \phi_7 CAI_h) \times DBH^{\phi_3}, (\phi_0 + \phi_1 DBH)\right) \quad (\text{Eqn 6.7})$$

where ϕ_0 - ϕ_7 are estimated parameters. Crown diameter (used for calculating CAI_h) and CAI_h were modelled exactly as in Chapter Five, again with a size dependent standard deviation:

$$CD \sim N(v_2 + v_3 DBH + v_4 PA + v_5 AVT + v_6 DL, (v_0 + v_1 DBH)) \quad (\text{Eqn 6.8})$$

where v_0 - v_6 are estimated parameters. Full details of model fitting, model selection and a comparison of model predictions and observations, for all processes, are given in Appendix D, tables D.1-D.6 and figures D.1-D.3 (Appendix D page 157).

6.2.3 Predictions of successional dominance

The original form of the PPA model makes analytical predictions for the early and late successional dominant species under simplifying canopy structure assumptions and assuming just two constant species specific growth and mortality rates, one for individuals in the understory and one for canopy trees (Purves et al., 2008). The predicted early successional dominant is the species which is able to grow to the tallest height in a completely open stand (i.e. in full light) and which has the largest share of the canopy at the earliest time of canopy closure. Purves et al. (2008) predict this to be the same species under the assumption of low interspecific differences in allometry and mortality rates in full light, and so the early successional species may be determined by a simple equation relating height and growth rates in light. As we used a continuous definition of the effect of asymmetric competition

on growth and mortality rates (in the form of the metric CAI_h , in contrast to the discrete canopy/understory) we could not apply the analytical equations of Purves et al. (2008) to predict early succession in Spain. Instead we used the simulation model to predict both the tallest species in the plot and the species with the largest share of the canopy after 30 years' growth in full light.

The original PPA model's predictions for the late-successional dominant species in a given area is the species with the tallest canopy closure in an equilibrium monoculture, that is, the tallest species which is able to regenerate under its own canopy to replace lost adults and maintain a closed canopy forest. However, we chose to test the predictions of our model for late successional dominance by simulating dynamics for each plot with all species found in that plot. We set each species with the same initial density as before and simulated dynamics for 500 years, recording the dominant species (the one with the largest share of the canopy) every 100 years.

6.2.4 Simulation steps

The model creates and follows cohorts of stems the same size of each species within a stand throughout their lives. At each one-year time step it creates cohorts of 1 cm DBH stems, the density of which (in stems/ha) is determined for each species by the crown area of large (>7.5 cm DBH) conspecifics and the crown area of all large trees within the stand, using equation 6.2. For each time step the simulation model then applies the species-specific growth function (equation 6.3) to each cohort's DBH, and reduces the density of each cohort according to the species-specific mortality function (equation 6.5). The simulator then recalculates height and crown width for each individual in each cohort (using species-specific equations 6.7-6.8), and its CAI_h value as well as the total crown area of large trees for each species and for the whole plot according to each cohort's density and size.

In order to prevent stems growing to a size unobserved in the data we restricted each stem to grow to no more than 10% larger than the largest stem observed in the inventory for that species (see Table 6.1). The inventory contained too few large trees to detect a senescence effect on mortality rates, despite this being found in many other systems (e.g. the Eastern US, Chapter Two; and forests in sub-boreal Umeki, 2002, temperate, Buchman et al., 1983; Monserud and Sterba, 1999; Coomes and Allen, 2007b or tropical, Chao et al., 2008). To avoid unrealistically large long-lived individuals surviving in the stand we increased the mortality rates of stems larger than the largest observed for their species by 25%. To aid computational speed we also removed cohorts of very low density (<0.1 stems/ha) from the simulation model at each time step.

We simulated dynamics in forest stands on a grid of cells of varying climate to reflect the observed climate in Spain. We simulated stands with varying average annual temperature (in steps of 0.2°C) and annual precipitation values (in steps of 20 mm) across the range found in Spain, at drought length values of 0.5, 1.5, 2.5, 3.5, 4.5 and 5.5 months drought (5783 gridcells in total). To avoid extrapolating rates far outside of the species ranges we calculated species' climatic ranges using the inventory data (see Fig. 6.1, Table 6.1), and only initialised plots with species found within those

climatic conditions (within 0.1°C temperature, 10 mm precipitation, 1 months drought), and only simulated for plots where more than one species was found (so removing plots where the predicted dominant species would be pre determined, see Table 6.1, Fig. 6.1).

To predict early successional dominance we initialised plots with a cohort of 500 1 cm DBH stems per hectare of each chosen species and applied the growth, allometry and mortality functions as described above for 30 years, but assumed no effect of competition for light (i.e. $CAI_h=0$ for all cohorts during the simulation), and no additional recruitment into the stand. To predict long-term successional dynamics we ran the simulator for 500 years with 500 initial 1 cm DBH stems for each species in each gridcell, and to provide a continuous size distribution in the early stages of the model we added an extra 100 1 cm DBH stems of each species into the stand in each of the first 10 years.

Table 6.1 The 14 species in the analysis, the maximum DBH of that species observed within the data and the upper limit drought length the species was simulated in (all were simulated in no drought).

Species	Maximum DBH (cm)	Maximum simulated drought length (months)
<i>Pinus sylvestris</i>	44.9	1.99
<i>Pinus uncinata</i>	43.9	0.10
<i>Pinus pinea</i>	46.1	5.03
<i>Pinus halepensis</i>	33.8	5.00
<i>Pinus nigra</i>	40.6	2.69
<i>Pinus pinaster</i>	44.2	3.73
<i>Quercus robur</i>	55.1	2.00
<i>Quercus petraea</i>	55.0	1.05
<i>Quercus pyrenaica</i>	52.9	3.04
<i>Quercus faginea</i>	52.6	3.46
<i>Quercus ilex</i>	60.5	4.35
<i>Quercus suber</i>	61.9	4.20
<i>Fagus sylvatica</i>	54.7	1.05
<i>Castanea sativa</i>	83.3	3.27
<i>Pinus sylvestris</i>	44.9	1.99

6.2.5 Observed species dominance

In IFN3 the dominant species was recorded in the field for each inventory plot, and we used this to test the model's predictions of early and late successional dominance. We selected plots from the data for which one of the 14 species in the study was recorded as dominant. We split the data by climate to create gridcells and determined average dominance within each gridcell as the species most often recorded as dominant in the inventory plots whose climatic range lay in the range of the gridcell. We

split the data by drought length in to six groups (0-1, 1-2, 2-3, 3-4, 4-5 and 5+ months drought), by annual precipitation on a 20 mm grid and by average annual temperature on a 0.2°C grid.

6.3 Results

6.3.1 Models of growth and mortality

Growth and mortality rates varied strongly with species, size, competition and climate, but the effects of size and competition were strongest (Fig. 6.2). Most species showed a strong increase in growth with size at small size, but for most species growth rates also slowed or declined in larger sizes. Mortality was also responsive to size, with almost all species showing declining rates from small to medium sized trees, with most species' mortality levelling around 20-40 cm DBH, although the mortality rates of *Q. suber* and *F. sylvatica* also rose in larger sized trees. Both growth and mortality were affected by increases in asymmetric competition (CAI_h), with growth of all species declining sharply in more competitive environments. Mortality rates also increased with competition, but there were much larger differences among species, with the Mediterranean angiosperm species appearing to suffer the least from increased competition. The effect of drought length, temperature and precipitation on growth and mortality were less consistent among species, with some species' rates responding positively and others negatively to changes in all three variables (see Figs. D.1 and D.2, Appendix D page 157)

Figure 6.1 Observed 95% climatic ranges of each species taken from all occurrences within the inventory data. Species were only simulated within the climatic range in which they were found in the data (*P.sy* = *Pinus sylvestris*, *P.un*=*P. uncinata*, *P.pa*=*P. pinea*, *P.ha*=*P. halepensis*, *P.ni*=*P. nigra*, *P.ps*=*P. pinaster*, *Q.ro*=*Quercus robur*, *Q.pe*=*Q. petraea*, *Q.py*=*Q. pyrenaica*, *Q.fa*=*Q. faginea*, *Q.il*=*Q. ilex*, *Q.su*=*Q. suber*, *F.sy*=*Fagus sylvatica*, *C.sa*=*Castanea sativa*).

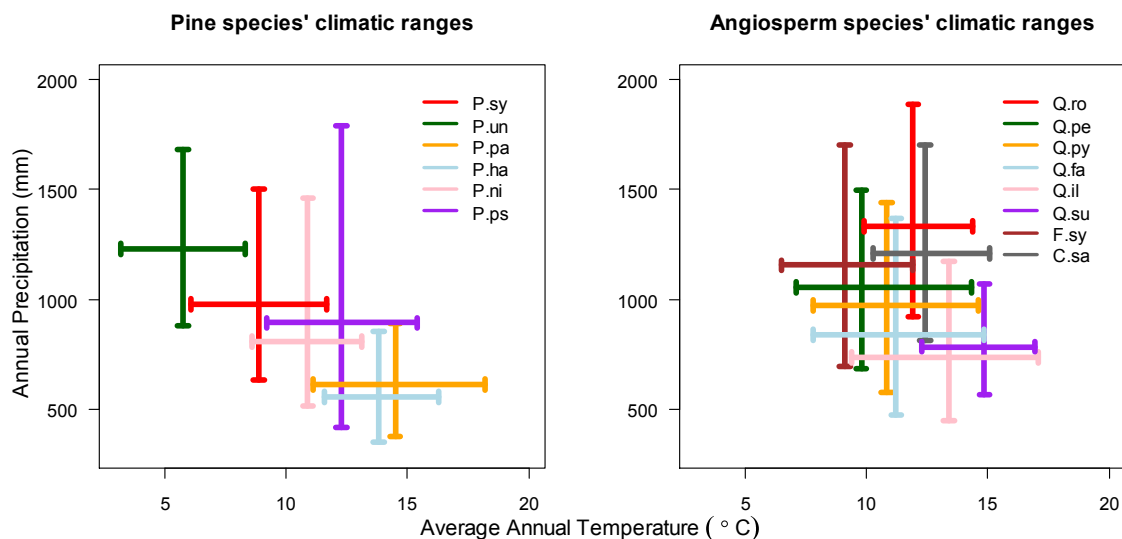
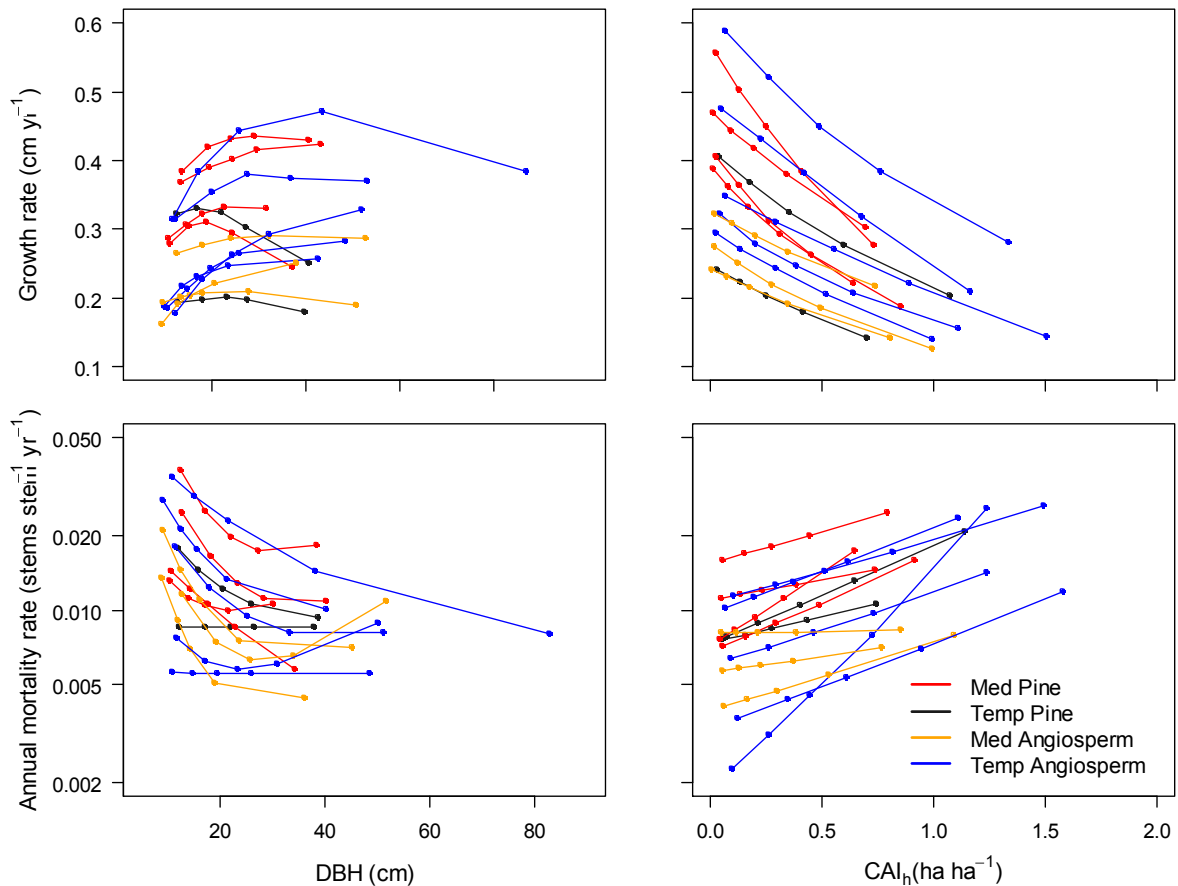


Figure 6.2 Average predicted annual growth and mortality rates of the 14 species along ranges of size and competition. Predictions were calculated along the gradient of each predictor (DBH or CAI_h) by varying only that predictor and holding all others at the species' average (see Table D.1 for average values), and then binning the data along the gradient to give the average. Species shown are Mediterranean pines (*Pinus pinea*, *P. halepensis*, *P. nigra*, *P. pinaster*), temperate pines (*P. sylvestris*, *P. uncinata*), Mediterranean angiosperms (*Quercus faginea*, *Q. ilex*, *Q. suber*) and temperate angiosperms (*Q. robur*, *Q. petraea*, *Q. pyrenaica*, *Fagus sylvatica*, *Castanea sativa*).



6.3.2 Observed and predicted pine dominance

The observed patterns of pine species' dominance (Fig. 6.3) were strongly determined by climate, with the mountain pine species (*P. uncinata* and *P. sylvestris*, and to a lesser extent *P. nigra*) dominating only in the cooler and wetter areas with the shortest drought, *P. pinaster* dominating in the warmer and wetter regions and *P. nigra* and *P. pinea* dominating in the warm areas with lower rainfall. In the very driest areas *P. halepensis* dominated (Fig. 6.4).

For each climatic gridcell we predicted what the early successional dominant species would be using two approaches- the tallest species after 30 years of stand development and the species with the largest share of the canopy area after 30 years. The two predictions were the same for only around 40% of the 5783 gridcells simulated. We found that the model predicted the observed patterns of pine

dominance well across the climatic gradients (compare Fig 6.3 and Fig 6.4, which shows predictions for dominance according to the species with the largest share of the canopy), but there were some mismatches, specifically the predicted dominance of both *P. halepensis* and *P. pinaster* was lower than observed, with *P. pinea* and *P. nigra* often predicted in their place, particularly in regions of low and medium drought (compare Fig 6.3 and Fig 6.4).

The predicted dominance according to share of the canopy area reproduced the observed pine dominance pattern better than the tallest species method, particularly in the areas of longest drought, where the predicted dominance according to height was solely *P. pinea*, whereas the predicted dominance according to the canopy share was *P. halepensis* in the cooler areas and *P. pinea* in the warmer and wetter areas (compare Fig. 6.4 and Fig. D.4, Appendix D page 157).

We analysed the mechanism of changes in dominance within the model for an example change in predicted pine dominance along a temperature gradient by examining the intraspecific variation in the component rates (growth, survival and crown diameter) along with changes in temperature (at drought length = 1.5 months, precipitation = 700 mm/year, Fig. 6.5). Along the temperature gradient in this region we found that *P. sylvestris* dominated in the coolest areas, *P. nigra* dominated in the middle of the temperature range and *P. pinea* dominated in the warmest areas. *P. sylvestris* dominated almost everywhere it was found because of its high growth and survival rates, and large crown diameter. However, in the cooler areas there was concurrent dominance of *P. nigra*, despite its low and declining growth rate, due to its extremely high survival rate. *P. pinea* had a low survival rate in the middle of the temperature range but this increased substantially and, despite a simultaneous decline in growth rates, led to dominance in the warmest area. There were small areas of *P. halepensis* dominance in the warmer part of the range, likely due to its low mortality rate, but despite its larger crown area it by and large lost out to both *P. pinea* (which had higher growth rates) and *P. nigra* (which had higher survival rates). Despite it occurring within this climatic region, *P. pinaster* was unable to dominate due to its low growth and high mortality rates.

Figure 6.3 Observed climatic range of **dominance** of the six pine species studied as recorded in the inventory. Each square is a cell of 0.1°C temperature $\times 10$ mm precipitation grid cell, representing the most often dominant species in the dataset in that range and in the stated range of drought length.

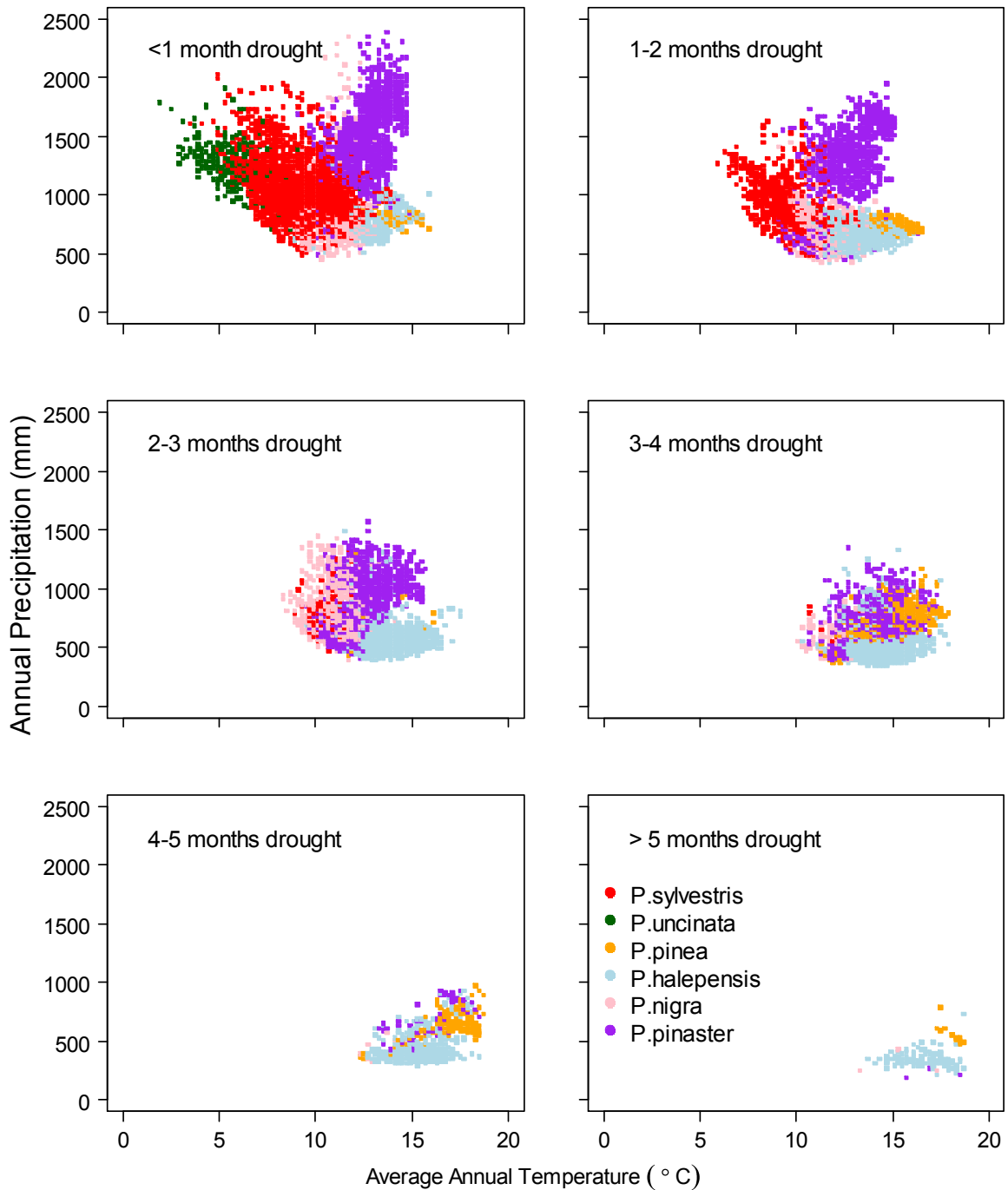


Figure 6.4 Predicted range of dominance of the six pine species studied determined as the species with the largest canopy area after 30 years of growth under full light, split by drought length and plotted along gradients of average annual temperature and annual precipitation.

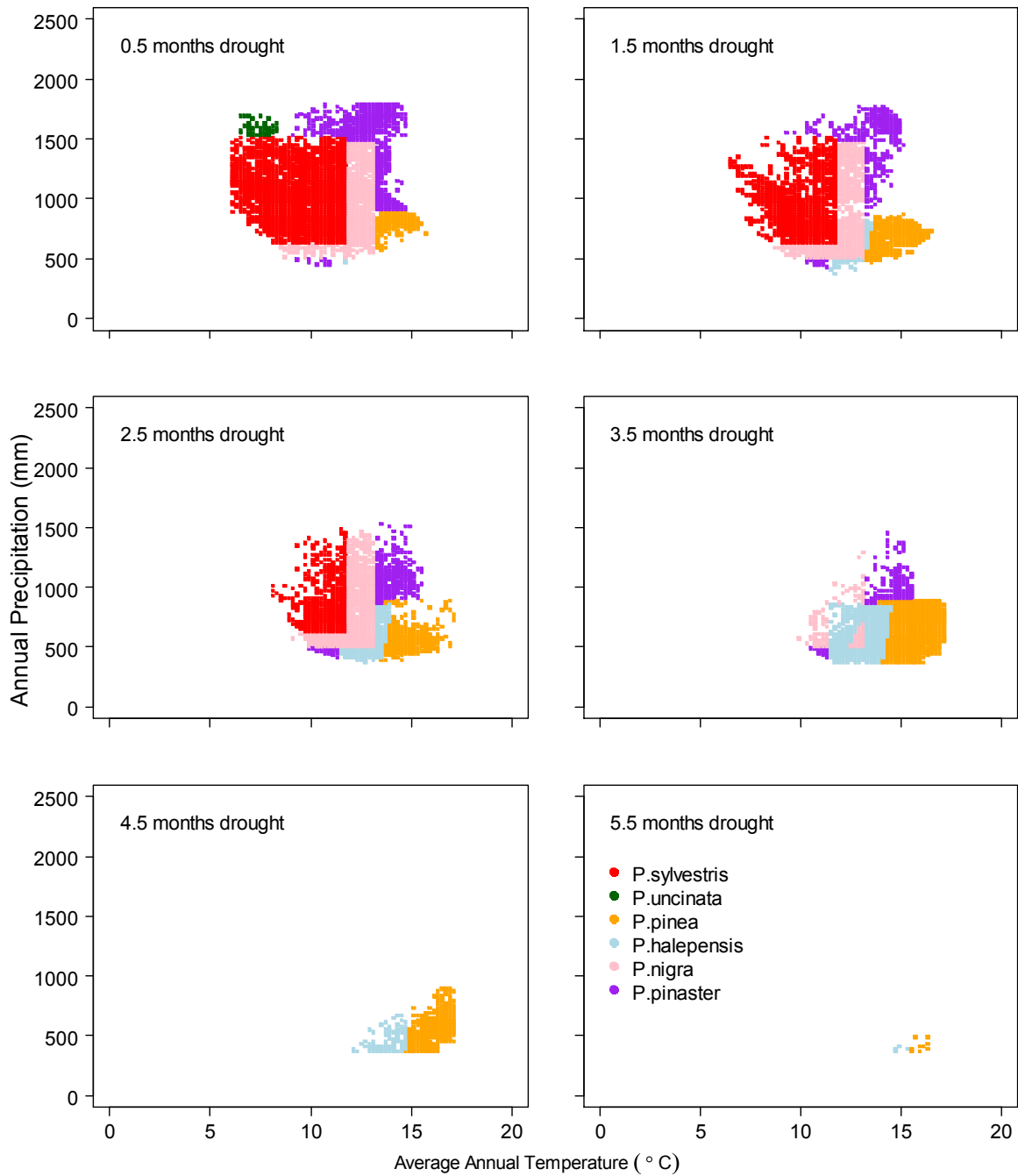
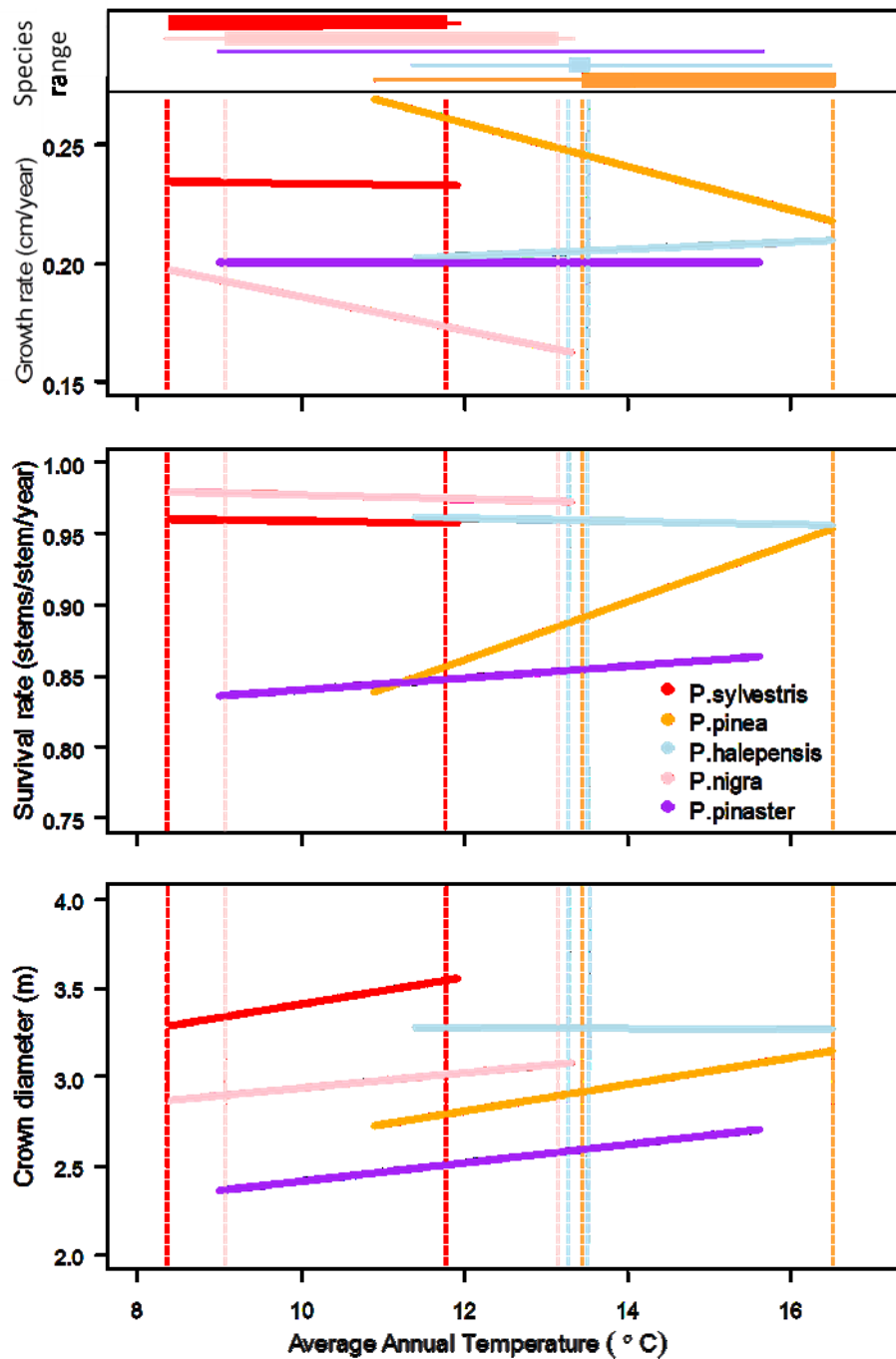


Figure 6.5 Predicted growth, survival and crown diameter of pine species (predicted for DBH=10 cm, $CAI_h=0.5$ ha/ha, drought length = 1.5 months and annual precipitation = 700 mm/year) plotted against average annual temperature, with each species shown in the range in which it was simulated in the model. Horizontal bars show the range (thin line) predicted dominance (thick line) of pine species in along average annual temperature, which overlap because they represent dominances within an annual precipitation range of 600-800 mm/year. *Pinus pinaster* was not predicted to be dominant in this range. Dotted lines show the edges of the ranges of dominance.



6.3.3 Observed and predicted angiosperm dominance

Both the ranges of occurrence and dominance of angiosperm species' ranges were less segregated and less well defined by climatic variation than pines (Fig. 6.1, and compare Figs. 6.3 and 6.6). There was little pattern of dominance in the areas of shortest drought length, whereas in parts with higher rainfall *F. sylvatica*, *Q. robur*, *Q. petraea* and *Q. pyrenaica* all dominated. In areas of intermediate drought, *Q. pyrenaica* and a few stands of *C. sativa* dominated where rainfall was higher, being replaced by *Q. suber* in the warmest parts. In the areas of longest drought, *Q. ilex* dominated most stands, with *Q. suber* dominating a small number of stands with higher rainfall.

We predicted species compositional dynamics from an initially completely bare stand over 500 years using the full climate and competitive-dependent model and examined the predicted transition in species' dominance (determined as largest share of the canopy) from pines to angiosperm species at 100 year intervals (Fig. 6.7). After 100 years of dynamics we found that most stands were still dominated by pine species, but large parts of the cooler areas of least drought were dominated by *F. sylvatica*.

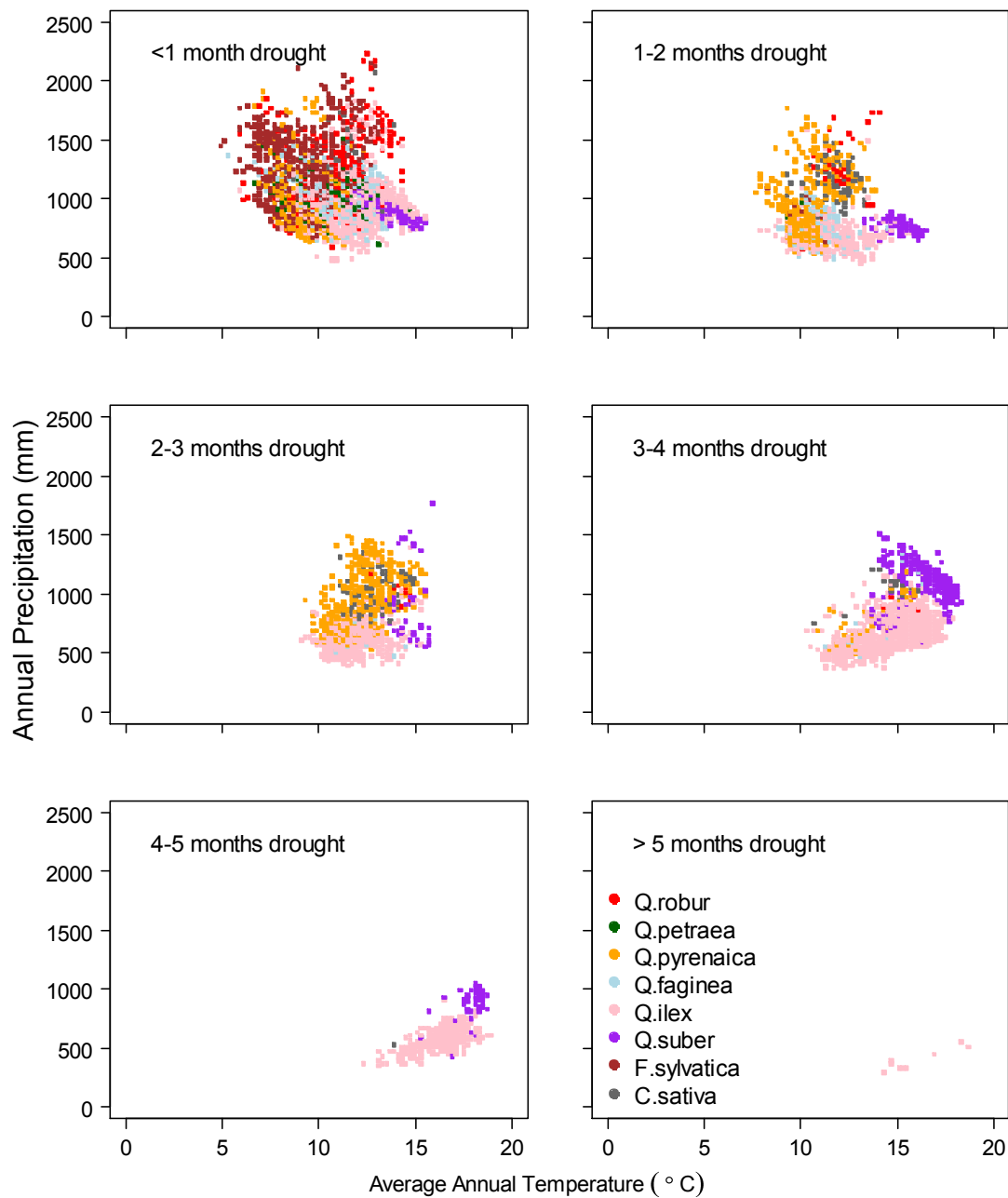
By 200-300 years the model predicted much higher levels of angiosperm dominance across the region, but in the areas of longer drought there were still large areas dominated by pine species. In areas of short drought (0-2 months) there was reduced dominance by *F. sylvatica* but increased dominance by deciduous species such as *Q. robur* and *C. sativa* in the warmest and wettest areas, and some dominance of *Q. pyrenaica* and *Q. petraea* in the cooler areas. In the warmest areas with lowest rainfall there was some dominance by the sclerophyllous *Q. ilex* and the semi-deciduous *Q. faginea*. In areas of medium drought (2-4) there was higher dominance by *Q. robur*, *Q. pyrenaica* and *C. sativa*, and dominance by both sclerophyllous oaks (*Q. suber* and *Q. ilex*) in the warmest and driest regions. In the very driest parts (4+ months of drought) only the two sclerophyllous oaks were found, with *Q. suber* in slightly wetter parts, *Q. ilex* in hottest and very driest areas and many pine dominated stands in the areas of least rainfall.

After 400-500 years of the model most stands were dominated by angiosperm species, and in the areas of shortest drought (0-2 months) most species distributions had not changed substantially. However, both *Q. pyrenaica* and *Q. faginea* were no longer dominant in any area. *Q. suber* still dominated some stands in the hottest areas but in areas of intermediate and long drought (2+ months) it had been outcompeted, primarily by *Q. ilex*. In these areas there were also still many stands dominated by pine species (almost exclusively *P. halepensis*, data not shown), particularly in areas with the very lowest rainfall.

It is difficult to directly compare the predictions of the model with the observed angiosperm dominance, since the inventory data does not give clear climatic patterns of dominance. This was especially evident in the areas of shortest drought, where both the model and the data show dominance of many different species without clear climatic differentiation. However, there were some

consistent patterns, such as the dominance of *F. sylvatica* in the coldest and wettest areas (compare Fig. 6.6 and Fig. 6.7) and the dominance of *Q. ilex* and *Q. suber* in the hottest areas with least rainfall.

Figure 6.6 Observed climatic range of dominance of the eight angiosperm species studied as recorded in the inventory. Each square is a cell of 0.1°C temperature $\times 10$ mm precipitation grid cell, representing the most often dominant species in the dataset in that range and in the stated range of drought length.



6.4 Discussion

6.4.1 Growth and mortality rates varied with size, climate and competition

We found that there was strong interspecific and intraspecific variation in growth and mortality. Growth for most species rose and then fell with stem size (DBH), but there were exceptions. Growth declined with all sizes in the inventory data (stems > 7.5 cm DBH) for *P. uncinata* and *Q. ilex*, and only increased with size for *F. sylvatica*. The size-related decline in growth has been found in many parts of the world (e.g. Mencuccini and Grace, 1996; Binkley et al., 2002; Coomes et al., 2012) and may be caused by the impact on large trees of nutrient or hydraulic limitations, increased respiratory costs, disease, herbivory or increased allocation of resources to reproduction (Zeide, 1993; Ryan and Yoder, 1997; Weiner and Thomas, 2001). Mortality rates of most species declined with stem size but two species, *P. uncinata* and *Q. petraea* showed almost no change in mortality with size. The minimum mortality rate occurred between 20 - 40 cm DBH for most species, and only two, *Q. suber* and *F. sylvatica*, showed a marked increase in mortality rates at large stem size. U-shaped size dependence of mortality, with high mortality in larger sizes has been found in many parts of the world (e.g. the Eastern US, Chapter Two; Buchman et al., 1983; Monserud and Sterba, 1999; Umeki, 2002; Coomes and Allen, 2007b; Chao et al., 2008), so we were surprised that this pattern was not more widespread in our data. Ninety per cent of the trees in the inventory were less than 40 cm DBH, and management practices may be removing large trees from the landscape in Spain before senescence effects occur in large trees (we filtered the data to remove stem loss due to management). Increases in asymmetric competition caused both decreases in growth rate and increases in mortality for all species, but there were more interspecific differences in the effect on mortality rates, with changes in rank mortality rates with increasing competition (Fig. 6.2). Growth and mortality rates for all species showed strong intraspecific variation along climatic gradients (Figs. D.1 and D.2, pages 167-168), but there were many differences among species and changes in ranks of rates across climatic gradients. Studies of growth rates along temperature, drought and precipitation gradients are common (e.g. Wickramasinghe, 1988; Corcuera et al., 2004; Coomes and Allen, 2007a; Martínez-Vilalta et al., 2011), but large-scale assessments of climate-driven intraspecific variation in mortality are more rare, though these studies typically also show strong variation in rates (van Mantgem and Stephenson, 2007; Adams et al., 2009).

Strong intraspecific variation in performance along climatic gradients implies that both growth and mortality rates are important in determining species dominance, and are likely to be primary drivers of competitive interactions and species composition. This is in contrast to our findings for intraspecific variation in allometry (Chapter Four) where we found little variation in rank in allometric scaling along the same climatic gradients.

6.4.2 *Early successional dominance was determined by both growth and mortality*

The patterns of observed dominance were better captured by predicting species dominance as the species with the largest share of the canopy rather than the tallest species in a region after 30 years of growth in the open. By examining the component parts of the model along an example temperature gradient we found that some shifts in canopy share dominance were due to differences in growth rates and others due to differences in mortality rates, but none appeared to be primarily driven by differences in crown area (Fig. 6.5). This implies that intraspecific variation in both growth and mortality rates along climatic gradients are important for determining shifts in the early successional dominant species, which was not simply the one with the fastest growth in full light. The importance of both growth and mortality in determining regeneration success have been observed in New Zealand forests (Kunstler et al., 2009). Here, we found that whilst a fast-growing and tall statured early successional species may be found in a particular region, an unfavourable climate may mean that too few individuals are able to survive to adult height to dominate the canopy.

6.4.3 *Mismatches in pine dominance are likely due to lack of fire dynamics*

The most striking mismatch between the early successional predicted species and the observed dominance of pine species was the reduced dominance of both *P. halepensis* and *P. pinaster* in our predictions. Although our model captured some dominance by both species in the warmer and drier areas, in many places where they were observed to be dominant our model wrongly predicted dominance by *P. nigra* and *P. pinea* (compare Fig. 6.3 and Fig. 6.4). We suggest that this is a result of our model not simulating the effects of fire on species dominance. Both *P. pinaster* and *P. halepensis* is a highly flammable serotinous species which is adapted to reproduce quickly after intense fires by reproducing at a young age and having serotinous cones which allow rapid seed dispersal and regeneration post fire (Tapias et al., 2004; Calvo et al., 2008). *P. nigra* and *P. pinea* are not serotinous and are unable to survive intense fires or quickly regenerate after them, although both have insulating bark which protects against low intensity fire damage (Rigolot, 2004; Pausas et al., 2008). Given the high frequency of fires in the hot and dry parts Spain, *P. halepensis* is therefore able to dominant in areas which, without fire, might be dominated by less fire-tolerant species (Agee, 1998). Both *P. halepensis* and *P. pinaster* can burn and re-establish a stand on a cycle of as little as 15 years (typically the cycle is 20-30 years). By promoting regular fires they are able to prevent succession by shade-tolerant angiosperm species indefinitely (Grove and Rackham, 2001), particularly in the driest areas where oaks are at the edge of their distributional limit, but this depends on both the intensity and the frequency of the fire regime (Zavala et al., 2000). In order to include these effects it would not be enough to simply simulate a frequent disturbance regime; we would also require detailed data on species-specific post-fire establishment and regeneration rates from recently burned stands.

6.4.4 Late successional dominance dynamics

The predicted late successional dominance distribution did not show the clear climatic differentiation found for the pine species, but the angiosperm species in the data also occupied much more similar observed climatic ranges than the pine species (Table 6.1 and Fig. 6.1). The model was able to predict a transition from pine to angiosperm species across the region but the time taken for this to happen varied with climate (Fig. 6.7), with slower dynamics in areas of longer drought. Some species showed much higher dominance over an intermediate time frame (e.g. dominance of *Q. faginea* and *Q. pyrenaica* after 200-300 years) but had disappeared after 500 years, suggesting that these may be recruitment limited under their own canopy. We also saw a rise and fall in dominance of *Q. suber* in the driest areas, where it was eventually outcompeted by *Q. ilex*, which may be a result of a lack of fire simulation in our model. *Q. suber* relies on fire to maintain dominance (Grove and Rackham, 2001), and in areas with low fire frequency *Q. ilex* is known to regenerate better (Curt et al., 2009).

We also found that pine species, and in particular *P. halepensis*, continued to dominate in the areas of very low rainfall even after 500 years. The relative abundance of oaks and pines is known to be strongly related to water availability and topography (Zavala et al., 2000), and although mixed stands are found in areas with intermediate droughts, pines form monospecific stands in the driest regions. *P. halepensis* plantations are known to survive in areas with precipitation as low as 300 mm/year whereas *Q. ilex* is found only sparsely in areas of less than 400 mm/year (Rodà, 1999).

6.4.5 Conclusions: climate-driven simulation models at a regional scale

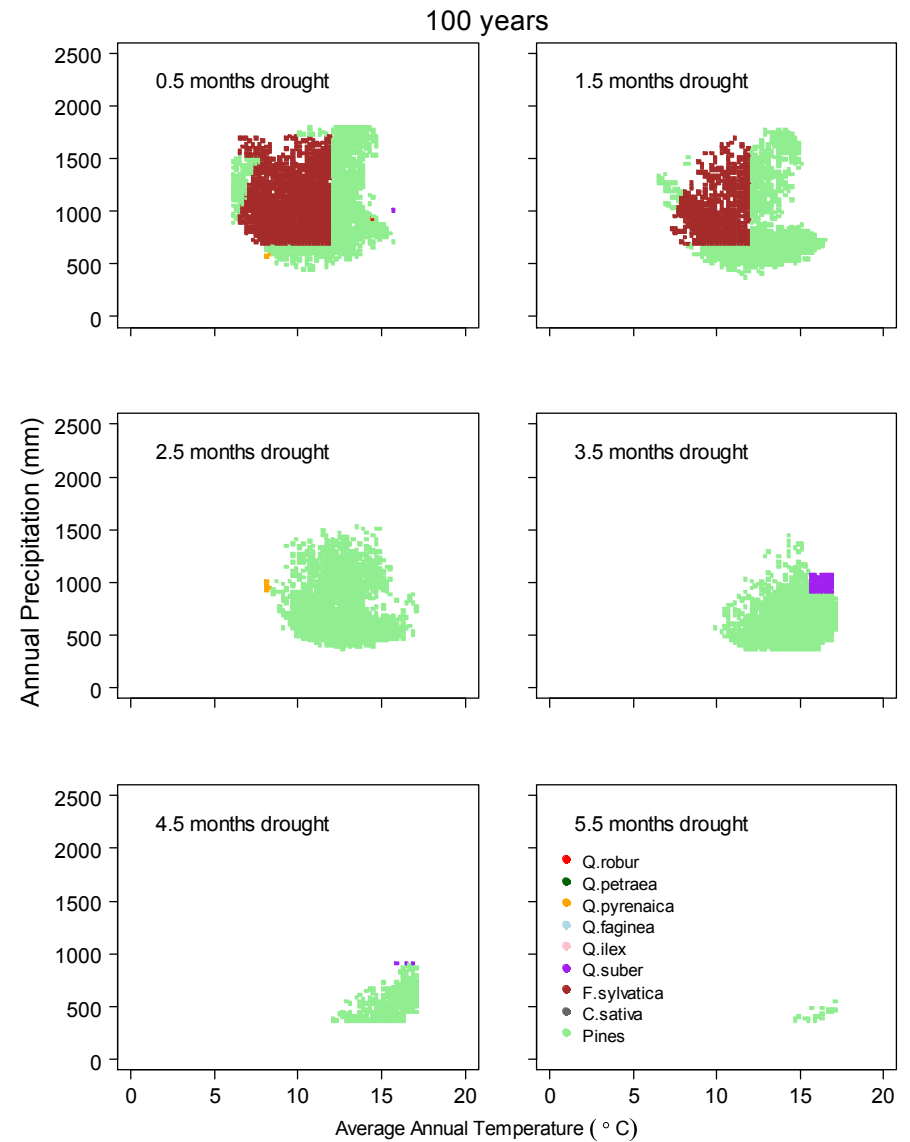
In this study we have demonstrated the straightforward way in which simple forest simulators may be parameterised to include climatic dependency of processes given appropriate inventory data. All processes within forest dynamics models are known to vary strongly with climate at regional scales and large national inventories, such as the one used here, provide the opportunity to study multiple species' dominance and succession across a wide variety of environmental conditions.

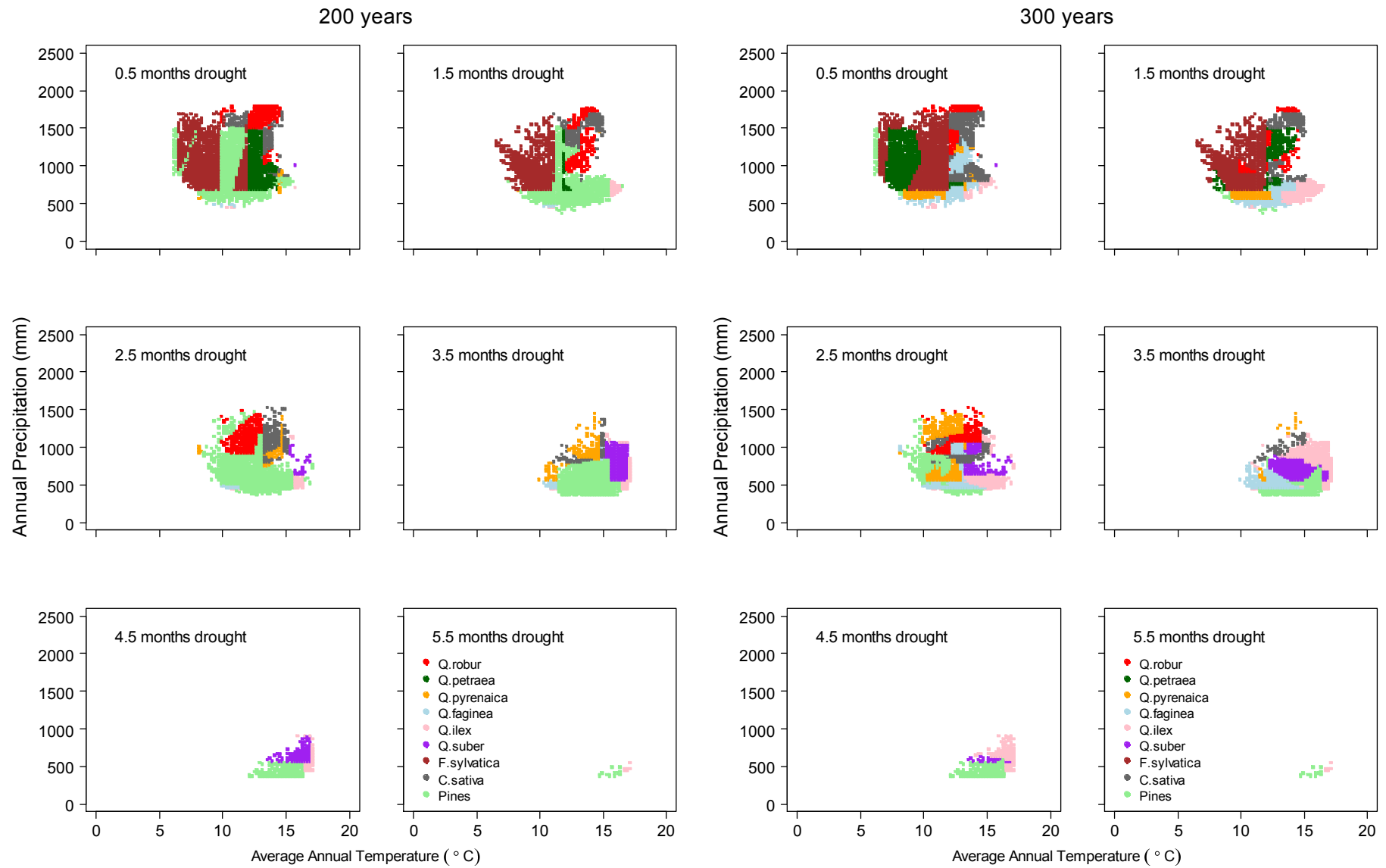
We believe that models such as the one presented in this chapter could be used as tools to predict changes in species composition with climate change at regional scales. However, we recognise that constraining the occurrence of species to within the range in which they were found in this study (Fig. 6.1) is unsatisfactory, and suggest that incorporating physiological-based climatic-dependency of growth and mortality could allow rates to be extrapolated outside of the range in which they were parameterised, to give new insight into forest dynamics in novel climates.

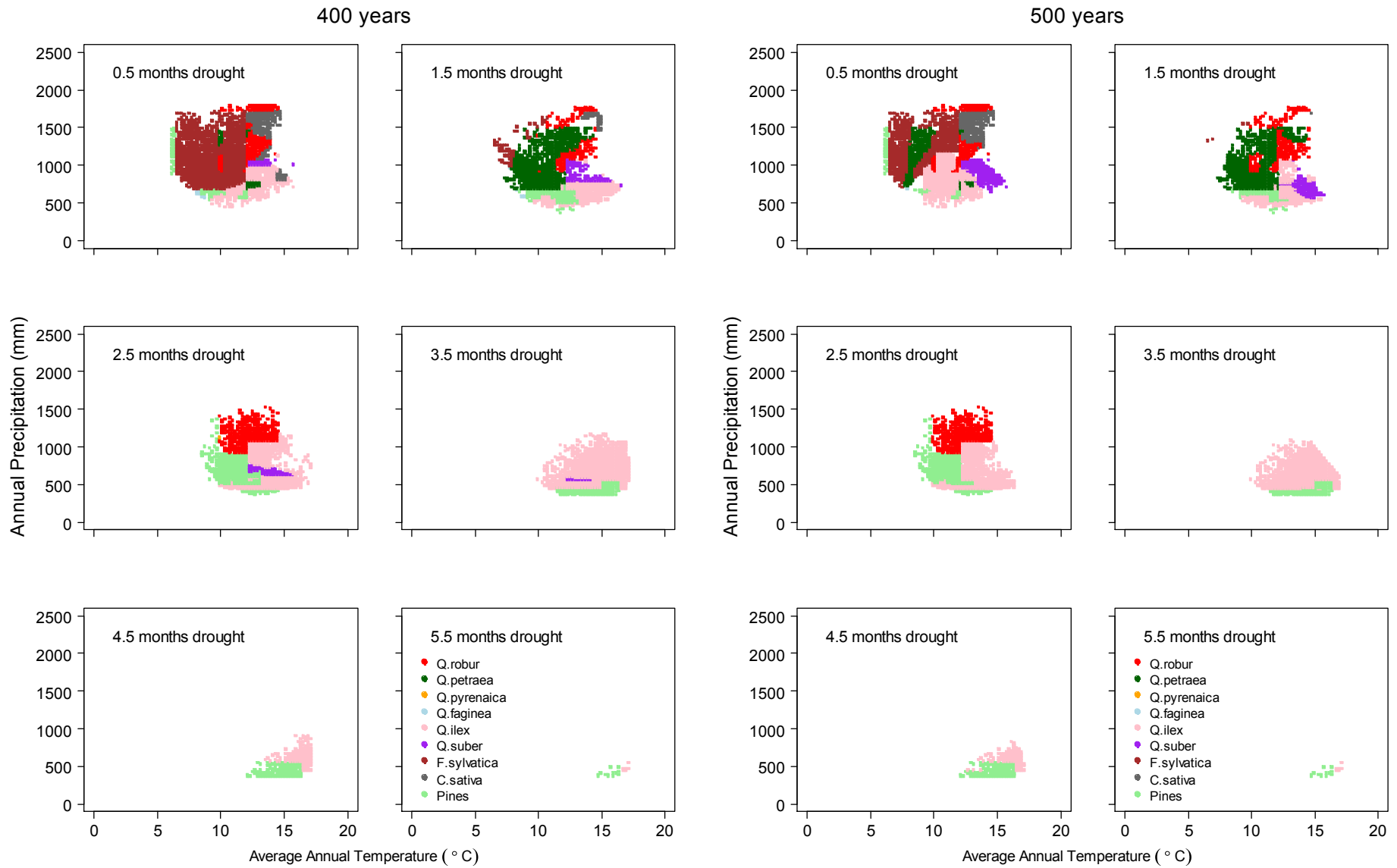
Despite this drawback, this study represents, to our knowledge, the first individual-based forest simulator incorporating both species-specific ecological and climatic drivers to reproduce regional patterns of species dominance. This approach has the potential to generate ecologically reasonable predictions of changes to forest structure, productivity, dynamics and species composition for many parts of the world and is an important step towards a better understanding of the mechanisms driving observed climate-forest type patterns.

Figure 6.7

Predicted range of dominance of the angiosperm species over 500 years of succession. Panels show succession after 100, 200, 300, 400 and 500 years, showing the gradual replacement of pine dominance (light green) by angiosperm dominance. Each panel is split by drought length and species' dominances are plotted along gradients of average annual temperature and annual precipitation.







Author contributions

Designed the study, analysed the data and performed statistical analysis: Emily Lines with support from David Coomes. Provided the data: Miguel Zavala. Wrote the simulation model code: Emily Lines and Drew Purves. Wrote the paper: Emily Lines with supervisory support from David Coomes.

7 Discussion

Analysing each of the four components of a typical forest dynamics model, (growth, mortality, allometry and recruitment) individually allows the investigation of the inter- and intra-specific differences in rates, which reveals the potential relative abilities of species to adapt to changes in climatic conditions. In this thesis I have shown that the examination of the regional-scale climatic-dependency of aboveground allometric functions and demographic rates parameterised from inventory data can give insight into intraspecific variation in species performance throughout their ranges. I have also demonstrated how the combination of these processes in a forest simulator can reveal the causes of observed shifts in the ability of species to dominant the forest across the landscape.

The geographical ranges of plant functional types on a continental scale are known to correlate with climate (Holdridge, 1947) and understanding the causes of observed ranges is a key question in ecological research and an important component towards understanding the possible impacts of climate change on species distributions and biodiversity (Guisan and Thuiller, 2005; Morin et al., 2007). However, empirical studies of the determinants of range shifts are fragmented and lag behind theoretical explanations (Gaston, 2009). Process-based models of species' distributions have shown promise in explaining the limitations of species performance at the edge of their ranges, whether due to climatic stresses on phenological, reproductive or survival processes (e.g. Morin et al., 2007, 2008). However, these models typically ignore competitive effects, although there is evidence to suggest the presence of competitors can alter species' responses to climatic variation (Leathwick and Austin, 2001). Climate is of course not the only factor affecting tree demographic processes and in this thesis I have found stem size and competitive environment to be the major determinants of variation in aboveground allometry and growth and mortality rates at the tree-level.

7.1 Tree size and competition as primary determinants of individual-level rates

Stem size was the single most important determinant of growth in Spain, and of mortality in both Spain (Chapter Six) and the Eastern US (Chapter Two). At small stem sizes I observed low growth and high mortality rates, as has been shown in many other studies (e.g. Bormann, 1965; Kobe et al., 1995; Kunstler et al., 2009), but I also found strong evidence from many species for declining growth

and increasing mortality for the largest trees (giving a U-shaped size-dependent mortality; Harcombe, 1987).

Declines in stem growth rate at larger sizes may be caused by internal factors such as limitations in hydraulic flow, increases in respiratory costs, self-shading leading to a decline in photosynthetic activity or increased allocation of resources to reproduction or external forces such as herbivory and disease, and the costs in protecting against these (Zeide, 1993; Ryan and Yoder, 1997; Weiner and Thomas, 2001; Meinzer et al., 2011). The size-related decline in individual tree growth has been found in many parts of the world (e.g. Mencuccini and Grace, 1996; Binkley et al., 2002; Coomes et al., 2012), and is a factor in age-related decline of whole-stand productivity that has been observed in many studies (e.g. Ryan et al., 1997).

Asymmetric competition (competition from taller trees) was found to be a determinant of both aboveground allometry and stem growth in Spain (Chapters Four and Six). Trees with more large neighbours grew taller and thinner and had narrower crowns than those in open areas, but had reduced stem growth rates when asymmetric competition was stronger. The plasticity of aboveground allometric to conditions means that trees are able to allocate resources to height growth means and so faster overtop their neighbours to reach the canopy and maximise light capture (Berntson and Wayne, 2000; Bragg, 2001; King et al., 2009).

Increases in mortality with size in larger trees has been observed from field measurements in many parts of the world (Buchman et al., 1983; Monserud and Sterba, 1999; Umeki, 2002; Coomes and Allen, 2007b; Caspersen et al., 2011), and I found increases in mortality in large sizes in all species in the Eastern US but very few in Spain. Increased mortality in large trees is likely to be due to a combination of factors including the higher exposure of canopy trees to strong winds and disturbance, disease and senescence (Busing and Pauley, 1994; Yang et al., 2003; Coomes and Allen, 2007b).

I found that competition was an important determinant of mortality rates in both Spain and the Eastern US, but that the effects in the two regions were different. I tested the effect of asymmetric competition on mortality rates in Spain and found that higher asymmetric competition increased mortality for almost all trees, and that its effect was stronger than that of symmetric competition, which has also been found in Norwegian forests (Eid and Tuhus, 2001). The mechanism for the negative effect of taller canopy cover is likely to be primarily the strong asymmetry of competition for light (Weiner, 1990), causing a reduction in performance in shade for many species. The magnitude of the effect however may depend on the species identities of the canopy and understory trees (He and Duncan, 2000) and the size of the suppressed tree (Kunstler et al., 2009). A more detailed study of Spanish forest mortality rates has revealed an interaction between competition and precipitation, so that in wetter sites where less light reaches the forest floor and competition for light is more intense (Coomes and Grubb, 2000), this increased asymmetric competition has an even larger impact on mortality rates (Ruiz-Benito et al. *in review*).

In the Eastern US I tested the effect of symmetric competition (total plot basal area) rather than asymmetric competition, and found that it had a broadly hump-shaped relationship with mortality, with low mortality in both the lowest and highest basal area plots, although there was strong interspecific differences, with some species showing no change in mortality rates with total plot basal area. Low mortality in the least dense stands is likely to be a result of lack of competition for resources such as water and light. However, the pattern seen for several species of lower mortality in areas with high basal area is less easy to explain. It may be a result of an unmodelled interaction between competition and resources, in that the most dense forests are likely to occur on sites with high levels of soil moisture and nutrients where overall tree performance could be higher, and could also be caused by inter-specific differences in response to competition. A study of the effects of plot density on mortality in Canadian forests found that the response varied between species and not all showed increases in mortality in denser plots (Yao et al., 2001). A possible future avenue of research would be to repeat this analysis using asymmetric rather than symmetric competition as a predictor, and to include interactions between competition and climate.

The effects of strong asymmetric competition, found in all these rates, are in contrast to metabolic scaling theory (West et al., 1997, 1999, 2009), which predicts whole-forest dynamics from metabolic rates and ignores asymmetric competition for light (Muller-Landau et al., 2006). The critical importance of including asymmetric competition for light in understanding whole forest dynamics has been highlighted in many studies (e.g. Muller-Landau et al., 2006; Coomes and Allen, 2007b; Coomes et al., 2011). I suggest that any forest simulator concerned with species dominance at a large scale will be able to reproduce observations more accurately with the inclusion of asymmetric competition in growth, mortality and allometry, but future research could test this by quantifying the improvement in predictive ability between simulators with symmetric and asymmetric competition.

7.2 Climate dependency of tree-level processes and inventory data

For the data tested in this study, models describing growth, mortality and allometry at regional scales were all improved by the inclusion of climatic dependency. Variation in climate and the influence of this on vegetation type and structure is very strong across Spain (Grove and Rackham, 2001), and this was evident in the climate dependency of individual-tree level processes I parameterised (Chapters Four and Six). Including climatic dependency along with the more commonly modelled competition-dependency of tree-level forest processes enabled the simulation model I parameterised for Spain to reproduce regional patterns of species dominance, and gave insight into the drivers behind shifts in dominance along climatic gradients (Chapter Six). Including a simple competition-dependent recruitment model (Chapter Five) meant that the simulator was able to reproduce dynamics of

succession in Spain; the commonly observed shift from dominance by *Pinus* species to dominance by angiosperm species in all but the driest areas (Rodà, 1999; Lookingbill and Zavala, 2000; Pausas et al., 2004; Capitano and Carcaillet, 2008; Santana et al., 2010).

Forest dynamics models which simulate individual tree-level processes have been shown to be able to reproduce a wide variety of forest properties such as stand structure, species composition and succession and productivity, and have been used to investigate critical questions for forestry, management, conservation and carbon storage (Pacala et al., 1996; Lindner et al., 1997; Kunstler et al., 2009; Zhang et al., 2009; Bohlman and Pacala, 2011; Caspersen et al., 2011; Coomes et al., 2012). However, such models typically do not include climatic dependency in processes at a regional scale, and are often parameterised from local-scale data. At small scales the lack of climate-dependency does not detract from the ability of the models to reproduce forest dynamics, but if individual tree-based forest simulators are to be used to answer questions on the large-scale effects of climate and land use change on forest dynamics then climate dependencies must be included as drivers of processes. Forest inventory datasets, available for many parts of the world, have the potential to be used for broad-scale forest dynamics models which reproduce species-climate distributions.

National forest inventories such as those used in this study typically do not contain detailed information such as soil nutrient levels, seed dispersal, or below ground dynamics which are necessary to parameterise processes for detailed individual based forest simulation models (e.g. SORTIE, Pacala et al., 1996) or the photosynthetic and respiratory measurements required for physiology-based models (e.g. HYBRID, Friend et al., 1993). The inclusion of climate and resource-driven physiological-based limitations to tree performance within existing forest simulation model frameworks has the potential to produce models which are able to both predict accurate rates in novel climatic conditions (extrapolated outside of the current species ranges) and the important ecological processes that current models are able to reproduce. Such an approach has been suggested (Wullschleger et al., 2001; Lichstein et al., 2010) and would be a major step towards the construction of forest models, currently able to reproduce local-scale dynamics, which are robustly predictive on a regional scale (Purves and Pacala, 2008).

7.3 Limitations of the use of forest inventory data for simulation models

Although they provide a wealth of information on variation in tree-level processes and forest properties at a large scale, there are important limitations to using forest inventories to parameterise forest models which should be considered when drawing conclusions from such studies on the climatic dependence of forest dynamics.

Performance of individual trees at a particular site may be strongly influenced by a variety of factors not recorded in inventory data. For example, allocation of resources to defend against and repair the damage done by herbivores reduces those available for growth (Herms and Mattson, 1992), and high levels of herbivory in seedlings have been found to increase mortality rates in future years (Eichhorn et al., 2010). Spatial heterogeneity in microsite quality is a strong determinant of juvenile performance, with understory cover, soil nutrients and canopy gaps all affecting seedling establishment and survival (e.g. Broncano et al., 1998; Kobe, 1999), and interspecific differences in performance in response to site quality influence coexistence and composition dynamics (Latham, 1992; Beckage and Clark, 2003).

Large scale disturbances such as fire, earthquakes and hurricanes can alter species composition and forest dynamics (Hickler et al., 2004; Keane et al., 2004; Liedloff and Cook, 2007; Uriarte et al., 2009; Coomes et al., 2012), and forest fires, a common form of disturbance in Spain, are known to influence vegetation composition (Carrión et al., 2001). I found clear mismatches between model predictions and species composition in Spain which I suspect have arisen because of the lack of consideration of fire dynamics in the model. In particular the model fails to predict the widespread dominance of two fire-adapted early successional species (*Pinus pinaster* and *P. halepensis*) which are able to reproduce at young age and are serotinous so are able to reestablish from the seed bank quickly following fire (Tapias et al., 2001; Calvo et al., 2008). These species achieve dominance through high fire frequency which reduces the seed bank of competitors over multiple cycles. To accurately describe such a mechanism would require multispecies data on survival and reproduction after fire, and data on fire intensity and frequency.

Although forest inventory data are common to many parts of the world, examples of measurements from more than one time period are much rarer. By parameterising models of dynamic processes using just two measurements it is necessary to make a space-for-time assumption. However, this ignores temporal and historical influences on currently observed forest properties. For example, episodes of stress such as disease or severe drought may influence tree performance for many years into the future (Franklin et al., 1987; Cherubini et al., 2002), meaning that poor performance observed in later years may be incorrectly assumed to be the result of current conditions. The observed forest species distribution in Spain cannot be disentangled from its very long history of human use, and forest degradation over the thousands of years of human activity in the region has dramatically changed areas of species dominance (Blondel, 2006). Recent agricultural land abandonment and new EU policy has led to an increase in forest cover since the mid 20th century (Barbero et al., 1990; Campos et al., 2005), so many forests in the region are not in equilibrium. This increase in forested land has also changed fire regimes in the region (Viedma et al., 2006; Chauchard et al., 2007) and means that the currently observed forest structure and dynamics are likely to have been influenced by different drivers than are currently observed.

The space for time assumption has another important implication- it means the ecotypic variation is ignored within the dataset, since it is assumed that an individual of a particular species in one location would perform in an identical manner to an individual of the same species in a different location if it were transplanted. However, many studies in the Mediterranean have shown ecotypic variation and the importance of seed provenance in tree performance (e.g. Balaguer et al., 2001; Chambel et al., 2007; Climent et al., 2008). For example, a planting experiment using seeds from multiple provenances found that the survival of *Pinus canariensis* seedlings in drought has high ecotypic variation, with seedlings from favourable sites (i.e. those with low or no drought) having much higher mortality rates (López et al., 2007). In the context of understanding the impacts of changing climate (particularly under increasing drought conditions) this assumption could lead a correlative model of forest dynamics to underestimate the impact on mortality and consequently incorrectly predict interspecific differences in performance.

Although I have been able to show that the approach of building a forest dynamics model using component parts parameterised from inventory data is able to reproduce aspects of observed species dominance and succession, the approach taken in this thesis has been correlative. To predict and quantify the effects of climate change on Mediterranean ecosystems requires a process-based approach which in particular addresses the effects of the likely increases in drought on demographic processes (Keenan et al., 2009). The inclusion of mechanistic processes within ecosystem models will dramatically improve understanding of species distributional limits (Kearney, 2006; Keenan et al., 2011). Approaches which incorporate process-based models of the climatic dependency of demographic rates into individual-based ecological models are therefore desirable both to fully understand the role of climate and competition in driving forest dynamics and species ranges, and to make robust predictions of the future of forests.

7.4 Concluding remarks

This thesis has demonstrated the flexibility of Bayesian statistical approaches for parameterising forest dynamics models with multiple drivers using large amounts of data. The flexibility of the approaches presented here, both in testing competing ecological hypotheses and in incorporating different types of data, means that they are invaluable tools for parameterising increasingly complex ecosystem models. I have also shown the wealth of information which may be extracted from national forest inventories to increase understanding of the relative importance and large-scale impacts of competitive and climatic drivers of forest structure. The procedures demonstrated in this thesis are easily applicable to other regions and future research will focus on translating these methods to other forest systems and testing their ability to reproduce species composition and successional dynamics.

The question of the amount of model detail necessary to accurately reproduce ecosystem function and predict dynamics is one which warrants further research. For example, in my climate-driven forest dynamics model (Chapter Six) I found that climatic dependence of growth and mortality may drive rank changes in species dominance, but allometric scaling appears to only have a secondary role. Simplifying assumptions can dramatically reduce the amount of data required to parameterise forest dynamics models (e.g. Purves et al., 2008), meaning that models can be parameterised from inventory data for many more regions of the world. Models of forest dynamics need only contain as much detail as is sufficient to accurately simulate the properties of interest. Rigorous comparison of ecological hypotheses should help to determine the level of detail required for a model and an understanding of the impacts of simplifying assumptions within a forest model will dramatically improve not only its predictions but also the ease with which it may be transferred to other ecosystems and scaled to larger geographical scales. The work presented in this thesis is an important step towards understanding how the dynamics and distribution of Mediterranean tree species is controlled by climate, and also represents a framework for specifying multi-species, multi-dependency forest models which can be translated to other regions of the world.

Appendix A: Eastern US mortality

Table A.1. Table comparing model fits using AIC and BIC. 36 models were run within which the four types of model predictor in equation 2.4 (constant, size, environment, basal area) were left out or included with forest-level (FL) or species specific (SS) effects. Total number of parameters, AIC and BIC scores and rankings are reported. Models without size and species effects were rejected strongly, and the addition of environmental and competition variables increased model fit significantly. The best-fit model, number 26, showed a very significant improvement on the next best using both AIC and BIC.

Model	Constant	Size	Environment	Basal Area	# parameters	AIC score	AIC rank	BIC score	BIC rank
1	FL	FL	-	-	3	285046.9	37	-142540.1	37
2	FL	SS	-	-	47	250075.5	26	-125298.2	23
3	SS	FL	-	-	25	250214.4	27	-125245.7	21
4	SS	SS	-	-	69	249993.7	24	-125379.2	24
5	FL	FL	FL	-	13	271511.5	35	-135827.8	34
6	FL	SS	FL	-	57	243591.3	12	-122111.5	8
7	SS	FL	FL	-	35	248196.5	18	-124292.2	17
8	SS	SS	FL	-	79	243336.2	11	-122105.8	7
9	FL	FL	SS	-	233	242284.9	9	-122433.5	9
10	FL	SS	SS	-	277	238863.2	4	-120966.4	4
11	SS	FL	SS	-	255	241014.1	6	-121919.9	6
12	SS	SS	SS	-	299	237455.7	3	-120384.6	2
13	FL	FL	-	FL	5	282448.5	36	-141252.0	36
14	FL	SS	-	FL	49	250312.1	28	-125427.6	25
15	SS	FL	-	FL	27	250028.6	25	-125163.9	20
16	SS	SS	-	FL	71	249753.9	22	-125270.3	22
17	FL	FL	-	SS	49	253033.1	30	-126788.1	30
18	FL	SS	-	SS	93	248935.0	20	-124982.8	19
19	SS	FL	-	SS	71	251300.0	29	-126043.4	29
20	SS	SS	-	SS	115	247667.0	17	-124470.7	18
21	FL	FL	FL	FL	15	270559.9	34	-135363.0	33
22	FL	SS	FL	FL	59	245060.7	14	-122857.3	13
23	SS	FL	FL	FL	37	247087.4	16	-123748.7	16
24	SS	SS	FL	FL	81	245586.3	15	-123242.0	14
25	FL	FL	SS	FL	235	248624.1	19	-125614.1	28
26	FL	SS	SS	FL	279	242284.7	8	-122688.2	11
27	SS	FL	SS	FL	257	244051.9	13	-123449.9	15
28	SS	SS	SS	FL	301	241561.7	7	-122448.6	10
29	FL	FL	FL	SS	59	254674.3	32	-127664.1	32
30	FL	SS	FL	SS	103	249889.8	23	-125515.6	26
31	SS	FL	FL	SS	81	253912.6	31	-127405.1	31
32	SS	SS	FL	SS	125	249701.3	21	-125543.3	27
33	FL	FL	SS	SS	279	242400.0	10	-122745.9	12
34	FL	SS	SS	SS	323	237318.7	2	-120449.0	3
35	SS	FL	SS	SS	301	239960.4	5	-121648.0	5
36	SS	SS	SS	SS	345	236303.6	1	-120063.3	1

Table A.2 Table of maximum likelihood estimators (MLEs), Bayesian means and 2.5% and 97.5% confidence levels calculated from the posterior distributions for each of the 15 parameters of Eqn (9) for each of the 21 common species parameterised by the adaptive MCMC algorithm. The burn-in for the algorithm was 750,000 iterations and the sampling was 250,000 iterations.

Parameter (from equation 2.9)	Species										
		<i>Acer rubrum</i>	<i>Pinus taeda</i>	<i>Quercus alba</i>	<i>Liquidambar styraciflua</i>	<i>Populus tremuloides</i>	<i>Acer saccharum</i>	<i>Quercus rubrum</i>	<i>Pinus echinata</i>	<i>Liriodendron tulipifera</i>	<i>Quercus velutina</i>
α_j	Mean	-3.187	-3.258	-3.256	-3.510	-5.675	-5.374	-3.538	-2.151	-2.994	-3.370
	MLE	-3.290	-3.261	-3.251	-3.857	-5.580	-5.012	-3.568	-2.164	-3.352	-3.389
	2.5%	-3.613	-3.540	-3.631	-4.067	-5.960	-5.830	-3.932	-2.647	-3.896	-3.742
	97.5%	-2.849	-2.953	-2.952	-2.907	-5.470	-4.887	-3.198	-1.732	-2.237	-3.014
β_{1j}	Mean	-0.279	-0.362	-0.308	-0.254	-0.131	-0.319	-0.214	-0.344	-0.290	-0.207
	MLE	-0.284	-0.366	-0.305	-0.265	-0.135	-0.320	-0.214	-0.347	-0.275	-0.215
	2.5%	-0.296	-0.376	-0.324	-0.271	-0.146	-0.346	-0.233	-0.368	-0.319	-0.223
	97.5%	-0.261	-0.349	-0.293	-0.238	-0.116	-0.293	-0.193	-0.319	-0.264	-0.190
β_{2j}	Mean	-0.045	-0.030	-0.028	-0.032	-0.047	-0.039	-0.032	-0.029	-0.026	-0.030
	MLE	-0.045	-0.030	-0.028	-0.032	-0.047	-0.040	-0.033	-0.029	-0.027	-0.030
	2.5%	-0.047	-0.031	-0.029	-0.033	-0.050	-0.041	-0.034	-0.031	-0.027	-0.032
	97.5%	-0.043	-0.029	-0.027	-0.031	-0.045	-0.037	-0.031	-0.028	-0.024	-0.029
β_{3j}	Mean	0.437	-1.146	0.395	-0.104	0.359	0.320	0.551	-0.185	-0.085	0.939
	MLE	0.429	-1.152	0.416	-0.092	0.378	0.325	0.536	-0.139	-0.185	0.879
	2.5%	0.378	-1.232	0.280	-0.205	0.257	0.174	0.441	-0.380	-0.279	0.819
	97.5%	0.491	-1.054	0.502	-0.009	0.458	0.456	0.660	0.020	0.124	1.046
β_{4j}	Mean	-0.163	0.367	-0.257	0.041	0.351	-0.583	-0.255	-0.147	-0.083	-0.279
	MLE	-0.143	0.372	-0.242	0.056	0.388	-0.557	-0.264	-0.162	-0.109	-0.295
	2.5%	-0.203	0.316	-0.310	-0.008	0.227	-0.693	-0.308	-0.220	-0.228	-0.333
	97.5%	-0.124	0.419	-0.200	0.090	0.470	-0.466	-0.203	-0.081	0.050	-0.229
β_{5j}	Mean	-0.340	0.015	-0.139	0.124	-1.916	-0.501	-0.169	-0.340	0.439	-0.137
	MLE	-0.344	-0.061	-0.108	0.065	-2.026	-0.468	-0.189	-0.388	0.349	-0.118
	2.5%	-0.415	-0.161	-0.275	-0.096	-2.185	-0.704	-0.291	-0.590	0.040	-0.279
	97.5%	-0.270	0.173	0.004	0.338	-1.648	-0.302	-0.040	-0.089	0.804	-0.002
β_{6j}	Mean	0.087	-0.295	0.060	-0.112	-0.695	-0.265	0.266	0.222	-0.466	0.062
	MLE	0.101	-0.354	0.046	-0.047	-0.640	-0.230	0.260	0.142	-0.396	0.073
	2.5%	0.045	-0.392	-0.048	-0.233	-0.799	-0.356	0.200	0.100	-0.686	-0.037
	97.5%	0.129	-0.192	0.162	0.006	-0.599	-0.179	0.328	0.343	-0.216	0.160

Parameter (from equation 2.9)	Species										
		<i>Acer rubrum</i>	<i>Pinus taeda</i>	<i>Quercus alba</i>	<i>Liquidambar styraciflua</i>	<i>Populus tremuloides</i>	<i>Acer saccarum</i>	<i>Quercus rubrum</i>	<i>Pinus echinata</i>	<i>Liriodendron tulipifera</i>	<i>Quercus velutina</i>
β_{7j}	Mean	0.625	2.915	-0.134	0.706	-2.849	1.424	0.426	-0.146	2.117	-0.722
	MLE	0.635	2.886	-0.019	0.679	-2.878	1.407	0.417	-0.194	2.148	-0.757
	2.5%	0.554	2.762	-0.346	0.290	-2.983	1.179	0.202	-0.856	1.610	-0.940
	97.5%	0.700	2.994	0.073	1.136	-2.661	1.695	0.673	0.426	2.589	-0.498
β_{8j}	Mean	0.240	-1.237	-0.066	-0.391	-1.064	1.126	-0.114	-0.142	-1.039	-0.343
	MLE	0.249	-1.246	-0.061	-0.503	-1.065	1.154	-0.154	-0.178	-1.128	-0.379
	2.5%	0.195	-1.328	-0.209	-0.648	-1.133	0.965	-0.282	-0.522	-1.399	-0.524
	97.5%	0.284	-1.132	0.082	-0.150	-0.983	1.272	0.061	0.313	-0.672	-0.166
β_{9j}	Mean	-0.264	-0.276	-0.144	0.013	0.086	0.057	-0.072	-0.108	0.304	-0.699
	MLE	-0.282	-0.217	-0.141	-0.088	0.076	0.024	-0.053	-0.054	0.111	-0.701
	2.5%	-0.307	-0.362	-0.261	-0.079	0.028	-0.064	-0.187	-0.261	0.130	-0.817
	97.5%	-0.219	-0.188	-0.019	0.101	0.138	0.167	0.044	0.040	0.472	-0.587
β_{10j}	Mean	0.100	-0.417	0.033	0.022	0.003	0.058	0.064	-0.085	0.262	0.190
	MLE	0.104	-0.407	0.046	-0.019	0.004	0.048	0.060	-0.082	0.277	0.171
	2.5%	0.053	-0.490	-0.016	-0.041	-0.028	-0.002	0.020	-0.156	0.153	0.143
	97.5%	0.143	-0.344	0.080	0.086	0.034	0.117	0.107	-0.012	0.377	0.243
β_{11j}	Mean	0.389	0.336	0.239	-0.209	0.295	-1.650	0.491	0.556	0.159	0.313
	MLE	0.291	0.381	0.165	-0.262	0.157	-1.701	0.547	0.535	0.153	0.332
	2.5%	0.159	0.188	-0.088	-0.538	0.111	-2.056	0.270	0.216	-0.727	0.071
	97.5%	0.588	0.539	0.488	0.227	0.458	-1.335	0.710	0.918	0.818	0.703
β_{12j}	Mean	0.129	0.092	0.108	0.040	0.104	-0.294	0.128	0.231	0.117	0.048
	MLE	0.110	0.098	0.113	0.035	0.075	-0.134	0.147	0.250	0.068	0.109
	2.5%	0.088	0.060	0.017	-0.016	0.071	-0.378	0.062	0.110	-0.044	-0.042
	97.5%	0.165	0.133	0.178	0.119	0.135	-0.216	0.193	0.337	0.237	0.177
β_{13j}	Mean	0.006	0.073	0.093	0.013	0.014	0.010	0.101	0.113	0.024	0.124
	MLE	0.004	0.071	0.035	0.017	0.015	0.022	0.102	0.112	-0.015	0.106
	2.5%	-0.003	0.062	0.068	0.001	0.006	-0.006	0.082	0.089	0.003	0.106
	97.5%	0.018	0.085	0.115	0.025	0.022	0.030	0.123	0.137	0.055	0.145
β_{14j}	Mean	-0.0002	-0.0007	-0.0016	-0.0001	-0.0002	-0.0003	-0.0021	-0.0015	-0.0006	-0.0022
	MLE	0.0000	-0.0007	-0.0010	0.0000	-0.0002	-0.0002	-0.0021	-0.0015	-0.0006	-0.0019
	2.5%	-0.0004	-0.0009	-0.0019	-0.0003	-0.0004	-0.0006	-0.0025	-0.0019	-0.0011	-0.0026
	97.5%	-0.0001	-0.0005	-0.0012	0.0001	-0.0001	-0.0001	-0.0017	-0.0011	-0.0003	-0.0019

Table A.2 continued

Parameter (from equation 2.9)	Species											
		<i>Quercus prinus</i>	<i>Quercus stellata</i>	<i>Carya spp</i>	<i>Thuja occidentalis</i>	<i>Nyssa sylvatica</i>	<i>Quercus nigra</i>	<i>Betula papyrifera</i>	<i>Fagus grandifolia</i>	<i>Pinus virginiana</i>	<i>Fraxinus americana</i>	<i>N.sylv. (biflora)</i>
α_j	Mean	-2.838	-3.810	-2.731	-2.313	-1.502	-2.570	-6.793	-3.634	-2.948	-4.487	-2.881
	MLE	-3.166	-3.410	-1.994	-2.257	-1.636	-2.496	-6.313	-2.650	-2.865	-4.509	-2.730
	2.5%	-3.447	-4.162	-3.185	-3.108	-2.502	-3.279	-7.546	-5.030	-3.700	-5.073	-3.474
	97.5%	-2.114	-3.402	-2.211	-1.626	-0.621	-1.805	-6.233	-2.139	-2.245	-3.858	-2.204
β_{1j}	Mean	-0.390	-0.333	-0.316	-0.226	-0.265	-0.227	-0.103	-0.363	-0.502	-0.251	-0.276
	MLE	-0.388	-0.335	-0.304	-0.266	-0.247	-0.231	-0.125	-0.359	-0.497	-0.235	-0.263
	2.5%	-0.421	-0.354	-0.343	-0.277	-0.308	-0.248	-0.138	-0.408	-0.548	-0.279	-0.314
	97.5%	-0.359	-0.313	-0.291	-0.173	-0.224	-0.206	-0.070	-0.315	-0.454	-0.223	-0.238
β_{2j}	Mean	-0.030	-0.033	-0.036	-0.055	-0.035	-0.033	-0.053	-0.040	-0.040	-0.030	-0.037
	MLE	-0.029	-0.033	-0.036	-0.056	-0.035	-0.033	-0.056	-0.041	-0.039	-0.030	-0.038
	2.5%	-0.031	-0.034	-0.038	-0.060	-0.037	-0.034	-0.061	-0.043	-0.042	-0.032	-0.040
	97.5%	-0.029	-0.032	-0.034	-0.050	-0.032	-0.031	-0.046	-0.038	-0.038	-0.027	-0.034
β_{3j}	Mean	0.885	-0.285	0.100	0.158	-0.403	-0.545	0.539	0.510	-0.163	0.899	0.180
	MLE	0.844	-0.316	0.084	0.162	-0.377	-0.505	0.472	0.444	-0.223	0.975	0.145
	2.5%	0.496	-0.468	-0.055	-0.307	-0.727	-0.689	0.363	0.355	-0.473	0.742	-0.063
	97.5%	1.262	-0.101	0.279	0.624	-0.079	-0.407	0.722	0.667	0.141	1.068	0.425
β_{4j}	Mean	0.369	-0.143	0.274	0.103	0.135	0.216	0.149	-0.230	0.458	-0.463	-0.183
	MLE	0.410	-0.130	0.315	0.100	0.137	0.220	0.078	-0.218	0.328	-0.436	-0.155
	2.5%	0.232	-0.218	0.201	-0.302	-0.144	0.150	0.016	-0.331	0.298	-0.553	-0.288
	97.5%	0.503	-0.070	0.347	0.504	0.375	0.285	0.280	-0.137	0.623	-0.374	-0.082
β_{5j}	Mean	0.158	-0.171	0.986	-0.471	-0.156	-0.469	-2.117	0.439	-0.081	0.479	0.133
	MLE	0.097	-0.117	0.967	-0.192	-0.056	-0.365	-1.365	0.481	-0.024	0.452	0.125
	2.5%	-0.167	-0.421	0.684	-1.040	-0.635	-0.881	-2.557	0.233	-0.336	0.249	-0.253
	97.5%	0.501	0.095	1.292	0.111	0.257	-0.136	-1.755	0.658	0.193	0.721	0.534
β_{6j}	Mean	-0.303	-0.191	-0.671	-0.197	0.033	-0.067	-0.895	-0.320	-0.208	-0.009	-0.090
	MLE	-0.247	-0.142	-0.691	-0.171	0.067	-0.047	-0.808	-0.308	-0.224	0.037	0.064
	2.5%	-0.560	-0.356	-0.874	-0.462	-0.192	-0.237	-1.101	-0.482	-0.387	-0.156	-0.288
	97.5%	-0.075	-0.031	-0.456	0.066	0.291	0.136	-0.755	-0.171	-0.035	0.121	0.115
β_{7j}	Mean	0.243	0.048	1.563	2.108	-1.433	-0.018	-2.116	-0.239	2.431	-0.133	1.531
	MLE	-0.181	-0.446	1.520	2.642	-0.654	0.129	-0.116	-0.219	2.615	-0.034	1.496
	2.5%	-0.450	-0.439	1.061	1.261	-2.269	-1.028	-2.862	-0.474	1.880	-0.398	0.910
	97.5%	0.952	0.535	1.964	2.831	-0.673	0.949	-1.153	-0.001	2.895	0.138	2.224

Parameter (from equation 2.9)	Species											
	<i>Quercus prinus</i>	<i>Quercus stellata</i>	<i>Carya</i> spp	<i>Thuja occidentalis</i>	<i>Nyssa sylvatica</i>	<i>Quercus nigra</i>	<i>Betula papyferia</i>	<i>Fagus grandifolia</i>	<i>Pinus virginiana</i>	<i>Fraxinus americana</i>	<i>N.sylv. (biflora)</i>	
β_{8j}	Mean	-1.636	-0.167	-1.411	0.668	0.565	-0.054	-0.537	0.656	-2.411	0.111	-1.094
	MLE	-1.805	-0.016	-1.450	0.769	0.548	0.039	-0.348	0.639	-2.332	0.100	-1.041
	2.5%	-2.217	-0.476	-1.720	0.414	0.207	-0.545	-0.813	0.522	-2.896	-0.071	-1.527
	97.5%	-1.080	0.143	-1.072	0.938	0.945	0.440	-0.145	0.794	-1.779	0.287	-0.701
β_{9j}	Mean	-0.261	-0.037	0.040	0.311	-0.277	-0.242	0.389	-0.008	0.297	0.195	-0.027
	MLE	-0.332	-0.017	0.013	0.314	-0.109	-0.258	0.415	-0.021	0.227	0.343	-0.161
	2.5%	-0.546	-0.176	-0.169	0.121	-0.472	-0.402	0.291	-0.136	0.078	0.016	-0.223
	97.5%	0.033	0.116	0.217	0.493	-0.087	-0.086	0.492	0.126	0.529	0.375	0.167
β_{10j}	Mean	0.719	0.035	0.179	0.013	-0.107	-0.058	0.107	0.210	0.961	0.148	-0.008
	MLE	0.655	0.003	0.190	0.016	-0.087	-0.075	0.060	0.161	1.006	0.137	-0.005
	2.5%	0.507	-0.026	0.074	-0.138	-0.243	-0.154	0.054	0.087	0.779	0.075	-0.108
	97.5%	0.927	0.095	0.280	0.164	0.028	0.035	0.156	0.328	1.151	0.218	0.094
β_{11j}	Mean	1.105	-0.527	0.866	-0.190	0.036	0.206	-0.246	-0.615	0.131	-1.220	0.419
	MLE	1.142	-0.318	1.067	-0.014	-0.079	0.345	-0.109	0.000	-0.082	-0.557	0.009
	2.5%	0.681	-0.983	0.583	-0.416	-0.633	-0.142	-0.450	-1.691	-0.579	-1.627	0.072
	97.5%	1.418	-0.239	1.105	0.060	0.489	0.610	-0.038	0.694	0.675	-0.680	0.730
β_{12j}	Mean	0.388	-0.088	0.111	-0.012	0.003	0.080	0.002	-0.133	-0.006	-0.175	0.124
	MLE	0.535	-0.007	0.157	-0.028	0.000	0.085	0.014	-0.035	-0.024	-0.109	0.053
	2.5%	0.201	-0.228	0.007	-0.051	-0.110	0.014	-0.036	-0.366	-0.295	-0.271	0.049
	97.5%	0.529	0.007	0.202	0.029	0.081	0.156	0.041	0.153	0.232	-0.058	0.191
β_{13j}	Mean	0.111	0.142	0.100	-0.025	-0.012	0.047	0.012	-0.018	0.131	-0.002	0.017
	MLE	0.029	0.130	0.031	-0.020	-0.006	0.032	0.007	-0.008	0.120	0.001	-0.004
	2.5%	0.075	0.120	0.071	-0.037	-0.025	0.017	-0.001	-0.030	0.092	-0.014	-0.010
	97.5%	0.143	0.168	0.125	-0.007	0.002	0.067	0.026	-0.004	0.176	0.012	0.050
β_{14j}	Mean	-0.0019	-0.0021	-0.0018	0.0002	0.0001	-0.0005	-0.0003	0.0000	-0.0021	-0.0001	-0.0005
	MLE	-0.0011	-0.0007	-0.0017	0.0002	0.0001	-0.0004	-0.0001	0.0001	-0.0018	0.0000	-0.0004
	2.5%	-0.0024	-0.0026	-0.0023	0.0000	-0.0001	-0.0009	-0.0005	-0.0002	-0.0028	-0.0003	-0.0010
	97.5%	-0.0014	-0.0017	-0.0013	0.0004	0.0002	0.0000	-0.0001	0.0001	-0.0015	0.0000	-0.0001

Figure A.1 Log annual mortality rates observed for the whole forest including rare species (orange) and the 21 common species (green), and the model predictions for the 21 species combined (purple) and each species individually (grey), plotted against maximum wind speed (m/sec). Species' error bars (grey) show parameter uncertainty, forest error bars (purple, orange and green) show the 95% confidence interval for the mortality rates predicted from the model-created and real datasets.

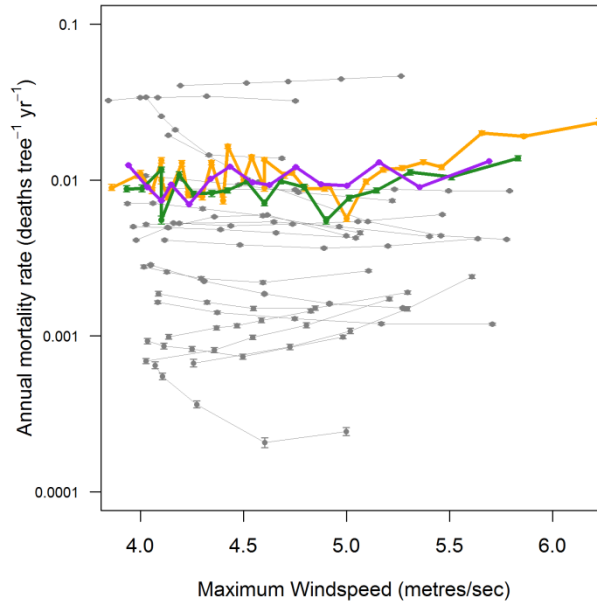


Figure A.2 Log annual mortality rates plotted against soil type for the predicted forest-level mortality rate for all 21 species (purple), the real forest-level mortality rates for the 21 species (green) and the whole forest including rare species (orange). Error bars (purple, orange and green) show the 95% confidence interval for the mortality rates predicted from the model-created and real datasets.

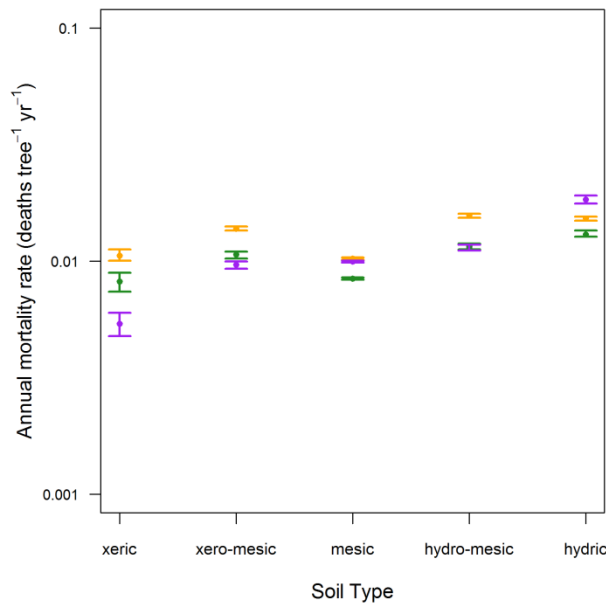


Figure A.3 Log annual mortality rates observed for the whole forest including rare species (orange) and the 21 common species (green), and the model predictions for the 21 species combined (purple) and each species individually (grey), plotted against plot basal area ($\text{m}^2/\text{hectare}$). Species' error bars (grey) show parameter uncertainty, forest error bars (purple, orange and green) show the 95% confidence interval for the mortality rates predicted from the model-created and real datasets.

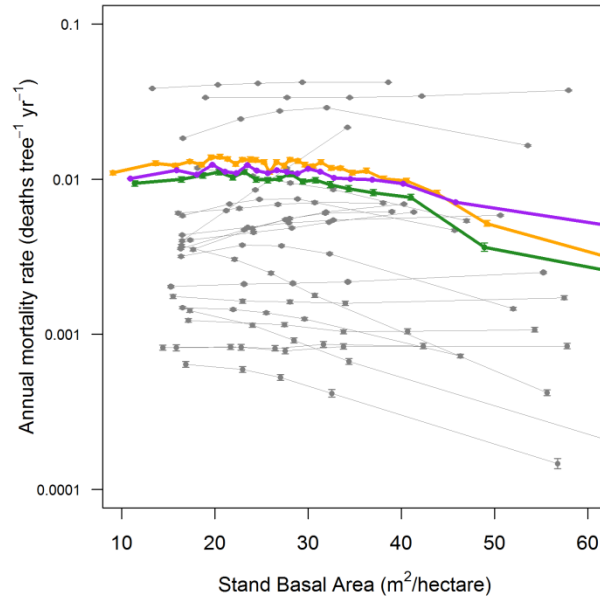


Figure A.4 Predicted versus observed plot-averaged annual mortality rate for all plots with at least 10 stems, showing the high correlation ($r^2=0.9$).

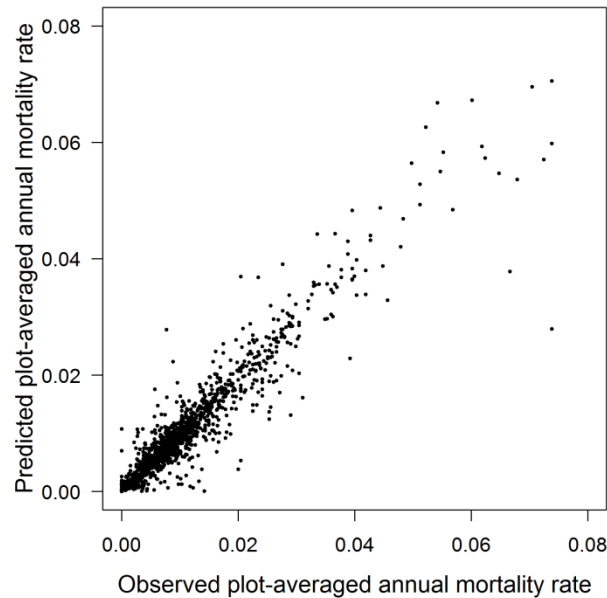


Figure A.5 Patterns of mortality due to regional variation in stand structure and environment alone. Maps of estimated annual forest-level mortality across the Eastern United States illustrating the contributions of variation in stand structure (stem size and plot basal area) and environment, modelled across the range of *Pinus taeda* to control for the effects of species composition. **(a)** Variation in forest structure alone (stem size and plot basal area), illustrated by removing environmental effects and modelling just the most common species (*P. taeda*). **(b)** The effect of variation in environment alone, illustrated by modelling *P. taeda* without stand structure variation (i.e. modelling a 20 cm DBH tree) across the region.

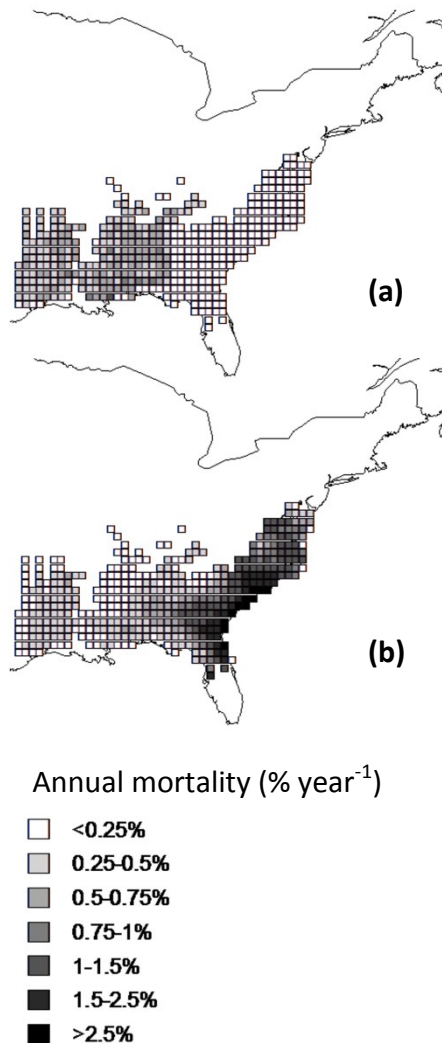
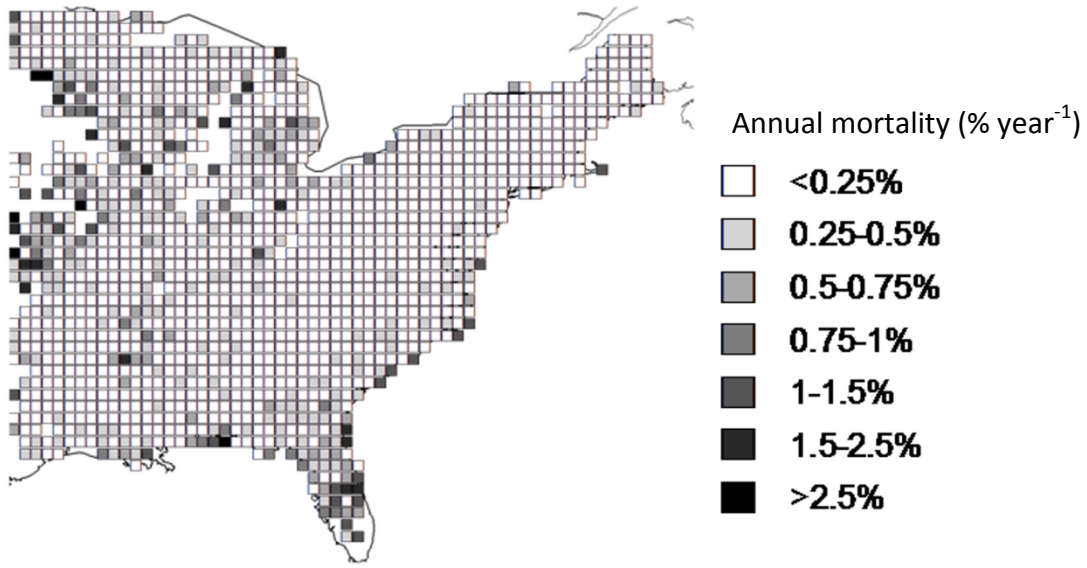


Figure A.6 Map of absolute difference between predicted and observed forest level mortality across the Eastern United States.



Appendix B: Aboveground allometry

Materials and Methods

Species-level traits

We found data for green wood density and modulus of elasticity (Young's modulus) in the literature (for density: Gutiérrez & Plaza 1967; Dietz 1975; Zanne et al. 2009; and for modulus of elasticity: U.S. Department of Agriculture Forest Service; Summitt & Sliker 1980; Gibson et al., 1981; Wessolly & Erb 1998; Borghetti et al. 2004; Alméras et al., 2005). When more than one estimate was given for European data we took the average.

Species' shade tolerance was represented using Ellenberg scores (Ellenberg, 1988), which range from 1 (plants typically found in deep shade) to 9 (mostly found in full light). Species' values were available for 28 species, accounting for 45% of the data, whilst for a further 24 species scores were calculated from average scores of other species of the same genus. In total 52 species, accounting for 94% of the data, were assigned shade-tolerance scores. We removed species which were non-native, and for those species which are frequently coppiced and/or pollarded we used the sub-dataset of high-quality, uncut stems. For height-diameter we parameterised the model for the 15 species for which we had information on wood density and modulus of elasticity, and which had at least 1000 samples within the dataset: in total over 550,000 stems. For one of these species we did not have a shade-tolerance score, but as we were primarily interested in the variables predicted by the *elastic similarity model* to have an effect, we preferred to include this species. For crown diameter-DBH there were 14 suitable species (over 175,000 stems in total) for which we had wood density and modulus of elasticity data, for which we had at least 1000 samples and which were native.

Choice of line-fitting methods

In this analysis we chose a method of line fitting which suited our aim to separate out the effects of several environmental variables on allometric scaling. These variables were partially correlated because, for example, denser forests are found in wetter places; which meant that the parameters associated with their effects were also likely to be partially correlated (Kruschke, 2010a). Bayesian methods provide the natural solution to such a problem, since instead of providing an estimate of the mean and variance of each parameter separately from all others, they provide parameter estimates in sets, each dependent on the others. These joint parameter estimates, drawn from the joint distribution of the model parameters, may therefore be used to make model predictions in a way that robustly accounts for correlation within a dataset. Although frequentist approaches such as generalised linear modelling allow the variance and covariance of parameters to be estimated, the approach is less

intuitive and flexible, and requires specification of parameter distributions, which are not easily selected well.

Reduced major axis (RMA) line fitting (also known as standardised major axis (SMA) line fitting) has become the most commonly used method for fitting allometric relationships and is routinely chosen over ordinary least squares regression (OLS) without specific justification, although in many cases OLS would be more appropriate (Smith, 2009). The main reason for this is that RMA line fitting assumes error in X as well as Y , often a reasonable assumption in allometry data. However, other factors ought to be included, and there are many excellent reviews in the literature which compare the assumptions and implications of these methods (e.g. Martin & Barbour 1989; Warton et al. 2006; Smith 2009). For example, error in the measurement of X should be considered relative to the error in Y . Another major difference is that RMA is a symmetric method (it produces the same line of best fit regardless of which variable is the predictor and which the response) whereas OLS is asymmetric. Choice of one or the other may therefore depend on whether finding the relationship between two variables or predicting one from the other is the aim.

Our Bayesian approach is more akin to OLS than it is to RMA, and although our primary aim was to choose a method which could accurately describe the response of height to a variety of co-varying predictors, RMA was also inappropriate because the diameter measurements were taken to the nearest 1 mm and H to the nearest 0.5 m. In these data, for a typical 15 cm DBH tree with a height of 10 m, this corresponds to measurement errors of 0.67% and 5% respectively, so the X variable was measured more accurately than the Y variable. We recognise that if we had used RMA methods then it is likely that the estimated slopes of our allometric relationships would have been greater, altering our comparisons of slope estimates with theoretical values.

The hierarchical Gibbs sampler

Hierarchical or multilevel modelling allows us to fit both individual species' allometric relationships and a 'universal' allometric relationship for all species together simultaneously. Hierarchical Gibbs sampling provides a natural way to constrain the allometry of less common species to be more similar to the population average (Gelfand et al., 1990; Lee, 1997; Gelman and Hill, 2007; Dietze et al., 2008). Rather than fit a universal 'species-average' allometric relationship we chose to use species covariates (Ellenberg score, wood density, modulus of elasticity) to constrain species with closer covariates to have closer allometries. This was done within the hierarchical Gibbs sampler by regressing the species-level parameters on the covariates at the across-species level (Gelman et al., 2004; Gelman and Hill, 2007; Dietze et al., 2008). By assuming normal distributions on parameter values and standard inverse-Gamma variance structures it is possible to fit the models using Gibbs samplers to find fully described posterior distributions, since prior and conditional distributions are conjugate (Lee, 1997).

We constructed a hierarchical normal Gibbs sampler to fit parameters to traditional power-law allometric equations, $y_{ij} = b_0 x_{ij}^{b_1}$, to describe the relationship between tree diameter (x_{ij}) and tree height and crown diameter (y_{ij}) following the methods used by Dietze *et al.* (2008). However, we decided not to fit the two models simultaneously as substantially more data were available to fit the height-DBH than crown diameter-DBH model.

The models take the form

$$y_{ij} = b_1 \log(x_{ij}) + \log(b_0) + \varepsilon_{ij} = \boldsymbol{\beta}_j \mathbf{x}_{ij} + \varepsilon_{ij} \quad (\text{Eqn B.1})$$

where, using the notation of Dietze *et al.* (2008), either $y_{ij} = \log(\text{height})$ or $\log(\text{crown diameter})$ (depending on the model), $\mathbf{x}_{ij} = \{1, \log(\text{DBH})\}$, $\boldsymbol{\beta}_j = \{\log(b_0), b_1\}$ and j is the species. We therefore assume that $y_{ij} \sim N(\boldsymbol{\beta}_j \mathbf{x}_{ij}, \sigma^2)$, where $\sigma^2 \sim IG(m, n)$ represents the inverse-gamma distributed variance. Moreover, we assume that all species' parameters have a common prior, $\boldsymbol{\beta}_j \sim N(\mathbf{B}, \Phi)$ where $\mathbf{B} = (B_0, B_1)$ and Φ are parameters to be fitted. This assumption makes the model hierarchical, which is an advantage because rare species' allometries will be constrained to be more similar to the universal allometry. In the fitting of the Gibbs sampler we used the standard conjugate hyperpriors, $\mathbf{B} \sim N(\mathbf{B}_0, \mathbf{V}_0)$ and $\Phi \sim \text{Inv-Wishart}(w, w\Psi)$. For the $\log(\text{height})$ - $\log(\text{diameter})$ model we used the MST prediction of 2/3 as a prior for the coefficient (b_1 in equation B.1) and a prior of 3 for the intercept ($\log(b_0)$). For the $\log(\text{crown diameter})$ - $\log(\text{diameter})$ model a prior of 3 for the intercept and 0 for the coefficient. For all parameters for the species level covariates we used a prior of 0. The prior \mathbf{V}_0 was the identity matrix, w was 1 and Ψ was the identity matrix.

To test the hypotheses based on species' differences in wood density, modulus of elasticity and shade tolerance, we fitted the Gibbs sampler with each included as a regression variable at the species level, that is we fitted

$$\boldsymbol{\beta}_j \sim N(\mathbf{ZB}, \Phi) \quad (\text{Eqn B.2})$$

where $\mathbf{Z} = \{z_1, z_2, z_3, z_4\}$ is a matrix of the covariates (as in Dietze *et al.*, 2008). We parameterised the model using a wide variety of different starting values for parameters, but none affected the significance of the fitted parameters or our conclusions.

The model was fitted using an algorithm written in C with code for sampling from standard distributions from Press *et al.* (1992), Lee (1997) and Kennedy & Gentle (2000) and model description from Gelfand *et al.* (1990), Gelman & Hill (2007) and Dietze *et al.* (2008).

Specifications of the MCMC sampler

We modelled DBH-H and DBH-CD relationships using an MCMC sampler. The models took the forms

$$y_{ij} \sim N\left(b_2 x_{ij}^{b_3}, (b_0 + b_1 x_{ij})^2\right) \quad (\text{Eqn B.3})$$

$$y_{ij} \sim N\left(b_2 + b_3 x_{ij}, (b_0 + b_1 x_{ij})^2\right) \quad (\text{Eqn B.4})$$

where (in equation B.3) y_{ij} is the H of each tree i of species j of DBH x_{ij} , and (in equation B.4) y_{ij} is the CD of each tree i of species j of DBH x_{ij} . In our final model b_2 and b_3 of equations B.3 and B.4 were linear functions of the environmental predictor variables:

$$\begin{aligned} b_2 &= a_0 + a_1(\text{competition index}) + a_2(\text{annual precipitation}) + a_3(\text{drought length}) \\ &\quad + a_4(\text{average temperature}) \\ b_3 &= c_0 + c_1(\text{competition index}) + c_2(\text{annual precipitation}) + c_3(\text{drought length}) \\ &\quad + c_4(\text{average temperature}) \end{aligned} \quad (\text{Eqn B.5})$$

We set wide and uninformative priors on all parameters of the MCMC sampler (Table B.4).

Convergence for the final models for DBH-H and DBH-CD was checked using the Gelman-Rubin statistic R (Gelman and Rubin, 1992) which assesses if a model has converged by comparing within and between chain variance for multiple chains. We fitted six chains using randomly chosen starting values for each parameter across a wide range (see Table B.4). We used a burn-in of 500,000 iterations and a sampling period of 500,000 for each chain. We applied the Gelman-Rubin statistic to each parameter and found that for most species convergence was achieved ($\sqrt{R} < 1.2$) within this number of iterations. However for the DBH-H model, a longer run was required to achieve convergence for seven species (*Abies alba*, *Arbutus glutinosa*, *Betula spp.*, *Juniperus thurifera*, *Pinus pinea*, *P. uncinata* and *Sorbus spp.*). For these we run six chains with a burn-in of 2,500,000 iterations and a sampling period of 1,500,000, after which convergence was achieved. For the DBH-CD models a burn-in of 500,000 and a sampling period of 500,000 for each of six chains was sufficient to achieve convergence for all species.

Additional Results

Hierarchical allometry

The fitted parameters for the across-species hierarchical allometry with species-level covariates are given in table S1 (parameters \mathbf{B} in equation B.2, height and DBH in cm), with 95% credible intervals on the given Bayesian means, where the coefficients of the covariates are for the normalised values. Overall, height for a given DBH increased with wood density, modulus of elasticity and Ellenberg score (i.e. decreased with shade tolerance). The effect of the Ellenberg score on the allometry was strongest and modulus of elasticity the weakest. However for all three covariates the central 95% of all parameters' posterior distributions contained 0, indicating that the effect is either not strong or not the same for all species, and therefore not well converged when species were combined. We found the

same result for crown diameter: none of the three covariates showed a clear positive or negative effect when tested in the hierarchical framework.

Tables and figures

Table B.1 Fitted intercept and gradient parameters for the across-species height/stem diameter and crown-diameter/stem diameter hierarchical Gibbs regression using species-level covariates (equation D.2), where height and diameter are both expressed in cm, and the 95% confidence interval of each parameter. All covariate regression parameters were non-significant.

	(constant)	Ellenberg score	Wood density	Modulus of elasticity
Height intercept	5.263 (4.911, 5.615)	-0.084 (-0.368, 0.201)	-0.001 (-0.274, 0.271)	-0.002 (-0.284, 0.280)
Height gradient	0.480 (0.396, 0.564)	0.027 (-0.055, 0.109)	-0.054 (-0.135, 0.028)	0.022 (-0.061, 0.104)
Crown diameter intercept	3.590 (3.065, 4.116)	0.039 (-0.372, 0.451)	-0.114 (-0.548, 0.320)	0.231 (-0.138, 0.600)
Crown diameter gradient	0.712 (0.602, 0.822)	0.022 (-0.095, 0.139)	0.083 (-0.033, 0.198)	-0.034 (-0.146, 0.078)

Table B.2 Fitted coefficient and exponent parameters, with 95% credible intervals, for all 26 species fitted together and for each species' height-diameter relationship (equation 2.3), where height and diameter are both expressed in cm for species with over 1000 individuals in the dataset. Neither the across-species model nor any individual species showed support for the 2/3 exponent, although the exponents of two species (*Pinus nigra* and *P. sylvestris*) were very close.

Species	Number	Coefficient b_2	Exponent b_3
Across-species model	696582	164.69 (163.48,165.91)	0.609 (0.606,0.611)
<i>Abies alba</i>	3961	198.10 (190.33,208.70)	0.62 (0.61,0.63)
<i>Acer campestre</i>	2194	287.98 (252.60,316.81)	0.44 (0.41,0.49)
<i>Alnus glutinosa</i>	3825	384.18 (362.56,404.69)	0.43 (0.42,0.45)
<i>Arbutus unedo</i>	2418	213.25 (196.76,233.55)	0.42 (0.38,0.45)
<i>Betula spp.</i>	7238	381.23 (357.38,399.61)	0.40 (0.38,0.42)
<i>Castanea sativa</i>	1162	682.24 (602.34,780.59)	0.16 (0.13,0.20)
<i>Corylus avellana</i>	1558	374.38 (344.95,400.12)	0.31 (0.28,0.35)
<i>Fagus sylvatica</i>	51479	350.88 (347.78,357.17)	0.46 (0.45,0.46)
<i>Ilex aquifolium</i>	1612	249.60 (215.62,281.44)	0.37 (0.32,0.42)
<i>Juniperus communis</i>	1465	154.74 (142.39,168.61)	0.42 (0.39,0.45)
<i>Juniperus thurifera</i>	7980	172.81 (168.12,177.53)	0.39 (0.39,0.40)
<i>Olea europaea</i>	2759	249.44 (232.14,272.62)	0.27 (0.24,0.29)
<i>Pinus halepensis</i>	88437	154.90 (153.73,156.04)	0.58 (0.57,0.58)
<i>Pinus nigra</i>	72548	128.13 (127.18,129.03)	0.67 (0.67,0.68)
<i>Pinus pinaster</i>	178622	163.06 (161.93,164.03)	0.63 (0.62,0.63)
<i>Pinus pinea</i>	25256	111.50 (108.87,114.18)	0.64 (0.63,0.65)
<i>Pinus sylvestris</i>	145446	142.44 (142.02,142.97)	0.66 (0.66,0.67)
<i>Pinus uncinata</i>	15239	169.00 (165.90,172.11)	0.58 (0.57,0.59)
<i>Quercus faginea</i>	3171	158.32 (146.91,171.77)	0.51 (0.48,0.54)
<i>Quercus ilex</i>	21551	202.44 (197.16,207.36)	0.34 (0.33,0.35)
<i>Quercus petraea</i>	13809	269.77 (256.35,280.01)	0.48 (0.47,0.50)
<i>Quercus pyrenaica</i>	4304	198.13 (183.32,213.11)	0.49 (0.47,0.52)
<i>Quercus robur</i>	26550	305.18 (297.30,310.49)	0.44 (0.44,0.45)
<i>Quercus suber</i>	3450	164.31 (147.53,179.68)	0.44 (0.42,0.48)
<i>Salix spp.</i>	2281	350.42 (323.84,383.45)	0.36 (0.32,0.39)
<i>Sorbus spp.</i>	1046	286.32 (256.75,323.22)	0.42 (0.37,0.45)

Table B.3 Spearman's rank correlation *p*-values for across-species predicted heights and crown diameters at given DBH and species' mean environmental conditions. Positive associations are indicated with (+), and negative relationships with (-).

Height				
DBH	Basal area of larger trees	Annual precipitation	Drought length	Average annual temperature
10	0.011 (+)	0.00001 (+)	0.0007 (-)	0.25 (-)
15	0.007 (+)	0.00001 (+)	0.002 (-)	0.156 (-)
20	0.0016 (+)	0.0001 (+)	0.0008(-)	0.097 (-)
Crown Diameter				
DBH	Basal area of larger trees	Annual precipitation	Drought length	Average annual temperature
10	0.197 (+)	0.048 (+)	0.064 (-)	0.240 (+)
15	0.573(+)	0.108 (+)	0.191(-)	0.584 (+)
20	0.682 (-)	0.112 (+)	0.186 (-)	0.627 (+)
Crown Diameter (angiosperms only)				
DBH	Basal area of larger trees	Annual precipitation	Drought length	Average annual temperature
15	0.011 (+)	0.022 (+)	0.005 (-)	0.132 (-)

Table B.4. Priors and initial value sampling ranges for each parameter for the final DBH-H and DBH-CD models (the same ranges were used for both). Gelman-Rubin convergence statistics were calculated using six chains, with initial parameter values were sampled randomly and uniformly across the given range for each parameter. Parameter names refer to equations D.3-D.5.

Parameter	b₀	b₁	a₀	c₀	a₁ - a₄	c₁ - c₄
Prior	U(-1000,1000)	U(-1000,1000)	U(-1000,1000)	U(-1000,1000)	U(-50,50)	U(-10,10)
Initial sampling distribution	U(100,300)	U(5,15)	U(100,800)	U(0,1)	U(-5,5)	U(-0.5,0.5)

Figure B.1 Height-diameter data for the 14 native species with over 1000 stems in the dataset for which H_{crit} (blue line) could be calculated, plotted with the MCMC-fitted allometry (green line), and the data. For most species the safety factor increased with size, and for many species, some specimens approached or even exceeded the hypothetical limit, particularly at small sizes.

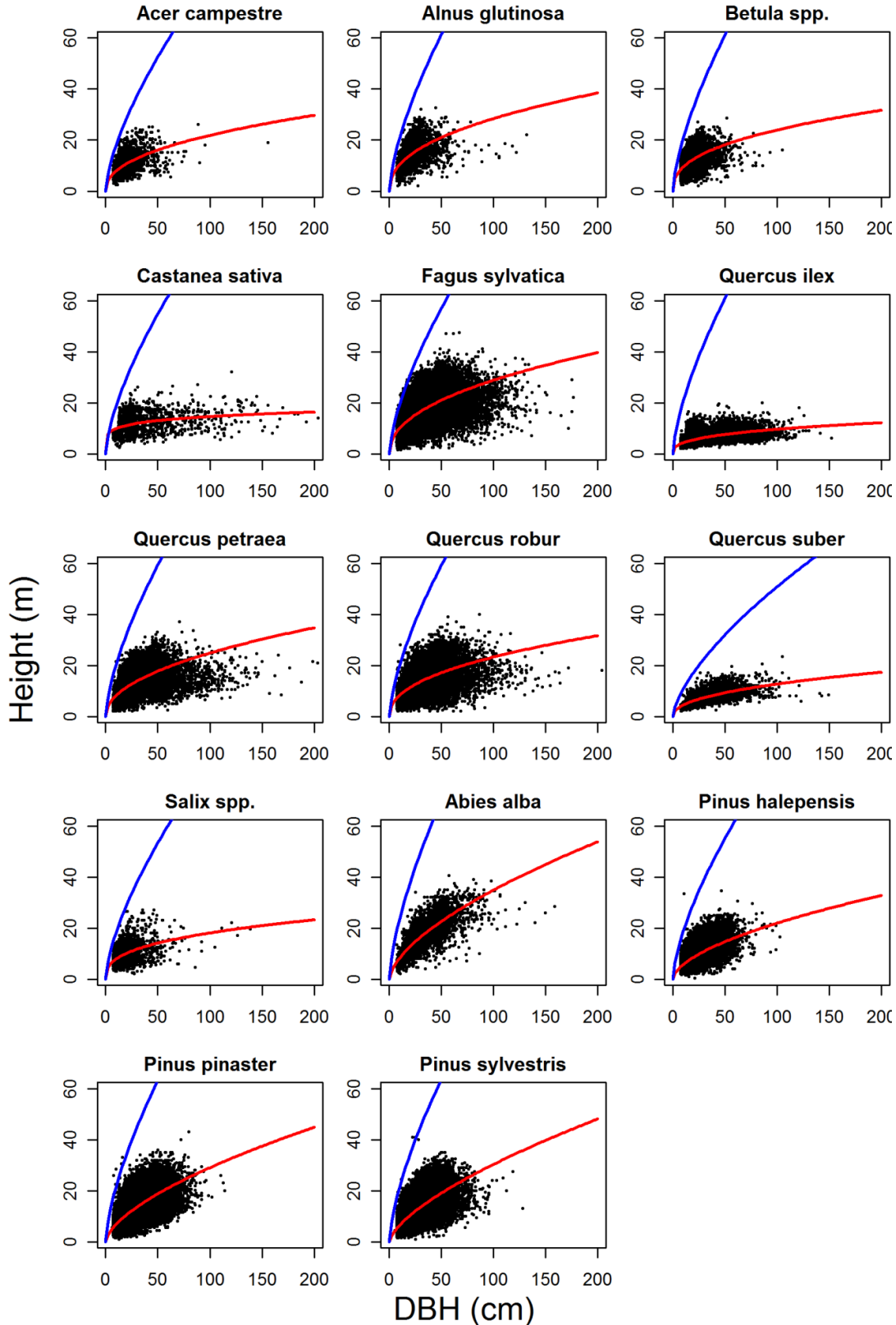


Figure B.2 As Fig. 4.2 (page 63), with species' names included. Predicted changes in height of 15-cm-DBH stems of 26 species in relation to (a) basal area of larger trees, (b) precipitation, (c) drought length, and (d) mean annual temperature. The symbols show height at the mean value of the environmental variables for the species - angiosperms (filled circles) and gymnosperms (open triangles) - whilst predicted variation in height is shown for ± 1 standard deviation in the environmental variable around the species' distribution mean (grey arrows). Estimates used in the predictions were produced using posterior estimates of the joint distribution of the parameters. Species' names are as follows: *P.sy*=*Pinus sylvestris*, *P.un*=*Pinus uncinata*, *P.pa*=*Pinus pinea*, *P.ha*=*Pinus halepensis*, *P.ni*=*Pinus nigra*, *P.pr*=*Pinus pinaster*, *A.al*=*Abies alba*, *J.co*=*Juniperus communis*, *J.th*=*Juniperus thurifera*, *Q.ro*=*Quercus robur*, *Q.pe*=*Quercus petraea*, *Q.py*=*Quercus pyrenaica**, *Q.fa*=*Quercus faginea**, *Q.il*=*Quercus ilex**, *Q.su*=*Quercus suber**, *A.gl*=*Alnus glutinosa*, *Sa.spp*=*Salix spp.*, *I.aq*=*Ilex aquifolium*, *O.eu*=*Olea europaea*, *A.un*=*Arbutus unedo*, *F.sy*=*Fagus sylvatica*, *C.sa*=*Castanea sativa**, *B.spp*=*Betula spp.*, *C.av*=*Corylus avellana*, *A.ca*=*Acer campestre*, *So.spp*=*Sorbus spp.* (*commonly coppiced/pollarded species so data was taken from a smaller database of trees with no signs of cutting at the time the inventory was taken).

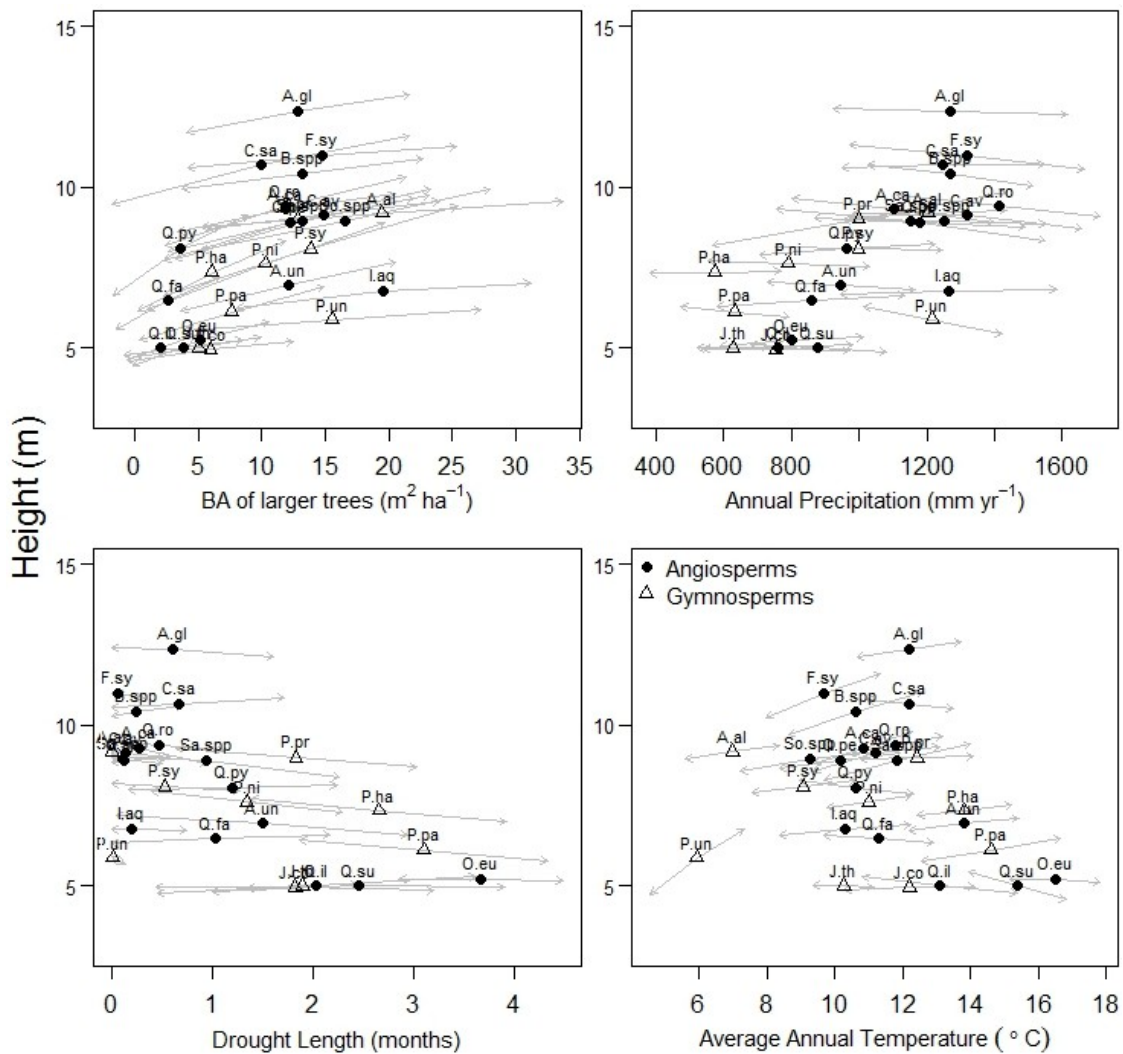
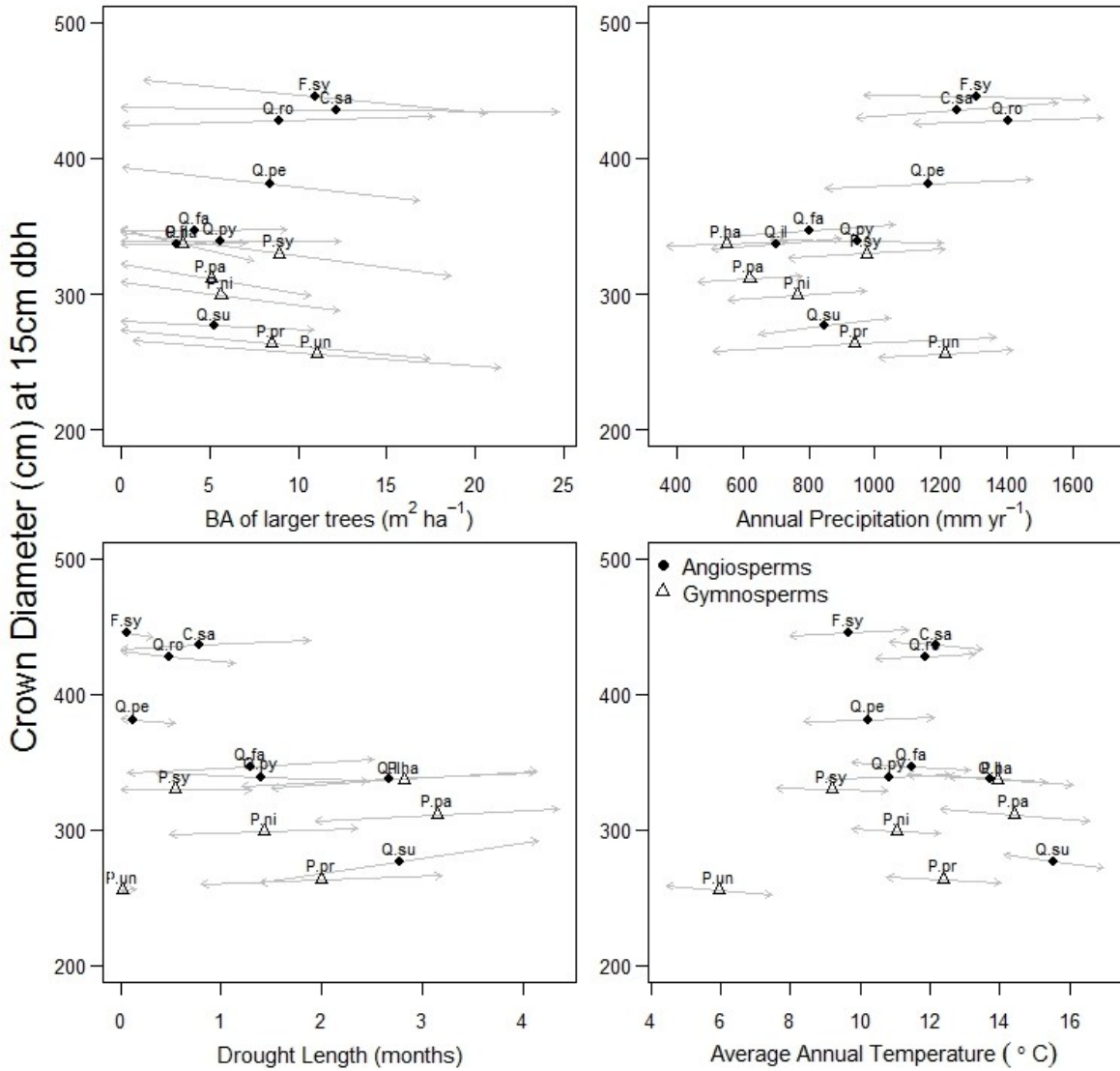


Figure B.3 As Fig. 4.3 (page 64), with species' names included. Predicted changes in crown diameter of 15-cm-DBH stems of 14 species in relation to (a) basal area of larger trees, (b) precipitation, (c) dry season length, and (d) mean annual temperature. The symbols show crown diameter at the mean value of the environmental variables for the species - angiosperms (filled circles) and gymnosperms (open triangles)- whilst predicted variation in crown diameter is shown for ± 1 standard deviation in the environmental variable around the mean (grey arrows). Estimates used in the predictions were produced using posterior estimates of the joint distribution of the parameters. Species' names are as in Fig. B.2.



Appendix C: ABC recruitment model

MCMC algorithm

We estimated parameters and credible intervals (CIs) of models of crown diameter, individual tree growth and annual mortality (described below) using an adaptive MCMC Metropolis algorithm (Lee, 1997; Gelman et al., 1999). We fitted several different functional forms for each model and compared them using the Akaike information criterion (Akaike, 1974). The MCMC algorithm compares parameter values using the log-likelihood of the data given the model. At each iteration the algorithm selects a parameter to alter and recalculates the likelihood. If the new parameter improves the likelihood then it is accepted by the algorithm. If not, it is accepted with probability of the ratio of the new and old likelihoods. In this way it returns not only a best-fit value for each parameter given the data but also estimates its distribution. The algorithm has two periods: burn-in and sampling. During the burn-in period (100,000-250,000 iterations of the algorithm) the algorithm alters the search range ("jumping distance") of each parameter value to achieve an optimal acceptance ratio of 25% (Gelman et al., 1999). After the burn-in period, the jumping distance is fixed (separately for each parameter). During sampling (100,000-250,000) iterations, parameter values are recorded every 100 iterations and the resulting parameter samples are taken as samples from the posterior distribution of each parameter. The resulting samples are then used to calculate mean and 95% confidence intervals for each parameter. We used non-informative uniform priors on all parameters so the MCMC algorithm needed to refer to the log-likelihood only. We used normalised mean annual temperature and mean annual precipitation values (taken from Gonzalo Jiménez, 2008). All models were fitted using an adaptive Metropolis algorithm written in C.

Construction of crown metric *CAI*

We parameterised models of crown diameter (CD) as a function of stem size (DBH) and climate for each species in order to calculate the crown area of adults in each plot, both in total and of each species individually. We used a subset of the IFN database in which two measurements of crown diameter were recorded for around four trees of particular silvicultural interest in each plot. The number of measurements for each species is shown in Table C.1. We parameterised DBH-CD equations using adaptive MCMC for the 30 species with more than 50 trees measurements in the data (in total >200,000 measurements), which accounted for >90% of the data. We tested a set of models

(see Table C.2 for functional forms tested) for crown diameter as a function of stem size and climate and selected the best model as the best for the most species and data (model 10, see Table C.2).

For each tree we used these functions to calculate, as a proportion of plot area, the total crown area of all taller trees in each plot, CAI_h , and the crown area of all conspecifics, CAI_{sp} in the plot. We also calculated the crown area of all trees in each plot, CAI_{pl} . Observed and predicted crown diameters are shown for each of the 30 fitted species in Fig. C.1. For species lacking allometric data we estimated the crown diameter-stem diameter relationship by either using the allometric equation of the single most closely related species or by averaging the allometric parameters of all the most closely related species if there was more than one at the closest distance (determined according to a phylogenetic tree created using the software *Phyloomatic*, Webb & Donoghue 2005, see Table C.3).

Construction of priors for growth and mortality functions

To construct priors for the growth and mortality functions within the ABC algorithm we fitted models to data of small trees from the second and third Spanish Forest Inventories (MMA, 1996, 2007). We selected plots that had been measured in both the second (IFN2) and third (IFN3) inventories and fitted models to trees that had stem diameter (DBH) < 10 cm in the IFN2, excluding individuals whose mortality was human induced. We fitted models to 16 species with >100 individual stems for both growth and mortality.

We compared the influence of three different predictors, initial stem size (DBH_1) and competition measured as crown area of all taller trees, CAI_h , and basal area of taller trees (BA_L) in the plot. All models were fitted with all parameters species-specific. We modelled the stem diameter measured in the IFN3 (DBH_2) as a function of the initial stem diameter measured in the IFN2 (DBH_1) and the growth rate using:

$$DBH_2 \sim N(DBH_1 + tGR, \omega_0^2) \quad (\text{Eqn C.1})$$

where GR is the predicted annual growth rate and t is the time interval (average 9 years).

We modelled the annual probability of mortality using a logistic function:

$$P(\text{mortality}) = 1/(1 + \exp(-k)) \quad (\text{Eqn C.2})$$

with corresponding likelihood:

$$\text{likelihood of data given model} = \begin{cases} [1 - P(\text{mortality})]^t & \text{if tree survived} \\ 1 - [1 - P(\text{mortality})]^t & \text{if tree died} \end{cases}$$

We compared a set of models with different functional forms and selected the best fit model according to AIC (see Tables C.4 and C.5, for model forms fitted for growth and mortality respectively).

Results of growth and mortality models

We compared seven models for annual growth and four for annual mortality rate (Tables C.4 and C.5). We calculated AIC values to compare models for each species individually. The best fit growth model for most species was a three parameter function with CAI_h as a predictor (model 3 in Table C.4), so we used this functional form for growth in the recruitment model. Similarly, the best fit model for mortality for most species was a two function with CAI_h as a predictor (model 3 in Table C.5). Individual species' parameter values and their corresponding 95% CIs for these two models are shown in Table C.6 and C.7. Predicted and observed values for DBH_2 , fitted using model 3 in Table C.4, are shown in Fig. C.2. Predicted and observed values for annual mortality rate, fitted using model 3 in Table C.5, are shown in Fig. C.3. Predicted growth and mortality rates for each species across the range of values of CAI_h in which it is found are shown in Fig. 5.2.

Table C.1 Amount of field data for each species used to estimate DBH-crown diameter allometric equations.

Species Name	Count
<i>Abies alba</i>	631
<i>Abies pinsapo</i>	63
<i>Castanea sativa</i>	4659
<i>Chamaecyparis lawsoniana</i>	177
<i>Eucalyptus camaldulensis</i>	1972
<i>Eucalyptus globules</i>	7127
<i>Eucalyptus nitens</i>	143
<i>Fagus sylvatica</i>	10292
<i>Larix spp.</i>	409
<i>Picea abies</i>	59
<i>Pinus halepensis</i>	30046
<i>Pinus nigra</i>	18455
<i>Pinus pinaster</i>	38086
<i>Pinus pinea</i>	8970
<i>Pinus radiata</i>	6609
<i>Pinus sylvestris</i>	28093
<i>Pinus uncinata</i>	2720
<i>Platanus spp.</i>	115
<i>Populus alba</i>	97
<i>Populus nigra</i>	1817
<i>Pseudotsuga menziesii</i>	172
<i>Quercus canariensis</i>	417
<i>Quercus faginea</i>	7845
<i>Quercus ilex</i>	36945
<i>Quercus petraea</i>	3660
<i>Quercus pyrenaica</i>	11832
<i>Quercus robur</i>	7958
<i>Quercus rubra</i>	304
<i>Quercus suber</i>	8693
<i>Robinia pseudoacacia</i>	214

Table C.2 Tested models of crown diameter (CD) as a function of stem size (DBH), drought length (DL), average annual temperature (AvT) and annual precipitation (PA), and the number of parameters in each model. Parameters fitted are denoted p_0 - p_6 . Average temperature and annual precipitation were normalised to aid convergence (using annual precipitation mean = 862, standard deviation = 378, average temperature mean = 12, standard deviation = 3).

Model #	Description	# parameters	AIC	AIC rank	#species' best model	% data best model
0	$CD \sim N(p_1+p_2DBH, p_0)$	3	5593348	11	1	0.07
1	$CD \sim N(p_2+p_3DBH, p_0+p_1DBH)$	4	5481178	7	5	16.92
2	$CD \sim N(p_1+p_2DBH+p_3DL, p_0)$	4	5584746	8	0	0.00
3	$CD \sim N(p_2+p_3DBH+p_4DL, p_0+p_1DBH)$	5	5472071	3	0	0.00
4	$CD \sim N(p_1+p_2DBH+p_3AvT, p_0)$	4	5588356	9	0	0.00
5	$CD \sim N(p_2+p_3DBH+p_4AvT, p_0+p_1DBH)$	5	5474664	5	2	1.98
6	$CD \sim N(p_1+p_2DBH + p_3PA, p_0)$	4	5590359	10	0	0.00
7	$CD \sim N(p_2+p_3DBH+p_4PA, p_0+p_1DBH)$	5	5478742	6	4	3.34
8	$CD \sim N(p_2+p_3DBH+p_4DL+p_5AvT, p_0+p_1DBH)$	6	5466517	2	2	2.90
9	$CD \sim N(p_2+p_3DBH+p_4PA+p_5AvT, p_0+p_1DBH)$	6	5472122	4	5	19.92
10	$CD \sim N(p_2+p_3DBH+p_4PA+p_5AvT+p_6DL, p_0+p_1DBH)$	7	5464760	1	12	54.87

Table C.3 IFN species code, species genus and family, the number of plots the species was found in, and the code of the species' crown diameter allometric equations used to calculate crown area for the species (in bold if the species had its own equation), assigned using nearest phylogenetic neighbour or neighbours, if there was more than one at the closest distance. If more than one species' code is listed then the average of those species' parameters was used. For 93% of the data we were able to use crown diameter equations fitted to the individual species' crown measurements.

IFN code	Species	Family	#Plots	IFN code(s) of species' allometric equation used to fit crown area.
31	<i>Abies alba</i>	Pinaceae	293	31
32	<i>Abies pinsapo</i>	Pinaceae	42	32
7	<i>Acacia spp.</i>	Mimosaceae	37	92
76	<i>Acer campestre</i>	Aceraceae	902	41,42,43,44,45,46,47,48,51,58,61,62,64,71,72, 79,92
54	<i>Alnus glutinosa</i>	Betulaceae	618	41,42,43,44,45,46,47,48,71,72
88	<i>Apollonias barbujana</i>	Lauraceae	4	41,42,43,44,45,46,47,48,51,58,61,62,64,71,72,79,92
68	<i>Arbutus unedo</i>	Ericaceae	743	41,42,43,44,45,46,47,48,51,58,61,62,64,71,72,92
73	<i>Betula spp.</i>	Betulaceae	1424	41,42,43,44,45,46,47,48,71,72
91	<i>Buxus sempervirens</i>	Buxaceae	29	41,42,43,44,45,46,47,48,51,58,61,62,64,71,72,92
98	<i>Carpinus betulus</i>	Coryloideae	5	41,42,43,44,45,46,47,48,71,72
72	<i>Castanea sativa</i>	Fagaceae	2396	72
17	<i>Cedrus atlantica</i>	Pinaceae	17	21,22,23,24,25,26,28,31,32,33,34,35
13	<i>Celtis australis</i>	Ulmaceae	18	41,42,43,44,45,46,47,48,71,72
67	<i>Ceratonia siliqua</i>	Fabaceae	218	92
18	<i>Chamaecyparis lawsoniana</i>	Cupressaceae	76	18
9	<i>Cornus sanguinea</i>	Cornaceae	1	41,42,43,44,45,46,47,48,51,58,61,62,64,71,72,92
74	<i>Corylus avellana</i>	Betulaceae	433	41,42,43,44,45,46,47,48,71,72
15	<i>Crataegus spp.</i>	Rosaceae	328	41,42,43,44,45,46,47,48,71,72
36	<i>Cupressus sempervirens</i>	Cupressaceae	71	18
83	<i>Erica arborea</i>	Ericaceae	183	41,42,43,44,45,46,47,48,51,58,61,62,64,71,72,92
62	<i>Eucalyptus camaldulensis</i>	Myrtaceae	691	62
61	<i>Eucalyptus globulus</i>	Myrtaceae	3006	61
64	<i>Eucalyptus nitens</i>	Myrtaceae	69	64
5	<i>Euonymus</i>	Celastraceae	1	51,58

<i>europaeus</i>				
71	<i>Fagus sylvatica</i>	Fagaceae	3549	71
3	<i>Frangula alnus</i>	Rhamnaceae	7	41,42,43,44,45,46,47,48,71,72
55	<i>Fraxinus angustifolia</i>	Oleaceae	761	41,42,43,44,45,46,47,48,51,58,61,62,64,71,72,92
1	<i>Heberdenia bahamensis</i>	Myrsinaceae	2	41,42,43,44,45,46,47,48,51,58,61,62,64,71,72,79,92
65	<i>Ilex aquifolium</i>	Aquifoliaceae	446	41,42,43,44,45,46,47,48,51,58,61,62,64,71,72,92
82	<i>Ilex canariensis</i>	Aquifoliaceae	114	41,42,43,44,45,46,47,48,51,58,61,62,64,71,72,92
75	<i>Juglans regia</i>	Juglandaceae	98	41,42,43,44,45,46,47,48,71,72
37	<i>Juniperus communis</i>	Cupressaceae	832	18
39	<i>Juniperus phoenicea</i>	Cupressaceae	203	18
38	<i>Juniperus thurifera</i>	Cupressaceae	1588	18
35	<i>Larix spp.</i>	Pinaceae	173	35
94	<i>Laurus nobilis</i>	Lauraceae	139	41,42,43,44,45,46,47,48,51,58,61,62,64,71,72,79,92
12	<i>Malus sylvestris</i>	Rosaceae	32	41,42,43,44,45,46,47,48,71,72
81	<i>Myrica faya</i>	Myricaceae	202	41,42,43,44,45,46,47,48,71,72
87	<i>Ocotea phoetens</i>	Lauraceae	2	41,42,43,44,45,46,47,48,51,58,61,62,64,71,72,79,92
66	<i>Olea europaea</i>	Oleaceae	743	41,42,43,44,45,46,47,48,51,58,61,62,64,71,72,92
63	Other/unknown eucalyptus species	Myrtaceae	1	61,62,64
89	Other/unknown laurel species	Lauraceae	6	41,42,43,44,45,46,47,48,51,58,61,62,64,71,72,79,92
29	Other/unknown pine species	Pinaceae	7	21,22,23,24,25,26,28
59	Other/unknown riparian species	Unknown (Angiosperm Average)	6	41,42,43,44,45,46,47,48,51,58,61,62,64,71,72,79,92
90	Other/unknown small trees	Unknown (Angiosperm Average)	1	41,42,43,44,45,46,47,48,51,58,61,62,64,71,72,79,92
99	Other/unknown species	Unknown (Angiosperm Average)	252	41,42,43,44,45,46,47,48,51,58,61,62,64,71,72,79,92
84	<i>Persea indica</i>	Lauraceae	43	41,42,43,44,45,46,47,48,51,58,61,62,64,71,72,79,92
8	<i>Phillyrea latifolia</i>	Oleaceae	96	41,42,43,44,45,46,47,48,51,58,61,62,64,71,72,92
69	<i>Phoenix spp.</i>	Arecaceae	12	41,42,43,44,45,46,47,48,51,58,61,62,64,71,72,79,92
86	<i>Picconia excelsa</i>	Oleaceae	16	41,42,43,44,45,46,47,48,51,58,61,62,64,71,72,92
33	<i>Picea abies</i>	Pinaceae	34	33

27	<i>Pinus canariensis</i>	Pinaceae	1448	23,24,26
24	<i>Pinus halepensis</i>	Pinaceae	10893	24
25	<i>Pinus nigra</i>	Pinaceae	6988	25
26	<i>Pinus pinaster</i>	Pinaceae	12372	26
23	<i>Pinus pinea</i>	Pinaceae	3288	23
28	<i>Pinus radiata</i>	Pinaceae	2368	28
21	<i>Pinus sylvestris</i>	Pinaceae	9221	21
22	<i>Pinus uncinata</i>	Pinaceae	929	22
93	<i>Pistacia terebinthus</i>	Anacardiaceae	39	61,62,64
79	<i>Platanus hispanica</i>	Platanaceae	72	79
51	<i>Populus alba</i>	Salicaceae	51	51
58	<i>Populus nigra</i>	Salicaceae	658	58
52	<i>Populus tremula</i>	Salicaceae	158	51,58
95	<i>Prunus spp.</i>	Rosaceae	324	41,42,43,44,45,46,47,48,71,72
34	<i>Pseudotsuga menziesii</i>	Pinaceae	80	34
16	<i>Pyrus spp.</i>	Rosaceae	30	41,42,43,44,45,46,47,48,71,72
47	<i>Quercus canariensis</i>	Fagaceae	220	47
44	<i>Quercus faginea</i>	Fagaceae	4373	44
45	<i>Quercus ilex</i>	Fagaceae	15714	45
42	<i>Quercus petraea</i>	Fagaceae	1695	42
43	<i>Quercus pyrenaica</i>	Fagaceae	4596	43
41	<i>Quercus robur</i>	Fagaceae	3821	41
48	<i>Quercus rubra</i>	Fagaceae	154	48
46	<i>Quercus suber</i>	Fagaceae	3537	46
4	<i>Rhamnus alaternus</i>	Rhamnaceae	11	41,42,43,44,45,46,47,48,71,72
96	<i>Rhus coriaria</i>	Anacardiaceae	4	61,62,64
92	<i>Robinia pseudoacacia</i>	Fabaceae	145	92
57	<i>Salix spp.</i>	Salicaceae	702	51,58
97	<i>Sambucus nigra</i>	Adoxaceae	47	41,42,43,44,45,46,47,48,51,58,61,62,64,71,72,92
78	<i>Sorbus spp.</i>	Rosaceae	492	41,42,43,44,45,46,47,48,71,72
53	<i>Tamarix spp.</i>	Tamaricaceae	7	41,42,43,44,45,46,47,48,51,58,61,62,64,71,72,92
14	<i>Taxus baccata</i>	Taxaceae	49	18
77	<i>Tilia spp.</i>	Malvaceae	123	61,62,64
56	<i>Ulmus minor</i>	Ulmaceae	246	41,42,43,44,45,46,47,48,71,72

Table C.4 Set of species-specific growth models tested with corresponding maximum log-likelihoods and AICs, and the number of species for which each model was the best fit (according to AIC) out of the fourteen in the analysis. Model 3 (shown in bold) provided the best fit for the largest number of species, and was therefore chosen.

Model number	Annual growth (GR in equation C.1)	Max log likelihood	# of parameters	AIC	# of species' best model
0	$GR=\omega_1$	-20151.7	2	40359.4	0
1	$GR=\omega_1 DBH$	-20190.1	2	40436.2	0
2	$GR=\omega_1/(1+\omega_2 BA_L)$	-19024.1	3	38132.2	4
3	$GR=\omega_1/(1+\omega_2 CAI_h)$	-19134.9	3	38353.7	6
4	$GR=\omega_1 DBH^{\omega_2}$	-20134.5	3	40353	0
5	$GR=\omega_1 DBH^{\omega_2}/(1+\omega_3 BA_L)$	-18986.5	4	38084.9	3
6	$GR=\omega_1 DBH^{\omega_2}/(1+\omega_3 CAI_h)$	-19125.7	4	38363.3	1

Table C.5 Set of species-specific mortality models tested, with corresponding maximum log-likelihoods and AICs, and the number of species for which each model was the best fit (according to AIC) out of the fourteen in the analysis. Model 3 (shown in bold) provided the best fit for the largest number of species, and was therefore chosen.

Model number	Annual probability of mortality P(mortality)=1/(1+exp(-k)) (equation C.2)	Max log likelihood	# of parameters	AIC	# of species' best model
0	$k=\tau_0$	-3550.79	1	7129.6	2
1	$k=\tau_0 + \tau_1 DBH$	-3541.05	2	7138.1	0
2	$k=\tau_0 + \tau_1 BA_L$	-3425.55	2	6907.6	5
3	$k=\tau_0 + \tau_1 CAI_h$	-3414.51	2	6885	7

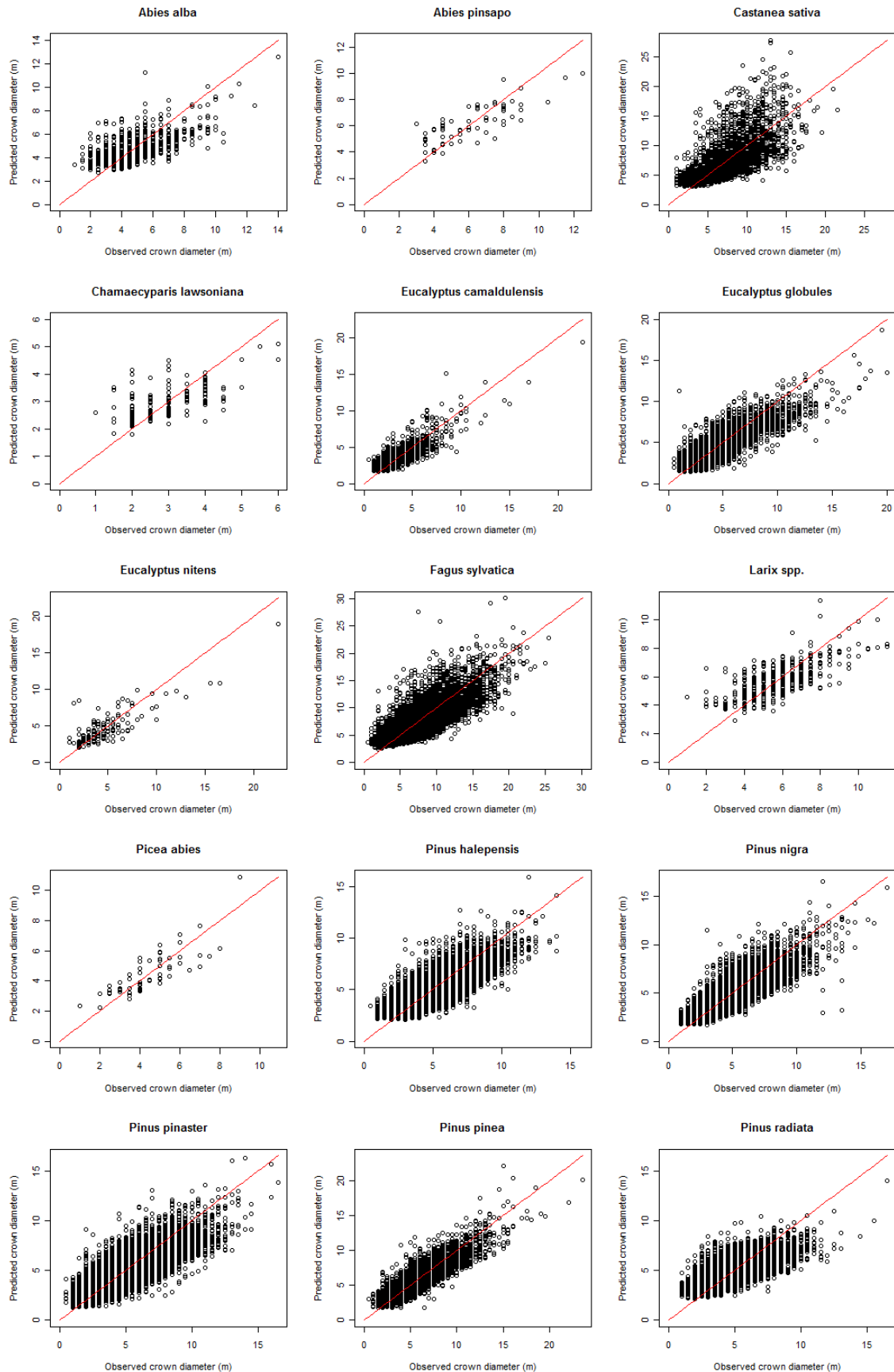
Table C.6 Parameter values and 95% confidence intervals for the chosen models for growth (equation C.1) for each of the fourteen species in the analysis (model 3 in table C.4). Parameters ω_1 and ω_2 formed prior mean values for parameters p_2 and p_3 in equation 5.5 in the ABC-SMC algorithm.

Species	ω_0	ω_1	ω_2
<i>Castanea sativa</i>	1.990 (1.972,2.008)	0.386 (0.334,0.437)	1.043 (0.662,1.424)
<i>Fagus sylvatica</i>	1.436 (1.381,1.491)	0.412 (0.374,0.451)	1.895 (1.557,2.233)
<i>Juniperus thurifera</i>	1.314 (1.235,1.393)	0.186 (0.165,0.208)	2.980 (1.524,4.435)
<i>Pinus halepensis</i>	1.994 (1.983,2.005)	0.342 (0.327,0.357)	1.855 (1.585,2.125)
<i>Pinus nigra</i>	1.907 (1.863,1.950)	0.499 (0.479,0.519)	3.167 (2.870,3.464)
<i>Pinus pinaster</i>	1.999 (1.998,2.001)	0.843 (0.812,0.874)	4.440 (4.080,4.800)
<i>Pinus pinea</i>	1.991 (1.975,2.007)	0.583 (0.535,0.632)	2.690 (2.073,3.306)
<i>Pinus sylvestris</i>	1.998 (1.995,2.002)	0.572 (0.553,0.591)	2.325 (2.146,2.505)
<i>Pinus uncinata</i>	1.840 (1.726,1.953)	0.486 (0.424,0.549)	3.445 (2.514,4.376)
<i>Quercus faginea</i>	1.096 (1.065,1.126)	0.177 (0.170,0.185)	0.872 (0.703,1.040)
<i>Quercus ilex</i>	1.499 (1.479,1.519)	0.161 (0.156,0.165)	0.459 (0.373,0.545)
<i>Quercus petraea</i>	1.524 (1.415,1.633)	0.327 (0.259,0.395)	1.964 (1.064,2.864)
<i>Quercus pyrenaica</i>	1.409 (1.377,1.441)	0.236 (0.226,0.246)	1.372 (1.191,1.553)
<i>Quercus suber</i>	1.572 (1.473,1.671)	0.311 (0.254,0.368)	2.329 (1.299,3.359)

Table C.7 Parameter values and 95% confidence intervals for the chosen models for mortality (equation C.2) for each of the fourteen species in the analysis (model 3 in table C.5). Parameters τ_0 and τ_1 formed prior mean values for parameters p_4 and p_5 in equation 5.5 in the ABC-SMC algorithm.

Species	τ_0	τ_1
<i>Castanea sativa</i>	-3.422 (-3.744,-3.100)	0.283 (0.004,0.563)
<i>Fagus sylvatica</i>	-5.818 (-6.229,-5.406)	0.834 (0.603,1.066)
<i>Juniperus thurifera</i>	-6.143 (-6.695,-5.591)	2.309 (1.011,3.607)
<i>Pinus halepensis</i>	-4.791 (-4.941,-4.641)	1.596 (1.330,1.862)
<i>Pinus nigra</i>	-4.782 (-4.929,-4.635)	0.923 (0.739,1.106)
<i>Pinus pinaster</i>	-4.011 (-4.144,-3.877)	1.687 (1.493,1.882)
<i>Pinus pinea</i>	-4.042 (-4.352,-3.732)	0.665 (0.157,1.174)
<i>Pinus sylvestris</i>	-5.381 (-5.543,-5.219)	1.554 (1.406,1.702)
<i>Pinus uncinata</i>	-5.966 (-6.569,-5.363)	2.549 (1.779,3.320)
<i>Quercus faginea</i>	-5.325 (-5.543,-5.107)	0.858 (0.538,1.177)
<i>Quercus ilex</i>	-5.242 (-5.341,-5.142)	0.788 (0.620,0.956)
<i>Quercus petraea</i>	-6.562 (-7.281,-5.843)	1.988 (1.391,2.586)
<i>Quercus pyrenaica</i>	-4.640 (-4.771,-4.508)	1.051 (0.898,1.204)
<i>Quercus suber</i>	-5.124 (-5.601,-4.647)	1.434 (0.772,2.097)

Figure C.1 Predicted vs observed crown diameters fitted using the chosen crown diameter model (model 10 in table C.2) for each of the 30 species for which we had >50 measurements in the dataset.. The one to one relationship is shown by the red line.



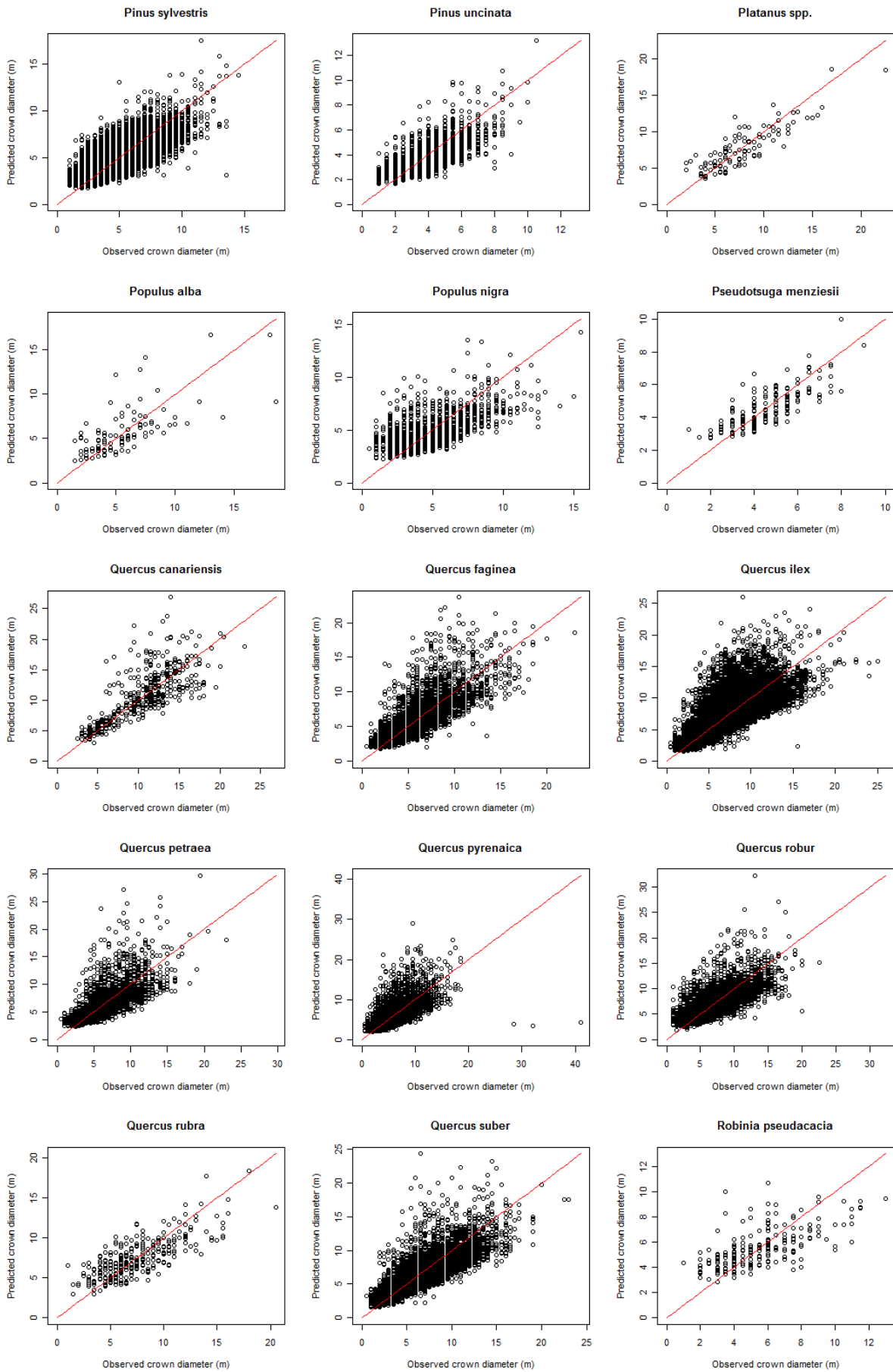


Figure C.2 Predicted and observed diameters fitted using the chosen growth model (model 3 in table C.4). Growth was predicted separately for each species using initial stem size (DBH_1) and CAI_h , and final observed diameter (DBH_2) is shown against predicted final diameter ($pDBH_2$). The one to one relationship is shown by the red line.

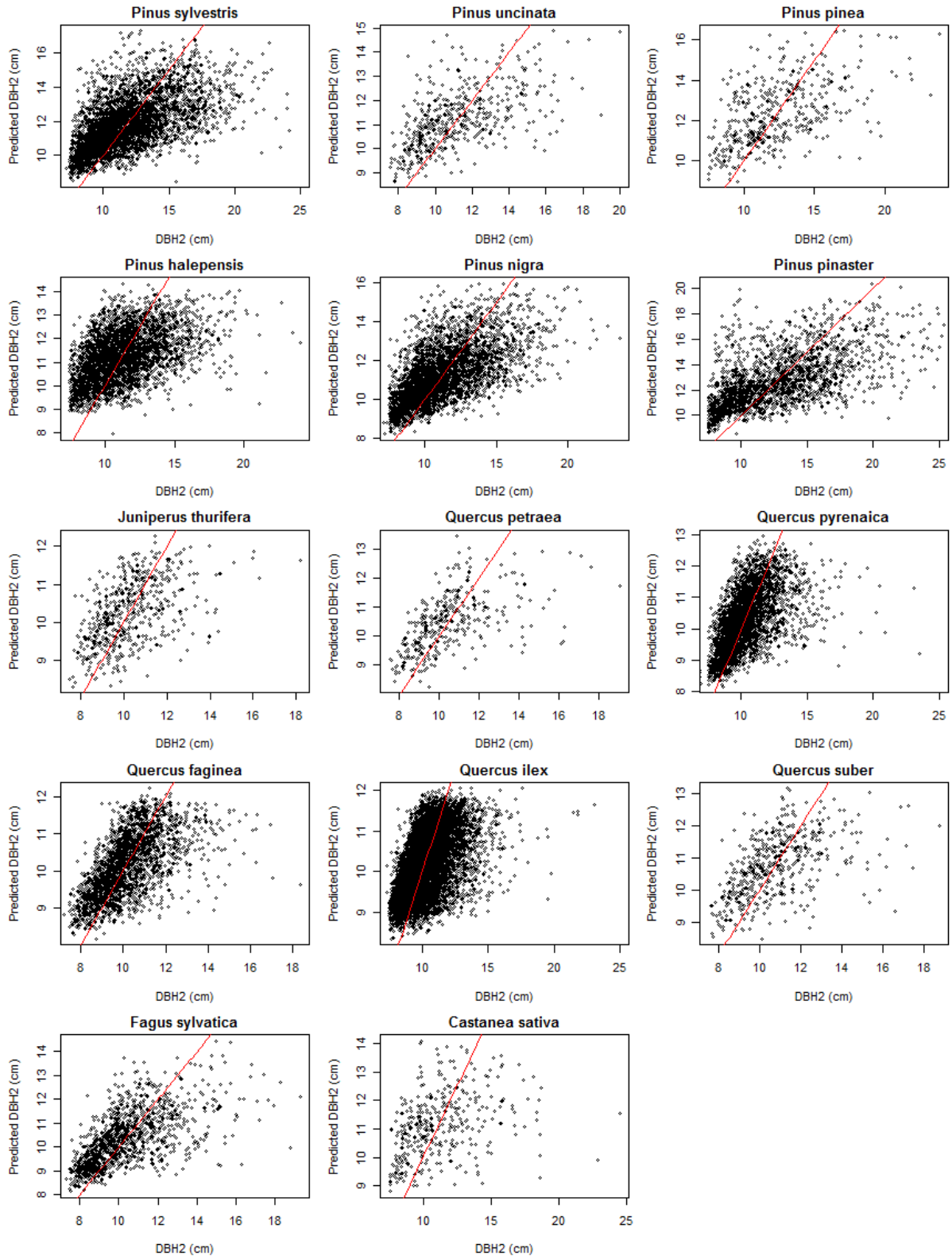
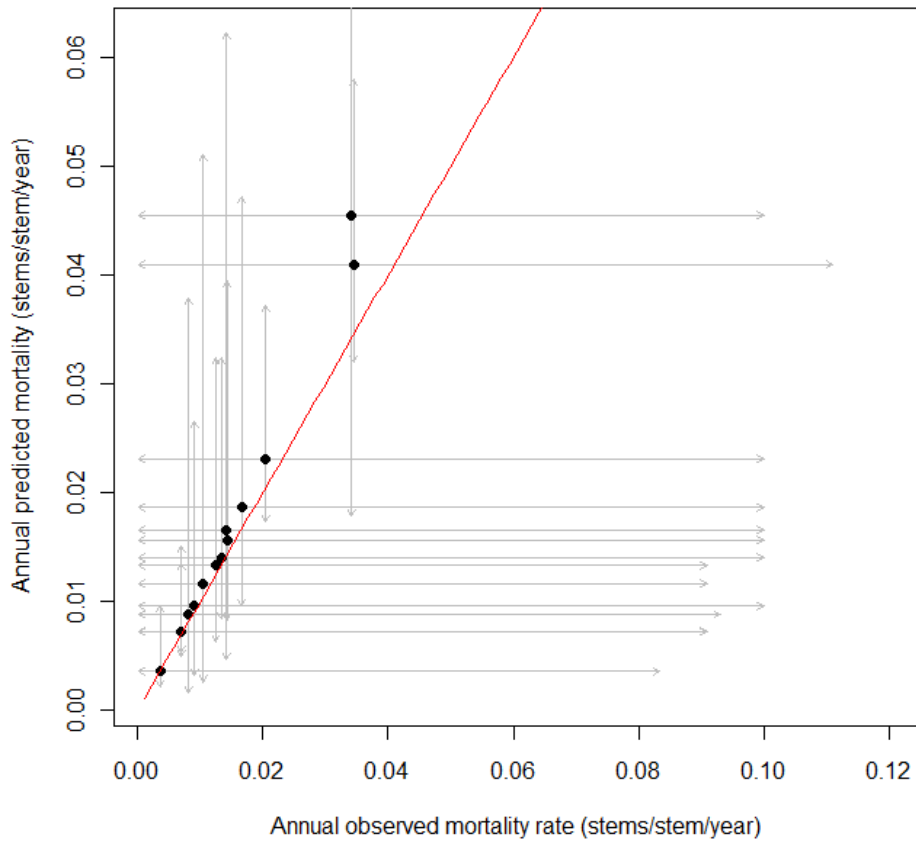


Figure C.3 Predicted and observed annual mortality fitted using the chosen mortality model (model 3 in table C.5). Mortality was predicted separately for each species using CAI_h and average rates for each species are shown with their 95% credible intervals. The one to one relationship is shown by the red line.



Appendix D: Simulation model

Data and species selection

The PPA modelling framework uses individual-based models of tree growth, mortality and allometry. We used data from the second and third Spanish forest inventories (IFN2 (1986-1996) and IFN3 (1997-2007), (MMA, 1996, 2007)) to derive growth and mortality functions, and allometry data from IFN2 only. We selected species for which we had at least 1000 points with which to parameterise the mortality model and at least 100 points to parameterise the growth and allometry models. We used a higher limit for the mortality model as it is a rare event with a discrete response (alive/dead) and requires more data to accurately parameterise the model. There were 14 species which satisfied this requirement (see Table D.1). Data on height and stem diameter were taken from IFN2. Spanish forests have a long history of human management, so for five species that are commonly coppiced/pollarded we used a smaller database of trees that showed no signs of cutting at the time the inventory was taken (these were *Quercus pyrenaica*, *Q. faginea*, *Q. ilex*, *Q. suber* and *Castanea sativa*). For a subset of the database (around 150,000 stems of 14 species of silvicultural interest), two measurements of crown diameter were recorded for around four trees per plot. For both stem diameter and crown diameter we used the average of the two measurements taken in the inventory in the model. The time between the two surveys ranged from 6-13 years, with an average of 11 years. In order to compare between IFN2 and IFN3 to derive growth and mortality rates we used only plots whose locations had been positively identified in IFN3. We also removed all plots not classified as thinning (stand density decreasing and mean stem size increasing over the time period of the two surveys), leaving 11,057 plots for the growth models. For mortality analyses we also removed plots which had evidence of management (recorded in IFN3), leaving 8,783 plots.

Submodel fitting methods: Growth, mortality and allometry

To construct the models and estimate mean and 95% credible intervals for their parameters we used an adaptive MCMC Metropolis algorithm to fit different functional forms and compared them using the Akaike information criterion (AIC, Akaike, 1974) (the MCMC algorithm is described in full in Chapters Two and Four). We used a burn-in period of between 250,000 and 500,000 (with a longer burn-in for models with more parameters) and a sampling period of 250,000 iterations, retaining every 100th sample parameter set. Details of the priors used are given in each section. All models were fitted using an adaptive Metropolis algorithm written in C (compiled using MS Visual Studio 2008). We took climate data from Gonzalo Jiménez (2008), the same data used in Chapter Four, to test as

possible predictors for each model. We also used canopy area of taller trees, CAI_h (Caspersen et al., 2011; Coomes et al., 2012), as derived for the Spanish data in Chapter Five, as a measure of the competition experienced by each tree, and tested this as a possible predictor for each model.

Growth

To model growth we used a simple power function dependent on stem diameter (DBH):

$$\frac{d(DBH)}{dt} = \alpha DBH^\beta \quad (\text{Eqn D.1})$$

where α and β are parameters to be estimated, with priors set as $U(-10,10)$. This integrates, for initial $DBH = DBH_0$ and final predicted DBH (after t years of growth) = $pDBH_t$, to give:

$$pDBH_t = \left[DBH_0^{1-\beta} + \alpha(1-\beta)t \right]^{1/(1-\beta)} \quad (\text{Eqn D.2})$$

In order to incorporate the size-dependent growth decline we also used a simpler form of the power law, which gives

$$pDBH_t = t \times \alpha DBH_0^\beta \exp(-\gamma DBH_0) + DBH_0 \quad (\text{Eqn D.3})$$

We used a normal distribution with standard deviation increasing linearly with initial size (DBH_0), so that to compare real and predicted DBH_t we used:

$$DBH_t \sim N(pDBH_t, \sigma^2), \quad \text{with} \quad \sigma = \rho_0 + \rho_1 DBH_0 \quad (\text{Eqn D.4})$$

where ρ_0 and ρ_1 are parameters to be estimated (with priors $U(0,10)$ and $U(-10,10)$ respectively). This model had corresponding likelihood within the MCMC run (with data X and model M dependent on parameters θ):

$$l(X|M, \theta) = \sum_i \ln \left\{ \left(\frac{1}{\sqrt{2\pi}\sigma} \right) \exp \left(-\frac{(DBH_t - pDBH_t)^2}{2\sigma^2} \right) \right\} \quad (\text{Eqn D.5})$$

We tested different functional forms for growth by incorporating the effects of competition and climate into the coefficient α . We modelled the effect of competition on growth using the area of taller trees (CAI_h) as a predictor of competition, applied in a two-parameter functional form proposed by Coomes and Allen (2007) assuming that the assimilation rate of the plant depends non-linearly on the light available, as a multiple of the coefficient α of the form:

$$\frac{1}{1 + \gamma \exp(\delta CAI_h)} \quad (\text{Eqn D.6})$$

where γ and δ are parameters to be estimated, with priors set as $U(-10,10)$.

To model the effect of temperature on growth we used Boltzmann-Arrhenius function which describes the temperature-dependency of metabolic rates (e.g. Enquist et al., 2003; Coomes and Allen, 2007), as a multiple of the coefficient α of the form:

$$\exp(-E/kT) \quad (\text{Eqn D.7})$$

where k is the Boltzmann constant (8.62×10^{-5} eV K^{-1}), T is the absolute temperature in Kelvin and E is the average activation energy (characterising the effect of temperature on biochemical reaction rates, Allen et al., 2005). The value of E varies between different organisms but has been found to be

around 0.62 eV for plants (Gillooly et al., 2001). We therefore fit the parameter E during the MCMC algorithm, but with a constrained prior of $U(0.55,0.7)$ to reflect this.

To model the effect of annual precipitation levels and drought length on growth we fit simple linear functions as multiples of the coefficient α . We also tested an alternative relationship between average annual temperature and growth, using a simple linear function of the same form:

$$(1 + \eta(\text{precipitation})) ; (1 + \lambda(\text{drought length})) ; (1 + \omega(\text{temperature})) \quad (\text{Eqn D.8})$$

where η , λ and ω were parameters to be estimated, with priors set as $U(-10,10)$. We normalised values for annual precipitation (mean = 862 mm, standard deviation = 378 mm) and average annual temperature (mean = 12°C, standard deviation = 3°C) to avoid parameter convergence problems.

We tested different combinations of these models as coefficients of the parameter α (equation D.1), initially just with one predictor at a time and subsequently with combinations of predictors to find the best fit according to AIC (see Table D.1 for model forms). All parameters were species-specific.

Mortality

We modelled annual probability of mortality for each individual tree i , as $P(\text{mortality}, i)$. Since $P(\text{mortality}, i)$ must lie between 0 and 1, we used a logistic transformation

$$P(\text{mortality}, i) = 1 / (1 + \exp(-k_i)) \quad (\text{Eqn D.9})$$

where k_i (which can vary from $\pm \infty$) is a function of the predictor variables. This had corresponding likelihood

$$l(X|M, \underline{\theta}) = \begin{cases} [1 - P(\text{mortality}, i)]^t & \text{if tree } i \text{ survived} \\ 1 - [1 - P(\text{mortality}, i)]^t & \text{if tree } i \text{ died} \end{cases} \quad (\text{Eqn D.10})$$

We used the method describe in Chapter Two to fit these models. Priors for all parameters were set as $U[-10,10]$. We tested different combinations of predictors within the parameter k_i (equation D.9) to choose the best fit model according to AIC (see Table D.3 for model forms), and normalised annual precipitation values and average annual temperature values as before. All parameters were species-specific.

Crown diameter and height allometry

For the PPA model we required models for height and crown diameter allometry. For the crown diameter allometry we used the equations derived in Chapter 5. The best fit model was a seven parameter model with size dependent standard deviation which predicted crown diameter (CD) as:

$$CD \sim N(v_2 + v_3 DBH + v_4 PA + v_5 AVT + v_6 DL, (v_0 + v_1 DBH)^2) \quad (\text{Eqn D.11})$$

where v_0 - v_6 are species-specific fitted parameters.

For the height allometry we used a simplified version of the model in Chapter Four. We fit a power function to describe the relationship between height (H) and stem diameter with size dependent standard deviation:

$$H \sim N \left((\phi_2 + \phi_4 PA + \phi_5 AVT + \phi_6 DL + \phi_7 CAI_h) \times DBH^{\phi_3}, (\phi_0 + \phi_1 DBH)^2 \right) \quad (\text{Eqn D.12})$$

where ϕ_0 - ϕ_7 are species-specific parameters to be fitted. For both equations we used normalised annual precipitation values and average annual temperature values as before

Results

We found that for both growth and mortality the best fit model had size, competition and climatic dependencies, and these high complexity models were the best fit to the majority of species representing the majority of data (Tables D.2 and D.3). The temperature dependency of growth was not well represented by the Boltzmann-Arrhenius function (equation D.7), as the AIC was worse than a simple linear function (Table D.2). We therefore discarded this function and used a linear equation to describe the relationship between growth and temperature. Parameter values and 95% credible intervals for the best fit growth and mortality functions are given in Tables D.4 and D.5, and the parameter values and intervals for the height-diameter relationship (equation D.12) are shown in Table D.6.

We found that both the size and competition dependency of growth rates was strong (Fig. D.1). All species had increasing growth with size, and most showed a strong decline in growth rates in larger sizes. All species showed a substantial decrease in growth rates in more competitive environments (with higher CAI_h). Responses of growth to changes in annual precipitation and drought rate were less consistent, but there was also no clear pattern of observed changes in growth along these gradients (Fig. D.1). However we found that, taking all data together, growth increased with temperature in cooler areas and decreased with temperature in warmer areas, and the predictions of the model were able to capture this pattern (compare black and blue lines, Fig. D.1).

Mortality rates were most strongly dependent on size and competition (Fig D.2). All species had high mortality rates in small stems, and lower mortality rates in larger stems, with the rates appearing to reach a minimum around 30-40 cm DBH. However, unlike the US mortality rates in Chapter Two, we did not find evidence of a U-shaped size dependency of mortality for most species (with higher mortality in larger stems). The model predicted for all species that mortality increases with temperature, drought and precipitation, but these did not match the observed patterns as well (Fig. D.2), possibly due to covariance with other factors (e.g. plots with higher competition in wetter areas). The relationship between height and size, competition and climate are shown in Fig D.3 and discussed further in Chapter Four.

Table D.1 Details of the data used for each model for the 14 species included in the analysis. Table shows the amount of data used for each species for each model and mean values of all predictors for each species (DBH= diameter breast height (mm), CAI_h = crown area of taller trees ($ha\ ha^{-1}$), DL= drought length (months), AVT = average annual temperature ($^{\circ}C$) and PA= annual precipitation ($mm\ year^{-1}$)). Details of the crown width allometry models are given in Chapter Five, "N/A" indicates a species for which we did not have crown data and so assigned a mean crown allometry based on nearest phylogenetic neighbour.

Species name	Growth data	Mortality data	Height data	Crown width data	Mean DBH	Mean CAI_h	Mean DL	Mean AVT	Mean PA
<i>Pinus sylvestris</i>	35272	30684	54457	2039	226.2	0.5	0.7	8.9	974.9
<i>Pinus uncinata</i>	2954	2596	3873	150	232.2	0.3	0.0	5.7	1218.
<i>Pinus pinea</i>	6971	5896	11210	1080	245.0	0.3	3.2	14.3	613.7
<i>Pinus halepensis</i>	14875	12196	24191	2973	186.5	0.3	2.8	13.9	549.3
<i>Pinus nigra</i>	14998	12187	22672	1289	199.2	0.4	1.4	10.8	810.7
<i>Pinus pinaster</i>	40363	32620	73836	3533	234.5	0.3	2.2	12.1	838.6
<i>Quercus robur</i>	1181	1952	5685	289	277.5	0.6	0.6	11.9	1335.
<i>Quercus petraea</i>	3613	1056	2020	107	239.3	0.6	0.1	9.3	1090.
<i>Quercus pyrenaica</i>	1354	7160	877	866	196.8	0.5	1.4	10.8	963.8
<i>Quercus faginea</i>	7714	2233	478	471	180.5	0.4	1.2	11.4	825.6
<i>Quercus ilex</i>	3298	9598	3581	3570	213.2	0.3	2.2	13.3	749.6
<i>Quercus suber</i>	11248	3673	762	756	286.2	0.3	2.6	15.4	880.8
<i>Fagus sylvatica</i>	6354	5423	8697	303	266.9	0.7	0.1	9.0	1164.
<i>Castanea sativa</i>	2042	1618	170	168	337.3	0.6	0.9	12.4	1213.

Table D.2 Comparison of different models for the coefficient of the annual growth model (parameter α in equation D.1), showing the different functional forms tested. DBH is stem diameter (cm), CAI_h is the crown area of taller trees ($ha\ ha^{-1}$), DL is drought length in months, AVT is average annual temperature (in $^{\circ}C$, and $nAVT$ is normalised as $nAVT=(AVT-12)/3$) and PA is annual precipitation (in $mm\ year^{-1}$, rescaled as $(precipitation-862)/378$). $\rho_0 - \rho_8$ are parameters that were estimated by the MCMC algorithm. Models are compared using the Akaike Information Criterion (AIC), for which the total for all species is shown. As models were fitted separately for each species we calculated the AIC for each species' models and compared these. The number of species for whom each model was the best (according to AIC) is also shown, as well as the total percentage of the data these species represent. Models 0-11 were fitted using the integrated growth function (equation D.2), whilst model 12 was fitted using the multiplicative growth function (equation D.3).

Model #	Annual growth model coefficient (α in equation D.1)	Parameters	AIC	AIC Rank	# species best model	% data best model
0	ρ_2	4	727574	12	0	0.0
1	$\rho_2/(1 + \rho_2/\rho_4 \exp(\rho_5 CAI_h))$	6	716597	7	0	0.0
2	$\rho_2(1 + \rho_4 DL)$	5	725831	9	0	0.0
3	$\rho_2(1 + \rho_4 PA)$	5	726928	11	0	0.0
4	$\rho_2(1 + \rho_4 nAVT)$	5	725880	10	0	0.0
5	$\rho_2 \exp\left(\frac{-\rho_6}{(8.62 * (AVT + 273.13))}\right)$	5	727603	13	0	0.0
6	$\rho_2(1 + \rho_6 DL)/(1 + \rho_2/\rho_4 \exp(\rho_5 CAI_h))$	7	714393	4	0	0.0
7	$\rho_2(1 + \rho_6 PA)/(1 + \rho_2/\rho_4 \exp(\rho_5 CAI_h))$	7	716481	6	1	2.6
8	$\rho_2(1 + \rho_6 nAVT)/(1 + \rho_2/\rho_4 \exp(\rho_5 CAI_h))$	7	714955	5	2	6.9
9	$\rho_2 \exp\left(\frac{-\rho_6}{(8.62 * (AVT + 273.13))}\right) / (1 + \rho_2/\rho_4 \exp(\rho_5 CAI_h))$	7	716626	8	0	0.0
10	$\rho_2 (1 + \rho_7 DL)(1 + \rho_8 PA) \exp\left(\frac{-\rho_6}{(8.62 * (AVT + 273.13))}\right) / (1 + \rho_2/\rho_4 \exp(\rho_5 CAI_h))$	9	714359	3	0	0.0
11	$\rho_2 (1 + \rho_7 DL)(1 + \rho_8 PA)(1 + \rho_6 nAVT) / (1 + \rho_2/\rho_4 \exp(\rho_5 CAI_h))$	9	712268	1	3	8.1
12	$\rho_2 (1 + \rho_7 DL)(1 + \rho_8 PA)(1 + \rho_6 nAVT) \exp(-\rho_9 DBH) / (1 + \rho_2/\rho_4 \exp(\rho_5 CAI_h))$	10	712724	2	8	82.4

Table D.3 Comparison of different models for annual probability of mortality, showing the different functional forms tested. *DBH* is stem diameter (mm), *CAI_h* is the crown area of taller trees ($ha\ ha^{-1}$), *DL* is drought length in months, *AVT* is average annual temperature (in °C, rescaled as $(\text{temperature} - 12)/3$) and *PA* is annual precipitation (in $mm\ year^{-1}$, rescaled as $(\text{precipitation} - 862)/378$). $\tau_0 - \tau_6$ are parameters that were estimated by the MCMC algorithm. Models are compared using the Akaike Information Criterion (AIC), for which the total for all species is shown. As models were fitted separately for each species we calculated the AIC for each species' models and compared these. The number of species for whom each model was the best (according to AIC) is also shown, as well as the total percentage of the data these species represent.

Model #	Logit (Annual probability of mortality) (k_i in equation D.9)	Parameters	AIC	AIC Rank	# species best model	% data best model
0	τ_0	1	112408	7	0	0.0
1	$\tau_0 + \tau_1 DBH \exp(\tau_2 DBH)$	3	109604	6	0	0.0
2	$\tau_0 + \tau_1 DBH \exp(\tau_2 DBH) + \tau_3 CAI_h$	4	107969	2	1	1.5
3	$\tau_0 + \tau_1 DBH \exp(\tau_2 DBH) + \tau_3 DL$	4	109136	3	0	0.0
4	$\tau_0 + \tau_1 DBH \exp(\tau_2 DBH) + \tau_3 AVT$	4	109279	5	1	2.8
5	$\tau_0 + \tau_1 DBH \exp(\tau_2 DBH) + \tau_3 PA$	4	109212	4	0	0.0
6	$\tau_0 + \tau_1 DBH \exp(\tau_2 DBH) + \tau_3 CAI_h + \tau_4 DL$ $+ \tau_5 AVT + \tau_6 PA$	7	107092	1	12	95.6

Table D.4 Parameter values for the chosen fit model (number 12 in Table D.2) for annual growth (cm year⁻¹) for each species showing Bayesian mean and 95% credible interval (CI).

Species	Annual growth model parameters	ρ_0	ρ_1	ρ_2	ρ_3	ρ_4	ρ_5	ρ_6	ρ_7	ρ_8	ρ_9
		Mean									
	95% CI										
<i>Castanea sativa</i>	Mean	1.972	0.047	2.779	0.482	0.138	0.358	-0.105	-0.067	0.248	0.012
	95% CI	(1.972, 1.972)	(0.047, 0.047)	(2.779, 2.779)	(0.482, 0.482)	(0.138, 0.138)	(0.358, 0.358)	(-0.105, -0.105)	(-0.067, -0.067)	(0.248, 0.248)	(0.012, 0.012)
<i>Fagus sylvatica</i>	Mean	1.107	0.039	0.337	0.233	0.995	1.131	0.310	-0.149	-0.004	0.002
	95% CI	(1.036, 1.179)	(0.036, 0.042)	(0.243, 0.520)	(0.157, 0.336)	(0.549, 1.788)	(0.841, 1.503)	(0.290, 0.328)	(-0.222, -0.074)	(-0.031, 0.023)	(0.000, 0.005)
<i>Pinus halepensis</i>	Mean	1.840	0.019	2.107	0.147	0.551	0.997	0.020	-0.066	0.205	0.008
	95% CI	(1.775, 1.905)	(0.016, 0.022)	(1.025, 2.944)	(0.032, 0.243)	(0.413, 0.740)	(0.887, 1.148)	(-0.009, 0.048)	(-0.076, -0.057)	(0.175, 0.233)	(0.003, 0.013)
<i>Pinus nigra</i>	Mean	1.890	0.005	1.541	0.386	0.281	0.872	-0.125	-0.021	0.243	0.031
	95% CI	(1.835, 1.943)	(0.003, 0.008)	(0.568, 2.885)	(0.284, 0.459)	(0.227, 0.345)	(0.775, 1.033)	(-0.154, -0.096)	(-0.032, -0.010)	(0.225, 0.260)	(0.026, 0.035)
<i>Pinus pinaster</i>	Mean	2.530	0.021	0.840	0.195	0.669	1.356	-0.001	0.026	0.165	0.011
	95% CI	(2.474, 2.584)	(0.019, 0.023)	(0.634, 1.143)	(0.142, 0.251)	(0.547, 0.795)	(1.197, 1.506)	(-0.015, 0.014)	(0.016, 0.037)	(0.154, 0.176)	(0.009, 0.014)
<i>Pinus pinea</i>	Mean	2.401	0.001	1.554	0.065	0.544	0.832	-0.105	0.135	0.242	0.003
	95% CI	(2.316, 2.491)	(-0.003, 0.004)	(0.615, 2.880)	(0.007, 0.162)	(0.365, 0.857)	(0.645, 1.164)	(-0.127, -0.083)	(0.106, 0.165)	(0.208, 0.273)	(0.000, 0.006)
<i>Pinus sylvestris</i>	Mean	2.258	0.000	2.152	0.202	0.388	0.700	-0.004	0.089	0.146	0.023
	95% CI	(2.223, 2.296)	(-0.002, 0.001)	(1.138, 2.925)	(0.151, 0.289)	(0.327, 0.440)	(0.660, 0.759)	(-0.021, 0.012)	(0.078, 0.100)	(0.132, 0.161)	(0.021, 0.027)
<i>Pinus uncinata</i>	Mean	1.644	0.005	1.840	0.039	0.553	0.987	0.136	0.845	0.006	0.013
	95% CI	(1.530, 1.751)	(0.001, 0.010)	(0.817, 2.920)	(0.002, 0.126)	(0.399, 0.873)	(0.762, 1.318)	(0.097, 0.170)	(0.637, 1.076)	(-0.055, 0.072)	(0.009, 0.018)
<i>Quercus faginea</i>	Mean	1.040	0.025	0.355	0.345	0.385	1.296	0.272	-0.039	0.179	0.008
	95% CI	(0.963, 1.117)	(0.021, 0.029)	(0.106, 1.218)	(0.185, 0.486)	(0.140, 0.947)	(0.696, 2.080)	(0.230, 0.312)	(-0.061, -0.015)	(0.128, 0.230)	(0.001, 0.014)
<i>Quercus ilex</i>	Mean	1.854	0.007	1.668	0.040	0.313	0.761	0.174	-0.014	0.141	0.007
	95% CI	(1.813, 1.895)	(0.006, 0.009)	(0.466, 2.918)	(0.003, 0.100)	(0.245, 0.545)	(0.630, 1.084)	(0.136, 0.211)	(-0.032, 0.006)	(0.098, 0.182)	(0.005, 0.010)
<i>Quercus robur</i>	Mean	1.495	0.082	0.915	0.039	1.836	1.407	0.384	-0.091	-0.052	0.004
	95% CI	(1.349, 1.645)	(0.076, 0.088)	(0.555, 2.006)	(0.001, 0.133)	(0.776, 4.160)	(0.893, 2.090)	(0.299, 0.466)	(-0.130, -0.051)	(-0.090, -0.008)	(0.001, 0.008)
<i>Quercus petraea</i>	Mean	1.387	0.017	1.494	0.332	0.179	0.620	0.177	0.131	0.116	0.006
	95% CI	(1.262, 1.513)	(0.012, 0.022)	(0.198, 2.920)	(0.171, 0.523)	(0.103, 0.377)	(0.458, 1.040)	(0.132, 0.220)	(0.029, 0.240)	(0.030, 0.209)	(0.001, 0.013)
<i>Quercus pyrenaica</i>	Mean	1.196	0.042	0.597	0.162	0.567	1.251	0.227	-0.052	0.044	0.003
	95% CI	(1.140, 1.253)	(0.039, 0.045)	(0.287, 2.288)	(0.092, 0.245)	(0.222, 0.941)	(0.737, 1.687)	(0.193, 0.258)	(-0.070, -0.033)	(0.017, 0.073)	(0.000, 0.007)
<i>Quercus robur</i>	Mean	1.495	0.082	0.915	0.039	1.836	1.407	0.384	-0.091	-0.052	0.004
	95% CI	(1.349, 1.645)	(0.076, 0.088)	(0.555, 2.006)	(0.001, 0.133)	(0.776, 4.160)	(0.893, 2.090)	(0.299, 0.466)	(-0.130, -0.051)	(-0.090, -0.008)	(0.001, 0.008)
<i>Quercus suber</i>	Mean	1.181	0.054	1.604	0.022	0.172	0.603	0.046	0.415	0.369	0.003
	95% CI	(1.066, 1.291)	(0.050, 0.059)	(0.437, 2.900)	(0.001, 0.072)	(0.139, 0.235)	(0.432, 0.812)	(-0.059, 0.169)	(0.326, 0.515)	(0.277, 0.456)	(0.000, 0.006)

Table D.5 Parameter values for the best fit model (number 6 in Table D.3) for annual mortality rate (stems $\text{stem}^{-1} \text{year}^{-1}$) for each species showing Bayesian mean and 95% credible interval (CI).

Species		Annual mortality model parameters						
		τ_0	τ_1	τ_2	τ_3	τ_4	τ_5	τ_6
<i>Castanea sativa</i>	Mean	-3.458	-0.005	-0.001	0.587	0.263	0.023	0.012
	95% CI	(-3.920, -3.015)	(-0.008, -0.003)	(-0.001, 0.000)	(0.394, 0.792)	(0.145, 0.387)	(-0.274, 0.328)	(-0.157, 0.182)
<i>Fagus sylvatica</i>	Mean	-4.017	-0.017	-0.004	0.780	0.524	0.099	-0.201
	95% CI	(-4.814, -3.302)	(-0.024, -0.009)	(-0.005, -0.003)	(0.614, 0.942)	(0.183, 0.855)	(-0.118, 0.304)	(-0.345, -0.065)
<i>Pinus halepensis</i>	Mean	-3.521	-0.014	-0.004	1.312	-0.071	0.076	0.060
	95% CI	(-4.019, -2.976)	(-0.022, -0.008)	(-0.005, -0.003)	(1.124, 1.499)	(-0.134, -0.003)	(-0.064, 0.212)	(-0.118, 0.241)
<i>Pinus nigra</i>	Mean	-3.969	-0.005	0.000	0.908	0.027	0.197	0.218
	95% CI	(-4.263, -3.612)	(-0.009, -0.003)	(-0.001, 0.001)	(0.770, 1.037)	(-0.035, 0.089)	(0.065, 0.335)	(0.137, 0.302)
<i>Pinus pinaster</i>	Mean	-1.758	-0.023	-0.003	0.610	0.089	-0.096	0.237
	95% CI	(-2.000, -1.503)	(-0.025, -0.020)	(-0.003, -0.003)	(0.528, 0.688)	(0.051, 0.127)	(-0.146, -0.040)	(0.198, 0.274)
<i>Pinus pinea</i>	Mean	-2.060	-0.019	-0.003	0.395	0.193	-0.727	0.223
	95% CI	(-2.580, -1.453)	(-0.024, -0.013)	(-0.003, -0.002)	(0.160, 0.634)	(0.093, 0.295)	(-0.889, -0.572)	(-0.002, 0.446)
<i>Pinus sylvestris</i>	Mean	-3.725	-0.010	-0.002	0.891	0.265	0.067	0.189
	95% CI	(-3.981, -3.456)	(-0.013, -0.007)	(-0.003, -0.002)	(0.824, 0.955)	(0.223, 0.306)	(-0.010, 0.146)	(0.133, 0.247)
<i>Pinus uncinata</i>	Mean	-5.296	0.013	-1.397	0.502	2.504	-0.154	0.003
	95% CI	(-5.964, -4.622)	(-0.935, 0.932)	(-2.850, -0.114)	(0.051, 0.963)	(2.063, 2.906)	(-0.463, 0.187)	(-0.262, 0.268)
<i>Quercus faginea</i>	Mean	-2.813	-0.028	-0.003	0.627	0.192	0.284	0.412
	95% CI	(-3.906, -1.902)	(-0.039, -0.015)	(-0.004, -0.002)	(0.291, 0.940)	(0.000, 0.392)	(-0.046, 0.616)	(0.079, 0.731)
<i>Quercus ilex</i>	Mean	-2.418	-0.020	-0.003	0.037	-0.048	0.327	0.232
	95% CI	(-2.781, -2.051)	(-0.024, -0.016)	(-0.003, -0.002)	(-0.146, 0.214)	(-0.109, 0.009)	(0.224, 0.428)	(0.088, 0.366)
<i>Quercus robur</i>	Mean	-3.400	-0.013	-0.002	0.652	-0.118	0.401	0.181
	95% CI	(-4.555, -2.438)	(-0.022, -0.003)	(-0.003, -0.001)	(0.377, 0.932)	(-0.339, 0.098)	(0.011, 0.784)	(-0.021, 0.388)
<i>Quercus petraea</i>	Mean	-5.625	0.028	-1.375	1.999	-0.084	0.377	-0.574
	95% CI	(-6.100, -5.139)	(-0.905, 0.926)	(-2.877, -0.057)	(1.609, 2.368)	(-0.718, 0.501)	(0.005, 0.724)	(-1.082, -0.086)
<i>Quercus pyrenaica</i>	Mean	-2.973	-0.013	-0.002	0.795	0.094	0.143	-0.146
	95% CI	(-3.382, -2.603)	(-0.017, -0.009)	(-0.003, -0.002)	(0.662, 0.925)	(0.016, 0.174)	(0.001, 0.291)	(-0.247, -0.048)
<i>Quercus suber</i>	Mean	-3.235	-0.025	-0.004	0.318	-0.019	0.630	-0.133
	95% CI	(-3.943, -2.591)	(-0.032, -0.018)	(-0.004, -0.003)	(-0.056, 0.695)	(-0.144, 0.111)	(0.299, 0.947)	(-0.357, 0.093)

Table D.6 Parameter values for the height-diameter allometric model (equation D.11, fit for both height and DBH in cm) for each species showing Bayesian mean and 95% credible interval (CI).

Species	Height-diameter model parameters (equation D.12)								
		ϕ_0	ϕ_1	ϕ_2	ϕ_3	ϕ_4	ϕ_5	ϕ_6	ϕ_7
<i>Castanea sativa</i>	Mean	369.743	-1.142	615.467	0.216	33.035	23.476	-43.610	-21.590
	95% CI	(297.406, 437.934)	(-2.408, 0.750)	(498.539, 753.552)	(0.157, 0.275)	(3.870, 48.916)	(-20.301, 48.483)	(-49.744, -31.050)	(-47.930, 28.712)
<i>Fagus sylvatica</i>	Mean	236.400	6.091	530.878	0.398	-15.437	49.639	-5.155	-47.601
	95% CI	(223.716, 248.372)	(5.626, 6.625)	(515.242, 545.224)	(0.389, 0.408)	(-18.611, -12.177)	(48.733, 49.990)	(-16.257, 5.556)	(-49.855, -43.692)
<i>Pinus halepensis</i>	Mean	112.928	5.469	172.257	0.576	12.758	26.670	-9.646	21.214
	95% CI	(112.928, 112.928)	(5.469, 5.469)	(172.257, 172.257)	(0.576, 0.576)	(12.758, 12.758)	(26.670, 26.670)	(-9.646, -9.646)	(21.214, 21.214)
<i>Pinus nigra</i>	Mean	63.340	8.263	119.976	0.718	5.597	9.465	-3.274	11.356
	95% CI	(58.310, 68.306)	(7.976, 8.541)	(117.508, 123.144)	(0.710, 0.725)	(5.040, 6.204)	(8.604, 10.379)	(-3.656, -2.873)	(10.181, 12.473)
<i>Pinus pinaster</i>	Mean	163.963	3.805	173.859	0.617	15.319	19.176	-8.098	4.954
	95% CI	(160.362, 167.399)	(3.654, 3.956)	(170.958, 175.953)	(0.613, 0.622)	(14.816, 15.842)	(18.513, 19.871)	(-8.549, -7.662)	(3.863, 6.013)
<i>Pinus pinea</i>	Mean	123.963	3.022	92.684	0.688	-0.818	13.146	-3.750	15.567
	95% CI	(117.313, 130.675)	(2.747, 3.299)	(87.898, 97.842)	(0.673, 0.701)	(-2.244, 0.573)	(12.209, 14.129)	(-4.318, 3.174)	(13.906, 17.111)
<i>Pinus sylvestris</i>	Mean	128.255	7.240	130.683	0.693	-0.216	0.399	-1.236	14.094
	95% CI	(124.204, 132.485)	(7.034, 7.435)	(128.295, 132.951)	(0.688, 0.699)	(-0.787, 0.367)	(-0.254, 1.086)	(-1.614, 0.829)	(13.385, 14.849)
<i>Pinus uncinata</i>	Mean	87.861	5.892	259.672	0.558	8.980	37.099	-37.428	-31.849
	95% CI	(87.861, 87.861)	(5.892, 5.892)	(259.672, 259.672)	(0.558, 0.558)	(8.980, 8.980)	(37.099, 37.099)	(-37.428, -37.428)	(-31.849, -31.849)
<i>Quercus faginea</i>	Mean	69.323	6.225	189.159	0.503	4.933	8.642	-12.874	31.954
	95% CI	(39.816, 98.931)	(4.650, 7.902)	(162.908, 220.221)	(0.452, 0.549)	(-4.279, 14.826)	(-0.197, 17.642)	(-18.342, -7.720)	(12.228, 47.352)
<i>Quercus ilex</i>	Mean	84.725	1.571	251.152	0.377	2.358	21.716	-26.286	-28.393
	95% CI	(79.055, 90.589)	(1.359, 1.779)	(240.666, 261.799)	(0.364, 0.390)	(-1.413, 6.214)	(18.685, 25.039)	(-28.701, -23.988)	(-38.525, -17.935)
<i>Quercus robur</i>	Mean	196.219	4.935	380.613	0.416	-19.204	23.682	-7.266	-48.759
	95% CI	(184.461, 208.673)	(4.477, 5.412)	(365.490, 397.081)	(0.403, 0.427)	(-23.468, -15.113)	(16.760, 30.922)	(-11.060, -3.547)	(-49.972, -45.982)
<i>Quercus petraea</i>	Mean	155.143	8.745	275.585	0.496	-4.780	2.417	-2.774	-22.563
	95% CI	(129.771, 180.021)	(7.494, 10.072)	(252.052, 299.669)	(0.469, 0.524)	(-11.854, 2.386)	(-3.511, 8.462)	(-11.781, 6.537)	(-32.762, -13.754)
<i>Quercus pyrenaica</i>	Mean	113.468	5.931	306.082	0.409	28.361	19.223	-21.095	16.261
	95% CI	(87.341, 141.647)	(4.621, 7.280)	(267.439, 351.366)	(0.367, 0.447)	(20.053, 37.476)	(8.121, 31.255)	(-29.189, -13.354)	(-3.981, 35.384)
<i>Quercus suber</i>	Mean	136.004	0.902	183.058	0.446	30.393	19.249	-11.918	-29.099
	95% CI	(116.457, 155.930)	(0.344, 1.479)	(157.201, 205.918)	(0.410, 0.489)	(23.925, 37.140)	(11.236, 27.702)	(-15.277, -8.625)	(-45.093, -13.147)

Figure D.1 Annual growth rate (cm year^{-1}) for the 14 selected species, with predictions plotted for each species (grey) and for all species together (blue), along with the observed growth rate along each gradient (black). Predicted growth was calculated along the gradient of each predictor by varying only that predictor and holding all others at the species' average (see table D.1 for average values), and then binning the data along the gradient to give average and 95% CIs.

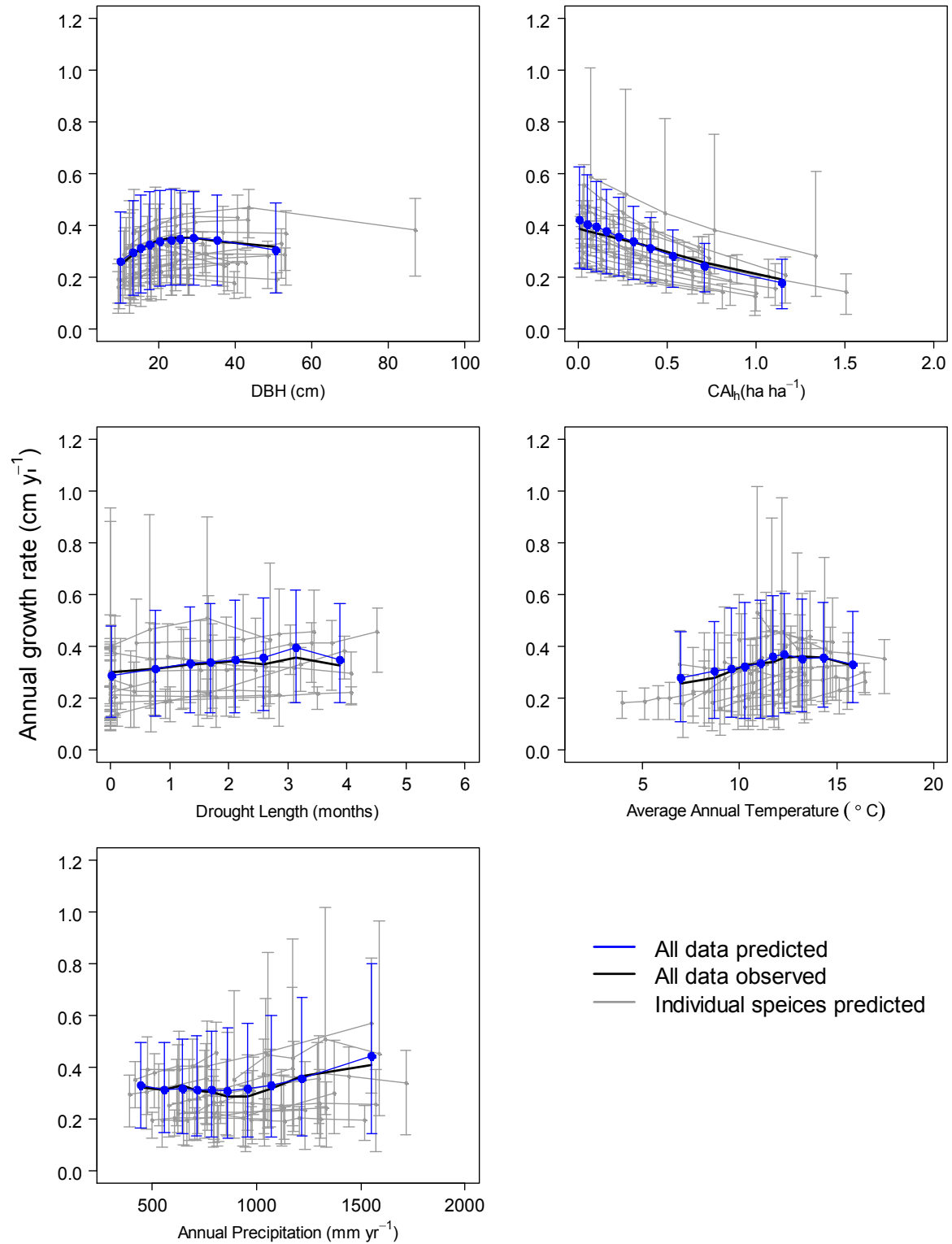


Figure D.2 Annual mortality rate (stems $\text{stem}^{-1} \text{ year}^{-1}$) for the 14 selected species, with predictions plotted for each species (grey) and for all species together (blue), along with the observed mortality rate along each gradient (black). Predicted mortality was calculated along the gradient of each predictor by varying only that predictor and holding all others at the species' average (see table D.1 for average values), and then binning the data along the gradient to give average and 95% CIs.

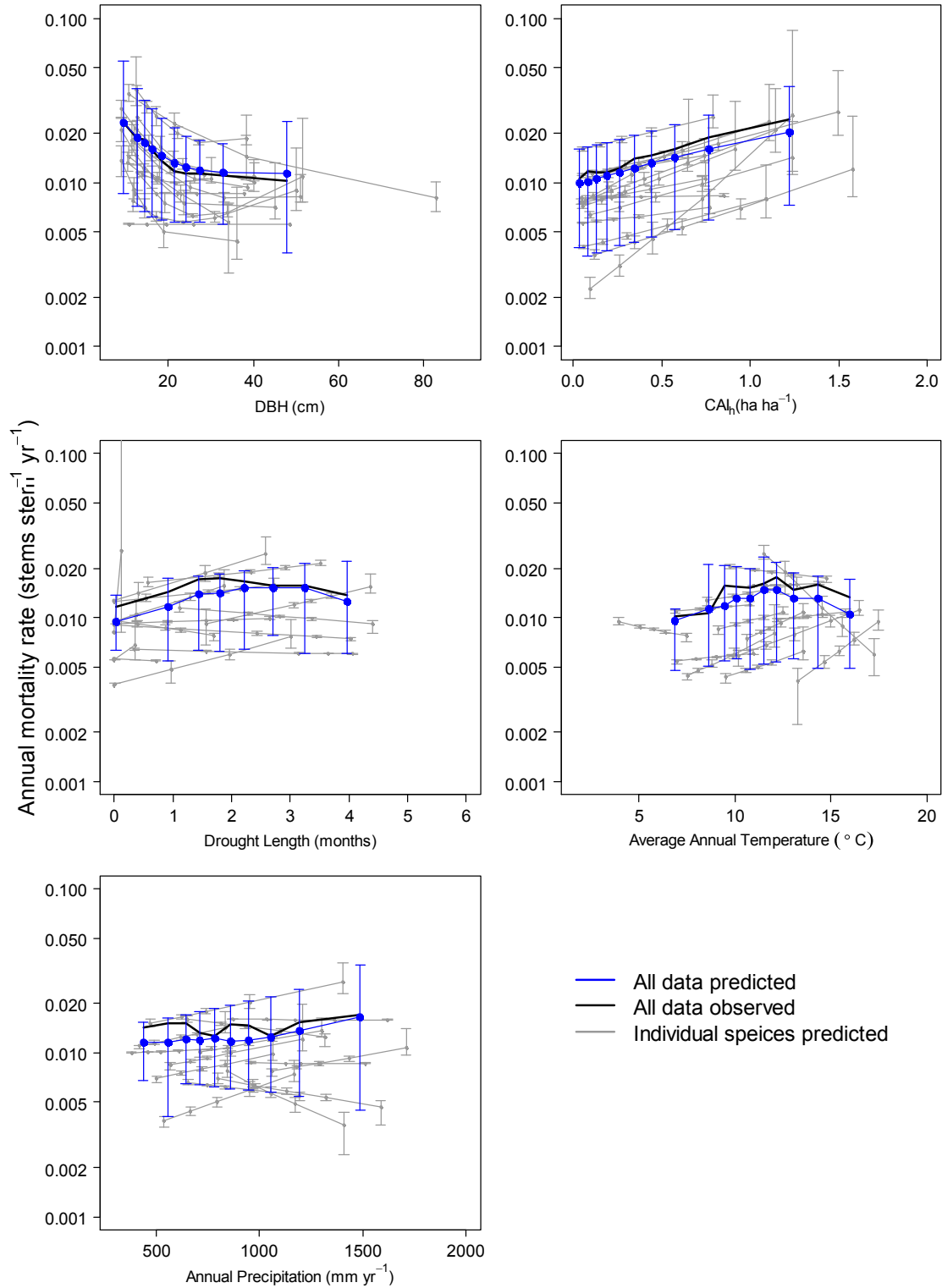


Figure D.3 Tree height (m) for the 14 selected species, with predictions plotted for each species (grey) and for all species together (blue), along with the observed heights rate along each gradient (black). Predicted height was calculated along the gradient of each predictor by varying only that predictor and holding all others at the species' average (see table D.1 for average values), and then binning the data along the gradient to give average and 95% CIs.

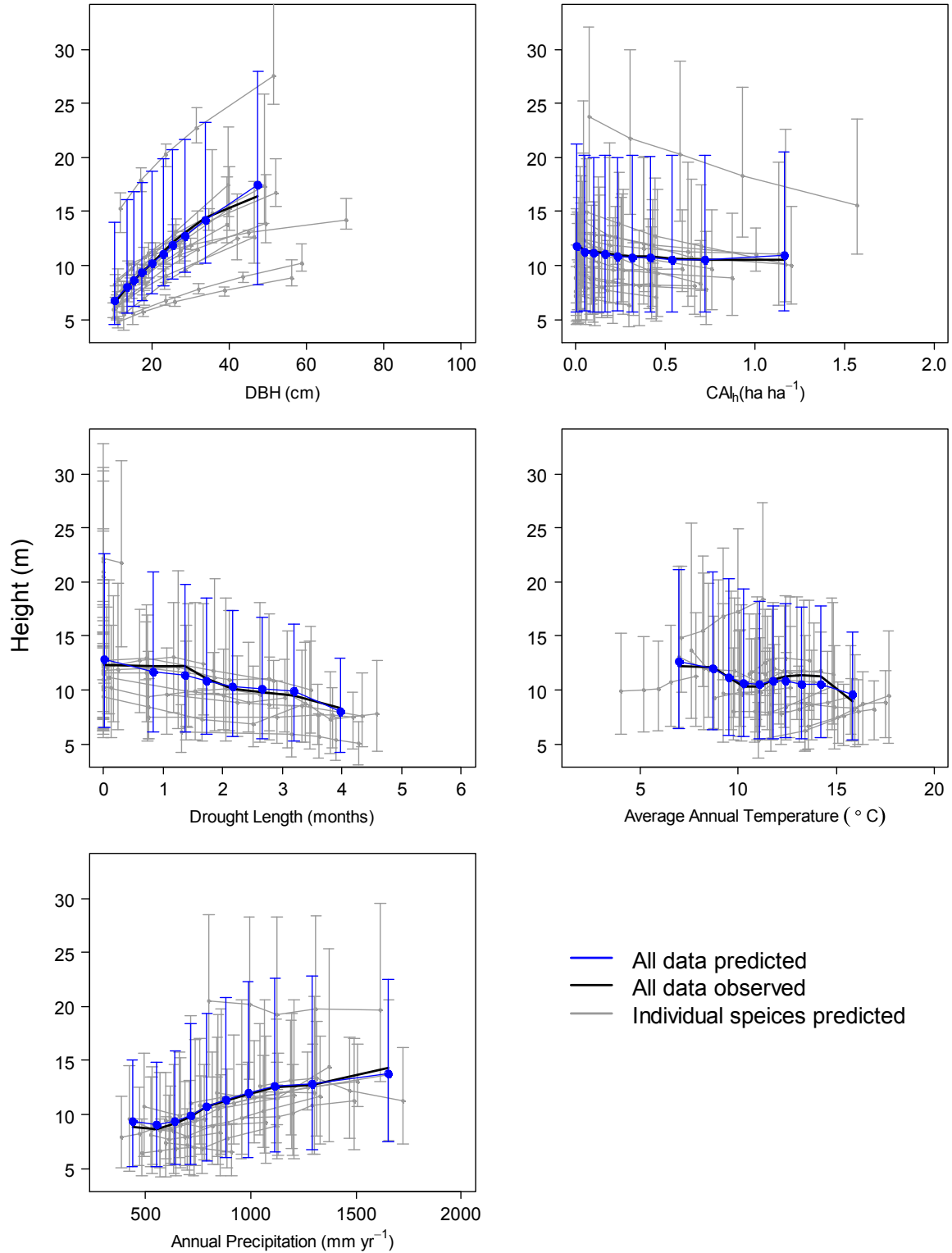
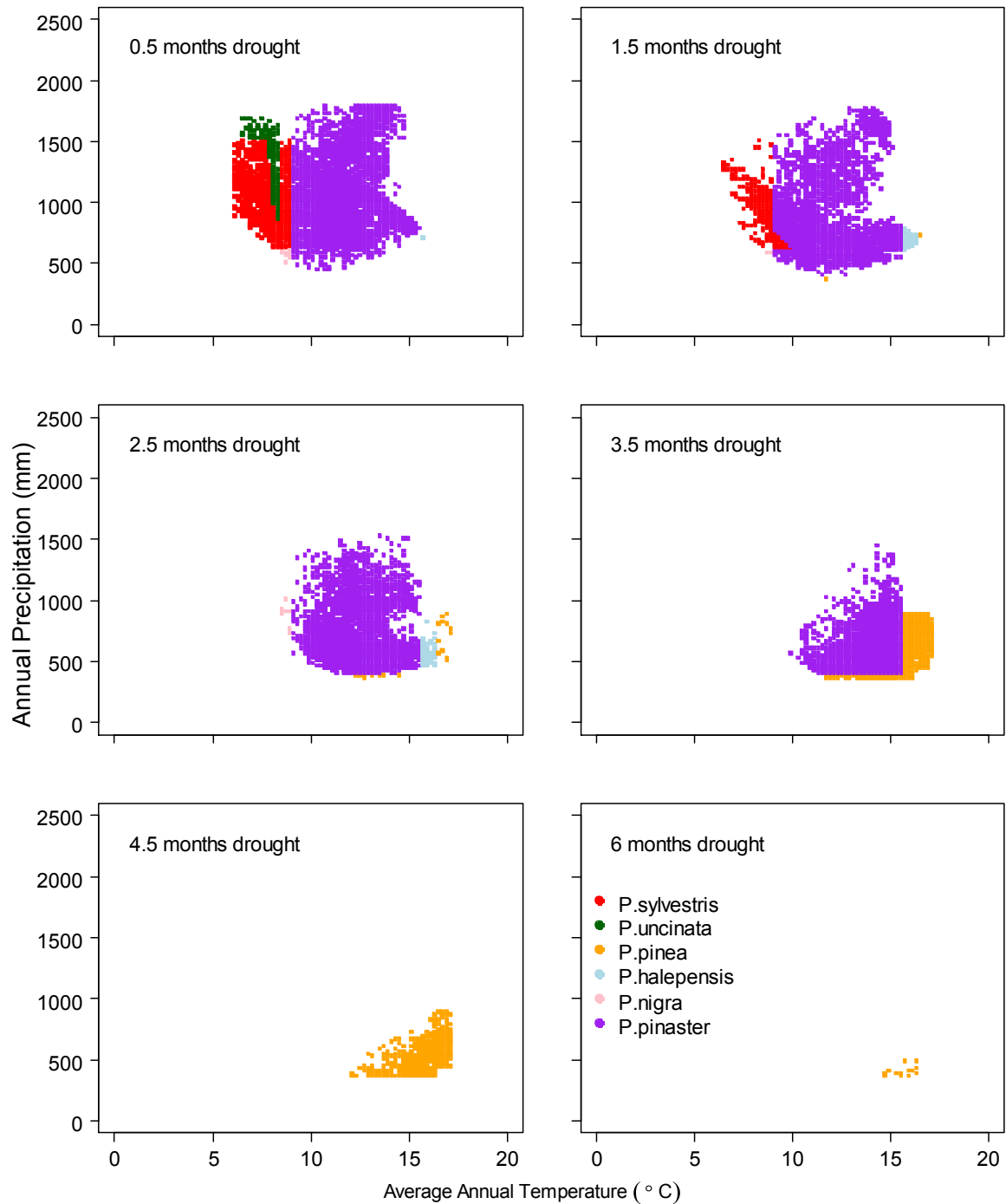


Figure D.4 Range of dominance of the six pine species studied as predicted by the simulation model with early successional dominance determined as the tallest species after 30 years of growth under full light, split by drought length and plotted along gradients of average annual temperature and annual precipitation. The simulation model reproduced the observed patterns of pine dominance (Fig 6.3 page 101) better when early successional dominance was determined as the species with the largest share of the canopy area after 30 years (Fig 6.4 page 102) than the tallest species (shown in this figure).



References

- Acquah, H.G., 2010. Comparison of Akaike information criterion (AIC) and Bayesian information criterion (BIC) in selection of an asymmetric price relationship. *Journal of Development and Agricultural Economics* 2, 1–6.
- Adams, H.D., Guardiola-Claramonte, M., Barron-Gafford, G.A., Villegas, J.C., Breshears, D.D., Zou, C.B., Troch, P.A., Huxman, T.E., 2009. Temperature sensitivity of drought-induced tree mortality portends increased regional die-off under global-change-type drought. *Proceedings of the National Academy of Sciences* 106, 7063–7066.
- Aerts, R., 1995. The advantages of being evergreen. *Trends in Ecology & Evolution* 10, 402–407.
- Agee, M., 1998. Fire and pine ecosystems, in: Richardson, D.M. (Ed.), *Ecology and Biogeography of Pinus*. Cambridge University Press, Cambridge, pp. 450–473.
- Agutter, P., Wheatley, D., 2004. Metabolic scaling: consensus or controversy? *Theoretical Biology and Medical Modelling* 1, 13.
- Akaike, H., 1974. A new look at the statistical model identification. *IEEE Transactions on Automatic Control* 19, 716–723.
- Allen, A.P., Gillooly, J.F., Brown, J.H., 2005. Linking the global carbon cycle to individual metabolism. *Functional Ecology* 19, 202–213.
- Alméras, T., Thibaut, A., Gril, J., 2005. Effect of circumferential heterogeneity of wood maturation strain, modulus of elasticity and radial growth on the regulation of stem orientation in trees. *Trees - Structure and Function* 19, 457–467.
- Andreu, L., Gutiérrez, E., Macias, M., Ribas, M., Bosch, O., Camarero, J.J., 2007. Climate increases regional tree growth variability in Iberian pine forests. *Global Change Biology* 13, 804–815.
- Bagnouls, F., Gaussen, H., 1957. Les climats biologiques et leur classification. *Annales de Géographie* 66, 193–220.
- Balaguer, L., Martínez-Ferri, E., Valladares, F., Pérez-Corona, M.E., Baquedano, F.J., Castillo, F.J., Manrique, E., 2001. Population divergence in the plasticity of the response of *Quercus coccifera* to the light environment. *Functional Ecology* 15, 124–135.
- Balster, H., Braun, P.W., Köhler, W., 1998. Cellular automata models for vegetation dynamics. *Ecological Modelling* 107, 113–125.
- Barbero, M., Bonin, G., Loisel, R., Quézel, P., 1990. Changes and disturbances of forest ecosystems caused by human activities in the western part of the Mediterranean basin. *Vegetatio* 87, 151–173.
- Barbéro, M., Loisel, R., Quézel, P., Richardson, D.M., Romane, F., 1998. Pines of the Mediterranean Basin, in: Richardson, D.M. (Ed.), *Ecology and Biogeography of Pinus*. Cambridge University Press, Cambridge, pp. 450–473.
- Batista, W.B., Platt, W.J., 2003. Tree population responses to hurricane disturbance: syndromes in a south-eastern USA old-growth forest. *Journal of Ecology* 91, 197–212.

- Beaumont, M.A., 2010. Approximate Bayesian computation in evolution and ecology. *Annual Review of Ecology, Evolution, and Systematics* 41, 379–406.
- Beaumont, M.A., Cornuet, J.-M., Marin, J.-M., Robert, C.P., 2009. Adaptive approximate Bayesian computation. *Biometrika* 96, 983–990.
- Beaumont, M.A., Zhang, W., Balding, D.J., 2002. Approximate Bayesian computation in population genetics. *Genetics* 162, 2025–2035.
- Beckage, B., Clark, J.S., 2003. Seedling survival and growth of three forest tree species: the role of spatial heterogeneity. *Ecology* 84, 1849–1861.
- Beckage, B., Clark, J.S., Clinton, B.D., Haines, B.L., 2000. A long-term study of tree seedling recruitment in southern Appalachian forests: the effects of canopy gaps and shrub understories. *Canadian Journal of Forest Research* 30, 1617–1631.
- Benito Garzón, M., Sánchez de Dios, R., Sainz Ollero, H., 2008. Effects of climate change on the distribution of Iberian tree species. *Applied Vegetation Science* 11, 169–178.
- Bergot, M., Cloppet, E., Pérarnaud, V., Déqué, M., Marçais, B., Desprez-Loustau, M., 2004. Simulation of potential range expansion of oak disease caused by *Phytophthora cinnamomi* under climate change. *Global Change Biology* 10, 1539–1552.
- Berntson, G.M., Wayne, P.M., 2000. Characterizing the size dependence of resource acquisition within crowded plant populations. *Ecology* 81, 1072–1085.
- Binkley, D., Stape, J.L., Ryan, M.G., Barnard, H.R., Fownes, J., 2002. Age-related decline in forest ecosystem growth: an individual-tree, stand-structure hypothesis. *Ecosystems* 5, 58–67.
- Blanco, J.A., Zavala, M.A., Imbert, J.B., Castillo, F.J., 2005. Sustainability of forest management practices: Evaluation through a simulation model of nutrient cycling. *Forest Ecology and Management* 213, 209–228.
- Blondel, J., 2006. The “design” of Mediterranean landscapes: a millennial story of humans and ecological systems during the historic period. *Human Ecology* 34, 713–729.
- Bloom, A.J., Chapin, F.S., Mooney, H.A., 1985. Resource limitation in plants — an economic analogy. *Annual Review of Ecology and Systematics* 16, 363–392.
- Blum, M.G.B., 2010. Approximate Bayesian computation: a nonparametric perspective. *Journal of the American Statistical Association* 105, 1178–1187.
- Blumler, M.A., 1991. Winter-deciduous versus evergreen habit in Mediterranean regions: a model. USDA Forest Service General Technical Report PSW-126. USDA Forest Service, Pacific Southwest Research Station, Albany, California, USA.
- Bohlman, S., Pacala, S., 2011. A forest structure model that determines crown layers and partitions growth and mortality rates for landscape-scale applications of tropical forests. *Journal of Ecology*.
- Bonan, G.B., 2008. Forests and climate change: forcings, feedbacks, and the climate benefits of forests. *Science* 320, 1444–1449.

- Bonan, G.B., Levis, S., Sitch, S., Vertenstein, M., Oleson, K.W., 2003. A dynamic global vegetation model for use with climate models: concepts and description of simulated vegetation dynamics. *Global Change Biology* 9, 1543–1566.
- Bonan, G.B., Sirois, L., 1992. Air temperature, tree growth, and the northern and southern range limits to *Picea mariana*. *Journal of Vegetation Science* 3, 495–506.
- Borghetti, M., Magnani, F., Fabrizio, A., Saracino, A., 2004. Facing drought in a Mediterranean post-fire community: tissue water relations in species with different life traits. *Acta Oecologica* 25, 67–72.
- Bormann, F.H., 1965. Changes in the Growth Pattern of White Pine Trees Undergoing Suppression. *Ecology* 46, 269–277.
- Bossel, H., Krieger, H., 1991. Simulation model of natural tropical forest dynamics. *Ecological Modelling* 59, 37–71.
- Botkin, D.B., Janak, J.F., Wallis, J.R., 1972. Some ecological consequences of a computer model of forest growth. *Journal of Ecology* 60, 849–872.
- Bragg, D., 2001. A local basal area adjustment for crown width prediction. *Northern Journal of Applied Forestry* 18, 22–28.
- Bréda, N., Huc, R., Granier, A., Dreyer, E., 2006. Temperate forest trees and stands under severe drought: a review of ecophysiological responses, adaptation processes and long-term consequences. *Annals of Forest Science* 63, 20.
- Broncano, M.J., Retana, J., Rodrigo, A., 2005. Predicting the recovery of *Pinus halepensis* and *Quercus ilex* forests after a large wildfire in northeastern Spain. *Plant Ecology* 180, 47–56.
- Broncano, M.J., Riba, M., Retana, J., 1998. Seed germination and seedling performance of two Mediterranean tree species, holm oak (*Quercus ilex* L.) and Aleppo pine (*Pinus halepensis* Mill.): a multifactor experimental approach. *Plant Ecology* 138, 17–26.
- Bruchert, F., Gardiner, B., 2006. The effect of wind exposure on the tree aerial architecture and biomechanics of Sitka spruce (*Picea sitchensis*, Pinaceae). *American Journal of Botany* 93, 1512–1521.
- Brus, D.J., Hengeveld, G.M., Walvoort, D.J.J., Goedhart, P.W., Heidema, A.H., Nabuurs, G.J., Gunia, K., 2011. Statistical mapping of tree species over Europe. *European Journal of Forest Research* 131, 145–157.
- Buchman, R.G., Pederson, S.P., Walters, N.R., 1983. A tree survival model with application to species of the Great Lakes region. *Canadian Journal of Forest Research* 13, 601–608.
- Bugmann, H., 2001. A review of forest gap models. *Climatic Change* 51, 259–305.
- Bugmann, H.K.M., Yan, X., Sykes, M.T., Martin, P., Lindner, M., Desanker, P.V., Cumming, S.G., 1996. A comparison of forest gap models: model structure and behaviour. *Climatic Change* 34, 289–313.
- Bürgi, M., Russell, E.W.B., Motzkin, G., 2000. Effects of postsettlement human activities on forest composition in the north-eastern United States: a comparative approach. *Journal of Biogeography* 27, 1123–1138.

- Burnham, K.P., Anderson, D.R., 2002. Model selection and multimodel inference: a practical information-theoretic approach. Springer.
- Burnham, K.P., Anderson, D.R., 2004. Multimodel inference. *Sociological Methods & Research* 33, 261–304.
- Busing, R.T., 1991. A spatial model of forest dynamics. *Vegetatio* 92, 167–179.
- Busing, R.T., Maily, D., 2004. Advances in spatial, individual-based modelling of forest dynamics. *Journal of Vegetation Science* 15, 831–842.
- Busing, R.T., Pauley, E.F., 1994. Mortality trends in a southern Appalachian red spruce population. *Forest Ecology and Management* 64, 41–45.
- Calvo, L., Santalla, S., Valbuena, L., Marcos, E., Tárrega, R., Luis-Calabuig, E., 2008. Post-fire natural regeneration of a *Pinus pinaster* forest in NW Spain. *Plant Ecology* 197, 81–90.
- Camarero, J., Gutiérrez, E., 2007. Response of *Pinus uncinata* recruitment to climate warming and changes in grazing pressure in an isolated population of the Iberian system (NE Spain). *Arctic, Antarctic, and Alpine Research* 39, 210–217.
- Campos, P., Caparros, A., Sanjurjo, E., 2005. Spain, in: Merlo, M., Croitoru, L. (Eds.), *Valuing Mediterranean Forests: Towards Total Economic Value*. CABI, p. 319.
- Canham, C.D., Finzi, A.C., Pacala, S.W., Burbank, D.H., 1994. Causes and consequences of resource heterogeneity in forests: interspecific variation in light transmission by canopy trees. *Canadian Journal of Forest Research* 24, 337–349.
- Canham, C.D., LePage, P.T., Coates, K.D., 2004. A neighborhood analysis of canopy tree competition: effects of shading versus crowding. *Canadian Journal of Forest Research* 34, 778–787.
- Capitania, R., Carcaillet, C., 2008. Post-fire Mediterranean vegetation dynamics and diversity: A discussion of succession models. *Forest Ecology and Management* 255, 431–439.
- Carrión, J.S., Andrade, A., Bennett, K.D., Navarro, C., Munuera, M., 2001. Crossing forest thresholds: inertia and collapse in a Holocene sequence from south-central Spain. *The Holocene* 11, 635–653.
- Carrión, J.S., Navarro, C., Navarro, J., Munuera, M., 2000. The distribution of cluster pine (*Pinus pinaster*) in Spain as derived from palaeoecological data: relationships with phytosociological classification. *The Holocene* 10, 243–252.
- Caspersen, J.P., Kobe, R.K., 2001. Interspecific variation in sapling mortality in relation to growth and soil moisture. *Oikos* 92, 160–168.
- Caspersen, J.P., Pacala, S.W., Jenkins, J.C., Hurtt, G.C., Moorcroft, P.R., Birdsey, R.A., 2000. Contributions of land-use history to carbon accumulation in U.S. forests. *Science* 290, 1148–1151.
- Caspersen, J.P., Vanderwel, M.C., Cole, W.G., Purves, D.W., 2011. How stand productivity results from size- and competition-dependent growth and mortality. *PLoS ONE* 6, e28660.

- Chambel, M.R., Climent, J., Alía, R., 2007. Divergence among species and populations of Mediterranean pines in biomass allocation of seedlings grown under two watering regimes. *Annals of Forest Science* 64, 87–97.
- Changhui, P., 2000a. Growth and yield models for uneven-aged stands: past, present and future. *Forest Ecology and Management* 132, 259–279.
- Changhui, P., 2000b. Understanding the role of forest simulation models in sustainable forest management. *Environmental Impact Assessment Review* 20, 481–501.
- Chao, K.-J., Phillips, O.L., Gloor, E., Monteagudo, A., Torres-Lezama, A., Martínez, R.V., 2008. Growth and wood density predict tree mortality in Amazon forests. *Journal of Ecology* 96, 281–292.
- Chauchard, S., Carcaillet, C., Guibal, F., 2007. Patterns of land-use abandonment control tree-recruitment and forest dynamics in Mediterranean mountains. *Ecosystems* 10, 936–948.
- Chave, J., 1999. Study of structural, successional and spatial patterns in tropical rain forests using TROLL, a spatially explicit forest model. *Ecological Modelling* 124, 233–254.
- Chave, J., Andalo, C., Brown, S., Cairns, M., Chambers, J., Eamus, D., Fölster, H., Fromard, F., Higuchi, N., Kira, T., Lescure, J.-P., Nelson, B., Ogawa, H., Puig, H., Riéra, B., Yamakura, T., 2005. Tree allometry and improved estimation of carbon stocks and balance in tropical forests. *Oecologia* 145, 87–99.
- Chen, H.Y.H., Klinka, K., 1998. Survival, growth, and allometry of planted *Larix occidentalis* seedlings in relation to light availability. *Forest Ecology and Management* 106, 169–179.
- Chen, X., Li, B.-L., 2003. Testing the allometric scaling relationships with seedlings of two tree species. *Acta Oecologica* 24, 125–129.
- Cherubini, P., Fontana, G., Rigling, D., Dobbertin, M., Brang, P., Innes, J.L., 2002. Tree-life history prior to death: two fungal root pathogens affect tree-ring growth differently. *Journal of Ecology* 90, 839–850.
- Civil Protection and Environmental Accidents Unit, 2001. Forest fires in southern Europe. Joint Research Centre of the European Commission.
- Clark, J.S., Macklin, E., Wood, L., 1998. Stages and spatial scales of recruitment limitation in southern Appalachian forests. *Ecological Monographs* 68, 213–235.
- Climent, J., Prada, M.A., Calama, R., Chambel, M.R., de Ron, D.S., Alía, R., 2008. To grow or to seed: ecotypic variation in reproductive allocation and cone production by young female Aleppo pine (*Pinus halepensis*, Pinaceae). *American Journal of Botany* 95, 833–842.
- Coomes, D.A., Allen, R.B., 2007a. Effects of size, competition and altitude on tree growth. *Journal of Ecology* 95, 1084–1097.
- Coomes, D.A., Allen, R.B., 2007b. Mortality and tree-size distributions in natural mixed-age forests. *Journal of Ecology* 95, 27–40.
- Coomes, D.A., Allen, R.B., 2009. Testing the Metabolic Scaling Theory of tree growth. *Journal of Ecology* 97, 1369–1373.

- Coomes, D.A., Duncan, R.P., Allen, R.B., Truscott, J., 2003. Disturbances prevent stem size-density distributions in natural forests from following scaling relationships. *Ecology Letters* 6, 980–989.
- Coomes, D.A., Grubb, P.J., 1998. Responses of juvenile trees to above- and belowground competition in nutrient-starved amazonian rain forest. *Ecology* 79, 768–782.
- Coomes, D.A., Grubb, P.J., 2000. Impacts of root competition in forests and wetlands: a theoretical framework and review of experiments. *Ecological Monographs* 70, 171–207.
- Coomes, D.A., Holdaway, R.J., Kobe, R.K., Lines, E.R., Allen, R.B., 2012. A general integrative framework for modelling woody biomass production and carbon sequestration rates in forests. *Journal of Ecology* 100, 42–64.
- Coomes, D.A., Lines, E.R., Allen, R.B., 2011. Moving on from Metabolic Scaling Theory: hierarchical models of tree growth and asymmetric competition for light. *Journal of Ecology* 99, 748–756.
- Corcuera, L., Camarero, J., Gil-Pelegrín, E., 2004. Effects of a severe drought on *Quercus ilex* radial growth and xylem anatomy. *Trees - Structure and Function* 18, 83–92.
- Cornuet, J.-M., Santos, F., Beaumont, M.A., Robert, C.P., Marin, J.-M., Balding, D.J., Guillemaud, T., Estoup, A., 2008. Inferring population history with DIY ABC: a user-friendly approach to approximate Bayesian computation. *Bioinformatics* 24, 2713–2719.
- Cox, P., 2001. Description of the “TRIFFID” dynamic global vegetation model. Hadley Centre Technical Note 24.
- Cox, P.M., Betts, R.A., Collins, M., Harris, P.P., Huntingford, C., Jones, C.D., 2004. Amazonian forest dieback under climate-carbon cycle projections for the 21st century. *Theoretical and Applied Climatology* 78, 137–156.
- Crawley, M., 1997. The structure of plant communities, in: *Plant Ecology*. Blackwell Science.
- Csilléry, K., Blum, M.G.B., Gaggiotti, O.E., François, O., 2010. Approximate Bayesian Computation (ABC) in practice. *Trends in Ecology & Evolution* 25, 410–418.
- Csilléry, K., François, O., Blum, M.G.B., 2012. abc: an R package for approximate Bayesian computation (ABC). *Methods in Ecology and Evolution*.
- Curt, T., Adra, W., Borgniet, L., 2009. Fire-driven oak regeneration in French Mediterranean ecosystems. *Forest Ecology and Management* 258, 2127–2135.
- Dale, V.H., Joyce, L.A., McNulty, S., Neilson, R.P., Ayres, M.P., Flannigan, M.D., Hanson, P.J., Irland, L.C., Lugo, A.E., Peterson, C.J., Simberloff, D., Swanson, F.J., Stocks, B.J., Michael Wotton, B., 2001. Climate change and forest disturbances. *BioScience* 51, 723.
- Damesin, C., Rambal, S., 1995. Field study of leaf photosynthetic performance by a Mediterranean deciduous oak tree (*Quercus pubescens*) during a severe summer drought. *New Phytologist* 131, 159–167.
- David, T., Ferreira, M., Cohen, S., Pereira, J., David, J., 2004. Constraints on transpiration from an evergreen oak tree in southern Portugal. *Agricultural and Forest Meteorology* 122, 193–205.
- Dennis, B., 1996. Discussion: Should ecologists become Bayesians? *Ecological Applications* 6, 1095.

- Deutschman, D.H., Simon A. Levin, Pacala, S.W., 1999. Error propagation in a forest succession model: the role of fine-scale heterogeneity in light. *Ecology* 80, 1927–1943.
- Devakumar, A., Gawai Prakash, P., Sathik, M., Jacob, J., 1999. Drought alters the canopy architecture and micro-climate of *Hevea brasiliensis* trees. *Trees* 13, 161–167.
- Didion, M., Kupferschmid, A.D., Lexer, M.J., Rammer, W., Seidl, R., Bugmann, H., 2009. Potentials and limitations of using large-scale forest inventory data for evaluating forest succession models. *Ecological Modelling* 220, 133–147.
- Dietz, P., 1975. Dichte und Rindengehalt von Industrieholz. *Holz Roh- Werkstoff* 33, 135–141.
- Dietze, M.C., Wolosin, M.S., Clark, J.S., 2008. Capturing diversity and interspecific variability in allometries: A hierarchical approach. *Forest Ecology and Management* 256, 1939–1948.
- Duhme, F., Hinckley, T.M., 1992. Daily and seasonal variation in water relations of macchia shrubs and trees in France (Montpellier) and Turkey (Antalya). *Vegetatio* 99-100, 185–198.
- Eichhorn, M.P., Nilus, R., Compton, S.G., Hartley, S.E., Burslem, D.F.R.P., 2010. Herbivory of tropical rain forest tree seedlings correlates with future mortality. *Ecology* 91, 1092–1101.
- Eid, T., Tuhus, E., 2001. Models for individual tree mortality in Norway. *Forest Ecology and Management* 154, 69–84.
- Ellenberg, H., 1988. *Vegetation ecology of central Europe*, 4th ed. Cambridge University Press.
- Ellison, A.M., 2004. Bayesian inference in ecology. *Ecology Letters* 7, 509–520.
- Enquist, B., West, G., Charnov, E., Brown, J., 1999. Allometric scaling of production and life-history variation in vascular plants. *Nature* 401, 907–911.
- Enquist, B.J., Allen, A.P., Brown, J.H., Gillooly, J.F., Kerkhoff, A.J., Niklas, K.J., Price, C.A., West, G.B., 2007. Biological scaling: Does the exception prove the rule? *Nature* 445, E9–E10.
- Enquist, B.J., Economo, E.P., Huxman, T.E., Allen, A.P., Ignace, D.D., Gillooly, J.F., 2003. Scaling metabolism from organisms to ecosystems. *Nature* 423, 639–642.
- Enquist, B.J., Niklas, K.J., 2002. Global allocation rules for patterns of biomass partitioning in seed plants. *Science* 295, 1517–1520.
- Enquist, B.J., West, G.B., Brown, J.H., 2009. Extensions and evaluations of a general quantitative theory of forest structure and dynamics. *Proceedings of the National Academy of Sciences* 106, 7046–7051.
- Esteban, L., Martín, J., de Palacios, P., García Fernández, F., López, R., 2010. Adaptive anatomy of *Pinus halepensis* trees from different Mediterranean environments in Spain. *Trees - Structure and Function* 24, 19–30.
- Esteban, L.G., de Palacios, P., Rodríguez-Losada Aguado, L., 2010. *Abies pinsapo* forests in Spain and Morocco: threats and conservation. *Oryx* 44, 276–284.
- Evans, T.P., Kelley, H., 2008. Assessing the transition from deforestation to forest regrowth with an agent-based model of land cover change for south-central Indiana (USA). *Geoforum* 39, 819–832.

- Fearnhead, P., Prangle, D., 2010. Constructing summary statistics for approximate Bayesian computation: semi-automatic ABC. arXiv:1004.1112.
- Feeley, K.J., Joseph Wright, S., Nur Supardi, M.N., Kassim, A.R., Davies, S.J., 2007. Decelerating growth in tropical forest trees. *Ecology Letters* 10, 461–469.
- FIA-DB, 2008. FIA Data Users Guide v4.0 (Online).
- Filella, I., Peñuelas, J., 2004. Indications of hydraulic lift by *Pinus halepensis* and its effects on the water relations of neighbour shrubs. *Biologia Plantarum* 47, 209–214.
- Fisher, R., McDowell, N., Purves, D., Moorcroft, P., Sitch, S., Cox, P., Huntingford, C., Meir, P., Ian Woodward, F., 2010. Assessing uncertainties in a second-generation dynamic vegetation model caused by ecological scale limitations. *New Phytologist* 187, 666–681.
- Foll, M., Beaumont, M.A., Gaggiotti, O., 2008. An approximate Bayesian computation approach to overcome biases that arise when using amplified fragment length polymorphism markers to study population structure. *Genetics* 179, 927–939.
- Foster, D., 1988. Disturbance history, community organization and vegetation dynamics of the old-growth Pisgah forest, south-western New Hampshire USA. *Journal of Ecology* 76, 105–134.
- FRA, 2000. Global Forest Resources Assessment. Food and Agriculture Organization of the United Nations.
- Franklin, J.F., Shugart, H.H., Harmon, M.E., 1987. Tree death as an ecological process. *BioScience* 37, 550–556.
- Friend, A.D., Schugart, H.H., Running, S.W., 1993. A physiology-based gap model of forest dynamics. *Ecology* 74, 792–797.
- Fuller, J., Foster, D., McLachlan, J., Drake, N., 1998. Impact of human activity on regional forest composition and dynamics in central New England. *Ecosystems* 1, 76–95.
- Galbraith, D., Levy, P.E., Sitch, S., Huntingford, C., Cox, P., Williams, M., Meir, P., 2010. Multiple mechanisms of Amazonian forest biomass losses in three dynamic global vegetation models under climate change. *New Phytologist* 187, 647–665.
- García Viñas, J.I., Lopez Leiva, C., Villares Muyo, J.M., Tostado Rivera, P., García Rodríguez, C., Ruiz del Castillo y Navascues, J., 2006. El Mapa Forestal de España escala 1:200.000. Metodología y análisis de resultados. *Forest Systems* 15.
- García-Gonzalo, J., Jäger, D., Lexer, M.J., Peltola, H., Briceño-Elizondo, E., Kellomäki, S., 2008. Does climate change affect optimal planning solutions for multi-objective forest management? *Allgemeine Forst- und Jagdzeitung* 179, 77–94.
- Gaston, K.J., 2009. Geographic range limits of species. *Proceedings of the Royal Society B: Biological Sciences* 276, 1391–1393.
- Gatti, P.L., 2005. Probability theory and mathematical statistics for engineers. Taylor & Francis.
- van Gelder, H.A., Poorter, L., Sterck, F.J., 2006. Wood mechanics, allometry, and life-history variation in a tropical rain forest tree community. *New Phytologist* 171, 367–378.

- Gelfand, A.E., Hills, S.E., Racine-Poon, A., Smith, A.F.M., 1990. Illustration of Bayesian inference in normal data models using Gibbs sampling. *Journal of the American Statistical Association* 85, 972–985.
- Gelman, A., Carlin, J.B., Stern, H.S., Rubin, D.B., 2004. *Bayesian data analysis*. Chapman & Hall/CRC Press.
- Gelman, A., Hill, J., 2007. *Data analysis using regression and multilevel/hierarchical models*. Cambridge University Press, Cambridge.
- Gelman, A., Roberts, G.O., Gilks, G.R., 1999. Efficient Metropolis Jumping Rules, in: *Bayesian Statistics 5*. Oxford University Press, pp. 599–607.
- Gelman, A., Rubin, D.B., 1992. Inference from iterative simulation using multiple sequences. *Statistical Science* 7, 457–472.
- Gibson, L.J., Easterling, K.E., Ashby, M.F., 1981. The structure and mechanics of cork. *Proceedings of the Royal Society A* 377, 99–117.
- Gillooly, J.F., Brown, J.H., West, G.B., Savage, V.M., Charnov, E.L., 2001. Effects of size and temperature on metabolic rate. *Science* 293, 2248–2251.
- Giudici, F., Zingg, A., 2005. Sprouting ability and mortality of chestnut (*Castanea sativa* Mill.) after coppicing. A case study. *Annals of Forest Science* 62, 11.
- Glenn-Lewin, D.C., Peet, R.K., Veblen, T.T., 1992. *Plant succession: theory and prediction*. Springer.
- Gómez-Aparicio, L., Pérez-Ramos, I.M., Mendoza, I., Matías, L., Quero, J.L., Castro, J., Zamora, R., Marañón, T., 2008. Oak seedling survival and growth along resource gradients in Mediterranean forests: implications for regeneration in current and future environmental scenarios. *Oikos* 117, 1683–1699.
- Gómez-Aparicio, L., Valladares, F., Zamora, R., 2006. Differential light responses of Mediterranean tree saplings: linking ecophysiology with regeneration niche in four co-occurring species. *Tree Physiology* 26, 947–958.
- Gómez-Aparicio, L., Zamora, R., Gómez, J.M., Hódar, J.A., Castro, J., Baraza, E., 2004. Applying plant facilitation to forest restoration: A meta-analysis of the use of shrubs as nurse plants. *Ecological Applications* 14, 1128–1138.
- Gómez-Aparicio, L., Zavala, M.A., Bonet, F.J., Zamora, R., 2009. Are pine plantations valid tools for restoring Mediterranean forests? An assessment along abiotic and biotic gradients. *Ecol Appl* 19, 2124–2141.
- Gonzalo Jiménez, J., 2008. *Diagnosis fitoclimática de la España peninsular. Actualización y análisis geostadístico aplicado*. Universidad Politécnica de Madrid: Thesis.
- de Graaf, N.R., Poels, R.L.H., Van Rompaey, R.S.A.R., 1999. Effect of silvicultural treatment on growth and mortality of rainforest in Surinam over long periods. *Forest Ecology and Management* 124, 123–135.
- Gracia, M., Retana, J., Roig, P., 2002. Mid-term successional patterns after fire of mixed pine–oak forests in NE Spain. *Acta Oecologica* 23, 405–411.

- Gratzer, G., Canham, C., Dieckmann, U., Fischer, A., Iwasa, Y., Law, R., Lexer, M.J., Sandmann, H., Spies, T.A., Splechtna, B.E., Szwagrzyk, J., 2004. Spatio-temporal development of forests-current trends in field methods and models. *Oikos* 107, 3–15.
- Gratzer, G., Darabant, A., Chhetri, P.B., Rai, P.B., Eckmüllner, O., 2004. Interspecific variation in the response of growth, crown morphology, and survivorship to light of six tree species in the conifer belt of the Bhutan Himalayas. *Canadian Journal of Forest Research* 34, 1093–1107.
- Green, D.G., 1989. Simulated effects of fire, dispersal and spatial pattern on competition within forest mosaics. *Vegetatio* 82, 139–153.
- Greenhill, A.G., 1881. Determination of the greatest height consistent with stability that a vertical pole or mast can be made, and of the greatest height to which a tree of given proportions can grow. *Proceedings of the Cambridge Philosophical Society* 4, 65–73.
- Grelaud, A., Robert, C., Marin, J.-M., Rodolphe, F., Taly, J.-F., 2008. ABC likelihood-free methods for model choice in Gibbs random fields. [arXiv:0807.2767](https://arxiv.org/abs/0807.2767).
- Grimm, V., Railsback, S., 2005. *Individual-based modelling in ecology*, 1st ed. Princeton University Press, Princeton.
- Grimm, V., Revilla, E., Berger, U., Jeltsch, F., Mooij, W.M., Railsback, S.F., Thulke, H.-H., Weiner, J., Wiegand, T., DeAngelis, D.L., 2005. Pattern-oriented modeling of agent-based complex systems: lessons from ecology. *Science* 310, 987–991.
- Grove, A., Rackham, O., 2001. *The nature of Mediterranean Europe: an ecological history*. Yale University Press, London, UK.
- Guisan, A., Thuiller, W., 2005. Predicting species distribution: offering more than simple habitat models. *Ecology Letters* 8, 993–1009.
- Gutiérrez, O.A., Plaza, P.F., 1967. *Características físico-mecánicas de las maderas Españolas*. Ministerio de Agricultura, Madrid.
- Hall, F.G., Botkin, D.B., Strelbel, D.E., Woods, K.D., Goetz, S.J., 1991. Large-scale patterns of forest succession as determined by remote sensing. *Ecology* 72, 628–640.
- Hampe, A., 2011. Plants on the move: The role of seed dispersal and initial population establishment for climate-driven range expansions. *Acta Oecologica* 37.
- Hanson, P.J., Todd, D.E., Amthor, J.S., 2001. A six-year study of sapling and large-tree growth and mortality responses to natural and induced variability in precipitation and throughfall. *Tree Physiology* 21, 345–358.
- Harcombe, P.A., 1987. Tree Life Tables. *BioScience* 37, 557–568.
- He, F., Duncan, R.P., 2000. Density-dependent effects on tree survival in an old-growth Douglas fir forest. *Journal of Ecology* 88, 676–688.
- He, H.S., Mladenoff, D.J., 1999. Spatially explicit and stochastic simulation of forest-landscape fire disturbance and succession. *Ecology* 80, 81–99.
- He, H.S., Mladenoff, D.J., Crow, T.R., 1999. Linking an ecosystem model and a landscape model to study forest species response to climate warming. *Ecological Modelling* 114, 213–233.

- Henry, H.A.L., Aarssen, L.W., 1999. The interpretation of stem diameter-height allometry in trees: biomechanical constraints, neighbour effects, or biased regressions? *Ecology Letters* 2, 89–97.
- Harms, D.A., Mattson, W.J., 1992. The Dilemma of Plants: To Grow or Defend. *The Quarterly Review of Biology* 67, 283–335.
- Herrera, C.M., 1992. Historical effects and sorting processes as explanations for contemporary ecological patterns: character syndromes in Mediterranean woody plants. *The American Naturalist* 140, 421–446.
- Hickler, T., Smith, B., Sykes, M.T., Davis, M.B., Sugita, S., Walker, K., 2004. Using a generalized vegetation model to simulate vegetation dynamics in northeastern USA. *Ecology* 85, 519–530.
- Hilborn, R., Mangel, M., 1997. *The Ecological Detective*. Princeton University Press, Princeton.
- Hobbs, N.T., Hilborn, R., 2006. Alternatives to statistical hypothesis testing in ecology: a guide to self teaching. *Ecological Applications* 16, 5–19.
- Holdridge, L.R., 1947. Determination of world plant formations from simple climatic data. *Science* 105, 367–368.
- Hooten, M.B., Larsen, D.R., Wikle, C.K., 2003. Predicting the spatial distribution of ground flora on large domains using a hierarchical Bayesian model. *Landscape ecology* 18, 487–502.
- Horn, H., 1971. *The adaptive geometry of trees*. Princeton University Press, Princeton.
- Huston, M., DeAngelis, D., Post, W., 1988. New computer models unify ecological theory. *BioScience* 38, 682–691.
- Huston, M., Smith, T., 1987. Plant succession: life history and competition. *The American Naturalist* 130, 168–198.
- Hynynen, J., Ahtikoski, A., Siitonen, J., Sievänen, R., Liski, J., 2005. Applying the MOTTI simulator to analyse the effects of alternative management schedules on timber and non-timber production. *Forest Ecology and Management* 207, 5–18.
- Hyvönen, R., Agren, G.I., Linder, S., Persson, T., Cotrufo, M.F., Ekblad, A., Freeman, M., Grelle, A., Janssens, I.A., Jarvis, P.G., Kellomäki, S., Lindroth, A., Loustau, D., Lundmark, T., Norby, R.J., Oren, R., Pilegaard, K., Ryan, M.G., Sigurdsson, B.D., Strömberg, M., van Oijen, M., Wallin, G., 2007. The likely impact of elevated CO₂, nitrogen deposition, increased temperature and management on carbon sequestration in temperate and boreal forest ecosystems: a literature review. *New Phytologist* 173, 463–480.
- Ibáñez, I., Clark, J.S., LaDeau, S., Lambers, J.H.R., 2007. Exploiting temporal variability to understand tree recruitment response to climate change. *Ecological Monographs* 77, 163–177.
- IPCC, 2007. *Climate Change 2007: Synthesis report*.
- Jabot, F., Chave, J., 2009. Inferring the parameters of the neutral theory of biodiversity using phylogenetic information and implications for tropical forests. *Ecology Letters* 12, 239–248.

- James, P.M.A., Fortin, M.-J., Sturtevant, B.R., Fall, A., Kneeshaw, D., 2010. Modelling spatial interactions among fire, spruce budworm, and logging in the boreal forest. *Ecosystems* 14, 60–75.
- Joffre, R., Rambal, S., Damesin, C., 1999. Functional attributes in Mediterranean-type ecosystems, in: Pugnaire, F.I., Valladares, F. (Eds.), *Handbook of Functional Plant Ecology*. CRC Press.
- Joffre, R., Rambal, S., Ratte, J.P., 1999. The dehesa system of southern Spain and Portugal as a natural ecosystem mimic. *Agroforestry Systems* 45, 57–79.
- Joffre, R., Vacher, J., Llanos, C., Long, G., 1988. The dehesa: an agrosilvopastoral system of the Mediterranean region with special reference to the Sierra Morena area of Spain. *Agroforestry Systems* 6, 71–96.
- Johnson, J.B., Omland, K.S., 2004. Model selection in ecology and evolution. *Trends in Ecology & Evolution* 19, 101–108.
- Jorritsma, I.T., van Hees, A.F., Mohren, G.M., 1999. Forest development in relation to ungulate grazing: a modeling approach. *Forest Ecology and Management* 120, 23–34.
- Joyce, L.A., 1995. Productivity of America's forests and climate change (General Technical Report RM-271). USDA Forest Service.
- Joyce, P., Marjoram, P., 2008. Approximately sufficient statistics and Bayesian computation. *Statistical Applications in Genetics and Molecular Biology* 7.
- Jump, A.S., Hunt, J.M., Peñuelas, J., 2006. Rapid climate change-related growth decline at the southern range edge of *Fagus sylvatica*. *Global Change Biology* 12, 2163–2174.
- Jung, H., Marjoram, P., 2011. Choice of summary statistic weights in approximate Bayesian computation. *Statistical Applications in Genetics and Molecular Biology* 10.
- Kaitaniemi, P., Lintunen, A., 2008. Precision of allometric scaling equations for trees can be improved by including the effect of ecological interactions. *Trees - Structure and Function* 22, 579–584.
- Karafyllidis, I., Thanailakis, A., 1997. A model for predicting forest fire spreading using cellular automata. *Ecological Modelling* 99, 87–97.
- Kardol, P., Todd, D.E., Hanson, P.J., Mulholland, P.J., 2010. Long-term successional forest dynamics: species and community responses to climatic variability. *Journal of Vegetation Science* 21, 627–642.
- Karin, G., 1996. Effects of root competition and canopy openness on survival and growth of tree seedlings in a tropical seasonal dry forest. *Forest Ecology and Management* 82, 33–48.
- Keane, R.E., Cary, G.J., Davies, I.D., Flannigan, M.D., Gardner, R.H., Lavorel, S., Lenihan, J.M., Li, C., Rupp, T.S., 2004. A classification of landscape fire succession models: spatial simulations of fire and vegetation dynamics. *Ecological Modelling* 179, 3–27.
- Keane, R.E., Ryan, K.C., Running, S.W., 1996. Simulating effects of fire on northern Rocky Mountain landscapes with the ecological process model FIRE-BGC. *Tree Physiology* 16, 319–331.
- Kearney, M., 2006. Habitat, environment and niche: what are we modelling? *Oikos* 115, 186–191.

- Keenan, T., García, R., Friend, A.D., Zaehle, S., Gracia, C., Sabate, S., 2009. Improved understanding of drought controls on seasonal variation in Mediterranean forest canopy CO₂ and water fluxes through combined in situ measurements and ecosystem modelling. *Biogeosciences* 6, 1423–1444.
- Keenan, T., Maria Serra, J., Lloret, F., Ninyerola, M., Sabate, S., 2011. Predicting the future of forests in the Mediterranean under climate change, with niche- and process-based models: CO₂ matters! *Global Change Biology* 17, 565–579.
- Kennedy, W., Gentle, J., 2000. *Statistical Computing*. Marcel Dekker.
- Kessell, S.R., Potter, M.W., 1980. A quantitative succession model for nine Montana forest communities. *Environmental Management* 4, 227–240.
- King, D.A., Davies, S.J., Supardi, M.N.N., Tan, S., 2005. Tree growth is related to light interception and wood density in two mixed dipterocarp forests of Malaysia. *Functional Ecology* 19, 445–453.
- King, D.A., Davies, S.J., Tan, S., Supardi, M.N.N., 2009. Trees approach gravitational limits to height in tall lowland forests of Malaysia. *Functional Ecology* 23, 284–291.
- King, J.S., Albaugh, T.J., Allen, H.L., Kress, L.W., 1999. Stand-level allometry in *Pinus taeda* as affected by irrigation and fertilization. *Tree Physiology* 19, 769–778.
- Kittel, T.G.F., Rosenbloom, N.A., Painter, T.H., Schimel, D.S., 1995. The VEMAP integrated database for modelling United States ecosystem/vegetation sensitivity to climate change. *Journal of Biogeography* 22, 867–62.
- Kobe, R.K., 1996. Intraspecific variation in sapling mortality and growth predicts geographic variation in forest composition. *Ecological Monographs* 66, 181.
- Kobe, R.K., 1999. Light gradient partitioning among tropical tree species through differential seedling mortality and growth. *Ecology* 80, 187–201.
- Kobe, R.K., Pacala, S.W., Silander, J.A., Canham, C.D., 1995. Juvenile tree survivorship as a component of shade tolerance. *Ecological Applications* 5, 517–532.
- Kohyama, T., 1991. A functional model describing sapling growth under a tropical forest canopy. *Functional Ecology* 5, 83–90.
- Kolbe, A.E., Buongiorno, J., Vasievich, M., 1999. Geographic extension of an uneven-aged, multi-species matrix growth model for northern hardwood forests. *Ecological Modelling* 121, 235–253.
- Krinner, G., Viovy, N., Noblet-Ducoudré, N. de, Ogée, J., Polcher, J., Friedlingstein, P., Ciais, P., Sitch, S., Prentice, I.C., 2005. A dynamic global vegetation model for studies of the coupled atmosphere-biosphere system. *Global Biogeochemical Cycles* 19.
- Kronfuss, H., Havranek, W., 1999. Effects of elevation and wind on the growth of *Pinus cembra* L. in a subalpine afforestation. *Phyton-Annales Rei Botanicae* 39, 99–106.
- Kruschke, J.K., 2010a. Bayesian data analysis. *Wiley Interdisciplinary Reviews: Cognitive Science* 1, 658–676.

- Kruschke, J.K., 2010b. What to believe: Bayesian methods for data analysis. *Trends in Cognitive Sciences* 14, 293–300.
- Kullback, S., Leibler, R.A., 1951. On information and sufficiency. *The Annals of Mathematical Statistics* 22, 79–86.
- Kunstler, G., Coomes, D.A., Canham, C.D., 2009. Size-dependence of growth and mortality influence the shade tolerance of trees in a lowland temperate rain forest. *Journal of Ecology* 97, 685–695.
- Kurz, W.A., Dymond, C.C., Stinson, G., Rampley, G.J., Neilson, E.T., Carroll, A.L., Ebata, T., Safranyik, L., 2008. Mountain pine beetle and forest carbon feedback to climate change. *Nature* 452, 987–990.
- Lapola, D.M., Oyama, M.D., Nobre, C.A., 2009. Exploring the range of climate biome projections for tropical South America: The role of CO₂ fertilization and seasonality. *Global Biogeochemical Cycles* 23.
- Latham, R.E., 1992. Co-Occurring Tree Species Change Rank in Seedling Performance with Resources Varied Experimentally. *Ecology* 73, 2129–2144.
- Lavorel, S., Díaz, S., Cornelissen, J., Garnier, E., Harrison, S., McIntyre, S., Pausas, J., Pérez-Harguindeguy, N., Roumet, C., Urcelay, C., 2007. Plant functional types: are we getting any closer to the Holy Grail?, in: *Terrestrial Ecosystems in a Changing World*. pp. 149–164.
- Leathwick, J.R., Austin, M.P., 2001. Competitive Interactions between Tree Species in New Zealand's Old-Growth Indigenous Forests. *Ecology* 82, 2560–2573.
- Lee, P.M., 1997. *Bayesian statistics: an introduction*, 3rd ed. Arnold.
- Leemans, R., 1991. Sensitivity analysis of a forest succession model. *Ecological Modelling* 53, 247–262.
- Leemans, R., Prentice, I.C., 1989. FORSKA, A General Forest Succession Model. Institute of Ecological Botany, Uppsala, Sweden.
- Lemoine, D., Granier, A., Cochard, H., 1999. Mechanism of freeze-induced embolism in *Fagus sylvatica* L. *Trees* 13, 206–210.
- Leuenberger, C., Wegmann, D., 2010. Bayesian computation and model selection without likelihoods. *Genetics* 184, 243–252.
- Lewis, S.L., 2006. Tropical forests and the changing earth system. *Philosophical transactions of the Royal Society B* 361, 195–210.
- Li, H., Han, X., Wu, J., 2005. Lack of evidence for 3/4 scaling of metabolism in terrestrial plants. *Journal of Integrative Plant Biology* 47, 1173–1183.
- Lichstein, J.W., Dushoff, J., Ogle, K., Chen, A., Purves, D.W., Caspersen, J.P., Pacala, S.W., 2010. Unlocking the forest inventory data: relating individual tree performance to unmeasured environmental factors. *Ecological Applications* 20, 684–699.
- Liedloff, A.C., Cook, G.D., 2007. Modelling the effects of rainfall variability and fire on tree populations in an Australian tropical savanna with the Flames simulation model. *Ecological Modelling* 201, 269–282.

- Linder, M., 2000. Developing adaptive forest management strategies to cope with climate change. *Tree Physiology* 20, 299–307.
- Lindner, M., Sievänen, R., Pretzsch, H., 1997. Improving the simulation of stand structure in a forest gap model. *Forest Ecology and Management* 95, 183–195.
- Liu, J., Ashton, P.S., 1995. Individual-based simulation models for forest succession and management. *Forest Ecology and Management* 73, 157–175.
- Liu, Y., Muller, R., 1993. Effect of drought and frost on radial growth of overstory and understory stems in a deciduous forest. *American Midland Naturalist* 129, 19–25.
- Lloret, F., Pausas, J.G., Vilà, M., 2003. Responses of Mediterranean plant species to different fire frequencies in Garraf Natural Park (Catalonia, Spain): field observations and modelling predictions. *Plant Ecology* 167, 223–235.
- Lloret, F., Peñuelas, J., Ogaya, R., 2004. Establishment of co-existing Mediterranean tree species under a varying soil moisture regime. *Journal of Vegetation Science* 15, 237–244.
- Loarie, S.R., Duffy, P.B., Hamilton, H., Asner, G.P., Field, C.B., Ackerly, D.D., 2009. The velocity of climate change. *Nature* 462, 1052–1055.
- Loehle, C., 1998. Height growth rate tradeoffs determine northern and southern range limits for trees. *Journal of Biogeography* 25, 735–742.
- Lookingbill, T.R., Zavala, M.A., 2000. Spatial pattern of *Quercus ilex* and *Quercus pubescens* recruitment in *Pinus halepensis* dominated woodlands. *Journal of Vegetation Science* 11, 607–612.
- Lopatin, E., 2007. Long-term trends in height growth of *Picea obovata* and *Pinus sylvestris* during the past 100 years in Komi Republic (north-western Russia). *Scandinavian Journal of Forest Research* 22, 310–323.
- López, R., Zehavi, A., Climent, J., Gil, L., 2007. Contrasting ecotypic differentiation for growth and survival in *Pinus canariensis*. *Australian Journal of Botany* 55, 759–769.
- López-Serrano, F.R., García-Morote, A., Andrés-Abellán, M., Tendero, A., del Cerro, A., 2005. Site and weather effects in allometries: A simple approach to climate change effect on pines. *Forest Ecology and Management* 215, 251–270.
- Lovett, G.M., Canham, C.D., Arthur, M.A., Weathers, K.C., Fitzhugh, R.D., 2006. Forest ecosystem responses to exotic pests and pathogens in eastern North America. *BioScience* 56, 395.
- Mäkelä, A., Landsberg, J., Ek, A.R., Burk, T.E., Ter-Mikaelian, M., Ågren, G.I., Oliver, C.D., Puttonen, P., 2000. Process-based models for forest ecosystem management: current state of the art and challenges for practical implementation. *Tree Physiology* 20, 289–298.
- Mäkelä, A., Valentine, H.T., 2006. Crown ratio influences allometric scaling in trees. *Ecology* 87, 2967–2972.
- van Mantgem, P.J., Stephenson, N.L., 2007. Apparent climatically induced increase of tree mortality rates in a temperate forest. *Ecology Letters* 10, 909–916.

- van Mantgem, P.J., Stephenson, N.L., Byrne, J.C., Daniels, L.D., Franklin, J.F., Fule, P.Z., Harmon, M.E., Larson, A.J., Smith, J.M., Taylor, A.H., Veblen, T.T., 2009. Widespread increase of tree mortality rates in the western United States. *Science* 323, 521–524.
- Marjoram, P., Molitor, J., Plagnol, V., Tavaré, S., 2003. Markov chain Monte Carlo without likelihoods. *Proceedings of the National Academy of Sciences* 100, 15324–15328.
- Markesteyn, L., Poorter, L., Paz, H., Sack, L., Bongers, F., 2011. Ecological differentiation in xylem cavitation resistance is associated with stem and leaf structural traits. *Plant, Cell & Environment* 34, 137–148.
- Martin, R.D., Barbour, A.D., 1989. Aspects of line-fitting in bivariate allometric analyses. *Folia Primatol.* 53, 65–81.
- Martín-Benito, D., Cherubini, P., del Río, M., Cañellas, I., 2008. Growth response to climate and drought in *Pinus nigra* Arn. trees of different crown classes. *Trees* 22, 363–373.
- Martínez-Vilalta, J., López, B.C., Loepfe, L., Lloret, F., 2011. Stand- and tree-level determinants of the drought response of Scots pine radial growth. *Oecologia*.
- Martínez-Vilalta, J., Prat, E., Oliveras, I., Piñol, J., 2002. Xylem hydraulic properties of roots and stems of nine Mediterranean woody species. *Oecologia* 133, 19–29.
- Matala, J., Ojansuu, R., Peltola, H., Sievänen, R., Kellomäki, S., 2005. Introducing effects of temperature and CO₂ elevation on tree growth into a statistical growth and yield model. *Ecological Modelling* 181, 173–190.
- McMahon, S.M., Harrison, S.P., Armbruster, W.S., Bartlein, P.J., Beale, C.M., Edwards, M.E., Kattge, J., Midgley, G., Morin, X., Prentice, I.C., 2011. Improving assessment and modelling of climate change impacts on global terrestrial biodiversity. *Trends in Ecology & Evolution* 26, 249–259.
- McMahon, S.M., Parker, G.G., Miller, D.R., 2010. Evidence for a recent increase in forest growth. *Proceedings of the National Academy of Sciences* 107, 3611–3615.
- McMahon, T., 1973. Size and shape in biology: elastic criteria impose limits on biological proportions, and consequently on metabolic rates. *Science* 179, 1201–1204.
- Mediavilla, S., Escudero, A., 2003. Stomatal responses to drought at a Mediterranean site: a comparative study of co-occurring woody species differing in leaf longevity. *Tree Physiology* 23, 987–996.
- van der Meer, P.J., Jorritsma, I.T.M., Kramer, K., 2002. Assessing climate change effects on long-term forest development: adjusting growth, phenology, and seed production in a gap model. *Forest Ecology and Management* 162, 39–52.
- Meinzer, F.C., Lachenbruch, B., Dawson, T.E., 2011. *Size- and Age-Related Changes in Tree Structure and Function*. Springer.
- Mencuccini, M., 2002. Hydraulic constraints in the functional scaling of trees. *Tree Physiology* 22, 553–565.
- Mencuccini, M., Grace, J., 1996. Hydraulic conductance, light interception and needle nutrient concentration in Scots pine stands and their relations with net primary productivity. *Tree Physiology* 16, 459–468.

- Méndez-Alonzo, R., Lopez-Portillo, J., Rivera-Monroy, V.H., 2008. Latitudinal variation in leaf and tree traits of the mangrove *Avicennia germinans* (Avicenniaceae) in the central region of the Gulf of Mexico. *Biotropica* 40, 449–456.
- Mendoza, I., Gómez-Aparicio, L., Zamora, R., Matías, L., 2009. Recruitment limitation of forest communities in a degraded Mediterranean landscape. *Journal of Vegetation Science* 20, 367–376.
- Mendoza, I., Zamora, R., Castro, J., 2009. A seeding experiment for testing tree-community recruitment under variable environments: Implications for forest regeneration and conservation in Mediterranean habitats. *Biological conservation* 142, 1491–1499.
- Miao, S., Zou, C.B., Breshears, D.D., 2009. Vegetation responses to extreme hydrological events: sequence matters. *American Naturalist* 173, 113–118.
- Millán, M.M., Estrela, M.J., Sanz, M.J., Mantilla, E., Martín, M., Pastor, F., Salvador, R., Vallejo, R., Alonso, L., Gangoiti, G., Ilardia, J.L., Navazo, M., Albizuri, A., Artíñano, B., Ciccioli, P., Kallos, G., Carvalho, R.A., Andrés, D., Hoff, A., Werhahn, J., Seufert, G., Versino, B., 2005. Climatic feedbacks and desertification: the Mediterranean model. *Journal of Climate* 18, 684–701.
- Millenium Ecosystems Assessment, 2005. Ecosystems and human well-being: biodiversity synthesis, Millenium Ecosystems Assessment. World Resources Institute, Washington DC.
- Mitchell, K.J., 1969. Simulation of the growth of even-aged stands of white spruce. *Yale University School of Forestry Bulletin* 1–48.
- Mitchell, S.R., Harmon, M.E., O'Connell, K.E.B., 2009. Forest fuel reduction alters fire severity and long-term carbon storage in three Pacific Northwest ecosystems. *Ecological Applications* 19, 643–655.
- MMA (Ministerio de Medio Ambiente), 1996. Segundo Inventario Forestal Nacional (1986–1996): bases de datos e información cartográfica. Banco de Datos de la Naturaleza. Ministerio de Medio Ambiente, Madrid, Spain.
- MMA (Ministerio de Medio Ambiente), 2007. Tercer Inventario Forestal Nacional (1997–2007): bases de datos e información cartográfica. Banco de Datos de la Naturaleza. Ministerio de Medio Ambiente, Madrid, Spain.
- Mohren, G.M.J., Burkhardt, H.E., 1994. Contrasts between biologically- based process models and management-oriented growth and yield models. *Forest Ecology and Management* 69, 1–5.
- Monserud, R.A., Sterba, H., 1999. Modeling individual tree mortality for Austrian forest species. *Forest Ecology and Management* 113, 109–123.
- Montoya, D., Zavala, M.A., Rodriguez, M.A., Purves, D.W., 2008. Animal versus wind dispersal and the robustness of tree species to deforestation. *Science* 320, 1502–1504.
- Moorcroft, P.R., Hurtt, G.C., Pacala, S.W., 2001. A method for scaling vegetation dynamics: The ecosystem demography model (ED). *Ecological Monographs* 71, 557–585.
- Del Moral, P., Doucet, A., Jasra, A., 2006. Sequential Monte Carlo samplers. *Journal of the Royal Statistical Society: Series B (Statistical Methodology)* 68, 411–436.

- Morales, P., Sykes, M.T., Prentice, I.C., Smith, P., Smith, B., Bugmann, H., Zierl, B., Friedlingstein, P., Viovy, N., Sabaté, S., Sánchez, A., Pla, E., Gracia, C.A., Sitch, S., Arneth, A., Ogee, J., 2005. Comparing and evaluating process-based ecosystem model predictions of carbon and water fluxes in major European forest biomes. *Global Change Biology* 11, 2211–2233.
- Moreno, G., Obrador, J.J., Cubera, E., Dupraz, C., 2005. Fine root distribution in dehesas of central-western Spain. *Plant and Soil* 277, 153–162.
- Morin, X., Augspurger, C., Chuine, I., 2007. Process-Based Modeling of Species' Distributions: What Limits Temperate Tree Species' Range Boundaries? *Ecology* 88, 2280–2291.
- Morin, X., Thuiller, W., 2009. Comparing niche- and process-based models to reduce prediction uncertainty in species range shifts under climate change. *Ecology* 90, 1301–1313.
- Morin, X., Viner, D., Chuine, I., 2008. Tree species range shifts at a continental scale: new predictive insights from a process-based model. *Journal of Ecology* 96, 784–794.
- Motzkin, G., Wilson, P., Foster, D., Allen, A., 1999. Vegetation patterns in heterogeneous landscapes: The importance of history and environment. *Journal of Vegetation Science* 10, 903–920.
- Muller-Landau, H.C., Condit, R.S., Chave, J., Thomas, S.C., Bohlman, S.A., Bunyavejchewin, S., Davies, S., Foster, R., Gunatilleke, S., Gunatilleke, N., Harms, K.E., Hart, T., Hubbell, S.P., Itoh, A., Kassim, A.R., LaFrankie, J.V., Lee, H.S., Losos, E., Makana, J.-R., Ohkubo, T., Sukumar, R., Sun, I.-F., Nur Supardi, M.N., Tan, S., Thompson, J., Valencia, R., Muñoz, G.V., Wills, C., Yamakura, T., Chuyong, G., Dattaraja, H.S., Esufali, S., Hall, P., Hernandez, C., Kenfack, D., Kiratiprayoon, S., Suresh, H.S., Thomas, D., Vallejo, M.I., Ashton, P., 2006. Testing metabolic ecology theory for allometric scaling of tree size, growth and mortality in tropical forests. *Ecology Letters* 9, 575–588.
- Muller-Landau, H.C., Condit, R.S., Harms, K.E., Marks, C.O., Thomas, S.C., Bunyavejchewin, S., Chuyong, G., Co, L., Davies, S., Foster, R., Gunatilleke, S., Gunatilleke, N., Hart, T., Hubbell, S.P., Itoh, A., Kassim, A.R., Kenfack, D., LaFrankie, J.V., Lagunzad, D., Lee, H.S., Losos, E., Makana, J.-R., Ohkubo, T., Samper, C., Sukumar, R., Sun, I.-F., Nur Supardi, M.N., Tan, S., Thomas, D., Thompson, J., Valencia, R., Vallejo, M.I., Muñoz, G.V., Yamakura, T., Zimmerman, J.K., Dattaraja, H.S., Esufali, S., Hall, P., He, F., Hernandez, C., Kiratiprayoon, S., Suresh, H.S., Wills, C., Ashton, P., 2006. Comparing tropical forest tree size distributions with the predictions of metabolic ecology and equilibrium models. *Ecology Letters* 9, 589–602.
- Muth, C., Bazzaz, F., 2003. Tree canopy displacement and neighborhood interactions. *Canadian Journal of Forest Research* 33, 1323–1330.
- Myers, N., Mittermeier, R.A., Mittermeier, C.G., da Fonseca, G.A.B., Kent, J., 2000. Biodiversity hotspots for conservation priorities. *Nature* 403, 853–858.
- Nathan, R., Muller-Landau, H.C., 2000. Spatial patterns of seed dispersal, their determinants and consequences for recruitment. *Trends in Ecology & Evolution* 15, 278–285.
- Návar, J., 2009. Allometric equations for tree species and carbon stocks for forests of northwestern Mexico. *Forest Ecology and Management* 257, 427–434.
- Neilson, R.P., Pitelka, L.F., Solomon, A.M., Nathan, R., Midgley, G.F., Fragoso, J.M.V., Lischke, H., Thompson, K., 2005. Forecasting regional to global plant migration in response to climate change. *BioScience* 55, 749.

- New, M., Hulme, M., Jones, P., 1999. Representing twentieth-century space-time climate variability. part I: development of a 1961-90 mean monthly terrestrial climatology. *Journal of Climate* 12, 829–856.
- Newton, A.C., Echeverría, C., Cantarello, E., Bolados, G., 2011. Projecting impacts of human disturbances to inform conservation planning and management in a dryland forest landscape. *Biological Conservation* 144, 1949–1960.
- Niinemets, Ü., Valladares, F., 2008. Tolerance to shade, drought, and waterlogging of temperate northern hemisphere trees and shrubs. *Ecological Monographs* 76, 521–547.
- Niklas, K.J., 1994. *Plant allometry: the scaling of form and process*. University of Chicago Press.
- Niklas, K.J., 1995. Size-dependent allometry of tree height, diameter and trunk-taper. *Annals of Botany* 75, 217–227.
- Niklas, K.J., Spatz, H.-C., 2004. Growth and hydraulic (not mechanical) constraints govern the scaling of tree height and mass. *Proceedings of the National Academy of Sciences of the United States of America* 101, 15661–15663.
- Nunes, M.A., Balding, D.J., 2010. On optimal selection of summary statistics for approximate Bayesian computation. *Statistical Applications in Genetics and Molecular Biology* 9, Article34.
- Pacala, S.W., Canham, C.D., Saponara, J., Silander, J.A., Kobe, R.K., Ribbens, E., 1996. Forest models defined by field measurements: estimation, error analysis and dynamics. *Ecological Monographs* 66, 1–43.
- Pacala, S.W., Canham, C.D., Silander, J.A., 1993. Forest models defined by field measurements: I. The design of a northeastern forest simulator. *Canadian Journal of Forest Research* 23, 1980–1988.
- Pacala, S.W., Canham, C.D., Silander, J.A., Kobe, R.K., 1994. Sapling growth as a function of resources in a north temperate forest. *Canadian Journal of Forest Research* 24, 2172–2183.
- Pacala, S.W., Deutschman, D.H., 1995. Details that matter: the spatial distribution of individual trees maintains forest ecosystem function. *Oikos* 74, 357–365.
- Pan, Y., Birdsey, R.A., Fang, J., Houghton, R., Kauppi, P.E., Kurz, W.A., Phillips, O.L., Shvidenko, A., Lewis, S.L., Canadell, J.G., Ciais, P., Jackson, R.B., Pacala, S.W., McGuire, A.D., Piao, S., Rautiainen, A., Sitch, S., Hayes, D., 2011. A large and persistent carbon sink in the world's forests. *Science* 333, 988–993.
- Pausas, J.G., 1997. Resprouting of *Quercus suber* in NE Spain after fire. *Journal of Vegetation Science* 8, 703–706.
- Pausas, J.G., Bladé, C., Valdecantos, A., Seva, J.P., Fuentes, D., Alloza, J.A., Vilagrosa, A., Bautista, S., Cortina, J., Vallejo, R., 2004. Pines and oaks in the restoration of Mediterranean landscapes of Spain: New perspectives for an old practice – a review. *Plant Ecology* 171, 209–220.
- Pausas, J.G., Llovet, J., Rodrigo, A., Vallejo, R., 2008. Are wildfires a disaster in the Mediterranean basin? – A review. *International Journal of Wildland Fire* 17, 713–723.

- Pausas, J.G., Ribeiro, E., Vallejo, R., 2004. Post-fire regeneration variability of *Pinus halepensis* in the eastern Iberian Peninsula. *Forest Ecology and Management* 203, 251–259.
- Peñuelas, J., Ogaya, R., Boada, M., Jump, A.S., 2007. Migration, invasion and decline: changes in recruitment and forest structure in a warming-linked shift of European beech forest in Catalonia (NE Spain). *Ecography* 30, 830–838.
- Pérez-Obiol, R., Jalut, G., Julià, R., Pèlach, A., Iriarte, M.J., Otto, T., Hernández-Beloqui, B., 2011. Mid-Holocene vegetation and climatic history of the Iberian Peninsula. *The Holocene* 21, 75–93.
- Phillips, O.L., Lewis, S.L., Baker, T.R., Chao, K.-J., Higuchi, N., 2008. The changing Amazon forest. *Philosophical Transactions of the Royal Society B* 363, 1819–1827.
- Platt, K.H., Allen, R.B., Coomes, D.A., Wiser, S.K., 2004. Mountain beech seedling responses to removal of below-ground competition and fertiliser addition. *New Zealand Journal Of Ecology* 28, 289–293.
- Plieninger, T., Modolell y Mainou, J., Konold, W., 2004. Land manager attitudes toward management, regeneration, and conservation of Spanish holm oak savannas (dehesas). *Landscape and Urban Planning* 66, 185–198.
- Plieninger, T., Pulido, F.J., Konold, W., 2003. Effects of land-use history on size structure of holm oak stands in Spanish dehesas: implications for conservation and restoration. *Environmental Conservation* 30, 61–70.
- Plieninger, T., Rolo, V., Moreno, G., 2010. Large-scale patterns of *Quercus ilex*, *Quercus suber*, and *Quercus pyrenaica* regeneration in central-western Spain. *Ecosystems* 13, 644–660.
- Pockman, W.T., Sperry, J.S., 2000. Vulnerability to xylem cavitation and the distribution of Sonoran Desert vegetation. *American Journal of Botany* 87, 1287–1299.
- Pol, D., 2004. Empirical problems of the hierarchical likelihood ratio test for model selection. *Systematic Biology* 53, 949–962.
- Poorter, L., McDonald, I., Alarcón, A., Fichtler, E., Licona, J., Peña-Claros, M., Sterck, F., Villegas, Z., Sass-Klaassen, U., 2010. The importance of wood traits and hydraulic conductance for the performance and life history strategies of 42 rainforest tree species. *New Phytologist* 185, 481–492.
- Porté, A., Bartelink, H.H., 2002. Modelling mixed forest growth: a review of models for forest management. *Ecological Modelling* 150, 141–188.
- Posada, D., Buckley, T.R., 2004. Model selection and model averaging in phylogenetics: advantages of Akaike Information Criterion and Bayesian approaches over likelihood ratio tests. *Systematic Biology* 53, 793–808.
- Poyatos, R., Latron, J., Llorens, P., 2003. Land use and land cover change after agricultural abandonment. *Mountain Research and Development* 23, 362–368.
- Prentice, I.C., Bondeau, A., Cramer, W., Harrison, S.P., Hickler, T., Lucht, W., Sitch, S., Smith, B., Sykes, M.T., 2007. Dynamic Global Vegetation Modeling: Quantifying Terrestrial Ecosystem Responses to Large-Scale Environmental Change, in: Canadell, J.G., Pataki, D.E., Pitelka, L.F. (Eds.), *Terrestrial Ecosystems in a Changing World*. Springer Berlin Heidelberg, Berlin, Heidelberg, pp. 175–192.

- Prentice, I.C., Sykes, M.T., Cramer, W., 1993. A simulation model for the transient effects of climate change on forest landscapes. *Ecological Modelling* 65, 51–70.
- Press, W.H., Flannery, B.P., Teukolsky, S.A., Vetterling, W.T., 1992. *Numerical Recipes in C: The Art of Scientific Computing*, 2nd ed. Cambridge University Press.
- Price, C.A., Enquist, B.J., Savage, V.M., 2007. A general model for allometric covariation in botanical form and function. *Proceedings of the National Academy of Sciences* 104, 13204–13209.
- Price, C.A., Ogle, K., White, E.P., Weitz, J.S., 2009. Evaluating scaling models in biology using hierarchical Bayesian approaches. *Ecol Lett* 12, 641–651.
- Price, D.T., Zimmerman, N.E., van der Meer, P.J., Lexer, M.J., Leadley, P., Jorri, I.T.M., Schaber, J., Clark, D.F., Lasch, P., McNu, S., Wu, J., Smith, B., 2001. Regeneration in gap models: Priority issues for studying forest responses to climate change. *Climatic change* 51, 475–508.
- Pritchard, J.K., Seielstad, M.T., Perez-Lezaun, A., Feldman, M.W., 1999. Population growth of human Y chromosomes: a study of Y chromosome microsatellites. *Molecular Biology and Evolution* 16, 1791–1798.
- Purves, D.W., 2009. The demography of range boundaries versus range cores in eastern US tree species. *Proceedings of the Royal Society B* 276, 1477–1484.
- Purves, D.W., Caspersen, J.P., Moorcroft, P.R., Hurtt, G.C., Pacala, S.W., 2004. Human-induced changes in US biogenic volatile organic compound emissions: evidence from long-term forest inventory data. *Global Change Biology* 10, 1737–1755.
- Purves, D.W., Lichstein, J.W., Pacala, S.W., 2007. Crown plasticity and competition for canopy space: a new spatially implicit model parameterized for 250 North American tree species. *PLoS ONE* 2, e870.
- Purves, D.W., Lichstein, J.W., Strigul, N., Pacala, S.W., 2008. Predicting and understanding forest dynamics using a simple tractable model. *Proceedings of the National Academy of Sciences* 105, 17018–17022.
- Purves, D.W., Pacala, S., 2008. Predictive models of forest dynamics. *Science* 320, 1452–1453.
- Quero, J.L., Villar, R., Marañón, T., Zamora, R., 2006. Interactions of drought and shade effects on seedlings of four *Quercus* species: physiological and structural leaf responses. *New Phytologist* 170, 819–834.
- Quillet, A., Peng, C., Garneau, M., 2010. Toward dynamic global vegetation models for simulating vegetation climate interactions and feedbacks: recent developments, limitations, and future challenges. *Environmental Reviews* 18, 333–353.
- Ramil-Rego, P., Muñoz-Sobrino, C., Rodríguez-Gutián, M., Gómez-Orellana, L., 1998. Differences in the vegetation of the North Iberian Peninsula during the last 16,000 years. *Plant Ecology* 138, 41–62.
- Reich, P.B., Tjoelker, M.G., Machado, J.-L., Oleksyn, J., 2006. Universal scaling of respiratory metabolism, size and nitrogen in plants. *Nature* 439, 457–461.
- Reille, M., Pons, A., 1992. The ecological significance of sclerophyllous oak forests in the western part of the Mediterranean basin: a note on pollen analytical data. *Vegetatio* 99/100, 13–17.

- Rey Benayas, 1998. Growth and survival in *Quercus ilex* L. seedlings after irrigation and artificial shading on Mediterranean set-aside agricultural land. *Annales des Sciences Forestières* 55, 7.
- Rhemtulla, J.M., Mladenoff, D.J., Clayton, M.K., 2009. Historical forest baselines reveal potential for continued carbon sequestration. *Proceedings of the National Academy of Sciences* 106, 6082–6087.
- Ribbens, E., Silander, J.A., Pacala, S.W., 1994. Seedling recruitment in forests: calibrating models to predict patterns of tree seedling dispersion. *Ecology* 75, 1794.
- Rigolot, E., 2004. Predicting postfire mortality of *Pinus halepensis* Mill. and *Pinus pinea* L. *Plant Ecology* 171, 139–151.
- Rizzo, D.M., Garbelotto, M., 2003. Sudden oak death: endangering California and Oregon forest ecosystems. *Frontiers in Ecology and the Environment* 1, 197–204.
- Rodà, F., 1999. *Ecology of Mediterranean evergreen oak forests*. Springer.
- Roderick, M., Berry, S., 2001. Linking wood density with tree growth and environment: a theoretical analysis based on the motion of water. *New Phytologist* 149, 473–485.
- Rodríguez-González, P.M., Stella, J.C., Campelo, F., Ferreira, M.T., Albuquerque, A., 2010. Subsidy or stress? Tree structure and growth in wetland forests along a hydrological gradient in Southern Europe. *Forest Ecology and Management* 259, 2015–2025.
- Rolland, C., 1993. Tree-ring and climate relationships for *Abies alba* in the internal alps. *Tree-Ring Bulletin* 53, 1–11.
- Rubiales, J.M., García-Amorena, I., Álvarez, S.G., Manzanque, F.G., 2008. The late Holocene extinction of *Pinus sylvestris* in the western Cantabrian range (Spain). *Journal of Biogeography* 35, 1840–1850.
- Ruiz-Benito, P., Lines, E.R., Coomes, D.A., Purves, D.W., Gómez-Aparicio, L., Zavala, M.A., Climatic effects on tree mortality are amplified by competition in Mediterranean forests (*in review*).
- Russell, E.W.B., Davis, R.B., Anderson, R.S., Rhodes, T.E., Anderson, D.S., 1993. Recent centuries of vegetational change in the glaciated north-eastern United States. *Journal of Ecology* 81, 647–664.
- Russo, S.E., Jenkins, K.L., Wiser, S.K., Uriarte, M., Duncan, R.P., Coomes, D.A., 2010. Interspecific relationships among growth, mortality and xylem traits of woody species from New Zealand. *Functional Ecology* 24, 253–262.
- Russo, S.E., Wiser, S.K., Coomes, D.A., 2007. Growth-size scaling relationships of woody plant species differ from predictions of the Metabolic Ecology Model. *Ecology Letters* 10, 889–901.
- Ryan, M.G., Binkley, D., Fownes, J.H., 1997. Age-Related Decline in Forest Productivity: Pattern and Process, in: *Advances in Ecological Research*. Academic Press, pp. 213–262.
- Ryan, M.G., Yoder, B.J., 1997. Hydraulic limits to tree height and tree growth. *Bioscience* 47, 235–242.

- Sabaté, S., Gracia, C.A., Sánchez, A., 2002. Likely effects of climate change on growth of *Quercus ilex*, *Pinus halepensis*, *Pinus pinaster*, *Pinus sylvestris* and *Fagus sylvatica* forests in the Mediterranean region. *Forest Ecology and Management* 462.
- Sands, P.J., Battaglia, M., Mummery, D., 2000. Application of process-based models to forest management: experience with PROMOD, a simple plantation productivity model. *Tree Physiology* 20, 383–392.
- Santana, V.M., Jaime Baeza, M., Marrs, R.H., Ramon Vallejo, V., 2010. Old-field secondary succession in SE Spain: can fire divert it? *Plant Ecology* 211, 337–349.
- Scarascia-Mugnozza, G., Oswald, H., Piussi, P., Radoglou, K., 2000. Forests of the Mediterranean region: gaps in knowledge and research needs. *Forest Ecology and Management* 132, 97–109.
- Scheiter, S., Higgins, S., 2009. Impacts of climate change on the vegetation of Africa: an adaptive dynamic vegetation modelling approach. *Global Change Biology* 15, 2224–2246.
- Schwarz, G., 1978. Estimating the dimension of a model. *The Annals of Statistics* 6, 461–464.
- Shibata, M., Nakashizuka, T., 1995. Seed and seedling demography of four co-occurring *Carpinus* species in a temperate deciduous forest. *Ecology* 76, 1099–1108.
- Shugart, H.H., Smith, T.M., 1996. A review of forest patch models and their application to global change research. *Climatic Change* 34.
- Shugart, H.H., West, D.C., 1977. Development of an Appalachian deciduous forest succession model and its application to assessment of the impact of the chestnut blight. *Journal of Environmental Management* 5, 161–179.
- Shugart, H.H., West, D.C., 1980. Forest succession models. *BioScience* 30, 308–313.
- Sisson, S.A., Fan, Y., Tanaka, M.M., 2007. Sequential Monte Carlo without likelihoods. *Proceedings of the National Academy of Sciences* 104, 1760–1765.
- Sisson, S.A., Fan, Y., Tanaka, M.M., 2009. Sequential Monte Carlo without likelihoods. Erratum 1041760. *Proceedings of the National Academy of Sciences* 106, 16889–16889.
- Sitch, S., Huntingford, C., Gedney, N., Levy, P.E., Lomas, M., Piao, S.L., Betts, R., Ciais, P., Cox, P., Friedlingstein, P., Jones, C.D., Prentice, I.C., Woodward, F.I., 2008. Evaluation of the terrestrial carbon cycle, future plant geography and climate-carbon cycle feedbacks using five Dynamic Global Vegetation Models (DGVMs). *Global Change Biology* 14, 2015–2039.
- Smit, C., Ouden, J., Díaz, M., 2008. Facilitation of *Quercus ilex* recruitment by shrubs in Mediterranean open woodlands. *Journal of Vegetation Science* 19, 193–200.
- Smith, R.J., 2009. Use and misuse of the reduced major axis for line-fitting. *American Journal of Physical Anthropology* 140, 476–486.
- Smith, W.B., 2002. Forest inventory and analysis: a national inventory and monitoring program. *Environmental Pollution* 116, S233–S242.
- Soares-Filho, B.S., Coutinho Cerqueira, G., Lopes Pennachin, C., 2002. DINAMICA—a stochastic cellular automata model designed to simulate the landscape dynamics in an Amazonian colonization frontier. *Ecological Modelling* 154, 217–235.

- Spiegelhalter, D.J., Best, N.G., Carlin, B.P., van der Linde, A., 2002. Bayesian measures of model complexity and fit. *Journal of the Royal Statistical Society, Series B (Statistical Methodology)* 64, 583–639.
- Straume, M., Johnson, M.L., 2010. Monte Carlo method for determining complete confidence probability distributions of estimated model parameters, in: *Essential Numerical Computer Methods*. Academic Press, p. 55.
- Strigul, N., Pristinski, D., Purves, D., Dushoff, J., Pacala, S., 2008. Scaling from trees to forests: tractable macroscopic equations for forest dynamics. *Ecological Monographs* 78, 523–545.
- Summitt, R., Sliker, A., 1980. *Handbook of materials science. Volume IV: Wood*. CRC Press.
- Swanson, M.E., 2009. Modeling the effects of alternative management strategies on forest carbon in the *Nothofagus* forests of Tierra del Fuego, Chile. *Forest Ecology and Management* 257, 1740–1750.
- Tabacchi, E., Planty-tabacchi, A., Salinas, M.J., Décamps, H., 1996. Landscape structure and diversity in riparian plant communities: a longitudinal comparative study. *Regulated Rivers: Research & Management* 12, 367–390.
- Tanaka, M.M., Francis, A.R., Luciani, F., Sisson, S.A., 2006. Using approximate Bayesian computation to estimate tuberculosis transmission parameters from genotype data. *Genetics* 173, 1511–1520.
- Tapias, R., Climent, J., Pardos, J.A., Gil, L., 2004. Life histories of Mediterranean pines. *Plant Ecology* 171, 53–68.
- Tapias, R., Gil, L., Fuentes-Utrilla, P., Pardos, J.A., 2001. Canopy seed banks in Mediterranean pines of south-eastern Spain: a comparison between *Pinus halepensis* Mill., *P. pinaster* Ait., *P. nigra* Arn. and *P. pinea* L. *Journal of Ecology* 89, 629–638.
- Tavaré, S., Balding, D.J., Griffiths, R.C., Donnelly, P., 1997. Inferring coalescence times from DNA sequence data. *Genetics* 145, 505–518.
- Taylor, A.R., Wang, J.R., Kurz, W.A., 2008. Effects of harvesting intensity on carbon stocks in eastern Canadian red spruce (*Picea rubens*) forests: An exploratory analysis using the CBM-CFS3 simulation model. *Forest Ecology and Management* 255, 3632–3641.
- Taylor, S.L., MacLean, D.A., 2007. Spatiotemporal patterns of mortality in declining balsam fir and spruce stands. *Forest Ecology and Management* 253, 188–201.
- Teixeira, A.M.G., Soares-Filho, B.S., Freitas, S.R., Metzger, J.P., 2009. Modeling landscape dynamics in an Atlantic Rainforest region: Implications for conservation. *Forest Ecology and Management* 257, 1219–1230.
- Thomas, R.Q., Canham, C.D., Weathers, K.C., Goodale, C.L., 2010. Increased tree carbon storage in response to nitrogen deposition in the US. *Nature Geoscience* 3, 13–17.
- Thompson, J., 2005. *Plant evolution and the Mediterranean*. Oxford University Press.
- Thornley, J.H.M., Cannell, M.G.R., 2004. Long-term effects of fire frequency on carbon storage and productivity of boreal forests: a modeling study. *Tree Physiology* 24, 765–773.

- Thornton, K., Andolfatto, P., 2006. Approximate Bayesian inference reveals evidence for a recent, severe bottleneck in a Netherlands population of *Drosophila melanogaster*. *Genetics* 172, 1607–1619.
- Tilman, D., 1988. Plant strategies and the dynamics and structure of plant communities. Princeton University Press.
- Tilman, D., HilleRisLambers, J., Harpole, S., Dybzinski, R., Fargione, J., Clark, C., Lehman, C., 2004. Does metabolic scaling theory apply to community ecology? It's a matter of scale. *Ecology* 85, 1797–1799.
- Toni, T., Welch, D., Strelkova, N., Ipsen, A., Stumpf, M.P.H., 2009. Approximate Bayesian computation scheme for parameter inference and model selection in dynamical systems. *Journal of The Royal Society Interface* 6, 187–202.
- Turner, I.M., 1994. Sclerophylly: primarily protective? *Functional Ecology* 8, 669–675.
- Tyree, M.T., Zimmermann, M.H., 2002. Xylem structure and the ascent of sap, 2nd ed. Springer-Verlag, Berlin.
- U.S. Department of Agriculture Forest Service, Technology transfer fact sheet mechanical properties of wood.
- Umeki, K., 2002. Tree mortality of five major species on Hokkaido Island, northern Japan. *Ecological Research* 17, 575–589.
- Urban, D.L., 1990. A versatile model to simulate forest pattern: a user's guide to ZELIG version 1.0. Department of Environmental Sciences, University of Virginia, Charlottesville, VA.
- Urban, D.L., Bonan, G.B., Smith, T.M., Shugart, H.H., 1991. Spatial applications of gap models. *Forest Ecology and Management* 42, 95–110.
- Urbieto, I.R., García, L.V., Zavala, M.A., Marañón, T., 2011. Mediterranean pine and oak distribution in southern Spain: Is there a mismatch between regeneration and adult distribution? *Journal of Vegetation Science* 22, 18–31.
- Urbieto, I.R., Pérez-Ramos, I.M., Zavala, M.A., Marañón, T., Kobe, R.K., 2008. Soil water content and emergence time control seedling establishment in three co-occurring Mediterranean oak species. *Canadian Journal of Forest Research* 38, 2382–2393.
- Urbieto, I.R., Zavala, M.A., Marañón, T., 2008. Human and non-human determinants of forest composition in southern Spain: evidence of shifts towards cork oak dominance as a result of management over the past century. *Journal of Biogeography* 35, 1688–1700.
- Uriarte, M., Canham, C.D., Thompson, J., Zimmerman, J.K., Murphy, L., Sabat, A.M., Fetcher, N., Haines, B.L., 2009. Natural disturbance and human land use as determinants of tropical forest dynamics: results from a forest simulator. *Ecological Monographs* 79, 423–443.
- Vaganov, E., Schulze, E.-D., Skomarkova, M., Knohl, A., Brand, W., Roscher, C., 2009. Intra-annual variability of anatomical structure and $\delta^{13}\text{C}$ values within tree rings of spruce and pine in alpine, temperate and boreal Europe. *Oecologia* 161, 729–745.
- Valbuena-Carabaña, M., de Heredia, U.L., Fuentes-Utrilla, P., González-Doncel, I., Gil, L., 2010. Historical and recent changes in the Spanish forests: A socio-economic process. *Review of Palaeobotany and Palynology* 162, 492–506.

- Valladares, F., Balaguer, L., Martinez-Ferri, E., Perez-Corona, E., Manrique, E., 2002. Plasticity, instability and canalization: is the phenotypic variation in seedlings of Sclerophyll oaks consistent with the environmental unpredictability of Mediterranean ecosystems? *New Phytologist* 156, 457–467.
- Valladares, F., Martinez-ferri, E., Balaguer, L., Perez-corona, E., Manrique, E., 2000. Low leaf-level response to light and nutrients in Mediterranean evergreen oaks: a conservative resource-use strategy? *New Phytologist* 148, 79–91.
- Vanclay, J.K., 1989. A growth model for north Queensland rainforests. *Forest Ecology and Management* 27, 245–271.
- Vanclay, J.K., 1995. Growth models for tropical forests: a synthesis of models and methods. *Forest Science* 41, 7–42.
- Viedma, O., Moreno, J.M., Rieiro, I., 2006. Interactions between land use/land cover change, forest fires and landscape structure in Sierra De Gredos (central Spain). *Environmental Conservation* 33, 212–222.
- Villela, D.M., Nascimento, M.T., Aragão, L.E.O.C., Gama, D.M. da, 2006. Effect of selective logging on forest structure and nutrient cycling in a seasonally dry Brazilian Atlantic forest. *Journal of Biogeography* 33, 506–516.
- Voelker, S.L., Muzika, R.-M., Guyette, R.P., 2008. Individual tree and stand level influences on the growth, vigor, and decline of red oaks in the Ozarks. *Forest Science* 54, 8–20.
- Wagenmakers, E.-J., Farrell, S., 2004. AIC model selection using Akaike weights. *Psychonomic Bulletin & Review* 11, 192–196.
- Wang, X., Fang, J., Tang, Z., Zhu, B., 2006. Climatic control of primary forest structure and DBH-height allometry in Northeast China. *Forest Ecology and Management* 234, 264–274.
- Warton, D.I., Wright, I.J., Falster, D.S., Westoby, M., 2006. Bivariate line-fitting methods for allometry. *Biological Reviews* 81, 259–291.
- Way, D., Oren, R., 2010. Differential responses to changes in growth temperature between trees from different functional groups and biomes: a review and synthesis of data. *Tree Physiology* doi: 10.1093/treephys/tpq015.
- Webb, C.O., Donoghue, M.J., 2005. Phylomatic: tree assembly for applied phylogenetics. *Molecular Ecology Notes* 5, 181–183.
- Wegmann, D., Leuenberger, C., Excoffier, L., 2009. Efficient approximate Bayesian computation coupled with Markov chain Monte Carlo without likelihood. *Genetics* 182, 1207–1218.
- Weiner, J., 1990. Asymmetric competition in plant populations. *Trends in Ecology & Evolution* 5, 360–364.
- Weiner, J., 2004. Allocation, plasticity and allometry in plants. *Perspectives in Plant Ecology, Evolution and Systematics* 6, 207–215.
- Weiner, J., Thomas, S.C., 2001. The nature of tree growth and the “age-related decline in forest productivity”. *Oikos* 94, 374–376.
- Wessolly, L., Erb, M., 1998. *Handbuch der Baumstatik und Baumkontrolle*. Patzer Verlag, Berlin.

- West, G.B., Brown, J.H., Enquist, B.J., 1997. A general model for the origin of allometric scaling laws in biology. *Science* 276, 122–126.
- West, G.B., Brown, J.H., Enquist, B.J., 1999. A general model for the structure and allometry of plant vascular systems. *Nature* 400, 664–667.
- West, G.B., Enquist, B.J., Brown, J.H., 2009. A general quantitative theory of forest structure and dynamics. *Proceedings of the National Academy of Sciences* 106, 7040–7045.
- Wickramasinghe, A., 1988. Modeling tree growth potential based on effective evapotranspiration. *Forest Science* 34, 864–881.
- Wolfslehner, B., Seidl, R., 2010. Harnessing ecosystem models and multi-criteria decision analysis for the support of forest management. *Environmental Management* 46, 850–861.
- Wullschlegel, S., Jackson, R., Currie, W., Friend, A., Luo, Y., Mouillot, F., Pan, Y., Shao, G., 2001. Below-ground processes in gap models for simulating forest response to global change. *Climatic Change* 51.
- Wunder, J., Bigler, C., Reineking, B., Fahse, L., Bugmann, H., 2006. Optimisation of tree mortality models based on growth patterns. *Ecological Modelling* 197, 196–206.
- Wyckoff, P.H., Clark, J.S., 2002. The relationship between growth and mortality for seven co-occurring tree species in the southern Appalachian Mountains. *Journal of Ecology* 90, 604–615.
- Wyckoff, P.H., Clark, J.S., 2005. Tree growth prediction using size and exposed crown area. *Canadian Journal of Forest Research* 35, 13–20.
- Yang, Y., Titus, S.J., Huang, S., 2003. Modeling individual tree mortality for white spruce in Alberta. *Ecological Modelling* 163, 209–222.
- Yao, X., Titus, S.J., MacDonald, S.E., 2001. A generalized logistic model of individual tree mortality for aspen, white spruce, and lodgepole pine in Alberta mixedwood forests. *Canadian Journal of Forest Research* 31, 283–291.
- Zanne, A.E., Lopez-Gonzalez, G., Coomes, D.A., Ilic, J., Jansen, S., Lewis, S.L., Miller, R.B., Swenson, N.G., Wiemann, M.C., Chave, J., 2009. Global wood density database. *Dryad*.
- Zavala, M.A., Espelta, J.M., Retana, J., 2000. Constraints and trade-offs in Mediterranean plant communities: The case of holm oak-Aleppo pine forests. *The Botanical Review* 66, 119–149.
- Zavala, M.A., Marcos, F., 1993. Ecological effects of harvesting biomass for energy in the Spanish Mediterranean. *Landscape and Urban Planning* 24, 227–231.
- Zeide, B., 1993. Analysis of growth equations. *Forest Science* 39, 594–616.
- Zhang, N., Shugart, H.H., Yan, X., 2009. Simulating the effects of climate changes on Eastern Eurasia forests. *Climatic Change* 95, 341–361.